Université de Montréal

Mécanismes d'activation de la voie lysosomale durant l'apoptose chimio-induite

par

Nicolas Parent

Programme de biologie moléculaire

Faculté de médecine

Thèse présentée à la Faculté de médecine
en vue de l'obtention du grade de philosophiæ doctor
en biologie moléculaire

août 2009

Université de Montréal
Faculté de médecine

Cette thèse intitulée

Mécanismes d'activation de la voie lysosomale durant l'apoptose chimio-induite

présentée par
Nicolas Parent

a été évaluée par un jury composé des personnes suivantes :

Marie-Josée Hebert, présidente-rapporteure
Richard Bertrand, directeur de recherche
Jean-François Cailhier, membre du jury
Éric Asselin, examinateur externe
Daniel Sinnett, représentant du doyen de la FES

Résumé

L'apoptose est une forme de mort cellulaire essentielle au développement et au maintien de l'homéostase chez les animaux multicellulaires. La machinerie apoptotique requiert la participation des caspases, des protéases conservées dans l'évolution et celle des organelles cytoplasmiques. Les lysosomes subissent des ruptures partielles, labilisation de la membrane lysosomale (LML), qui entraînent l'activation des cathepsines dans le cytoplasme de cellules cancéreuses humaines en apoptose induite par la camptothecin (CPT), incluant les histiocytes humains U-937. Ces modifications lysosomales se manifestent tôt durant l'activation de l'apoptose, concomitamment avec la perméabilisation de la mitochondrie et l'activation des caspases.

Une étude protéomique quantitative et comparative a permis d'identifier des changements précoces dans l'expression/localisation de protéines lysosomales de cellules U-937 en apoptose. Lors de deux expériences indépendantes, sur plus de 538 protéines lysosomales identifiées et quantifiées grâce au marquage isobarique iTRAQ et LC-ESI-MS/MS, 18 protéines augmentent et 9 diminuent dans les lysosomes purifiés de cellules en cours d'apoptose comparativement aux cellules contrôles. Les candidats validés par immuno-buvardage et microscopie confocale incluent le stérol-4-alpha-carboxylate 3-déhydrogénase, le prosaposin et la protéine kinase C delta (PKC-δ). Des expériences fonctionnelles ont démontrées que la translocation de PKC-δ aux lysosomes est requise pour la LML puisque la réduction de son expression par ARN interférents ou l'inhibition de son activité à l'aide du rottlerin empêche la LML lors de l'apoptose induite par la CPT. La translocation de PKC-δ aux lysosomes conduit à la phosphorylation et l'activation de la sphingomyelinase acide lysosomale (ASM), et à l'accroissement subséquent du contenu en céramide (CER) à la membrane lysosomale. Cette accumulation de CER endogène aux lysosomes est un évènement critique pour la LML induite par la CPT car l'inhibition de l'activité de PKC-δ ou de ASM diminue la formation de CER et la LML.

Ces résultats révèlent un nouveau mécanisme par lequel la PKC-δ active l'ASM qui conduit à son tour à l'accumulation de CER à la membrane lysosomale et déclenche la LML et l'activation de la voie lysosomale de l'apoptose induite par la CPT. En somme, ce

mécanisme confirme l'importance du métabolisme des sphingolipides dans l'activation de la voie lysosomale de l'apoptose.

Mots-clés : Apoptose, lysosome, PKC-δ, sphingolipides, céramide, iTRAQ, membrane lipidique, cellules U-937.

Abstract

Apoptosis is a distinct form of regulated cell death which is essential for the development and homeostasis maintenance of multicellular animals. Apoptosis is an evolutionary conserved process involving a specific molecular pathway, known as the caspase cascade, and the different cytoplasmic organelles. A lysosomal pathway, characterized by partial rupture, labilization of lysosomal membranes (LML), and cathepsin activation in the cytoplasm, is evoked during camptothecin-induced apoptosis in human cancer cells, including human histiocytic lymphoma U-937 cells. These lysosomal events begin rapidly and simultaneously with mitochondrial permeabilization and caspase activation within 3 h after drug treatment.

Comparative and quantitative proteome analyses were performed to identify early changes in lysosomal protein expression/localization from U-937 cells undergoing apoptosis. In two independent experiments, among a total of more than 538 proteins putatively identified and quantitated by iTRAQ isobaric labelling and LC-ESI-MS/MS, 18 proteins were found to be upregulated and 9 downregulated in lysosomes purified from early apoptotic compared to control cells. Protein expression was validated by Western blotting on enriched lysosome fractions, and protein localization confirmed by fluorescence confocal microscopy of representative protein candidates, whose functions are associated with lysosomal membrane fluidity and dynamics. These include sterol-4-alpha-carboxylate 3-dehydrogenase (NSDHL), prosaposin (PSAP) and protein kinase C delta (PKC-δ). Functional experiments demonstrate that PKC-δ translocation to lysosomes is required for LML, as silencing its expression with RNA interference or suppressing its activity with the inhibitor rottlerin prevents CPT-induced LLM. PKC-δ translocation to lysosomes is associated with lysosomal acidic sphingomyelinase (ASM) phosphorylation and activation, which in turn leads to an increase of ceramide (CER) content at lysosomes. The accumulation of endogenous CER at lysosomes is a critical event for CPT-induced LLM as suppressing PKC-δ or ASM activity reduces both CPT-mediated CER generation at lysosomes and CPT-induced LLM.

These findings reveal a novel mechanism by which PKC-δ mediates ASM phosphorylation/activation and CER accumulation at lysosomes in CPT-induced LLM, rapidly activating the lysosomal pathway of apoptosis after CPT treatment. Taken together, these results confirm the importance of sphingolipid metabolism in the activation of the lysosomal pathway of apoptosis.

Keywords : Apoptosis, lysosome, PKC-δ, sphingolipids, céramide, iTRAQ, lipid membrane, U-937 cells.

Table des matières

Liste des tableaux

Proteomic analysis of enriched lysosomes at early phase of camptothecin induced apoptosis in human U-937 cells

Liste des figures

À tous ceux qui cherchent

Remerciements

Je tiens à exprimer toute ma gratitude à mes collègues qui ont fait de ces dernières années une des périodes les plus heureuses de ma vie. C'est grâce à leur support et à leur bonne humeur que chacune des journées passées au laboratoire et au centre de recherche furent un véritable plaisir.

Pour la confiance que tu m'as accordée avec cet ambitieux projet, et pour toute l'énergie que tu as déployée pour me permettre de me réaliser, je te suis mille fois reconnaissant Richard. Non seulement j'ai pu profiter de ton incroyable flair scientifique, mais pour toute la générosité que tu as fait preuve envers moi, j'ai été acceuilli dans ton laboratoire comme dans une seconde famille. Tes qualités humaines témoignent de l'amour et du respect que tu as pour tes étudiants. Merci pour la chance immense que j'ai eu de passer ces dernières années avec toi Richard.

Enfin, à ma famille et amis, je ne peux que difficilement vous rendre le mérite qui vous revient. Vous avez contribué, loin du laboratoire, à l'aboutissement de mes travaux par votre soutien inconditionnel et persistant. À Karyne pour tout son amour, ses mots et sa présence. À mon garçon Ulysse, sans lui nul ne sait si un jour cette thèse aurait été écrite.

À vous tous, je vous aime!

Introduction

L'étude de la mort vise à comprendre la vie. La vie telle que nous la connaissons nécessite un peu de mort, à tous les jours, pour survivre à ce qui la menace. Si les cellules meurent dès nos premières heures, c'est pour que notre vie puisse prendre forme. Si nos cellules meurent durant notre vie, c'est pour que la vie puisse vivre. Un organisme pluricellulaire est un écosystème finement régulé et, c'est à la mort qu'il le doit!

La mort cellulaire est programmée lorsqu'elle survient durant le développement, non seulement au stade embryonnaire, mais aussi ultérieurement pour l'établissement de processus physiologiques cruciaux pour l'organisme tels que le système immunitaire et la mémoire. L'apoptose est une forme de mort cellulaire programmée et, bien qu'elle ne soit pas la seule forme de mort cellulaire programmée, elle est celle avec la plus grande occurrence (revu dans [1]). L'apoptose préserve aussi notre homéostase en éliminant les cellules indésirables ou endommagées afin de contrôler le renouvellement et l'intégrité cellulaire et tissulaire. Une perte de contrôle des mécanismes de régulation de l'apoptose est présente dans une variété de pathologies humaines [2-5] et le cancer [6-11].

Ce travail se veut, dans un premier temps, une revue de la littérature concernant les mécanismes d'initiation de l'apoptose, avec une attention particulière portée sur la participation du compartiment lysosomal et ses molécules associées. Les rôles des sphingolipides membranaires dans le processus apoptotique seront abordés afin de mieux illustrer les différents modèles qui ont été suggérés pour expliquer la rupture des organelles, celle observée à la membrane lysosomale plus précisément. Dans un second temps, il sera judicieux d'exposer les principes moléculaires de la voie des lysosomes dans l'apoptose appliquées à la thérapeutique du cancer. Dans un troisième temps, seront présentés les résultats de recherches qui ont permis d'élucider un mécanisme d'activation de la voie lysosomale dans l'apoptose impliquant la protéine PKC-δ et les céramides. Enfin, une brève synthèse des résultats, suivie d'éléments de discussion, permettra de mieux situer ces nouvelles connaissances et leur portée dans ce vaste champ d'étude qu'est l'apoptose.

I- L'apoptose

La cellule apoptotique

Récemment, plusieurs auteurs reconnus se sont réunis en comité, le « Nomenclature Committee on Cell Death 2009 », avec l'ambition de systématiser les diverses formes de morts cellulaires (Tableau 1a., page 16) [12]. Afin de mieux encadrer l'appellation « apoptose », ils ont émis une série de recommandations sur la classification expérimentale des cellules en apoptose. Ainsi, l'apoptose se définit suivant un ensemble de modifications spécifiquement retrouvées dans une cellule (Tableau 1).

Tableau 1 : Modifications associées à l'apoptose.

Morphologiques	Biochimiques
Arrondissement de la cellule	Activation des membres pro-apoptotiques de la famille des Bcl-2
Rétraction des pseudopodes	Activation des caspases
Contraction cellulaire et nucléaire	Dissipation du potentiel membranaire mitochondrial ($\Delta\Psi m$)
Fragmentation du noyau	Perméabilisation de la membrane externe mitochondriale
Modifications mineures des organelles cytoplasmiques	Fragmentation oligonucléosomale de l'ADN
Bourgeonnement de la membrane plasmique	Externalisation des phosphatidylsérine à la membrane externe
Phagocytose des corps apoptotiques, *in vivo*	Surproduction d'espèces oxygénées réactives (ROS)
	Accumulation de fragments d'ADN

Bien qu'il ne soit pas essentiel de retrouver la totalité des modifications mentionnées, il est à l'inverse hasardeux de parler d'apoptose suite à l'observation d'une seule de ces manifestations. Par exemple, l'activation seule des caspases ne constituent pas nécessairement la signature de la cellule en cours d'apoptose puisque l'on reconnaît à ces dernières plusieurs fonctions non-apoptotiques, notamment durant l'inflammation, la différenciation et la prolifération cellulaire (revu dans [13]). Toutefois, l'activation des caspases dans un contexte apoptotique, c'est-à-dire en présence d'autres altérations

cellulaires décrites dans le tableau 1, demeure une étape-clé dans la signalisation de l'apoptose.

Tableau 1a: Caractéristiques morphologiques des principales formes de mort cellulaire.

Apoptose	Nécrose	Mort autophagique
• Condensation de la chromatine importante • Réduction du cytoplasme • Fragmentation nucléaire • Altérations mineures des organelles • Bourgeonnement de la membrane • Phagocyté par les cellules environnantes *in vivo*	• Condensation de la chromatine modérée • Rupture de la membrane plasmatique • Gonflement des organelles et du cytoplasme • Entraîne généralement de l'inflammation *in vivo*	• Condensation de la chromatine absente • Vacuolisation massive du cytoplasme • Accumulation de vacuoles autophagiques • Peu ou pas de phagocyté *in vivo*

Les caspases

Les caspases (*cysteinyl aspartate-specific proteinase*) jouent un rôle central dans la cascade apoptotique. Selon l'analyse phylogénique des divers membres de cette famille conservée des insectes jusqu'à nous, on regroupe chez les mammifères les caspases associées au contrôle de l'inflammation, soit les caspases-1, -4, -5, -11 et -12. À ce groupe sont associées, les caspases-2 et -14 moins conservées. Un deuxième groupe comprend les caspases-3, -6 et -7 appelés caspases effectrices. Enfin, un troisième groupe phylogénique inclut les caspases-8, -9, et -10, celles-ci impliquées dans l'initiation de l'apoptose (revu dans [14]). Les caspases sont des protéases à motif cystéine, synthétisées sous forme de zymogènes inactifs et ultérieurement activées, soit par proximité à l'intérieur de complexes protéiques, soit suivant la maturation protéolytique des sous-unités large et petite (revu dans [15]). En plus des régions qui constitueront les deux sous-unités de l'enzyme active, les procaspases possèdent un prodomaine dans la région amino-terminale d'une longueur variable, associée en partie à son rôle dans le processus apoptotique. Les caspases initiatrices (caspases-2, -8, -9 et -10) sont caractérisées par un long prodomaine (>90 acides aminés) tandis que le prodomain des caspases effectrices (caspases-3, -6 et -7) est plus

court (20-30 acides aminés) ou absent. Finalement, on retrouve deux modules d'interaction protéine-protéine distincts sur les longs prodomaines, DED (*death effector domain*) et CARD (*caspase-activating recruitment domain*), qui permettront aux caspases initiatrices d'être recrutées et d'initier le processus moléculaire apoptotique (revu dans [16]).

La cascade des caspases

Les caspases orchestrent l'essentiel des modifications biochimiques et morphologiques associées au phénotype de la cellule apoptotique, par la protéolyse en cascade d'une foule de protéines indispensables aux fonctions cellulaires normales (pour une revue exhaustive des substrats des caspases, voir [17]). Les zymogènes des caspases constituent eux-aussi des substrats pour les caspases initiatrices actives. Ceci permettra d'une part, à amplifier la réponse apoptotique en activant plus de caspases initiatrices (i.e. caspases-2, -8, -9 et -10) et d'autre part, à poursuivre la cascade signalétique en activant les caspases effectrices (i.e. caspases-3, -6 et -7) : c'est la cascade des caspases [18]. Toutefois, l'activité des caspases n'est pas indispensable à la mort cellulaire dans des conditions pro-apoptotiques dans certains contextes. Il existe d'ailleurs quelques exemples où l'inhibition des caspases n'empêche pas les cellules de mourir, suggérant la participation active d'autres protéases à la signalisation de l'apoptose ou d'autres formes de mort cellulaire [8-10]. Il n'est demeure pas moins que l'activation des caspases est généralement considérée comme une étape critique dans l'initiation de l'apoptose. La mort cellulaire observée suivant l'inhibition des caspases pourrait s'agir plutôt de nécrose [19], de mort autophagique [20] ou simplement, de mort cellulaire caspase-indépendante (revu dans [21]).

L'initiation de l'apoptose

Face à l'extrême diversité des signaux qui induisent l'apoptose, aussi bien de sources endogènes qu'exogènes, on en conclu que l'initiation de l'apoptose et l'activation des caspases puissent emprunter des voies signalétiques distinctes et se produire à différents

endroits dans la cellule. On remarque d'ailleurs que la signalisation de l'apoptose n'est pas qu'une simple série linéaire d'événements qui amène ultimement la cellule à sa destruction, mais plutôt l'intervention de deux voies signalétiques, voire même de multiples voies, initiées simultanément ou séquentiellement au sein d'une même cellule. Des voies signalétiques initiant l'apoptose siégeant à la membrane plasmique, à la mitochondrie, au réticulum endoplasmique et dans les lysosomes ont été décrites au long des trente dernières années. La description des principales voies d'initiation de l'apoptose sera brièvement abordée avec l'emphase sur la voie lysosomale et les rôles qui lui sont connues dans le processus apoptotique.

La voie des récepteurs de mort, ou extrinsèque

Il existe une famille de récepteurs membranaires pouvant induire la mort cellulaire par l'entremise des caspases initiatrices. La liaison des ligands aux récepteurs de mort de la famille de TNF (*tumor necrosis factor*), regroupant Fas/APO-1/CD95, TNF-R1, DR-3, DR-4, DR-5 et DR-6 (revu dans [22]) enclenche l'assemblage de complexes de signalisation, le DISC (*death-inducing signalling complex*), comprenant les protéines adaptatrices FADD/MORT1, TRADD et RIP et les procaspases-8 et/ou -10. La proximité, résultant de l'agrégation de plusieurs molécules de procaspases au niveau des récepteurs de mort, permettra leur activation par auto-protéolyse. Cette première voie d'initiation de l'apoptose par les caspases est la voie extrinsèque ou la voie des récepteurs de mort cellulaire (revu dans [23]). Une fois activées, les caspases-8 et/ou -10 pourront transmettre le signal apoptotique en clivant directement les caspases effectrices ou engager la voie mitochondriale par l'entremise du clivage de la protéine Bid, une protéine BH3-unique pro-apoptotique de la famille des Bcl-2, en une forme tronquée et active, tBid (Figure 1, page 26).

La voie mitochondriale, ou intrinsèque

La perméabilisation modérée de la membrane externe de la mitochondrie, la MOMP (*mitochondrial outer-membrane permeabilization*), résulte en la libération dans le cytosol

de plusieurs molécules proapoptotiques; il s'agit de la voie mitochondriale de l'apoptose, dite intrinsèque (revu dans [24]). Les protéines de la famille des Bcl-2 régulent la MOMP. Ces protéines se caractérisent par diverses combinaisons de domaines BH classés de 1 à 4. On retrouve les protéines anti-apoptotiques Bcl-2, Bcl-xL, Mcl-1, A-1/Bf-1/Grs, Bcl-w, Brag-1, Boo/Diva, Bcl-B/Bcl-2L-10 et Bcl-xES, constituées d'au moins un domaine BH1 et BH2 ou de tous les quatre domaines BH, et les protéines pro-apoptotiques Bax, Bak, Bcl-xS, Mtd/Bok/Bod, Bcl-rambo et Bcl-gL comportant des combinaisons de domaines BH1 à BH3. Enfin, une troisième classe comprend les activateurs, contenant seulement le domaine BH3, dont Bik/Nbk, Bid, Hrk, Bad, Bim, Puma/Bbc3, Noxa et Bmf. (revu dans [25]). Les différents homologues de Bcl-2 exercent leur action sur la membrane mitochondriale en interagissant physiquement et en formant un réseau complexe et dynamique d'homo- et d'hétéro-oligomères (revu dans [26]).

On retrouve dans l'espace inter-membranaire de la mitochondrie une panoplie de molécules pro-apoptotiques incluant le cytochrome c [27, 28], les protéines Smac/DIABLO [29, 30], OMI/Htra2 [31-33], AIF[34], EndoG [35] ainsi qu'une réserve de procaspases-2, -3, -8 et -9 [36-39]. Suite à l'activation de la voie mitochondriale, la MOMP entraînera la relâche de ces facteurs dans le cytosol qui pourront interagir pour favoriser positivement la cascade des caspases et l'induction de l'apoptose (revu dans [24]). Le cytochrome *c* ainsi relâché, facilitera l'assemblage d'un complexe multiprotéique comprenant Apaf-1, caspase-9 et le cytochrome *c*, nommé l'apoptosome qui conduira à l'activation de la caspase-9 [5-7]. Les procaspases-3 et -7 sont ensuite recrutées à l'apoptosome actif où elles sont clivées et activées par la caspase-9 [40, 41]. Les souris déficientes pour l'expression de Apaf-1 et de caspase-9 montrent des phénotypes similaires, ce qui en a inspiré plusieurs à soutenir que la caspase -9 ne pourrait être activée que dans le contexte de l'apoptosome [34-37]. Cependant, la nécessité de l'apoptosome pour l'activation de la caspase-9 est remise en cause par des observations qui montrent l'indépendance de l'activation de la caspase-9, d'Apaf-1 et de l'apoptosome [42-44]. Conséquemment, certains auteurs ont proposé que la forme clivée de caspase-9, par exemple par l'action de la caspase-8, pourrait former, avec l'aide ou non d'adaptateurs, des dimères actifs et outrepasser la voie mitochondriale [43, 44].

La voie du réticulum endoplasmique

La caspase-12 médie une voie spécifique de l'apoptose suivant l'exposition à des agents déstabilisant le réticulum endoplasmique [45-47]. La procaspase-12 est localisée dans le réticulum endoplasmique et relâchée dans le cytosol durant l'apoptose, un événement qui coïncide avec l'activation des caspases-3 et -9 indépendamment [47] ou non [46] de la voie mitochondriale. Il est aussi intéressant de noter que la caspase-12 active la caspase-9 *in vitro* [47]. Par ailleurs, il apparaîtrait que les protéines pro-apoptotiques de la famille des Bcl-2, Bax et Bak, contriburaient aussi à la voie de l'apoptose du réticulum endoplasmique en régulant l'efflux de Ca^{2+} du réticulum endoplasmique, affectant positivement plusieurs facteurs pro-apoptotiques [48]. Enfin, la protéine salubrinal protège le réticulum endoplasmique de l'apoptose causée par divers agents de stress spécifiques au réticulum endoplasmique [49]. L'effet protecteur de la protéine salubrinal implique le facteur de traduction eEF-2 (*elongation factor eukaryotic translation elongation factor 2*) qui permettrait de réduire l'inhibition qui affecte la traduction lors de stress au réticulum endoplasmique [50].

Ces voies d'initiation de l'apoptose illustrent bien que les organelles agissent comme des sentinelles aux aguets de la moindre source de stress qui pourraient perturber leurs fonctions physiologiques normales. Dans ce sens, le compartiment lysosomal à la particularité d'être une structure dangereuse pour la cellule de par sa nature, mais bénéfique de par ses fonctions. Suivant un bref aperçu des lysosomes, ses rôles et fonctions dans l'apoptose et les autres formes de mort cellulaire seront exposées.

II- Le compartiment lysosomal

Les lysosomes

Christian de Duve décrivait en 1955 l'existence d'une structure vacuolaire riche en enzymes hydrolytiques, au sein de cellules hépatiques de rat qu'il nomma lysosome [51].

Issu du système endosomal, le lysosome acquiert en cours de maturation un ensemble d'enzymes lytiques dont le fonctionnement est optimal à pH acide (revu dans [52]). Les lysosomes sont des organelles cytosoliques hautement dynamiques qui reçoivent les produits de la biosynthèse (via le réseau du *trans*-Golgi), de l'endocytose et des processus autophagiques, et où s'effectue la majorité de l'activité de dégradation dans les cellules eucaryotes. La régulation des activités de dégradation sera déterminante pour le maintien de l'homéostase (revu dans [53]). Les pathologies liées au dysfonctionnement lysosomal ou à l'expression des enzymes lysosomales sont nombreuses : maladies congénitales, troubles associés au vieillissement dont certaines maladies neuro-dégénératives, cardiovasculaires et cancer (revu dans [54-56]). Certaines molécules de la pharmacopée peuvent aussi entraîner certains effets néfastes dûs à l'activité lysosomale perturbée (revu dans [57]). Enfin, il existe certains types cellulaires possédants des lysosomes spécialisés auxquels sont associées des fonctions cellulaires uniques et dont le dysfonctionnement est responsable de pathologies (revu dans [58]).

Les lysosomes dans la mort cellulaire

Les lysosomes jouent des rôles fondamentaux dans trois différents types de mort cellulaire : 1- la nécrose, qui peut être induite par une sortie soudaine et massive des hydrolases contenues dans les lysosomes [59], 2- l'apoptose, induite par une relâche limitée de protéines pro-apoptotiques lysosomales suivant l'apparition de ruptures modérées à la membrane des lysosomes, un phénomène aussi décrit comme la labilisation de la membrane lysosomale (LML), et 3- la mort cellulaire autophagique, lorsque la régulation de l'autophagie est perturbée.

Il y a trois formes d'autophagie : la microautophagie, la macroautophagie et l'autophagie à l'aide de protéine chaperones (CMA). Dans les deux premières, de larges portions du cytoplasme peuvent être séquestrées de manière spécifique ou non, alors que la CMA ne touche que des protéines solubles spécifiquement ciblées. La microautophagie se caractérise par la séquestration directe de constituants cytosoliques aux lysosomes suivant l'invagination de la membrane lysososmale. Quant à elle, la macroautophagie fait intervenir

des vésicules où les constituants cytosoliques y sont séquestrés: les autophagosomes. Ces deniers viendront fusionner avec des lysosomes afin de former des autophagolysosomes, permettant à leur contenu d'être dégradé par les hydrolases lysosomales. Les produits de dégradation seront relâchés dans le cytosol par l'entremise de perméases lysosomales pour être éventuellement réassimilés par la cellule (revu dans [60]).

D'une part, l'autophagie est un processus catabolique permettant aux cellules de survivre à une carence nutritive en suppléant elle-même à ses besoins à partir de l'autodégradation de quelques unes de ses organelles et macromolécules (revu dans [61]). D'autre part, l'autophagie favorise la survie cellulaire en éliminant des protéines et des organelles défectueuses ou endommagées de même que certains parasites intracellulaires d'origine bactérienne notamment (revu dans [60]). Au contraire, l'exacerbation du processus autophagique, comme par exemple lors de la surexpression des protéines de l'autophagie Berclin-1 [62] ou Atg1, entraîne la mort cellulaire de manière contrôlée (revu dans [63] et tableau 1a en page 15a). et parfois similaire à l'apoptose [64, 65].

D'ailleurs, l'apoptose et la mort cellulaire autophagique partagent plusieurs similitudes quant aux signaux qui les induisent, en particulier les substances pouvant entraîner un stress cellulaire, ainsi que des protéines qui inhibe ces processus, dont les protéines de la famille de Bcl-2, la protéine Bcl-2 et la protéine Bcl-xL [62, 66]. Ces similitudes suggèrent l'existence de voies signalétiques communes aux deux processus. Bien qu'il n'y ait que très peu de données décrivant l'interrelation moléculaire entre l'autophagie et l'apoptose, il a été montré récemment que la protéine Beclin-1 y jouerait un rôle clé [67]. Beclin-1 est une protéine contenant un domaine BH3, caractéristique des protéines de la famille des Bcl-2 activatrices de la MOMP. Il apparaît que la protéine Beclin-1 dans sa forme entière ne joue pas de rôles dans le processus apoptotique; elle est clairement est une stimulatrice de l'autophagie. Par l'entremise de son domaine BH3, la protéine Beclin-1 empêche l'action anti-autophagique de la protéine Bcl-2 ou de la protéine Bcl-xL en se liant à celles-ci (revu dans [68]). Cependant, ce même domaine BH3 de la protéine Beclin-1 constitue un substrat pour les caspases 2 et 7. Une fois clivée, le fragment de la protéine Beclin-1 nouvellement formé perd son activité pro-autophagique et acquiert

la capacité d'induire la relâche mitochondriale de facteurs pro-apoptotiques pour ainsi favoriser l'apoptose [67].

On remarque dans certains modèles expérimentaux que l'inhibition de l'apoptose peut entraîner la mort cellulaire autophagique. En effet, il est observé dans un modèle murin déficient pour les protéines pro-apoptotiques Bax et Bak [69] ainsi que dans diverses lignées de cellules humaines traitées avec l'inhibiteur pan-caspases Z-VAD-fmk [70, 71], que l'inhibition de l'apoptose de manière prolongée conduit à la mort cellulaire autophagique. Cette mort cellulaire autophagique représenterait un choix ultime pour la cellule résistante à l'apoptose qui serait incapable de composer avec une perte trop importante de ses constituants cytosoliques [63].

Bien qu'il apparaisse que l'apoptose soit le programme de mort prédominant et serait habituellement privilégié sur la mort autophagique, ces deux processus de mort cellulaire pourraient partager une relation beaucoup plus intime qu'à première vue. Plusieurs scénarios ont été avancés par le groupe de Kroemer afin de mettre en relation les fonctions apparemment cytoprotectrices de l'autophagie et la mort cellulaire apoptotique. D'abord, l'autophagie précédant l'apoptose pourrait faciliter le processus apoptotique en débutant les réactions cataboliques visant à détruire une cellule destinée à mourir. Ensuite, la contribution de l'autophagie à maintenir des niveaux énergétiques cellulaires optimaux favoriserait la mise en action du processus apoptotique [72, 73].

L'environnement acide des lysosomes dans l'apoptose

L'une des premières observations, suggérant une implication du compartiment lysosomal dans l'initiation de l'apoptose, fût l'acidification cytosolique, un événement qui se produit tôt suivant l'induction de l'apoptose [74-78]. Dans les cellules Jurkat par exemple, les signes d'acidification touchent près de 80% des cellules en cours d'apoptose, quatre heures suivant l'exposition aux rayons ultra-violets (UV) [77]. Dans les cellules U-937, le pH cytosolique décroît de 7,2 ± 0,1 à 5,8 ± 0,1 tandis que le pH intra-lysosomal passe de 4,3 ± 0,4 à 5,2 ± 0,3 quatre heures après le traitement au TNF-α [76].

L'acidification du cytosol pourrait, d'une part, contribuer à l'activation des caspases. Des expériences *in vitro* soutiennent que le pH optimal pour l'activation des caspases se situe près de pH 6,4. À pH 7,4, soit l'acidité normale du cytosol, l'activité des caspases n'atteint que 25% de la valeur optimale [75]. D'autre part, l'acidification faciliterait la dimérisation des membres pro-apoptotiques de la famille des Bcl-2 et leur capacité à provoquer la perméabilisation de la membrane mitochondriale [79]. En plus du contenu acide, les lysosomes vont relâcher dans le cytosol leurs puissantes hydrolases, les cathepsines.

Les cathepsines

Il existe trois types de cathepsines, classées selon leur spécificité catalytique : soit sur la sérine (cathepsines A et G), l'acide aspartique (cathepsines D et E) ou sur la cystéine (cathepsines B, C, H, F, L, O, S, V, W et X/Z). Les rôles des cathepsines ont longtemps été associés strictement à leur fonction de dégradation à l'intérieur des lysosomes, alors que leur fonction extra-lysosomale a été ignorée à cause de l'instabilité de ces protéases à pH neutre, limitant leur durée de vie, allant de quelques minutes (cathepsine L) [80] à quelques heures (cathepsine S) [81]. Il existe pourtant des inhibiteurs endogènes dans le cytosol, les stefines, aussi appelées cystatines, qui limitent l'activité des cathepsines à motif cystéine volontairement ou accidentellement relâchées [82]. Lors de la LML et de la sortie modérée des cathepsines hors du compartiment lysosomal, l'action inhibitrice des stefines serait légèrement surchargée, ce qui permettrait aux cathepsines d'induire l'apoptose. Ainsi, on remarque que chez les souris déficientes en stefine B, l'apoptose neuronale s'observe même en absence d'atteinte de la membrane lysosomale, probablement attribuable à l'activité basale des cathepsines hors des lysosomes [83].

Rôles des lysosomes dans la cascade apoptotique

Dépendamment du type cellulaire et du stimulus utilisé, la voie lysosomale de l'apoptose se distingue en deux phases, précoce, où elle initie ou contribue à initier la cascade apoptotique (initiation), et tardive, alors que l'apoptose est entamée et que les

protéases lysosomales vont participer à la destruction finale de la cellule (exécution). Le tableau 2 recense les observations directes de l'implication de la voie lysosomale dans l'apoptose et la fonction, telle que rapportée, qu'elle occupe au sein de ce processus. L'importance de la voie lysosomale pour le phénotype apoptotique est indiquée, à savoir qu'elle est requis (requis) ou dispensable lorsque d'autres voies sont en jeux (coopération).

L'activation des caspases par les lysosomes

Il n'existe que peu d'évidences concernant le rôle directe des cathepsines dans l'activation des caspases, notamment parce que les pro-caspases font de piètres substrats pour les cathepsines [84, 85]. Cependant, deux groupes ont rapportés l'existence d'une fonction pro-apoptotique pour la lactoferrine lysosomale, une protéase à motif sérine impliquée dans la régulation du métabolisme du fer [86-88]. La lactoferrine a la capacité de cliver et d'activer la caspase-3 et de provoquer l'apoptose [89]. L'inhibition de cette dernière, à l'aide d'ARN interférents ou d'agents chélateurs du fer, diminue l'apoptose des cellules [89]. La dépendance au fer pour l'action pro-apoptotique de la lactoferrine est d'un intérêt particulier. En effet, les chélateurs du fer protègent divers types de cellules cancéreuses de l'apoptose induite par le stress oxydatif [90, 91]. Les lysosomes constituent le compartiment cytoplasmique contenant le plus de fer de faible poids moléculaire, attribuable à la dégradation autophagique normale de métalloprotéines, telles que les cytochromes mitochondriaux [92]. Dans l'environnement acide du lysosome, le fer libre réduit (Fe^{2+}) catalyse rapidement dans des réactions de type Fenton, la conversion des molécules de H_2O_2 en radicaux libres HO· générant un stress oxydatif. Le pH acide du compartiment lysosomal le rend donc particulièrement sensible au stress oxydatif.

L'activation de la voie mitochondriale par les lysosomes

Plusieurs travaux démontrent néanmoins que l'action pro-apoptotique des cathepsines se manifeste dans la phase précoce du processus apoptotique et que, dans

certains contextes, l'activité des cathepsines est requise pour le phénotype apoptotique (voir tableau 2). Un des mécanismes le mieux décrit est l'activation, suivant le clivage par les

Tableau 1 : Répertoire des observations sur l'activation de la voie lysosomale conduisant à l'apoptose.

Stimuli apoptotique	Contexte cellulaire	Fonction(s)	Réf.
Dommages à l'ADN			
Étoposide	LML précède l'activation de la caspase-3. indépendamment du cytochrome c dans les cellules P39.	Initiation	[93]
Camptothécine	LML et MOMP simultanées dans les cellules U-937 et Namalwa.	Initiation / Exécution	[94]
Camptothécine	Cathepsines requises pour MOMP dans les cellules MCF-7.	Initiation/ Coopération	[95]
Stress oxydatif			
ROS	Cathepsines à motif cystéine clivent Bid dans les neutrophiles.	Initiation / Coopération	[96]
ROS	LML et relâche de la cathepsine D induisent l'apoptose des cardiomyocytes.	Initiation	[97]
ROS	LML et relâche de la cathepsine D précèdent l'activation de la caspase-3 dans les fibroblastes.	Initiation	[98]
ROS	Cathepsine D induit la MOMP et l'apoptose dans les neuroblastomes.	Initiation	[91]
ROS	LML induite à des doses modérées de H_2O_2 dans les cellules Jurkat.	Initiation	[99] [100]
ROS	LML précède l'apoptose dans les cellules D384.	Initiation	[101]
Acide hypochloreux	LML induite par les calpaïnes dans les neurones.	Initiation / Coopération	[102]
Récepteurs de mort			
TNF-α	LML inhibée dans les hépatocyte $Bid^{-/-}$.	Initiation / Coopération	[103]
TNF-α	LML indépendante de la MOMP mais dépendante de la caspase-9 dans les fibroblastes.	Initiation / Exécution	[44]
TNF-α	Expression de Spi2A via NF-κB réduit l'apoptose des MEF.	Initiation / Coopération	[104]
TNF-α	LML dépendante de caspase-8 dans les hépatocytes; réduction de l'apoptose dans les $Bid^{-/-}$.	Initiation / Coopération	[105]
TNF-α	Hépatocyte Cathepsine $B^{-/-}$ résistant à l'apoptose.	Requis	[106] [107]
TNF-α / FasL / interféron-γ	Inhibition de la cathepsine D empêche l'apoptose des cellules HeLa et U-937.	Requis	[108]
FasL	Cathepsines et caspases requises pour l'apoptose des lymphocytes B.	Requis	[109]
TRAIL	Internalisation et migration de DR-5 aux lysosomes et LML dans les cellules Huh-7.	Requis	[110]
Agents lysomotropiques et photosensibilisateurs			
N-dodecylimidazole	S'accumule dans les lysosomes dans les cellules HL-60.	Initiation	[111]
O-methyl-L-serine dodecylamide hydrochloride	LML induit l'apoptose dans les lymphocytes B en absence d'activité de la caspase-3.	Requis	[112]
O-methyl-L-serine dodecylamide hydrochloride	LML précède l'activation des caspases et de l'apoptose des neurones.	Initiation	[113]
L-leucyl-L-leucine methyl ester	S'accumule dans les lysosomes dans les cellules U-937.	Initiation	[114]
L-leucyl-L-leucine methyl ester	LML induit le clivage de Bid dans les cellules HeLa et HEK293.	Initiation / Coopération	[115]
Quinolones + UV	LML induite dans les fibroblastes $Bid^{-/-}$.	Initiation / Coopération	[116]
Hydroxychloroqui-ne (*N*-aspartyl chlorin e6)	LML précède l'activation de la voie mitochondriale des cellules HeLa, BJAB et fibroblastes.	Initiation / Coopération	[117]
	LML précède l'apoptose dans les cellules 1c1c7.	Initiation / Coopération	[118]
ATX-s10-PDT	S'accumule aux lysosomes des cellules MCF-7 et G361.	Initiation	[119] [120]
3-aminopropanal	S'accumule dans les lysosomes des neurones et cellules gliales suivant l'ischémie cérébrale.	Initiation	[121]
Sphingolipides et analogues			
Sphingosine	Inhibition des cathepsines réduit l'apoptose des cellules Jurkat et J774.	Initiation / Coopération	[122]
HePC (miltefosine)	LML induite après l'activation de la caspase-3.	Exécution	[123]
N-myristoylamino-(4-nitrophenyl)-propandiol-1,3	L'inhibition de la ceramidase acide induit la LML puis l'apoptose des cellules DU145.	Initiation	[124]

Stimuli apoptotique	Contexte cellulaire	Fonction(s)	Réf.
Drogues ciblant les microtubules			
Paclitaxel / epothilone B	Inhibition des cathepsines à motif cystéine et la cathepsine B inhibe l'apoptose des cellules NCI-H460, SW1573 et A549.	Requis	[125]
Vincristine	LML précède l'activation de la voie mitochondriale et l'apoptose des cellules HeLa.	Initiation / Coopération	[126]
Divers			
Bafilomycine A_1	LML et relâche de la cathepsine D précèdent l'activation de la caspase-3 dans les MKN-1 et P39.	Initiation	[93, 127]
Globulines anti-thymocytes	Cathepsine B induit l'apoptose des lymphocytes T.	Requis	[128]
VIH	LML précède la MOMP dans les lymphocytes T CD4+.	Initiation	[129]
Carence en sérum	Sur-expression de cathepsines B et D sensibilise les cellules PC-12 à l'apoptose.	Coopération	[130]
Carence en facteur de croissance / FasL / ROS	LML précède l'apoptose des cellules Jurkat.	Initiation	[131]
benzo[*a*]pyrene	LML et relâche de la lactoferrine induisent l'activation de la caspase-3 dans les cellules F258.	Initiation	[86]
D-galactosamine	LML et relâche de la lactoferrine induisent l'activation de la caspase-3 dans les hépatocytes.	Initiation	[88]
Déplétion de Hsp70	LML induite et inhibition de la cathepsine B réduit l'apoptose.	Initiation / Coopération	[132]
Zinc ($ZnCl_2$) + clioquinol	Accumulation du Zn^{2+} dans les lysosomes précédant l'induction de la LML dans les cellules DU145.	Initiation	[133]
Silice	Inhibition de la cathepsine D réduit l'activation des caspases dans les macrophages.	Initiation	[134]
Rétinoïques artificiels	LML induit l'apoptose.	Initiation	[135]
α-tocopheryl succinate	LML précède la MOMP et l'apoptose des cellules Jurkat.	Initiation	[136]
Liaison du récepteur des cellules B	LML et relâche de la cathepsine B induisent l'apoptose des cellules DT40.	Initiation	[137]
p53 thermo-inductible	LML précède la MOMP et l'apoptose des cellules M1-tp53.	Initiation	[138]
Staurosporine	Cathepsine D relâchée dans les lymphocytes T.	Initiation	[139]
Staurosporine	Cathepsine D induit la MOMP dans les fibroblastes.	Initiation	[140]

cathepsines relâchées après la LML, de la protéine pro-apoptotique de la famille des Bcl-2, Bid. Des expériences utilisant des extraits purifiés de lysosomes, ont montré qu'ils induisaient le clivage de Bid [84, 115, 118]. Les sites de clivage des cathepsines (arginine 65 ou arginine 71) sur la protéine Bid diffèrent du site de la caspase-8 (acide aspartique 59) et de la granzyme B (acide aspartique 75), bien qu'ils se situent dans la même région, soit dans la boucle entre les hélices-α 2 et 3 [115] (Figure 1, page 26). La forme tronquée de Bid, tBid, ainsi générée conserve tout de même son potentiel d'activer la MOMP, contribuant à l'activation de la voie mitochondriale [115]. À noter que la protéolyse de Bid est attribuable aux cathepsines à motifs cystéines, puisque le motif catalytique de la cathepsine à motif acide aspartique ne correspond pas au site de clivage de Bid [84] et que le pepstatin A, un inhibiteur spécifique à ce type de cathepsines, n'inhibe pas le clivage de Bid [118]. Par contre, certains auteurs envisageraient un mécanisme en deux étapes où la cathepsine D (acide aspartique) active la cathepsine B (cystéine), qui ensuite clive la protéine Bid [141].

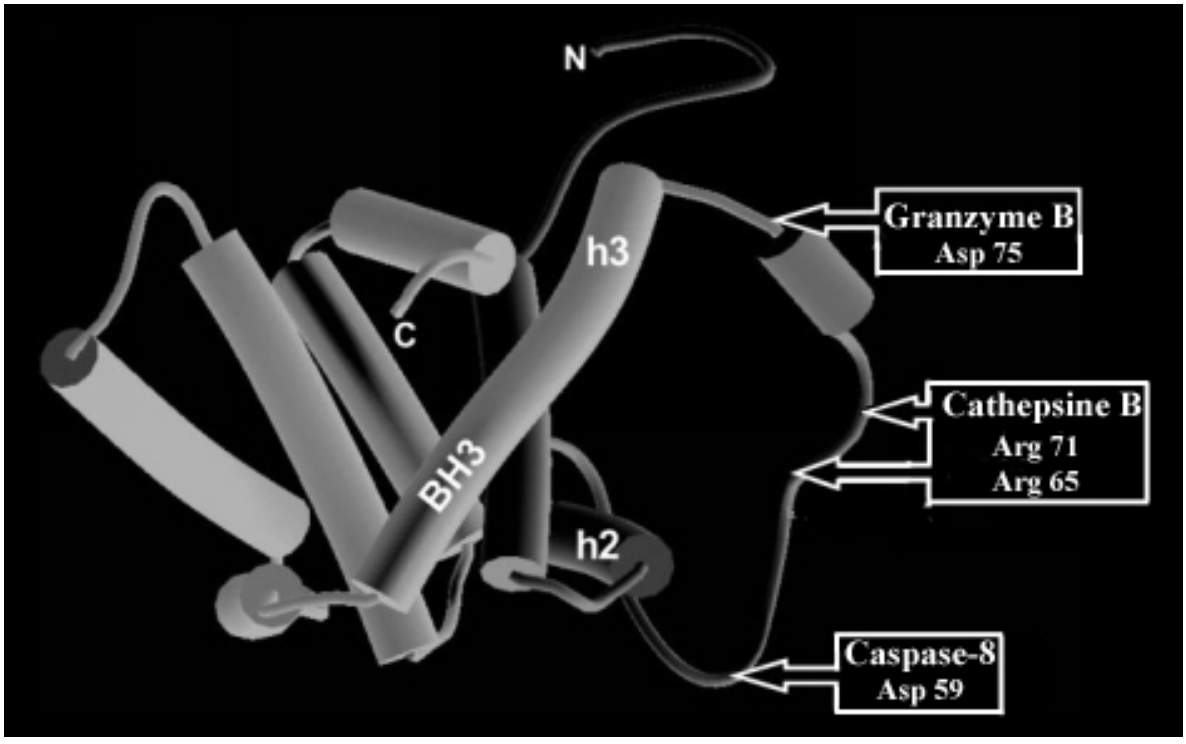

Figure 1 : Représentation schématisée de la protéine Bid. Les sites de protéolyse de la protéine ainsi que les protéases associées sont désignés. Les hélices-α 2 et 3 (h2 et h3) et le domaine BH3 sont indiqués. Figure modifiée de [84].

En dépit de l'indiscutable potentiel pro-apoptotique des cathepsines, de par leur nature à dégrader, peu de substrats hors des lysosomes leur sont connus. Pourtant, il est établi que les cathepsines peuvent, à elles seules, induire l'apoptose. Par exemple, la micro-injection cytosolique de cathepsine D active dans des fibroblastes [142] ou l'ajout de cathepsine B purifiée dans un système de cellules HeLa perméabilisées à la digitonine, induisent un phénotype apoptotique [143]. Les mécanismes moléculaires qu'emprunteraient les protéases lysosomales pour l'exécution de l'apoptose sont à élucider. L'étude des dégradomes, soit l'identification peptidique à haut débit de l'ensemble des produits de dégradation des protéases, est un champ de recherche prometteur (revu dans [144]).

L'implication des lysosomes au processus apoptotique d'une multitude de modèles expérimentaux a été rapportée ces vingt dernières années, et de nouvelles observations s'ajoutent à chaque jour. Il n'en demeure pas moins que les mécanismes par lesquels s'initient la LML sont peu nombreux et ne font toujours pas l'unanimité. Afin d'illustrer les différentes hypothèses avancées sur les causes probables de la LML, il est nécessaire d'aborder la membrane lysosomale et ses constituants principaux, les sphingolipides.

III- Les sphingolipides

La structure

Les sphingolipides constituent, avec les glycérophospholipides, la majeure partie des lipides dans les divers types de membranes des animaux. Le cœur des sphingolipides est formé d'une queue hydrophobe de sphingosine, un acide gras non-ramifié lié à un groupement amide qui constitue la tête polaire auquelle va s'ajouter différents groupements, afin de générer la diversité des sphingolipides. Par exemple, un groupement hydroxyle pour former un céramide ou une phosphocholine pour former une sphingomyéline (Figure 2, page 28). Les acides gras, constituant les sphingolipides les plus communément retrouvés dans la cellules eucaryotes, ont une longueur variant entre 16 et 24 carbones, la chaîne à 18 carbones étant généralement la plus représentée (revu dans [145]).

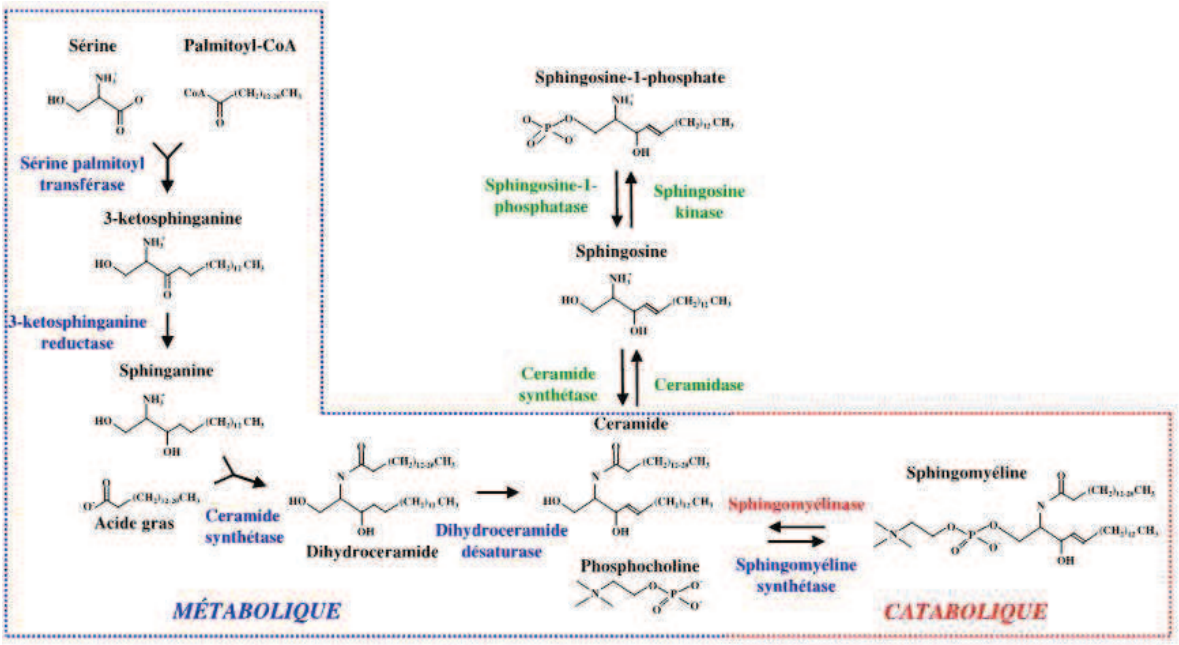

Figure 2 : Voies de biosynthèses des sphingolipides.

La biosynthèse

Les sphingolipides sont principalement issus de deux voies, l'une métabolique et l'autre catabolique (revu dans [146]) (Figure 2, page 28). La voie métabolique, ou *de novo*, requiert l'action coordonnée de la sérine palmitoyl transférase et la céramide synthétase pour former les céramides. La sérine palmitoyl transférase catalyse d'abord la condensation de sérine et de palmitoyl-CoA en 3-ketosphinganine qui est ensuite réduit en sphinganine et acylée par la céramide synthétase pour former le dihydrocéramide. Finalement, l'oxydation de la molécule permet l'introduction d'un lien insaturé en position C4-C5 pour former le céramide. La formation de sphingomyéline requiert l'action de la sphingomyéline synthase afin de condenser une phosphocholine et un céramide. Les sphingolipides issus de la voie *de novo* sont synthétisés à l'intérieur du réticulum endoplasmique et vont emprunter le transit endosomal pour rejoindre les diverses membranes de la cellule [147].

À l'inverse, la voie catabolique conduit à la dégradation de la sphingomyéline déjà existente par les sphingomyélinases. Il existe au moins cinq sphingomyélinases classées

selon le pH où l'enzyme est active, reflétant du coup leur localisation cellulaire et leur dépendance aux ions Zn^{2+} ou Mg^{2+}. Ainsi, on retrouve la sphingomyélinase acide (ASM) aux lysosomes, la sphingomyélinase acide dépendante du Zn^{2+} qui est une forme sécrétoire, la sphingomyélinase neutre dépendante du Mg^{2+} qui est associée à la membrane plasmique et à la mitochondrie, une sphingomyélinase neutre indépendante du Mg^{2+} et une sphingomyélinase alcaline dans le réticulum endoplasmique et l'appareil de Golgi (revu dans [148]). Enfin, les céramides générés par les sphingomyelinases pourront être dégradés et donner un ensemble d'autres sphingolipides (Figure 2, page 28). Les céramides seront phosphorylés par la céramide kinase pour former du céramide-1-phosphate. La ceramidase va, quant à elle dé-acyler les céramides pour donner des sphingosines. À leur tour, les sphingosines, par l'entremise de la sphingosine-1-phosphate lyase, pourront être dégradés en plusieurs types de glycérophospholipides.

La régulation du métabolisme des sphingolipides est cruciale pour l'organisme. Plusieurs pathologies sont associées à la déficience de certaines de ces enzymes, menant à l'accumulation des sphingolipides. Les lipoïdoses comprennent la maladie de Gaucher (glucocéramide), de Krabbe (cérébrosides), de Niemann Pick (sphingomyélines) et de Sandhoff (gangliosides) [149]. De plus, il semble exister un lien entre la perturbation du métabolisme des sphingolipides et la progression du cancer (revu dans [150]). Dans plusieurs types de cancers les niveaux des céramides, particulièrement des céramides à 18 carbones, sont réduits, tandis que la concentration en sphingosine-1-phosphate est augmentée, indiquant probablement un métabolisme des céramides plus élevé comparativement aux tissus normaux (revu dans [151])

Céramide et l'apoptose

L'idée que les fonctions des sphingolipides n'étaient pas restreintes à de simples constituants membranaires, est venue des travaux d'Okazaki qui démontraient que la liaison de la vitamine D à son récepteur induisait l'activation de l'ASM et la génération de céramides, une étape requise pour l'activation d'une voie de différenciation dans les cellules HL-60 [152]. Par la suite, les céramides, ainsi que d'autres sphingolipides ont été

identifiés comme des acteurs importants dans la signalisation de plusieurs processus cellulaires, incluant la prolifération cellulaire (revu dans [153]) et l'apoptose (revu dans [154]).

Les données issues de nombreux modèles cellulaires en présence de signaux de stress montrent que l'accumulation des céramides [155-159] ou des sphingosines [160-162] accompagne et même précède l'apparition des différentes manifestations biochimiques et morphologiques de l'apoptose, suggérant que les sphingolipides constituent des signaux inducteurs de l'apoptose. Ainsi, l'ajout exogène de sphingosines [163-165], de céramides [166-168], de sphingomyélinase [169] ou d'agents pharmacologiques qui perturbent le métabolisme des céramides [156, 170, 171], mime les effets de l'induction de l'apoptose. Les différents modèles génétiquement déficients quant à la génération des céramides (cellules Nieman-Pick, souris $ASM^{-/-}$ et souris $FAN^{-/-}$ (*factor associated with neutral sphingolyelinasease activation*)) ont démontrés la fonction pro-apoptotique des céramides [172-175]. Inversement, l'inhibition de l'expression de la sphingomyéline synthase 1 dans les cellules Jurkat, s'accompagne d'une accumulation du contenu cellulaire en céramides et rends les cellules plus sensibles à l'apoptose induite par les photo-dommages[176].

Il demeure toutefois incertain si ces effets sont totalement attribuables à l'augmentation des céramides ou à la diminution de sphingomyélines, puisqu'il a été montré que l'inhibition de l'expression des sphingomyélines synthase 1 et 2 réduisait l'apoptose induite par le LPS dans les cellules dérivées des macrophages THP-1 [177]. De plus, la surexpression stable de la sphingomyéline synthase 1 et 2 dans les cellules CHO, augmente le contenu en sphingomyéline et accroît la sensibilité à l'apoptose induite par le TNF-α [177]. Ces effets pro-apoptotiques pourraient être attribués à l'augmentation simultanée du contenu en céramides, vraisemblablement imputable à un métabolisme des sphingolipides plus élevé, puisque dans d'autres modèles, l'ajout exogène de sphingomyélines a un effet protecteur contre l'apoptose [178]. Alternativement, il est possible que cette divergence d'observations s'explique par un contexte cellulaire particulier aux stimuli apoptotiques. Enfin, l'apparition de nouveaux métabolites ne semble pas être en cause. Une étude s'est penchée sur l'importance des métabolites des céramides dans le processus apoptotique. Saumois et collègues ont montré que l'inhibition de la

glucosylcéramide synthase ou que l'inhibition de la ceramidase n'avait pas d'influence notable sur les paramètres apoptotiques, démontrant que les céramides étaient bien responsables de l'apoptose observée dans leur système [179].

Cibles moléculaires des céramides

Les céramides, comme signaux de stress, constituent un caractère conservé dans l'évolution que l'on retrouve, au moins, dès l'apparition des levures [180]. Plusieurs protéines impliquées dans des voies signalétiques sont des cibles directes des céramides, dont KSR (*kinase suppressor of RAS*) [181, 182], CAPP (*céramide-activated protein phosphatase*)[183], c-RAF-1 [184, 185], les petites protéines G RAS et RAC [186], la phospholipase A_2 [187], cathepsine D [188] et les PKC [189]. D'autres cibles, cette fois indirect, sont connues pour les céramides, incluant CRAC (*calcium release- activated calcium channel*) [190], les JNKs (*c-Jun N-terminal kinases*) qui signalent l'apoptose dans une diversité de cellules [191, 192], et Bad via une voie implicant RAS, KSR,c-RAF-1 et MEK-1 et l'inactivation d'AKT [193]. Enfin, les céramides pourraient aussi agir directement sur la chaîne respiratoire mitochondriale [194] et conduire à une surproduction de ROS toxiques pour la mitochondrie [195].

Alors que la plupart des partenaires directs aient été déterminés *in vitro*, les propriétés physiques des céramides les limitent cependant à une association stricte avec les membranes, ce qui laisse des doutes quant à la possibilité que de telles interactions aient lieu *in vivo*. Ainsi, il est difficile de considérer les céramides comme des seconds messagers, un terme s'appliquant mieux aux petites molécules qui peuvent diffuser dans la cellule. Plusieurs fonctions des céramides, cette fois liées à leur seule qualité de lipide neutre, sont d'ailleurs avancées.

Micro-domaines membranaires riches en céramides

La forme sécrétoire de l'ASM se retrouve à la face externe de la membrane plasmique où elle modifie sa composition [196]. Suivant la stimulation de Fas ou de CD40, à l'aide des ligands respectifs, la forme sécrétoire de l'ASM se retrouve à la face externe de la membrane plasmique et participe à l'activation des récepteurs et à leur signalisation [197, 198]. Il y aurait entre 40 et 70% de la sphingomyéline cellulaire qui serait contenue dans les rafts, des micro-domaines membranaires majoritairement composés de cholestérol et de glycosphingolipides formant des sortes d'îlots flottants sur les membranes [199]. La forme sécretoire d'ASM modifierait la composition des rafts, et l'augmentation du contenu en céramides permettrait une réorganisation des rafts en plateforme plus large, alors que les céramides forment un réseau entre eux via des liens de ponts hydrogènes et possiblement d'interactions de type van der Waal [200]. Ce type de plateforme favoriserait l'oligomérisation des récepteurs et la transmission inter-membranaire du signal [201]. Enfin, en facilitant le recrutement et la stabilisation de molécules intracellulaires à la face interne de la membrane plasmique, les plateformes de céramides réguleraient la signalisation de voies telles que PI3K-Akt-Bad dans un contexte apoptotique [202].

Régulation de la fluidité membranaire par les céramides

On attribue aussi aux micro-domaines de céramides un rôle dans le transport endosomal, en favorisant le bourgeonnement des membranes et la formation de vésicules lipidiques telles que les exosomes [203]. Les sphingomyélines forment des structures plutôt compactes dûes au fait que la tête hydrophile et les deux chaînes acyles sont de dimensions comparables. L'hydrolyse des sphingomyélines par les sphingomyélinases retire la phosphorylcholine de la tête polaire, modifiant la symétrie quant à son insertion dans la couche lipidique, la queue hydrophobe demeurant intacte. La structure dorénavant formée de céramides sera de forme conique (Figure 3, page 33). Ainsi, l'accumulation de cônes de céramides sur une des deux couches lipidiques va augmenter sa flexibilité en formant une courbure concave de la membrane du sens de l'accumulation (revu dans [204]). De plus,

l'accumulation de cônes de céramides va accroître la propension à former des phases hexagonales II dans la membrane, ce qui va favoriser la fusion des membranes entre elles (revu dans [205]).

Les sphingolipides sont des constituants dynamiques dont l'influence sur divers processus cellulaires, incluant l'apoptose, est certaine. Il existe d'ailleurs un lien entre les propriétés des sphingolipides et l'activation de la voie lysosomale.

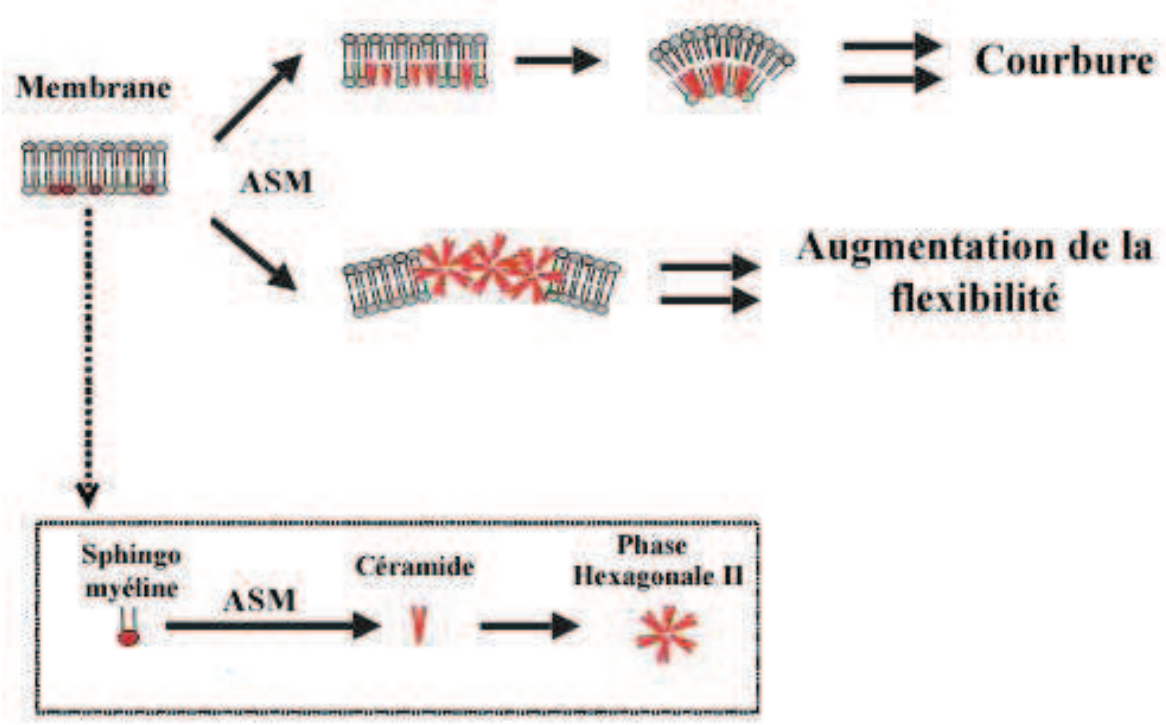

Figure 3 : Modifications membranaires par les sphingolipides. Figure modifiée de [204]

IV- Labilisation de la membrane lysosomale

Plusieurs mécanismes ont été avancés pour expliquer la déstabilisation membranaire et la LML lors du processus apoptotique. Parmi ceux-ci, il a été avancé que des protéines pouvaient transloquer à la membrane lysosomale pour induire ces changements, incluant la protéine Bax, LAPF et les phospholipases C et A_2. D'autres modèles reposent sur les propriétés physiques des sphingolipides qui composent la membrane lysosomale et la dynamique des changements accompagnant le processus apoptotique, dont la formation de canaux et la peroxydation.

La protéine Bax

Kagedal et collègues ont montré que la protéine pro-apoptotique de la famille des Bcl-2 , Bax, était activée et retrouvée insérée à la membrane de la mitochondrie et des lysosomes suivant l'induction de l'apoptose à l'aide de la staurosporine [206]. Outre la capacité de Bax à induire la MOMP et d'activer la voie mitochondriale, il semblerait que Bax pourrait aussi induire la voie lysosomale et la relâche de la cathepsine D. Ainsi, l'ajout de la protéine Bax recombinante à des extraits de lysosomes purifiées provoque la relâche des cathepsines [206]. La protéine Bax agirait en synergie avec les céramides pour favoriser la formation de canaux de céramides dans les membranes de phospholipides et permettre leur perméabilisation [207].

La protéine LAPF

Récemment, un rôle pour la protéine LAPF (*lysosome-associated and apoptosis-inducing protein containing PH and FYVE domains*) a été décrit dans l'activation de la voie lysosomale dans les cellules de fibrosarcome murin L929 exposées au TNF-α et dans les cellules de carcinome MCF-7 soumises à des radiations ionisantes [208]. Suivant l'induction de l'apoptose, la protéine LAPF interagit spécifiquement avec p53, lorsque

celle-ci est phosphorylée sur ses sérines 15 et 18. Ils migrent ensuite ensemble aux lysosomes où ils participent à l'activation de la LML [209], un effet qui semble indépendant de l'activité transcriptionnelle de la protéine p53. L'effet direct de p53 dans l'apoptose, en l'absence de sa capacité transcriptionnelle, a déjà été rapporté [210, 211]. De plus, p53 peut activer directement la procaspase-3 dans un système acellulaire [212], voire même complexer avec Bcl-xL et Bcl-2 à la membrane mitochondriale et induire sa perméabilisation [213]. Enfin, il a été montré que dans les cellule M1-t-p53, une lignée leucémique myéloïde transfectée avec un gène p53 thermo-inductible, p53 peut induire la voie lysosomale de manière précoce précédant la cascade apoptotique [138].

Déstabilisation osmotique

Les lysosomes sont des organelles particulièrement sensibles aux variations de tonicité du milieu cytosolique. L'activité de la phospholipase C, sous la régulation du Ca^{2+} cytosolique, augmente la perméabilité de la membrane des lysosomes dans un environnement hypotonique [214]. De plus l'augmentation importante du Ca^{2+} cytosolique rend la membrane lysosomale plus susceptible aux chocs osmotiques, permettant l'influx d'eau et l'augmentation de la taille des lysosomes allant jusqu'à leur rupture [214]. Il est intéressant de souligner que la relâche de Ca^{2+} accompagne les signaux de stress qui ciblent le réticulum endoplasmique, et qu'elle participe de manière générale à l'activation de l'apoptose (revu dans [215]).

Une autre phospholipase est aussi mise en cause dans la déstabilisation osmotique. L'activation de la phospholipase A_2, par micro-injection d'une forme active ou par l'utilisation d'un agoniste, induit la LML et l'apoptose [216]. La déstabilisation de la membrane lysosomale serait le résultat d'une perméabilité accrue aux échanges ioniques [217]. Le lysophosphatidylcholine, un sphingolipide issu de la dégradation de la phosphatidylcholine par la phospholipase A_2, participerait à l'augmentation de la perméabilité membranaire et à l'influx lysosomal du potassium [218].

Les canaux de sphingolipides

Les récents travaux de Siskind ont porté sur la capacité qu'ont les sphingolipides à former des canaux au niveau des membranes lipidiques où ils s'accumulent, les rendant ainsi perméables. Les canaux constitués par les sphingosines apparaissent et disparaissent rapidement, et sont d'une taille d'environ 2 nm de diamètre [219], tandis que les canaux composés de céramides se forment progressivement pour atteindre un diamètre maximal de 10 nm [220]. Les céramides sont liés entre-eux par des ponts hydrogène formés sur leur groupement amine pour créer des cylindres stables permettant le passage de molécules ayant jusqu'à 60 kDa de taille (Figure 4, page 36). Le groupement ammonium libre des sphingosines ne permet pas de former des canaux de structures comparables, ce qui expliquerait l'instabilité des canaux-sphingosines [219]. Enfin, il semble que le double lien en position 4, 5 soit aussi requis à la formation des canaux-céramides puisque l'ajout de dihydrocéramides, des céramides dont l'acide gras est saturé, à des liposomes, inhibe la perméabilisation induite par des céramides [221].

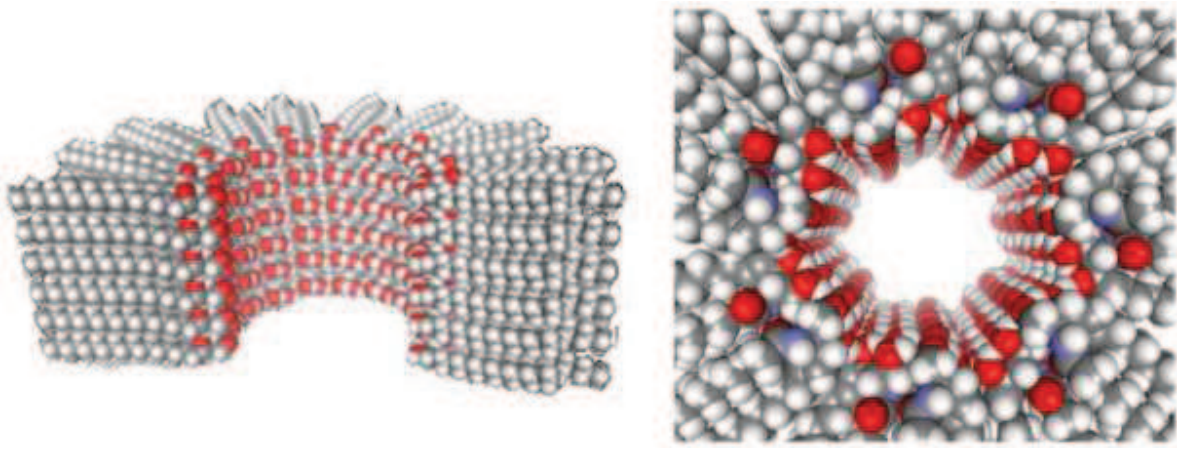

Figure 4 : Modèle structural des canaux-céramides. La vue en coupe tranversale (à gauche) et la vue de haut (à droite) montre un canal-céramide composé de 12 colonnes de molécules de céramide. Les atomes d'hydrogène, responsable des interactions entre les molécules de céramide sont représentés en rouge. Figure modifiée de [222].

Puisque l'accumulation de céramides durant la phase d'initiation de l'apoptose s'observe dans de nombreux modèles, l'importance des canaux formés de phospholipides pourrait être considérable lors de la libération cytosolique de molécules pro-apoptotiques. À l'aide de mitochondries isolées, il a été montré que les canaux-céramides permettaient le passage de l'espace inter-membranaire au cytosol de certaines molécules pro-apoptotiques associées à l'activation de la voie mitochondriale, soit le cytochrome c (12 kDa), l'endonuclease G (28 kDa), AIF (57 kDa) et Smac/DIABLO (42 kDa)[223].

La peroxydation

Le stress oxydatif cellulaire résulte de la surcharge des molécules antioxydantes par les pro-oxidants, et aura pour conséquence d'altérer structuralement les biomolécules telles que les acides nucléiques, les protéines, les carbohydrates et les lipides. Le stress oxydatif est au centre de plusieurs événements cellulaires dont la prolifération, la réponse immunitaire, la nécrose et l'apoptose (revu dans [224]). L'implication du stress oxydatif dans le processus apoptotique est basée sur l'utilisation d'antioxydants, particulièrement d'antioxydants lipidiques, qui ont pour effets de protéger les mitochondries [225] et les lysosomes [97]. Possiblement plus apte à empêcher l'oxydation des lipides, de par sa nature lipophile, le α-tocophérol, préviendrait la peroxydation des lipides membranaires et stabiliserait les membranes (revu dans [226]).

Sur les phospholipides, le stress oxydatif cause des réactions de peroxydation en trois étapes (Figure 5, page 38). La réaction initiale entre un radical hydroxyl (HO·) et un phospholipide va engendrer un radical lipidique (L·) (1) qui a son tour réagira avec une molécule d'O_2 pour former un radical lipide peroxyl (LOO·) (2). Ce dernier, en présence d'un autre acide gras (LH), va générer un lipide hydroperoxyde (LOOH) et un second radical lipidique (L·) (3) qui à son tour reformera un radical lipide peroxyl (LOO·) (2). Le lipide hydroperoxyde (LOOH) quant à lui pourra être clivé par des métaux réducteurs tels que le Fe^{2+} pour produire un radical lipide alkoxyl (LO·) (4). Les radicaux lipide alkoxyl (LO·) et lipide peroxyl (LOO·) stimuleront enfin une réaction de peroxydation des lipides

environnants. Une telle réaction en chaîne des lipides au sein d'une membrane perturbera sa fluidité et sa perméabilité (revu dans [227]). La peroxydation des lipides de la membrane mitochondriale a déjà été mise en cause dans l'activation de la MOMP [228]. Le lien insaturé des sphingolipides les rend d'autant plus vulnérable qu'on les retrouve dans l'environnement acide des lysosomes où le Fe^{2+} est abondant.

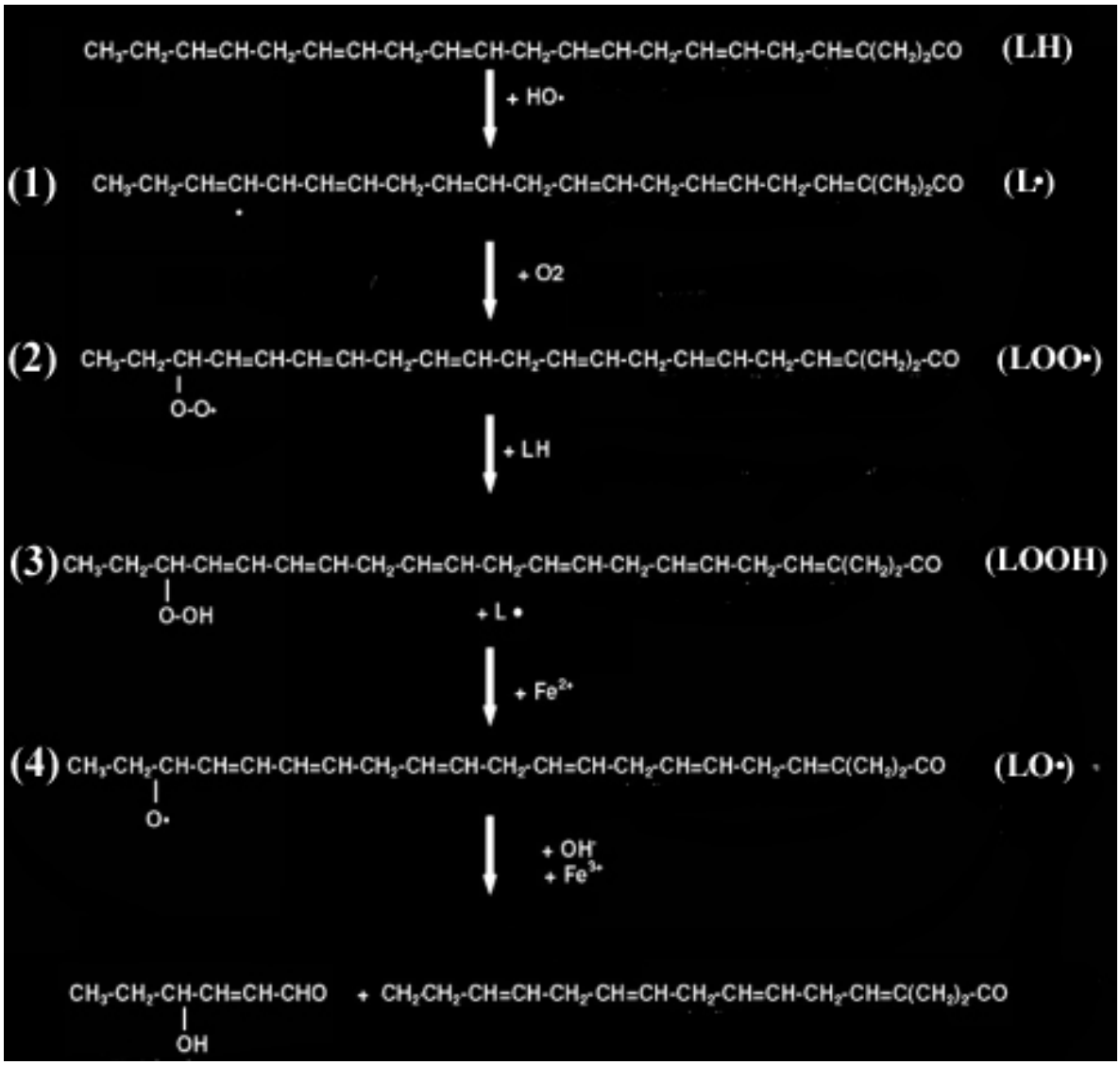

Figure 5 : Réactions de peroxydation des lipides. Un acide docosahexaenoïque (22:6) est représenté. Figure modifiée de [226].

Pertinence du projet

Selon l'Organisation Mondiale de la Santé, il y aurait eu en 2004 près de 7,4 millions de décès liés au cancer, soit 13% de la mortalité mondiale. Les prévisions ne sont guère encourageantes et l'incidence devrait augmenter pour atteindre 12 millions de décès d'ici 2030 [229]. Bien que l'efficacité des traitements se soit accrue avec le temps, il n'en demeure pas moins que l'attention de la communauté médicale, de même que celle des grandes pharmaceutiques, est tournée vers la recherche de nouvelles cibles thérapeutiques pour le traitement du cancer. L'intérêt pour les voies d'initiation de l'apoptose est donc considérable.

Les voies d'initiation de l'apoptose les mieux décrites sont sans doutes les voies mitochondriales et des récepteurs de mort. La connaissance grandissante de ces voies de signalisation a permit la conception de stratégies nouvelles pour lutter plus efficacement contre les tumeurs malignes. Plusieurs molécules ont ainsi été conçues afin d'interférer dans les interactions entre certaines protéines de la familles des Bcl-2, aux fonctions anti-apoptotiques à la mitochondrie, et dont l'expression augmente durant la tumorigénèse (revu dans [230]). Similairement, les récepteurs de mort sont considérés comme des cibles potentielles, et différentes approches sont actuellement en essais cliniques (revu dans [231]).

Le compartiment lysosomal constitue une cible prometteuse. D'une part, la progression métastasiques de cellules du cancer du sein s'accompagne d'une augmentation de la taille des lysosomes [232]. D'une autre part, la cathepsine D constitue un marqueur pronostique défavorable pour certaines tumeurs dont celles du cancer du sein [138, 233]. Ces différences entre certains tissus normaux et cancéreux offrent une fenêtre thérapeutique intéressante, puisque la taille d'un lysosome est directement liée à sa susceptibilité à la rupture, et l'activation des cathepsines dans le cytosol conduit à différentes formes de mort cellulaire. Il a d'ailleurs été observé que l'immortalisation spontanée de fibroblastes embryonnaires murins (MEF) amplifiait de près de mille fois leur sensibilité à l'apoptose

induite par la voie lysosomale via le TNF-α, comparativement aux MEF sauvages [234]. Enfin, la tumorigénèse s'accompagne d'une acidification intra-lysosomale et pourrait, en partie, engendrer le développement de résistances à la chimiothérapie [235]. Il a été proposé que les agents chimiothérapeutiques, souvent des acides faibles prédisposés à la protonation, étaient séquestrés dans un environnement acide, tel que celui retrouvé dans les lysosomes, diminuant du coup la concentration cytosolique de ces molécules [236].

Parmi les approches thérapeutiques envisagées, la combinaison de molécules ciblant spécifiquement les lysosomes pour les déstabiliser et d'agents chimiothérapeutiques déjà utilisés, permettrait de contrer le phénomène de résistance.

Ainsi, l'utilisation combinée de siramesine, un ligand des récepteurs de type sigma-2, connu pour induire la LML, et d'agents déstabilisateurs du réseau de microtubules, incluant la vincristine et son analogue la vinorelbine, permet de détruire massivement par apoptose des cellules MCF-7 résistantes à ces derniers, et ce à des doses de siramesine tolérée par les cellules [126]. La toxicité neuronale étant la principale contrainte à l'utilisation de la vincristine [237], l'approche combinée permettrait de réduire la toxicité tout en conservant une activité anti-tumorale adéquate.

Les quinolones, une famille d'antibactériens de synthèse couramment utilisée dans la prophylaxie et le traitement de diverses infections, sont lysosomotropes. La structure des quinolones favorise leur accumulation dans les lysosomes où ils agiraient possiblement à la manière de détergents ou, pourraient causer des photo-dommages localement sur la membrane lysosomale. Certains auteurs ont même proposé que les effets indésirables associés aux quinolones, en particulier une médication au norfloxacin et l'exposition au soleil, pourraient être utilisés en chimiothérapie [238]. Par exemple, la combinaison de quinolones, ciprofloxacin et norfloxacin, et de rayons ultra-violets induit l'apoptose via l'activation de la voie lysosomale [116]. De plus, il a été montré qu'un traitement au ciprofloxacin, à des doses n'induisant pas d'effets toxiques notables, augmentait la sensibilité des cellules de cancer de la prostate hormono-résistantes, aux effets antiprolifératifs de l'étoposide, un agent génotoxique utilisé en chimiothérapie [239]. Similairement, le clioquinol est une molécule qui possède des propriétés anticancéreuses

démontrées *in vitro* et *in vivo* [240]. Combiné avec le chlorure de zinc, le clioquinol induit l'apoptose via l'accumulation de Zn^{2+} intra-lysosomale et la LML [133]. Enfin, la chloroquinine déstabilise les lysosomes et sensibilise des cellules de cancer du sein aux radiations ionisantes [241].

Ces observations expérimentales illustrent le potentiel du compartiment lysosomale pour lutter contre le cancer. Les résultats obtenus dans le laboratoire procurent une meilleure compréhension des mécanismes moléculaires responsables de l'activation de la voie lysosomale durant l'apoptose induite à l'aide de la camptothecin, un agent chimiothérapeutique. Ils fournissent des pistes nouvelles dans l'élaboration de cibles thérapeutiques qui pourront éventuellement être évaluées pour le traitement du cancer.

Hypothèses et objectifs de l'étude

Hypothèses

1. À l'instar de l'activation de la voie mitochondriale, des facteurs protéiques migrent vers les lysosomes et provoquent la labilisation de la membrane lysosomale durant la phase précoce de l'apoptose.

2. La labilisation de la membrane lysosomale est dépendante de l'altération de la composition en sphingolipides observée durant l'apoptose.

Objectif principal du projet de doctorat

L'étude des mécanismes responsables de l'induction de la voie lysosomale de l'apoptose de cellules cancéreuses exposées à des agents chimiothérapeutiques.

Objectifs spécifiques

1-a. Identification, à partir du protéome de lysosomes purifiés de cellules, des protéines dont le profil d'expression est modifié durant la phase précoce de l'apoptose induite par des dommages à l'ADN.

1-b. Validation fonctionnelle des protéines identifiées dans l'objectif spécifique 1-a quant à leur participation à la labilisation de la membrane lysosomale.

2-a. Mesure du contenu en sphingolipides des membranes de lysosomes purifiés de cellules apoptotiques.

2-b. Évaluation de l'impact de l'inhibition des voies de biosynthèse des sphingolipides sur la labilisation de la membrane lysosomale.

Proteomic analysis of enriched lysosomes at early phase of camptothecin-induced apoptosis in human U-937 cells

Nicolas Parent[1], Eric Winstall[2], Myriam Beauchemin[1], Claudie Paquet[1], Guy G. Poirier[2] and Richard Bertrand[1,3,4]

Affiliations des auteurs:

[1]Centre de recherche du Centre hospitalier de l'Université de Montréal (CHUM) - Hôpital Notre Dame et Institut du Cancer de Montréal, Montréal (Qc) H2L 4M1, Canada,

[2]Centre de recherche du Centre hospitalier de l'Université Laval (CHUQ), Québec (Qc) G1V 4G2, Canada et

[3]Département de Médecine, Université de Montréal, Montréal (Qc) H3C 3J7, Canada.

Article publié dans:

Journal of Proteomics (2009); volume 72, pages 960 à 973

Contribution des co-auteurs :

Nicolas Parent : expérimentateur principal, hypothèse et approches développées en collaboration avec Richard Bertrand; article co-rédigé avec Richard Bertrand

Éric Winstall : analyse iTRAQ

Myriam Beauchemin : microscopie sur les figures 2d) et 4

Claudie Paquet : figure 1c)

Richard Bertrand : instigateur principal

Proteomic analysis of enriched lysosomes at early phase of camptothecin-induced apoptosis in human U-937 cells

Nicolas Parent[1], Eric Winstall[2], Myriam Beauchemin[1], Claudie Paquet[1], Guy G. Poirier[2] and Richard Bertrand[1,3,4]

[1]Centre de recherche, Centre hospitalier de l'Université of Montréal (CHUM), Hôpital Notre- Dame and Institut du cancer de Montréal, Montréal (QC) H2L 4M1, Canada,
[2]Centre de recherche, Centre hospitalier de l'Université Laval (CHUL), Québec (QC) G1V 4G2, Canada, and
[3]Département de médecine, Université de Montréal, Montréal (QC) H3C 3J7, Canada.

Running title: Lysosomal pathway of CPT-induced apoptosis
Key words: Apoptosis / Camptothecin / Lysosome / iTRAQ reagent / LC-ESI-MS/MS / Confocal Microscopy

[4]**Correspondence to**: Richard Bertrand, CRCHUM, Hôpital Notre-Dame and Institut du cancer de Montréal, 1560 Sherbrooke St. East (Room Y-5634), Montreal (QC) H2L 4M1, Canada
Phone: (1-514) 890 8000 ext 26615; Fax: (1-514) 412 7591;

Abbreviations: Ac-DEVD-AMC: acetyl-Asp-Glu-Val-Asp-7-amino-4-methylcoumarin; AO: acridine orange; BH: Bcl-2 homology; CPT: 20-S-camptothecin lactone; EF: error factor; ER: endoplasmic reticulum; FC: fold change; iTRAQ: isobaric tag for relative and absolute quantitation; Ig: immunoglobulin; JC-1: 5,5',6,6'-tetrachloro-1,1',3,3'-tetraethylbenzimidazolyl-carbocyanide iodide; MMTS: methylmethane-thiosulfonate; NSDHL: sterol-4-alpha-carboxylate 3-dehydrogenase; PI: propidium iodide; PKC-δ: protein kinase C delta; PSAP: prosaposin; RCA: relative colocalization area; SD: standard deviation; SE: standard error; Z-RR-AMC: benzyloxycarbonyl-Arg-Arg-7-amino-4-methylcoumarin; 1-D/IEF: one-dimensional isoelectric focusing; ↓ΔΨm: loss of mitochondrial transmembrane potential.

ABSTRACT

A lysosomal pathway, characterized by partial rupture or labilization of lysosomal membranes and cathepsin activation, is evoked during camptothecin-induced apoptosis in human cancer cells, including human histiocytic lymphoma U-937 cells. These lysosomal events begin rapidly and simultaneously with mitochondrial permeabilization and caspase activation within 3 h after drug treatment. In this study, comparative and quantitative proteome analyses were performed to identify early changes in lysosomal protein expression/localization from U-937 cells undergoing apoptosis. In 2 independent experiments, among a total of more than 538 proteins putatively identified and quantitated by iTRAQ isobaric labeling and LC-ESI-MS/MS, 18 proteins were found to be upregulated and 9 downregulated in lysosomes purified from early apoptotic compared to control cells. Protein expression was validated by Western blotting on enriched lysosome fractions, and protein localization confirmed by fluorescence confocal microscopy of representative protein candidates, whose functions are associated with lysosomal membrane fluidity and dynamics. These include sterol-4-alpha-carboxylate 3-dehydrogenase (NSDHL), prosaposin (PSAP) and protein kinase C delta (PKC-δ). This comparative proteome analysis provides the basis for novel hypothesis and rationale functional experimentation, where the 3 validated candidate proteins are associated with lysosomal membrane fluidity and dynamics, particularly cholesterol, sphingolipid and glycosphingolipid metabolism.

INTRODUCTION

The lysosomal pathway of apoptosis involves moderate rupture of lysosomes, often referred to as small-scale lysosomal rupture or lysosomal labilization, and subsequent release of lysosomal cathepsins into the cytosol [1-4]. Lysosomal rupture and cathepsin activation have been linked to apoptosis after various insults, including oxidative stress [5], lysosomotropic photo sensitizer agents [6, 7], serum withdrawal [5], Fas and tumor necrosis factor-alpha (TNF-α) ligation [5, 8], increased sphingosine [9] and endogenous ceramide levels [10], DNA-damaging [11, 12] and microtubule-stabilizing agents [13]. During 20-S-camptothecin (CPT)-induced apoptosis in U-937 and Namalwa cancer cells, lysosomal labilization and cathepsin B activation occur rapidly and simultaneously with mitochondrial permeabilization and caspase activation, effects prevented by Bcl-xL, indicating that lysosomal rupture may be related, in part, to mitochondrial disruption [12].

Alterations of mitochondrial functions, such as mitochondrial permeability transition, transmembrane potential disruption, ATP/ADP exchange and cytochrome c release, are early events involved in the initiation step of apoptosis induced by most chemotherapeutic agents [14-20]. Members of the Bcl-2 family of proteins are critical regulators of the mitochondrial pathway of apoptosis that either promote cell survival (e.g. Bcl-2, Bcl-xL, Bcl-w, Mcl-1) or facilitate cell death. The pro-cell death members are subdivided into 2 classes: multidomain proteins that contain Bcl-2 homology (BH) domains 1-3 (e.g. Bax, Bak), and BH3-only proteins constituted of a unique BH3 motif (e.g. Bad, Bid, Bik, Bim, Puma, Noxa, Hkr) [21, 22]. Relative amounts and localization of death agonists and antagonists greatly influence the cell's ability to undergo apoptosis. Because it provides binding ability, the BH3 motif has become a potent mediator of cell death and is

often uniquely required for cell-killing activity [23, 24]. Two distinct models have been proposed to explain the killing activity of BH3-only proteins [22]. The *direct activation model* proposes that after a death stimulus, BH3-only proteins promote apoptosis by binding to and inhibiting pro-survival Bcl-2 family members, or by binding to other death agonists, like multidomain Bax and Bak proteins, which become activated and exert their pro-apoptotic activities at the mitochondrial level. BH3-only proteins that neutralize pro-survival proteins are referred to as BH3 "enabler or sensitizing" proteins, while those that bind pro-apoptotic Bax or Bak are called BH3 "activator or activating" proteins [25-27]. The *indirect activation model* suggests that all BH3-only proteins solely engage pro-survival proteins and act by preventing them from inhibiting Bax or Bak activation [28-30].

In contrast, the exact mechanisms that influence lysosomal membrane stability during apoptosis induced by DNA-damaging agents are, yet, not resolved. The best-studied models have associated lysosomal membrane rupture with oxidative stress, accumulation of redox-active iron and the occurrence of a lipid peroxidative chain reaction (for review see [4]). It has also been reported that sphingosine, a metabolite of the sphingomyelin and ceramide pathway, and lysophosphatidylcholine, a phospholipase A2-produced lipid metabolite, are capable of eliciting relatively selective damage to the lysosomal membrane, provoking lysosomal rupture [9, 31]. Although the exact mechanisms behind the relative activity of sphingosine and lysophosphatidylcholine for lysosome destabilization have not been fully clarified, it has been proposed that sphingosine is a lysosomotropic detergent because its long hydrophobic tail and polar head contain a proton-trapping group that is attracted by the acidic lysosomal vacuolar compartment [9], while lysophosphatidylcholine changes lysosomal osmotic sensitivity provoking entry of potassium ions leading to losses of membrane and lysosomal integrity [31]. Only a few proteins have been associated with

lysosome labilization during apoptosis. First, cytosolic phospholipase A2 was proposed to attack the lysosomal membrane, provoking its destabilization [32]. Other studies have suggested that phospholipase A2 and C could osmotically destabilize the lysosome membrane via a K(+)/H(+) exchange process [33-36], effects associated with lysophosphatidylcholine [31]. More recently, the accumulation of lysosome-associated apoptosis-inducing protein containing pleckstrin homology and FYVE domains (LAPF) on lysosomal membranes was also linked with lysosomal rupture and activation of a lysosomal-mitochondrial pathway of apoptosis [37].

In this study, to identify proteins putatively associated with lysosome labilization in the early phase of apoptosis induced by DNA-damaging agents, comparative and quantitative proteomic analyses of enriched lysosomes were performed in CPT-induced apoptosis of human histiocytic lymphoma U-937 cells. A significant proportion of the proteins putatively quantitated and identified by iTRAQ reagent labeling and LC-ESI-MS/MS play a role in membrane dynamics and fluidity, vesicle trafficking, redox regulation, cellular stress response and signaling pathways. In 2 independent experiments, 2 proteins were reproducibly found to be upregulated (>1.5) and 2 downregulated (<0.75) in lysosomes purified from early apoptotic compared to control cells. Considering the dynamic nature of small membrane-bound organelles and the restrictive and limiting criteria of the study consisting of experiments performed at very early phase of apoptosis when approximately less than 10% of the lysosome population presents partial membrane disruption or labilization, 16 candidate proteins found to be upregulated , and 7 downregulated, in 1 experiment only, were also considered. Finally, a rationale approach for validation of representative candidate protein was taken, based on the fundamental

biological question addressed in this study, which is related to biomembrane fluidity and dynamics.

MATERIALS AND METHODS

Cell line, chemicals and drug treatment. Human histiocytic lymphoma U-937 cells obtained from the American Type Culture Collection (Manassas, VA), were grown in suspension at 37°C under 5% CO_2 in RPMI-1640 medium supplemented with 10% heat-inactivated fetal bovine serum, 2 mM glutamine, 100 U/ml penicillin and 100 μg/ml streptomycin (Gibco-BRL Life Technologies, Grand Island, NY). CPT, Histodenz™, Hoechst 33342 and propidium iodide (PI) were obtained from the Sigma-Aldrich Company (St. Louis, MO). Percoll™ was purchased from GE Healthcare Bio-Sciences AB (Uppsala, Sweden). Acridine orange (AO), 5,5',6,6'-tetrachloro-1,1',3,3'-tetraethylbenzimidazolyl-carbocyanideiodide (JC-1), LysoTracker RED/DND-99, MitoTracker Green/FM and ER-Tracker Red dye were purchased from Molecular Probes (Eugene, OR). The fluorogenic peptide derivatives acetyl-Asp-Glu-Val-Asp-7-amino-4-methylcoumarin (Ac-DEVD-AMC) and benzyloxycarbonyl-Arg-Arg-7-amino-4-methylcoumarin (Z-RR-AMC) were acquired from Calbiochem-Novobiochem Corporation (San Diego, CA). All other chemicals were of reagent grade and purchased either from the Sigma-Aldrich Company, ICN BioMedicals (Costa Mesa, CA) or other local sources. For drug treatment, U-937 cells were treated with CPT at a concentration of 1.0 μM for 30 min, and then grown in drug-free medium.

Loss of mitochondrial transmembrane potential (↓$\Delta\Psi$m) and lysosomal rupture. ↓$\Delta\Psi$m was assessed by JC-1 staining [12, 38]. At the indicated times (h) after CPT treatment, 1 x 10^6 cells were incubated with 10 μg/ml JC-1 in complete culture medium for 15 min at

room temperature, washed twice, resuspended in 500 μl of PBS and submitted to flow cytometry analysis. To assess lysosomal rupture, at various times after drug treatment, 1 x 10^6 cells were incubated with 1 μM AO in complete culture medium for 15 min at 37°C; then, the cells were washed twice and resuspended in 500 μl of fresh culture medium before analysis by flow cytometry (uptake method) [5, 12]. Loss of JC-1 orange fluorescence was measured with the FL2 channel, loss of lysosomal AO red fluorescence with the FL3 channel, and increased cytosolic AO green fluorescence with the FL1 channel of a Coulter EPICS XL-MLC Flow Cytometer. At least 10,000 cells per sample were acquired in histograms, and the results are expressed as the percentage of total cells presenting $\downarrow\Delta\Psi m$ or lysosomal rupture.

Analysis of DNA fragmentation. The kinetics of DNA fragmentation were monitored and quantitated by DNA filter elution assays, and the results expressed as percentages of DNA fragmentation [39]. DNA content was also measured by flow cytometry after PI staining with recording on the FL2 channel of the Coulter EPICS XL-MLC Flow Cytometer. The results are expressed as percentages of cells presenting hypoploid DNA content (sub-G1 peak).

Enzymatic assays. For the measurement of enzyme activities, cellular extracts were prepared in lysis buffer containing 100 mM Hepes (pH 7.5), 5 mM EDTA, 5 mM DTT, 20% (v/v) glycerol and 0.3% (v/v) Igepal. Protein aliquots (100 μg) were incubated with 200 μM of the caspase-3-like substrate Ac-DEVD-AMC or with 20 μM of the cathepsin B substrate Z-RR-AMC, in reaction assay mixtures (500 μl) containing 100 mM Hepes (pH 7.5), 100 mM NaCl, 10% glycerol, 0.1% (w/v) CHAPS, 10 mM DTT and 1 mM EDTA for caspase-3-like activity, and 0.4 mM sodium acetate buffer (pH 5.5) and 4 mM EDTA for cathepsin B activity. Enzymatic activities were determined as initial velocities at 37°C in a

dual luminescence fluorometer at an excitation wavelength of 380 nm and an emission wavelength of 460 nm, and expressed as relative intensity/min/mg.

Subcellular fractionation. A 2-step sequential density gradient centrifugation protocol was modified from Storrie and Madden [40] and Paquet et al. [41] for lysosome isolation. A schematic representation of the procedure is illustrated in Supplemental Figure 1. First, control and CPT-treated U-937 cells (5.0×10^8) were swelled in deionized water for 4 min on ice, and the samples adjusted to 220 mM mannitol, 70 mM sucrose, 10 mM Hepes-KOH (pH 7.4) and 1.0 mM EDTA (isotonic buffer). The cells were then disrupted by passing the samples 30-fold through a 26G3/8 needle, and subsequently centrifuged at 1,000 x g for 15 min to pellet unbroken cells and nuclei. Supernatants containing mitochondria, lysosomes and other vesicles were adjusted to 8 mM calcium chloride and centrifuged at 5,000 g for 15 min to pellet the rough endoplasmic reticulum and mitochondria. Then, the supernatants were layered on top of the first gradient consisting, from bottom to top, of 2 ml of 35% (w/v) Histodenz™, 2 ml of 17% (w/v) Histodenz™, and 5 ml of 6% (v/v) Percoll™ in isotonic buffer. After centrifugation at 50,500 x g for 1 h at 4°C, a set of 2 discrete bands appears at the interfaces of 17/35% Histodenz™ and 6% Percoll™/17% Histodenz™. The upper band, at the 6% Percoll™/17% Histodenz™ interface, contained small mitochondria and lysosomes that needed further separation by the second gradient to obtain pure organelle fractions. This interface was collected and adjusted to 35% Histodenz™ by mixing with a 80% (w/v) Histodenz™ solution. The sample was then placed at the bottom of the second gradient and overlaid with 2 ml of 17% Histodenz™ and 5 ml of 5% Histodenz™. The tube was filled to the top with isotonic buffer, and centrifuged at 50,500 x g for 1 h at 4°C. Two distinct bands appeared: the upper one at the 5/17% Histodenz™ interface contains lysosomes, while the lower one, at the 17/35% Histodenz™ interface,

contained small mitochondria. To pellet the lysosomes, the interface was diluted with the largest possible volume of isotonic buffer and centrifuged at 53,000 x g for 1 h at 4°C.

Protein digestion and iTRAQ labeling. Relative quantification experiments were performed in duplicate in distinct lysosome preparations. Protein aliquots of lysosomes isolated from normal or apoptotic cells were acetone-precipitated. Each protein pellet was then solubilized in 0.5 M triethylammonium bicarbonate, pH 8.5, supplemented with 0.1% (w/v) SDS. Twenty-five and 80 µg of proteins were used for iTRAQ labeling in the first and second experiment, respectively. Protein cysteine residues were reduced with 5 mM Tris (2-Carboxyethyl) phosphine for 1 h at 60°C and then blocked with 8 mM methyl methane-thiosulfonate (MMTS) for 10 min at room temperature. Protein samples were digested with 5 µg of modified porcine trypsin in the presence of 10 mM $CaCl_2$ for 18 h at 37°C. The final SDS concentration at this point was 0.05% (w/v). The efficiency of protein digestion was assessed by SDS-polyacrylamide gel electrophoresis in undigested and digested aliquots of proteins. In both experiments, tryptic peptides from normal cell lysosomes and apoptotic cell lysosomes were labeled with iTRAQ 114 and iTRAQ 117 reagents, respectively, according to the manufacturer's protocol (Applied Biosystems, Foster City, CA). Labeled samples were then combined and dried in a vacuum concentrator.

Isoelectric focusing of iTRAQ-labeled peptides. Lyophilized iTRAQ-labeled peptides were resuspended in 325 µL of Milli-Q water containing 0.25% (v/v) ampholyte (Bio-Lyte 3/10 Ampholyte, Bio-Rad, Hercules, CA). The resulting solution served to rehydrate an 18-cm IPG gel strip (pH 5 to 8) from Bio-Rad, for 10 h. Conditions for isoelectric focusing of peptides were as follows: 250 V for 15 min, 10,000 V for 3 h, 10,000 V for 60,000 V•h and then at 50 V until the peptides were extracted. Excess overlaying oil was gently blotted

away from the IPG strip, which was cut into 36 pieces of 5 mm each. The IPG strip pieces were transferred to a 96-well plate, and peptides were eluted from the gel pieces by 2 successive extractions (15 min each with shaking) that were subsequently pooled. The first extraction was in 100 µL of a 1% formic acid, 2% acetonitrile solution, and the second extraction was in 100 µL of a 1% formic acid, 50% acetonitrile solution. The extracted peptides were then dried in a vacuum concentrator and resuspended in 25 µL of a 0.1% formic acid solution.

MS of iTRAQ-labeled peptides. For each analysis, 5 µL of the peptide solution was injected into the nano LC-ESI-MS/MS system. MS analyses were performed in a QStar XL Hybrid ESI quadrupole time of flight tandem mass spectrometer (Applied Biosystems/MDS Sciex) interfaced with an integrated online capillary LC system consisting of an autosampler, switching pump, and micro-pump (LC Packings, Sunnyvale CA). Peptides were first trapped and concentrated on a 300-µm i.d. x 5-mm C18 reverse-phase pre-column (LC Packings) at a flow rate of 15 µL/min. The peptide mixture was then separated on a 75-µm i.d. x 10-cm BioBasic (New Objective Inc., Woburn, MA) C18 reverse-phase capillary column at a flow rate of 200 nL/min. The gradient started at 98% buffer A (0.1% formic acid in water) and 2% buffer B (0.1% formic acid in acetonitrile) for 5 min, followed by an increase from 2% to 25% in buffer B over 85 min, then from 25% to 40% buffer B over 10 min, and 40% to 80% buffer B over 5 min. The column was washed with 80% buffer B for 5 min and equilibrated at 2% buffer B for 20 min. Eluted peptides were electrosprayed through a distal-coated silica tip (15 µm i.d.) (New Objective Inc.) with an ion spray voltage of 2,800 V. Data acquisition on the mass spectrometer was in the positive ion mode within a mass range of 400 to 1,600 m/z for precursor ions for a 1- sec period. Information-dependent acquisition of the MS/MS data was performed on the 3 most

abundant peptides exceeding 15 counts with +2 to +4 charge states within a 100 to 2,000 m/z value window. Time summation of the MS/MS events was set to 3 sec. Fragmented target ions were dynamically excluded for 60 sec with 100 ppm mass tolerance.

Data analysis. For iTRAQ, raw data file (.wiff) processing, protein identification, protein quantification, and statistical analyses were undertaken with ProteinPilot v.2.0 software (Applied Biosystems, MDS-Sciex) running the Paragon algorithm [42]. Searches were conducted against a subset of the UniRef100 protein database (version 12.7) containing only entries from Homo sapiens (83 425 protein sequences). The search parameters allowed a peptide and fragment mass deviation of up to 0.2 Da and 1 missed trypsin cleavage. Cysteine modification by MMTS, oxidation of methionine as well as iTRAQ labeling of N-termini of the peptides and side chains of lysine and tyrosine residues were allowed. Peak areas for each of the 4 reporter ions (m/z: 114 and 117) were corrected to account for isotopic overlap according to the manufacturer's instructions. Protein identification and quantification results were calculated and viewed with ProteinPilot v.2.0. Protein iTRAQ ratios were corrected for experimental bias by the median average protein ratio as correction factor. Only peptides above 80% confidence were used for identification and quantification, and only proteins, including at least 2 peptides above 80% confidence, were considered. The quantification results were reviewed manually for all proteins found to be differentially expressed (iTRAQ ratio > 1.5 or < 0.75) and for those included in Table 1 and in Supplemental Table 1 and 2. Briefly, this validation step included the examination of the MS/MS spectrum assigned to each identified peptide looking specifically for: 1) the presence of the iTRAQ reporter peaks, 2) a good representation of both x and y ions with preferences toward the presence of more than 3 consecutive assigned ions, 3) the assignment of all major peaks of the spectrum, and 4) the signal-to-noise ratio of peaks

assigned to peptide fragment ions. Assigned spectra that failed to pass these requirements were not included in the calculation of the protein iTRAQ ratio and not considered for protein identification. Quantification data from very low intensity spectra were removed from the protein ratio calculation. Doubtful identifications were rejected. iTRAQ ratios presented in Table 1 and Supplementary Table 1 represent protein ratios calculated by ProteinPilot v.2.0 based on the weighted average Log ratios of peptides. The significance of the changes in protein expression is reported in Table 1 and Supplementaty Table 1 as a p-value calculated by the ProteinPilot software v 2.0 and reporting the probability that the observed ratio is different from 1 by chance. The accuracy of iTRAQ protein ratios can be assessed from the error factors (EF) values calculated by the ProteinPilot software v.2.0 and reported in Table I and Supplementary Table I. The true value for the average protein ratio is expected to be found between [(reported ratio)*(EF)] and [(reported ratio)÷(EF)], 95% of the time. Standard deviation (S.D.) was calculated by MicrosoftExcel software v.11.2.3. Functional classification of proteins identified in this study was based on information from UniPro Knowledgebase and from published literature in Medline.

Immunoblotting. For immunoblot experiments, pellets of purified lysosomes were lysed in buffer containing 50 mM Tris (pH 7.4), 120 mM NaCl, 1% Triton X-100, 1 mM sodium orthovanadate, 2 mM phenylmethylsulfonyl fluoride, 5 mM sodium pyrophosphate and a cocktail of protease inhibitors (Complete^{TM}, Roche Molecular Biochemicals, Laval, QC, Canada) at 4°C for 30 min, centrifuged, and the supernatants analyzed by immunoblotting. The primary antibodies in this study were: anti-LAMP-1 mouse mAb LY1C6, EMD BioSciences, Inc (La Jolla, CA); anti-LAMP-1 rabbit pAb H-228, Santa Cruz Biotechnology, Inc. (Santa Cruz, CA), anti-porin 31HL (VDAC-1) mouse mAb 89-173/025, EMD BioSciences, Inc.; anti-Calnexin rabbit pAb sc-11397, Santa Cruz

Biotechnology, Inc.; anti-NSDHL (sterol-4-alpha-carboxylate 3-dehydrogenase) rabbit pAb HPA000248, Atlas Antibodies AB (Stockholm, Sweden); anti-protein kinase C-delta (PKC-δ) pAb 658-676, EMD BioSciences, Inc.; anti-prosaposin (PSAP) mouse mAb 1D1-C12, Abnova Corp.; and anti-ERp19 rabbit pAb 10291, Abcam Inc. The secondary antibodies were horseradish peroxidase-conjugated sheep anti-mouse immunoglobulin (Ig) and horseradish peroxidase-conjugated donkey anti-rabbit Ig secondary antibodies (GE Healthcare Bio-Sciences AB). ECL reagents also were from GE Healthcare Bio-Sciences AB. Relative densitometry analysis of Westerns blots are based on integrated *Volume* value (intensity x mm^2) normalized to corresponding loading control (LAMP-1) *Volume* value, performed with Quantity One software (BioRad, Hercules, CA.). The data are expressed as relative ratios (control:CPT-treated) and represent the means of *n* independent experiments in distinct lysosome preparations.

Immunofluorescence microscopy. For enriched lysosome staining *in vitro*, aliquots of the preparations were labeled for 20 min in the presence of LysoTracker RED/DND-99 (10 μg/ml), MitoTracker Green/FM (10 μg/ml), ER-Tracker Red dye (10 μg/ml) or Hoechst 33342 (10 μg/ml) in isotonic buffer, washed twice and spread on glass slides. Images were generated with a Nikon Optiphot-2 microscope equipped with Omega Optical Emission/Excitation Filter Sets XF-21, XF102-2 and XF05-2 and mounted with a thermoelectrically-cooled CCD camera (Model DC330E, DageMTI Inc., Michigan City, IN) hooked up to a PC computer. For co-localization experiments, control and CPT-treated U-937 cells were spread by cytocentrifugation on glass slides and fixed in ice-cold methanol:acetone for 2-3 min. Nonspecific binding sites were blocked with 5% BSA in the presence of irrelevant antibodies (anti-sheep IgG, 10 μg/ml; Sigma-Aldrich) then, the slides were incubated sequentially with the first antibody (candidate proteins) at 10 μg/ml,

followed by a fluorescein-conjugated secondary Ab (InVitrogen Molecular Probe; 1:25 v/v), then LysoTracker Red DND-99 or ER-Tracker Red dye or anti-LAMP1 staining at 10 μg/ml and a Texas-red linked secondary Ab (GE Healthcare Bio-Sciences AB; 1:25 v/v). Each antibody incubation for 60 min was followed by several washes in phosphate-buffered solution. Total cells were stained with hematoxylin, and nuclei, with the DNA intercalator Hoechst 33342. The slides were mounted with polyvinyl alcohol 4-88 mounting medium (Sigma-Aldrich). Images were generated and analyzed with a Leica TC S SP5 Confocal Microscope mounted with 3 lasers, Argon, SS561 and HeNe, and equipped for spectral imaging and analysis. *Relative colocalization area* (RCA) values were calculated according to the formula: $[(\mu m2)^{YELLOW} / (\mu m2)^{RED} + (\mu m2)^{GREEN} + (\mu m2)^{YELLOW}] \times 100$, where each color was assigned to a defined color spectrum by Clemex Vision software (Version 3.0.036, Clemex, Longueuil, QC, Canada).

RESULTS

Lysosomes are disrupted after CPT treatment in U-937 cells. Human histiocytic lymphoma U-937 cells are highly sensitive to DNA damage and rapidly die by apoptosis after short, 30-min treatment with the DNA-damaging drug CPT, a DNA topoisomerase I inhibitor [12, 43, 44]. The apoptotic death of these cells is associated with quick involvement of a mitochondrial and lysosomal pathway, within 2 to 3 h after drug treatment. $\downarrow\Delta\Psi m$ (Fig. 1a), lysosome membrane labilization (Fig. 1b), activation of caspase-3-like and cathepsin B enzymes (Fig. 1c), DNA fragmentation and sub-G1 cell populations (Fig. 1d) rapidly appear in CPT-treated U-937 cells [12]. Alterations of mitochondrial functions and mitochondrial membrane permeabilization have been studied extensively in the past. For a better understanding of the molecular mechanisms provoking lysosomal rupture, highly-enriched lysosomes were obtained from control and CPT-treated U-937 cells by 2-step sequential density gradient centrifugation, 3 h after treatment. A schematic view of the purification procedure appears in Supplemental Figure 1. The purity of these lysosome preparations was established first by *in vitro* staining with the fluorescent biomarkers LysoTracker RED/DND-99 (lysosome), MitoTracker Green/FM (mitochondria), ER-Tracker Red dye (endoplasmic reticulum, ER) and Hoechst 33342 (nucleus), observed under a fluorescent microscope (Fig. 2a). In parallel, the purified preparations were incubated and labeled with specific antibodies directed against the protein biomarker LAMP-1 (lysosome), VDAC-1 (mitochondria), Calnexin (ER) and Nucleolin (nucleus) and monitored by fluorescence microscopy (Fig. 2b). The micrographs show much stronger staining with LysoTracker RED/DND-99 (Fig. 2a) and LAMP-1 (Fig. 2b), revealing high enrichment of the preparations. Similarly, detection of the protein biomarkers by Western blotting (Fig. 2c) indicates similar high enrichment of the lysosome

preparations, with high LAMP-1 expression. Finally, fluorescence confocal microscopy experiments were performed to validate LAMP-1 colocalization with the fluorescent biomarker LysoTracker RED/DND-99 (Fig. 2d). The micrographs reveal strong colocalization between LAMP-1 and LysoTracker RED/DND 99 with a *RCA* value of 39.0% ± 2.7 (n=3), while VDAC-1:LAMP-1 (*RCA*: 11.3% ± 1.2; n=3), Calnexin:LAMP-1 (*RCA*: 2.3% ± 0.2; n=3) and Nucleolin:LAMP-1 (*RCA*: 1.9% ± 0.9; n=3) do not significantly colocalize together (Fig. 2d).

Differentially expressed proteins identified by MS of iTRAQ-labeled peptides. Proteins of enriched lysosomes obtained from control and at early phase of CPT-treated U-937 cells (3 h post-treatment) were trypsin-digested, labeled with iTRAQ114 and iTRAQ117 reagents, respectively, combined and fractionated by 1-D/IEF. The isoelectric focusing strips were cut into 36 pieces and the peptides eluted. Nano-LC separation, ionization, quantitation and identification of the peptides were performed by the nano-LC-ESI-MS/MS system. A functional classification of proteins identified in this study (reference experiment) is presented in Fig. 3, with data in Supplemental Table 1. Only proteins including at least 2 peptides above 80% confidence, were considered. A significant proportion of all proteins identified in this study has been identified by others, including 55 of the 103 proteins (53.3%) analysed by Hu Z.-Z. et al. [45] and 94 of the 222 proteins (42.3%) reported by Casey T.M. et al. [46], although the lysosome purification in these studies were carried on different tissues or cell types. In the 2 independent experiments on distinct lysosome preparations, 2 proteins were reproducibly found to be upregulated with a mean fold change (FC) >1.50 and 2 were downregulated with mean FC <0.75 in lysosomes purified from apoptotic compared to control cells (Table 1; Level 1). To gain more valuable information of the analysis, and considering the dynamic nature of membrane-

bound small vesicules, particularly in a biological context of early phase apoptosis where less than 10% of the lysosome population presents partial membrane disruption or labilization, candidate proteins identified as differentially expressed in 1 experiment only were also considered, and included an additional 16 proteins upregulated and 7 downregulated (Table 1; Level 2 and 3). Peptide listing with identification and quantitation data of the candidate proteins are presented in Supplemental Table 2 with the annotated-spectra for unique-peptide-based protein identification provided in Supplemental Table 3.

Expression and localization validation by Western blotting and fluorescence confocal microscopy. Considering the fundamental biological question behind this study, which is to understand lysosomal membrane disruption at early phase of apoptosis, a rationale approach for validation of representative candidate protein was taken, based on their function associated with biomembrane fluidity and dynamics. Western blotting analysis was first performed on candidate proteins, including sterol-4-alpha-carboxylate3-dehydrogenase (NSDHL) (Fig. 4a, upper panel), prosaposin (PSAP) (Fig. 4b, upper panel) and protein kinase C delta (PKC-δ) (Fig. 4c, upper panel). Expression levels of NSDHL, PSAP and PKC-δ appeared to be higher at very early phase of apoptosis activation in lysosome preparations obtained from CPT-treated cells (3 h post-treatment) compared to control cells, with relative ratios (control:CPT-treated; 50 μg protein per lane) of 1:1.30 ± 0.12 (NSDHL; n=3), 1:1.56 (PSAP; n=2) and 1:1.32 (PKC-δ; n=2). Values are based on relative integrated *Volume* value (intensity x mm^2) normalized to LAMP-1 *Volume* value, and represent the means of independent experiments (n) on distinct lysosome preparations.

To confirm the localization of candidate proteins, colocalization experiments were visualized by fluorescent confocal microscopy with LAMP-1 as lysosome biomarker. As shown in Fig. 4 (lower panels), all candidate proteins colocalize to lysosomes with *RCA*

values of 15.5% ± 3.0 (n= 6) and 26.2% ± 5.8 (n= 6) for NSDHL:LAMP-1, 19.3% ± 0.9 (n=4) and 30.8% ± 2.6 (n=4) for PSAP:LAMP-1, and 23.2% ± 2.8 (n=6) and 33.7% ± 2.7 (n=6) for PKC-δ:LAMP-1, in control and CPT-treated cells, respectively. The annotated-spectra and iTRAQ reporter peaks for peptides of validated proteins presented in figure 4 are provided in Supplemental Table 4.

DISCUSSION

Proteomics methods have been recently deployed to identify lysosome proteins (reviewed in [47]). The major aim of our study was to identify candidate proteins that accumulate at lysosomes, with a restrictive and limiting criteria consisting of very early phase of apoptosis when approximately less than 10% of the lysosome population presents partial membrane disruption or labilization in cells induced to undergo apoptosis by CPT, a DNA topoisomerase I inhibitor. By utilizing subcellular fractionation, iTRAQ reagent labeling, 1-D/IEF and LC-ESI-MS/MS-based technology for protein quantitation and identification, we were able to identify candidate proteins which are differentially expressed in lysosomes obtained from human cells triggered to undergo apoptosis. Recently, Yu and al. have reported subcellular proteome analysis of camptothecin analogue-treated NB4 cells, focusing on nuclear, ER, mitochondria and cytosolic proteins [48]. To the best of our knowledge, this is the first study describing the lysosome proteome at very early phase of CPT-induced apoptosis.

Only a few proteins have been shown to accumulate in lysosomes where they contribute to lysosome rupture or labilization during apoptosis, including phospholipase A2 and C, and LAPF [33-37]. These proteins were not detected in our study. This discrepancy could be due to the subcellular fractionation protocol used in these experiments, and to variations in biological responses, depending on the stimuli that provoke lysosomal

labilization. Indeed, organelle purification and fractionation are challenging, particularly for membrane-bound small organelles like lysosome-related organelles, where communication with each other and remodeling occur frequently by complex membrane dynamics and transmembrane protein trafficking [45, 49]. In addition to the dynamic nature of the organelles themselves, membrane-bound cellular organelles could often share comparable densities, which render purification to complete homogeneity by density gradient centrifugation untenable, if not impossible. Nevertheless, sequential density gradient centrifugation represents the best current technology and leads to high enrichment of organelles [45, 49]. Because of these intrinsic limitations in membrane-bound organelle purification, in addition to validating protein candidate expression by Western blotting, protein candidate localization was also visualized by high-resolution fluorescence confocal microscopy. Keeping in mind the dynamic nature of these organelles, and the restrictive and limiting criteria of the study consisting of experiments performed at very early phase of apoptosis when approximately less than 10% of the lysosome population presents partial membrane disruption or labilization, the expression and localization of representative protein candidates, initially identified in 1 experiment only, were also considered.

With these various approaches, 3 representative candidate proteins were validated, including NSDHL, PSAP and PKC-δ. NSDHL is a catalytic enzyme involved in cholesterol biosynthesis, removing 2 C-4 methyl groups in post-squalene cholesterol biosynthesis [50]. In turn, cholesterol, an essential component of biomembranes, is a major determinant of membrane fluidity. Membranes enriched in cholesterol with glycosphingolipids, sphingolipids and phospholipids can lead to the formation of lipid rafts and non-raft shell lipids with protein microdomain formation [51]. Interestingly, cholesterol content is know to be key determinant during endocytosis where lysosomal membranes are formed and

prepared for digestion by a controlled lipid-sorting process [52]. Cholesterol accumulation to lysosomes has been associated with lysosomal dysfunctions in Niemann-Pick type C disease provoking autophagic stress and increased cell death [53-56], and cholesterol oxidation products have been reported to cause lysosomal destabilization and apoptosis [57]. Similarly, treatment of cells with inhibitors that block cholesterol transport out of the lysosome, including the amphiphile 3-beta-(2-(diethylamino)ethoxy)androst-5-en-17-one (U18666A), has been reported to provoke apoptosis [58, 59], although cholesterol accumulation in mitochondrial membranes leads to inefficient Bax oligomerization [60]. Thus, molecular interplay between cholesterol segregation and partitioning, and cholesterol-dependent protein microdomain formation appear to contribute to many cellular functions, including lysosome-endocytosis, lysosome-autophagy and lysosome-apoptosis regulation. Further investigations to understand the role of NSDHL in cholesterol-mediated effect during early phase of lysosomal disruption during apoptosis will be challenging for the near future.

PKC-δ has been demonstrated to regulate apoptosis in response to various stimuli, including DNA-damaging agents [61-63]. The apoptotic function of PKC-δ has been associated with its localization and with the activation of multiple signaling proteins, including JNK, p38, ATM, AKT, cAbl, p73, DNA-PK, lamin, scramblase and, more recently, acid sphingomyelinase [64-66]. Interestingly, upon phorbol 12-myristate 13-acetate treament, PKC-δ has been shown to rapidly translocate to lysosomes where it phosphorylates and activates lysosomal acid sphingomyelinase, a key enzyme that catalyzes the degradation of membrane-bound sphingomyelin into phosphorylcholine and ceramide [66, 67]. Formed of a single peptidic chain, PKC-δ contains an inhibitory pseudosubstrate domain that occludes the substrate-binding pocket, two membrane-binding

domains (termed C1 and C2) and a conserved catalytic domain. The C1 domain forms a hydrophobic globular structure and coordinates with two Zn^{2+} ions to allow diaglycerol and phorbol ester binding and insertion inside apolar milieu of membranes [68, 69]. The C2 domain comprise a characteristic 8-stranded antiparallel β-sandwich that also binds phospholipids but unlike other PKC isoforms, the C2 domain of PKC-δ does not required presence of Ca^{2+} ions. Upon its activation, PKC-δ autoinhibitory domain moves to open the phorbol ester-binding pocket and allows interaction of C1 and C2 domains with membrane lipids, resulting in its translocation from the cytosol to sub-cellular membranes, including lysosomal membrane [66, 67, 70]. In this study, the observed increase in PKC-δ re-localization at lysosomes after CPT treatment strongly suggests that activation of acid sphingomyelinase, in turn, could raise ceramide levels, an event often associated with apoptosis induction [71]. DNA damaging agents including etoposide and NSC606985, a CPT analog, have been reported to induce a caspase-dependent proteolytic activation of PKC-δ into a 41-kDa catalytic fragment that activates the kinase [72-74]. In this study, with analysis performed at very early phase of apoptosis, the translocation of PKC-δ to lysosomes was not associated with its proteolytic cleavage, consistent with a previous study that has reported that PKC-δ cleavage occurred 24 h after NSC606985 treatment in U-937 cells [74].

Similarly, PSAP, the other candidate protein validated in this study, is the precursor of 4 lysosomal sphingolipid activator proteins (saposin A-D), that also play key roles in acid sphingomyelinase activation [75, 76], and lysosomal membrane digestion during endocytosis [52]. PSAP and the saposins are membrane-pertubating and lipid-binding proteins that are essential for glycosphingolipid degradation of lysosomal membranes [52].

Recruited together at lysosomes after CPT treatment, NSDHL, PKC-δ and PSAP could possibly have drastic effects, leading to membrane fluidity, rapid ceramide accumulation, major changes in sphingolipid content, with glycosphingolipid degradation and lysosomal membrane disruption.

Several proteins associated with ER stress have also been identified by the proteomic approach. In U937 cells, we also noticed that CPT triggered typical morphological rearrangements of cells undergoing ER stress, with cells showing ER undergoing clumping and forming aggregates and/or small vesicles, 3 h post-CPT treatment [77, 78] (data not shown). However, the connection between ER stress, appearance of aggregates and/or small vesicles and lysosome impairment has not been well documented. Given the importance of autophagy during organelle damage and stress, and the relation between autophagy and apoptosis, it will be of interest to pursue future studies in that direction.

In conclusion, iTRAQ reagent labeling with 1-D/IEF and LC-ESI-MS/MS approaches combined with the validation of expression/localization of candidate proteins, have permitted the identification of novel proteins that accumulate in lysosomes in the early phase of CPT-induced lysosome labilization and apoptosis. The exact consequences of accumulating these proteins in lysosomes for lysosome labilization and apoptosis are, yet, unknown. All of our 3 validated candidate proteins are related to biomembrane fluidity and dynamics, particularly cholesterol, sphingolipid and glycosphingolipid metabolism. Further functional studies are underway to investigate their importance for lysosome dysfunction and labilization during CPT-induced apoptosis.

Acknowledgements

This work was supported by a grant from the Canadian Institutes of Health Research to R.B. G.G.P. is a recipient of a Canadian Research Chair in Proteomics. N.P. obtained studentships from the Faculté des études supérieures (Université de Montréal) and from the Institut du cancer de Montréal and Canderel Inc. (Montréal, QC). CP received fellowship from Fonds de la recherche en santé du Québec (FRSQ). The authors thank Mr. Ovid Da Silva (Research Support Office, Research Centre, CHUM) for editing this manuscript.

REFERENCES

[1] Brunk UT, Neuzil J, Eaton JW. Lysosomal involvement in apoptosis. Redox Rep 2001;6:91-7.

[2] Turk B, Stoka V, Rozman-Pungercar J, Cirman T, Droga-Mazovec G, Oreic K, et al. Apoptotic pathways: involvement of lysosomal proteases. Biol Chem 2002;383:1035-44.

[3] Guicciardi ME, Leist M, Gores GJ. Lysosomes in cell death. Oncogene 2004;23:2881-90.

[4] Terman A, Kurz T, Gustafsson B, Brunk UT. Lysosomal labilization. IUBMB Life 2006;58:531-9.

[5] Brunk UT, Svensson I. Oxidative stress, growth factor starvation and Fas activation may all cause apoptosis through lysosoma leak. Redox Rep 1999;4:3-11.

[6] Brunk UT, Dalen H, Roberg K, Hellquist HB. Photo-oxidative disruption of lysosomal membranes causes apoptosis of cultured human fibroblasts. Free Radic Biol Med 1997;23:616-26.

[7] Boya P, Andreau K, Poncet D, Zamzami N, Perfettini JL, Metivier D, et al. Lysosomal membrane permeabilization induces cell death in a mitochondrion-dependent fashion. J Exp Med 2003;197:1323-34.

[8] Guicciardi ME, Deussing J, Miyoshi H, Bronk SF, Svingen PA, Peters C, et al. Cathepsin B contributes to TNF-alpha-mediated hepatocyte apoptosis by promoting mitochondrial release of cytochrome c. J Clin Invest 2000;106:1127-37.

[9] Kagedal K, Zhao M, Svensson I, Brunk UT. Sphingosine-induced apoptosis is dependent on lysosomal proteases. Biochem J 2001;359:335-43.

[10] Heinrich M, Wickel M, Schneider-Brachert W, Sandberg C, Gahr J, Schwandner R, et al. Cathepsin D targeted by acid sphingomyelinase-derived ceramide. EMBO J 1999;18:5252-63.

[11] Hishita T, Tada-Oikawa T, Tohyama K, Miura Y, Nishihara T, Tohyama Y, et al. Caspase-3 activation by lysosomal enzymes in cytochrome c-independent apoptosis in myelodysplastic syndrome-derived cell line P39. Cancer Res 2001;61:2878-84.

[12] Paquet C, Beauchemin M, Bertrand R. Caspase- and mitochondrial dysfunction-dependent mechanisms of lysosomal leakage and cathepsin B activation in DNA damage-induced apoptosis. Leukemia 2005;19:784-91.

[13] Broker LE, Huisman C, Span SW, Rodriguez JA, Kruyt FA, Giaccone G. Cathepsin B mediates caspase-independent cell death induced by microtubule stabilizing agents in non-small cell lung cancer cells. Cancer Res 2004;64:27-30.

[14] Kluck RM, Martin SJ, Hoffman BM, Zhou JS, Green DR, Newmeyer DD. Cytochrome C activation of Cpp32-like proteolysis plays a critical role in a Xenopus cell-free apoptosis system. EMBO J 1997;16:4639-49.

[15] Marzo I, Brenner C, Zamzami N, Jurgensmeier JM, Susin SA, Vieira HLA, et al. Bax and adenine nucleotide translocator cooperate in the mitochondrial control of apoptosis. Science 1998;281:2027-31.

[16] Matsuyama S, Xu QL, Velours J, Reed JC. The mitochondrial F0F1-ATPase proton pump is required for function of the proapoptotic protein Bax in yeast and mammalian cells. Mol Cell 1998;1:327-36.

[17] Shimizu S, Narita M, Tsujimoto Y. Bcl-2 family proteins regulate the release of apoptogenic cytochrome c by the mitochondrial channel VDAC. Nature 1999;399:483-7.

[18] Vander Heiden MG, Chandel NS, Williamson EK, Schumacker PT, Thompson CB. Bcl-X(L) regulates the membrane potential and volume homeostasis of mitochondria. Cell 1997;91:627-37.

[19] Vander Heiden MG, Thompson CB. Bcl-2 proteins: regulators of apoptosis or of mitochondrial homeostasis? Nat Cell Biol 1999;1:E209-E16.

[20] Kroemer G, Galluzzi L, Brenner C. Mitochondrial membrane permeabilization in cell death. Physiol Rev 2007;87:99-163.

[21] Reed JC. Proapoptotic multidomain Bcl-2/Bax-family proteins: mechanisms, physiological roles, and therapeutic opportunities. Cell Death Differ 2006;13:1378-86.

[22] Adams JM, Cory S. The Bcl-2 apoptotic switch in cancer development and therapy. Oncogene 2007;26:1324-37.

[23] Chittenden T, Flemington C, Houghton AB, Ebb RG, Gallo GJ, Elangovan B, et al. A conserved domain in Bak, distinct from BH1 and BH2, mediates cell death and protein binding functions. EMBO J 1995;14:5589-96.

[24] Polster BM, Kinnally KW, Fiskum G. BH3 death domain peptide induces cell type-selective mitochondrial outer membrane permeability. J Biol Chem 2001;276:37887-94.

[25] Chittenden T. BH3 domains: intracellular death-ligands critical for initiating apoptosis. Cancer Cell 2002;2:165-6.

[26] Kuwana T, Bouchier-Hayes L, Chipuk JE, Bonzon C, Sullivan BA, Green DR, et al. BH3 domains of BH3-only proteins differentially regulate Bax-mediated mitochondrial membrane permeabilization both directly and indirectly. Mol Cell 2005;17:525-35.

[27] Kim H, Rafiuddin-Shah M, Tu HC, Jeffers JR, Zambetti GP, Hsieh JJ, et al. Hierarchical regulation of mitochondrion-dependent apoptosis by Bcl-2 subfamilies. Nat Cell Biol 2006;8:1348-58.

[28] Chen L, Willis SN, Wei A, Smith BJ, Fletcher JI, Hinds MG, et al. Differential targeting of prosurvival Bcl-2 proteins by their BH3-only ligands allows complementary apoptotic function. Mol Cell 2005;17:393-403.

[29] Willis SN, Chen L, Dewson G, Wei A, Naik E, Fletcher JI, et al. Proapoptotic Bak is sequestered by Mcl-1 and Bcl-xL, but not Bcl-2, until displaced by BH3-only proteins. Genes Dev 2005;19:1294-305.

[30] Willis SN, Fletcher JI, Kaufmann T, van Delft MF, Chen L, Czabotar PE, et al. Apoptosis initiated when BH3 ligands engage multiple Bcl-2 homologs, not Bax or Bak. Science 2007;315:856-9.

[31] Hu JS, Li YB, Wang JW, Sun L, Zhang GJ. Mechanism of lysophosphatidylcholine-induced lysosome destabilization. J Membr Biol 2007;215:27-35.

[32] Zhao M, Brunk UT, Eaton JW. Delayed oxidant-induced cell death involves activation of phospholipase A2. FEBS Lett 2001;509:399-404.

[33] Hiraoka M, Abe A, Lu Y, Yang K, Han X, Gross RW, et al. Lysosomal phospholipase A2 and phospholipidosis. Mol Cell Biol 2006;26:6139-48.

[34] Wang X, Wang LL, Zhang GJ. Guanosine 5'-[gamma-thio]triphosphate-mediated activation of cytosol phospholipase C caused lysosomal destabilization. J Membr Biol 2006;211:55-63.

[35] Wang X, Zhao HF, Zhang GJ. Mechanism of cytosol phospholipase C and sphingomyelinase-induced lysosome destabilization. Biochimie 2006;88:913-22.

[36] Zhao HF, Wang X, Zhang GJ. Lysosome destabilization by cytosolic extracts, putative involvement of Ca(2+)/phospholipase C. FEBS Lett 2005;579:1551-6.

[37] Chen W, Li N, Chen T, Han Y, Li C, Wang Y, et al. The lysosome-associated apoptosis-inducing protein containing the pleckstrin homology (PH) and FYVE domains (LAPF), representative of a novel family of PH and FYVE domain-containing proteins, induces caspase-independent apoptosis via the lysosomal-mitochondrial pathway. J Biol Chem 2005;280:40985-95.

[38] Salvioli S, Ardizzoni A, Franceschi C, Cossarizza A. Jc-1, but not Dioc(6)(3) or rhodamine 123, is a reliable fluorescent probe to assess Delta-Psi changes in intact cells; Implications for studies on mitochondrial functionality during apoptosis. FEBS Lett 1997;411:77-82.

[39] Bertrand R, Sarang M, Jenkin J, Kerrigan D, Pommier Y. Differential induction of secondary DNA fragmentation by topoisomerase II inhibitors in human tumor cell lines with amplified c-myc expression. Cancer Res 1991;51:6280-5.

[40] Storrie B, Madden EA. Isolation of subcellular organelles. Methods Enzymol 1990;182:203-25.

[41] Paquet C, Schmitt E, Beauchemin M, Bertrand R. Activation of multidomain and BH3-only pro-apoptotic Bcl-2 family members in p53-defective cells. Apoptosis 2004;9:815-31.

[42] Shilov IV, Seymour SL, Patel AA, Loboda A, Tang WH, Keating SP, et al. The Paragon Algorithm, a next generation search engine that uses sequence temperature values and feature probabilities to identify peptides from tandem mass spectra. Mol Cell Proteomics 2007;6:1638-55.

[43] Schmitt E, Cimoli G, Steyaert A, Bertrand R. Bcl-xL modulates apoptosis induced by anticancer drugs and delays DEVDase and DNA fragmentation-promoting activities. Exp Cell Res 1998;240:107-21.

[44] Sané AT, Bertrand R. Distinct steps in DNA fragmentation pathway during camptothecin-induced apoptosis involved caspase-, benzyloxycarbonyl- and N-tosyl-L-phenylalanylchloromethyl ketone-sensitive activities. Cancer Res 1998;58:3066-72.

[45] Hu ZZ, Valencia JC, Huang H, Chi A, Shabanowitz J, Hearing VJ, et al. Comparative bioinformatics analyses and profiling of lysosome-related organelle proteomes. Int J Mass Spectrom 2007;259:147-60.

[46] Casey TM, Meade JL, Hewitt EW. Organelle proteomics: identification of the exocytic machinery associated with the natural killer cell secretory lysosome. Mol Cell Proteomics 2007;6:767-80.

[47] Callahan JW, Bagshaw RD, Mahuran DJ. The integral membrane of lysosomes: its proteins and their roles in disease. J Proteomics 2009;72:23-33.

[48] Yu Y, Wang LS, Shen SM, Xia L, Zhang L, Zhu YS, et al. Subcellular proteome analysis of camptothecin analogue NSC606985-treated acute myeloid leukemic cells. J Proteome Res 2007;6:3808-18.

[49] Takamori S, Holt M, Stenius K, Lemke EA, Gronborg M, Riedel D, et al. Molecular anatomy of a trafficking organelle. Cell 2006;127:831-46.

[50] Caldas H, Herman GE. NSDHL, an enzyme involved in cholesterol biosynthesis, traffics through the Golgi and accumulates on ER membranes and on the surface of lipid droplets. Hum Mol Genet 2003;12:2981-91.

[51] Haucke V, DiPaolo G. Lipids and lipid modifications in the regulation of membrane traffic. Curr Opin Cell Biol 2007;19:426-35.

[52] Kolter T, Sandhoff K. Principles of lysosomal membrane digestion: stimulation of sphingolipid degradation by sphingolipid activator proteins and anionic lysosomal lipids. Annu Rev Cell Dev Biol 2005;21:81-103.

[53] Beltroy EP, Liu B, Dietschy JM, Turley SD. Lysosomal unesterified cholesterol content correlates with liver cell death in murine Niemann-Pick type C disease. J Lipid Res 2007;48:869-81.

[54] Bi X, Liao G. Autophagic-lysosomal dysfunction and neurodegeneration in Niemann-Pick Type C mice: lipid starvation or indigestion? Autophagy 2007;3:646-8.

[55] Liao G, Yao Y, Liu J, Yu Z, Cheung S, Xie A, et al. Cholesterol accumulation is associated with lysosomal dysfunction and autophagic stress in Npc1 -/- mouse brain. Am J Pathol 2007;171:962-75.

[56] Pacheco CD, Lieberman AP. Lipid trafficking defects increase Beclin-1 and activate autophagy in Niemann-Pick type C disease. Autophagy 2007;3:487-9.

[57] Yuan XM, Li W, Brunk UT, Dalen H, Chang YH, Sevanian A. Lysosomal destabilization during macrophage damage induced by cholesterol oxidation products. Free Radic Biol Med 2000;28:208-18.

[58] Koh CH, Cheung NS. Cellular mechanism of U18666A-mediated apoptosis in cultured murine cortical neurons: bridging Niemann-Pick disease type C and Alzheimer's disease. Cell Signal 2006;18:1844-53.

[59] Koh CH, Qi RZ, Qu D, Melendez A, Manikandan J, Bay BH, et al. U18666A-mediated apoptosis in cultured murine cortical neurons: role of caspases, calpains and kinases. Cell Signal 2006;18:1572-83.

[60] Lucken-Ardjomande S, Montessuit S, Martinou JC. Bax activation and stress-induced apoptosis delayed by the accumulation of cholesterol in mitochondrial membranes. Cell Death Differ 2008;15:484-93.

[61] Brodie C, Blumberg PM. Regulation of cell apoptosis by protein kinase C delta. Apoptosis 2003;8:19-27.

[62] Basu A. Involvement of protein kinase C delta in DNA damage-induced apoptosis. J Cell Mol Med 2003;7:341-50.

[63] Blass M, Kronfeld I, Kazimirsky G, Blumberg PM, Brodie C. Tyrosine phosphorylation of protein kinase C delta is essential for its apoptotic effect in response to etoposide. Mol Cell Biol 2002;22:182-95.

[64] Yoshida K. PKC delta signaling: Mechanisms of DNA damage response and apoptosis. Cell Signal 2007;9:892-901.

[65] Gomel R, Xiang C, Finniss S, Lee HK, Lu W, Okhrimenko H, et al. The localization of protein kinase C delta in different subcellular sites affects its proapoptotic and antiapoptotic functions and the activation of distinct downstream signaling pathways. Mol Cancer Res 2007;5:627-39.

[66] Zeidan YH, Hannun YA. Activation of acid sphingomyelinase by protein kinase C delta-mediated phosphorylation. J Biol Chem 2007;282:11549-61.

[67] Zeidan YH, Wu BX, Jenkins RW, Obeid LM, Hannun YA. A novel role for protein kinase C delta-mediated phosphorylation of acid sphingomyelinase in UV light-induced mitochondrial injury. FASEB J 2008;22:183-93.

[68] Chow W. Membrane targeting by C1 and C2 domains. J Biol Chem 2001;276:32407-10.

[69] Zhang G, Kazanietz MG, Blumberg PM, Hurley JH. Crystal structure of the Cys2 activator-binding domain of protein kinase Cδ in complex with phorbol esters. Cell 1995;81:917-24.

[70] Wang QJ, Bhattacharyya D, Garfield S, Nacro K, Marquez VE, Blumberg PM. Differential localization of protein kinase C delta by phorbol esters and related compounds using a fusion protein with green fluorescent protein. J Biol Chem 1999;274:37233-9.

[71] Siskind LJ. Mitochondrial ceramide and the induction of apoptosis. J Bioenerg Biomembr 2005;37:143-53.

[72] Khwaja A, Tatton L. Caspase-mediated proteolysis and activation of protein kinase Cdelta plays a central role in neutrophil apoptosis. Blood 1999;94:291-301.

[73] Shin SY, Kim CG, Ko J, Min DS, Chang JS, Ohba M, et al. Transcriptional and post-transcriptional regulation of the PKC delta gene by etoposide in L1210 murine leukemia cells: implication of PKC delta autoregulation. J Mol Biol 2004;340:681-93.

[74] Song MG, Gao SM, Du KM, Xu M, Yu Y, Zhou YH, et al. Nanomolar concentration of NSC606985, a camptothecin analog, induces leukemic-cell apoptosis through protein kinase Cdelta-dependent mechanisms. Blood 2005;105:3714-21.

[75] Linke T, Wilkening G, Lansmann S, Moczall H, Bartelsen O, Weisgerber J, et al. Stimulation of acid sphingomyelinase activity by lysosomal lipids and sphingolipid activator proteins. Biol Chem 2001;382:283-90.

[76] Ferlinz K, Linke T, Bartelsen O, Weiler M, Sandhoff K. Stimulation of lysosomal sphingomyelin degradation by sphingolipid activator proteins. Chem Phys Lipids 1999;102:35-43.

[77] Terrinoni A, Ranalli M, Cadot B, Leta A, Bagetta G, Vousden KH, et al. p73-alpha is capable of inducing scotin and ER stress. Oncogene 2004;23:3721-5.

[78] Moenner M, Pluquet O, Bouchecareilh M, Chevet E. Integrated endoplasmic reticulum stress responses in cancer. Cancer Res 2007;67:10631-4.

FIGURE LEGENDS

Fig. 1 Parameters of CPT-induced apoptosis in U-937 cells. U-937 cells were treated with 1.0 μM CPT for 30 min. At the indicated times (h) after CPT treatment, a) the percentage of total cells with $\downarrow\Delta\Psi m$, b) the percentage of total cells with lysosome rupture or labilization, c) the kinetics of caspase-3-like (open circles) and cathepsin B (closed circles) activities, and d) the percentage of DNA fragmentation (open circles) and sub-G_1 death cells (closed circles) were quantified as described in Experimental Procedures. Symbols represent the means ± SE of at least 4 independent experiments.

Fig. 2 Purity of enriched lysosome preparations obtained by 2-step sequential density gradients. Lysosomes from U-937 cells were purified by 2-step sequential density gradients and **a)** U-937 cells and enriched lysosome preparations were stained *in situ* with the fluorescent biomarkers LysoTracker RED/DND-99 (lysosome), MitoTracker Green/FM (mitochondria), ER-Tracker Red dye (endoplasmic reticulum, ER) and Hoechst 33342 (nucleus), and observed under a fluorescent microscope. Hematoxylin staining is also shown; **b)** Cells and enriched lysosome preparations were labeled with specific antibodies directed against the protein biomarkers LAMP-1 (lysosome), VDAC-1 (mitochondria), Calnexin (ER) and Nucleolin (nucleus) and monitored by fluorescence microscopy; **c)** Protein aliquots of enriched lysosome preparations were run on SDS-PAGE for Western blotting using anti-LAMP-1 (lysosome biomarker), anti-VDAC-1 (mitochondria biomarker), anti-Calnexin (ER biomarker) and anti-Nucleolin (nuclear biomarker) to monitor the purity of the lysosome preparations; **d)** Colocalization of LAMP-1 with the

fluorescent biomarker LysoTracker RED/DND-99. Note that VDAC-1:LAMP-1, Calnexin:LAMP-1 and Nucleolin:LAMP-1 do not significantly colocalized together. All representative of 3 or 4 independent experiments.

Fig. 3 Functional classification of the proteins identified in 1 reference experiment. All data associated with this graph are presented in Supplemental Table 1. Only proteins including at least 2 peptides above 80% confidence were considered.

Fig. 4 Validation of differentially-expressed representative protein candidates. To validate the expression/localization of representative candidate proteins, in the **upper panels**, protein aliquots (10 and 50 μg) of enriched lysosome preparations obtained from control (C) and CPT-treated cells (3 h post-treatment; CPT) were run on SDS-PAGE for Western blotting using specific antibodies against NSDHL (**a**), PSAP (**b**) and PKC-δ (**c**). LAMP-1 serves as a loading control; protein extracts obtained from whole cells are antibody controls. Relative ratios after CPT treatment were determined by relative densitometry analysis of light radiographs normalized to LAMP-1 intensity levels. Data in the Results section represent the means of (n) independent experiments. **Lower panels:** colocalization of NSDHL (**a**), PSAP (**b**) and PKC-δ (**c**) (fluorescein- labeled) and LAMP-1 (Red Texas-labeled), in control (C) and CPT-treated cells (3 h post-treatment; CPT). Data in the Results section are expressed as *Relative Colocalization Area* (*RCA*) values, and represent the means ± SD of (n) independent experiments.

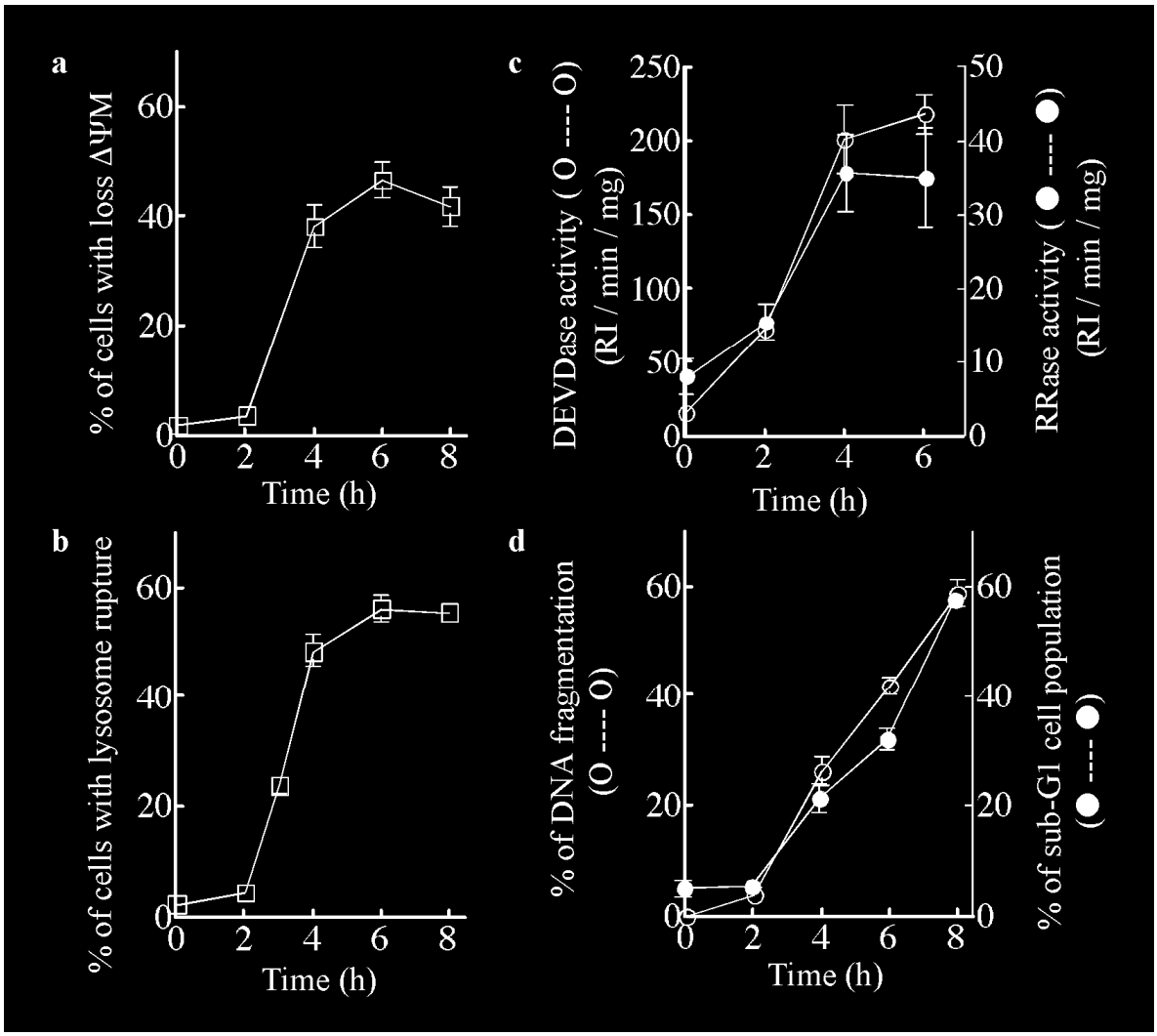
a
% of cells with loss ΔΨM
Time (h)
b
% of cells with lysosome rupture
Time (h)
c
DEVDase activity (O ---- O)
(RI / min / mg)
RRase activity (● ---- ●)
(RI / min / mg)
Time (h)
d
% of DNA fragmentation
(O ---- O)
% of sub-G1 cell population
(● ---- ●)
Time (h)

Figure 1

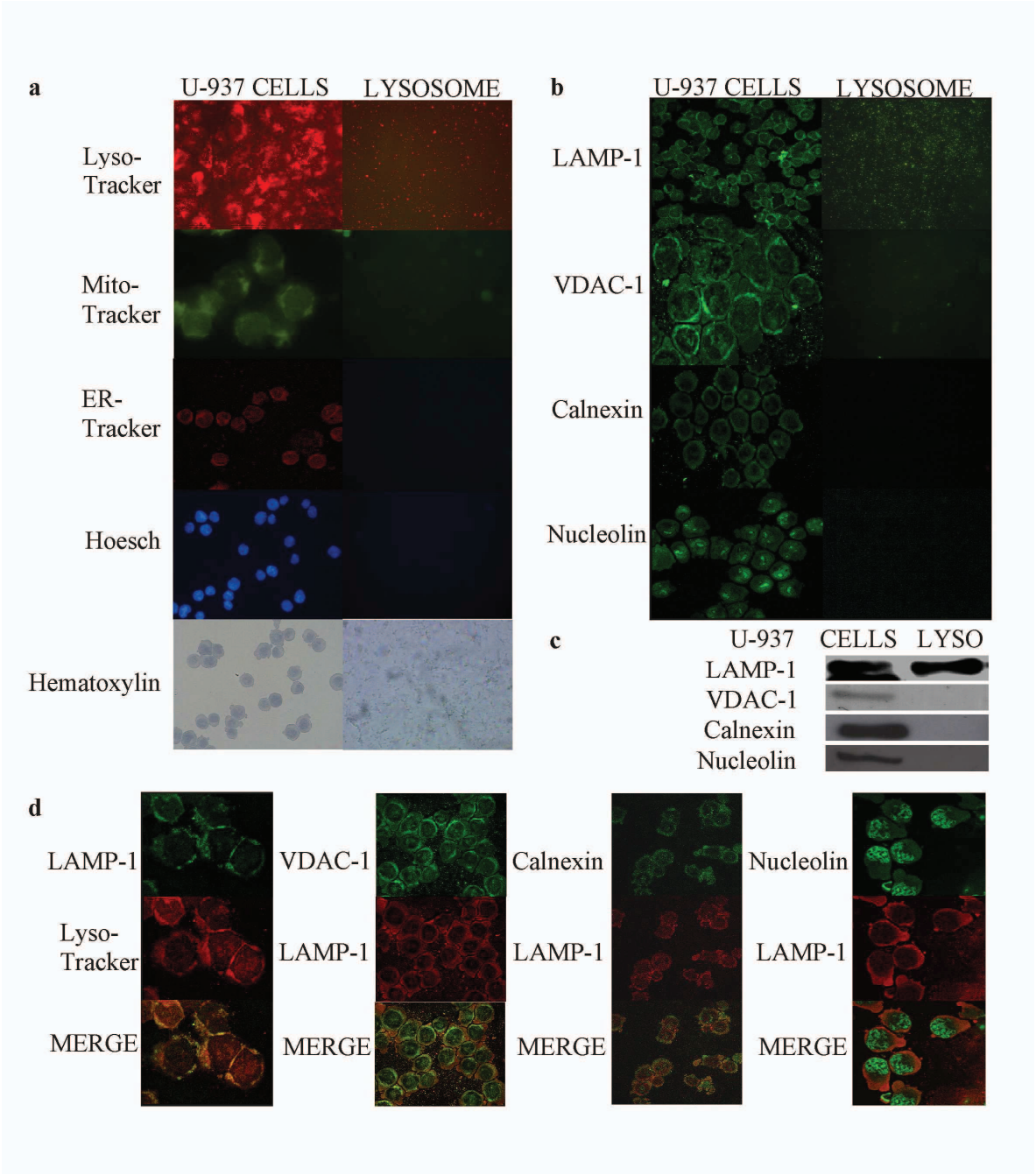
a
U-937 CELLS
LYSOSOME
Lyso-Tracker
Mito-Tracker
ER-Tracker
Hoesch
Hematoxylin
b
U-937 CELLS
LYSOSOME
LAMP-1
VDAC-1
Calnexin
Nucleolin
c
U-937
CELLS
LYSO
LAMP-1
VDAC-1
Calnexin
Nucleolin
d
LAMP-1
Lyso-Tracker
MERGE
VDAC-1
LAMP-1
MERGE
Calnexin
LAMP-1
MERGE
Nucleolin
LAMP-1
MERGE

Figure 2

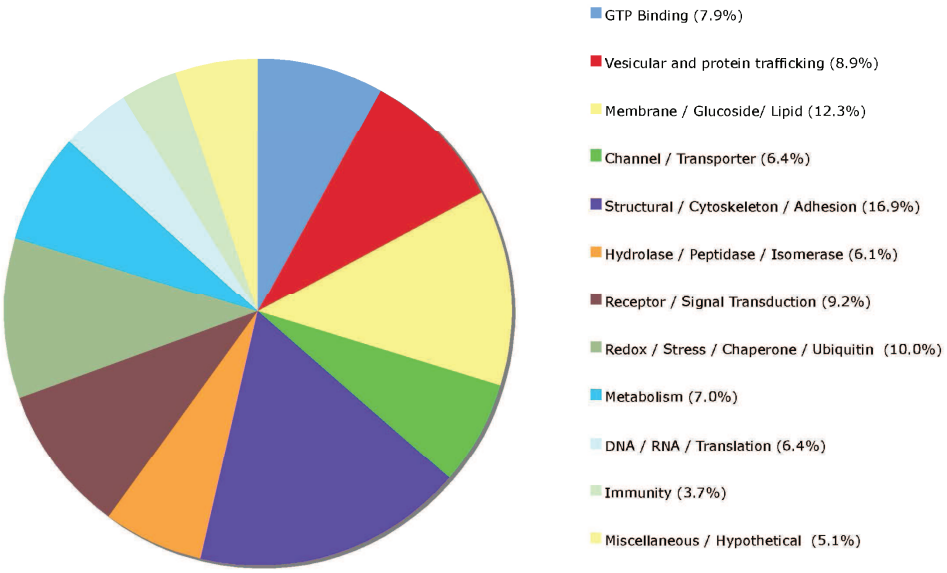
GTP Binding (7.9%)
Vesicular and protein trafficking (8.9%)
Membrane / Glucoside/ Lipid (12.3%)
Channel / Transporter (6.4%)
Structural / Cytoskeleton / Adhesion (16.9%)
Hydrolase / Peptidase / Isomerase (6.1%)
Receptor / Signal Transduction (9.2%)
Redox / Stress / Chaperone / Ubiquitin (10.0%)
Metabolism (7.0%)
DNA / RNA / Translation (6.4%)
Immunity (3.7%)
Miscellaneous / Hypothetical (5.1%)

Figure 3

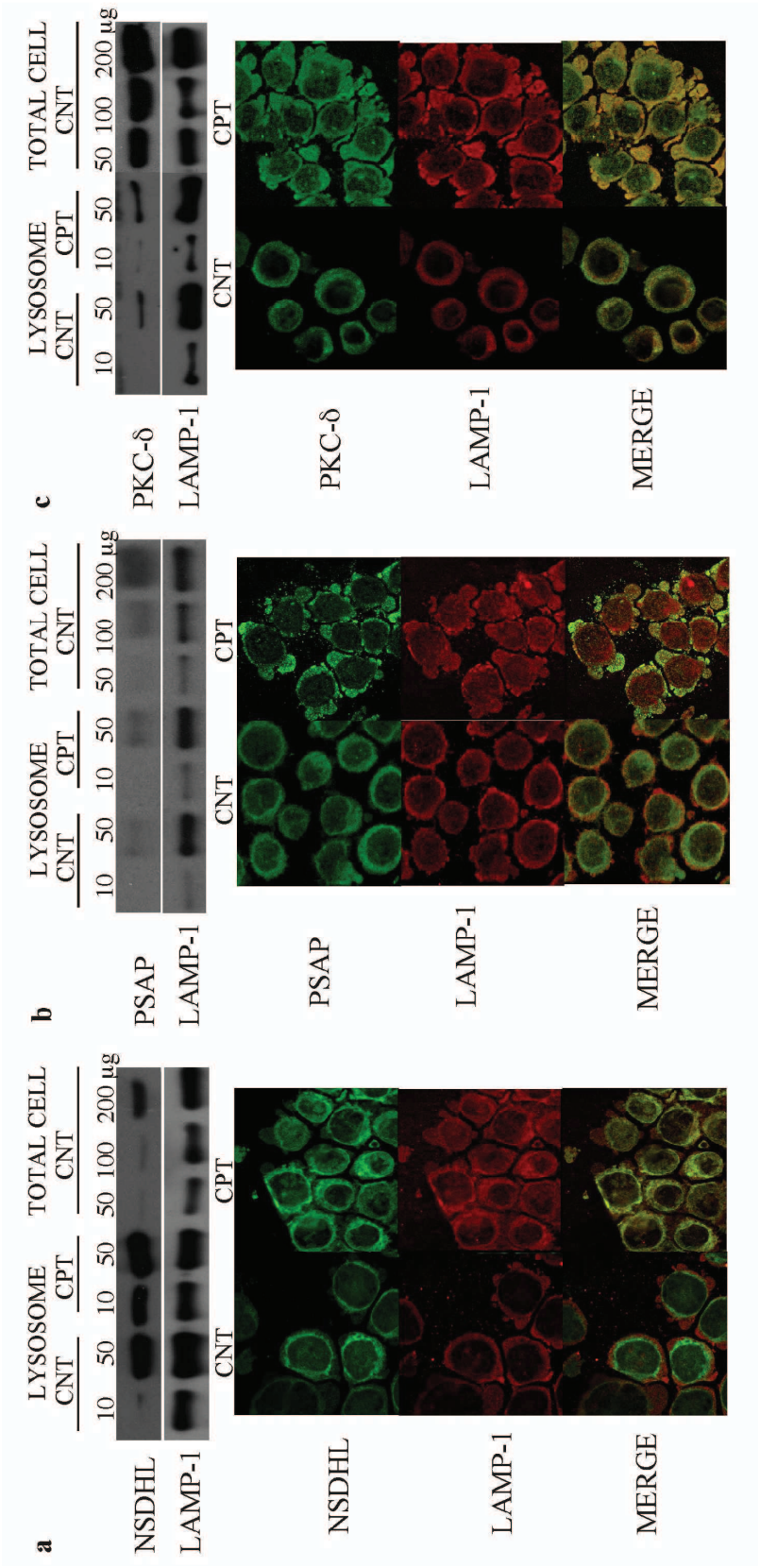
a
LYSOSOME
CNT
CPT
TOTAL CELL
CNT
10 50 10 50 50 100 200 μg
NSDHL
LAMP-1
CNT
CPT
NSDHL
LAMP-1
MERGE
b
LYSOSOME
CNT
CPT
TOTAL CELL
CNT
10 50 10 50 50 100 200 μg
PSAP
LAMP-1
CNT
CPT
PSAP
LAMP-1
MERGE
c
LYSOSOME
CNT
CPT
TOTAL CELL
CNT
10 50 10 50 50 100 200 μg
PKC-δ
LAMP-1
CNT
CPT
PKC-δ
LAMP-1
MERGE

Figure 4

TABLE 1: CANDIDATE PROTEINS DIFFERENTIALLY EXPRESSED IN ENRICHED LYSOSOME PREPARATIONS FROM EARLY APOPTOTIC U937 CELLS

A

Accession Number	Name and *Synonym*	Experiment 1						Experiment 2					
		unique peptide (*total* count)	% Cov	Ratio	± S.D. or (± range)	P-Value	EF	*unique* peptide (*total* count)	% Cov	Ratio	± S.D. or (± range)	P-Value	EF
LEVEL 1													
UP10000456547 UPI000047EFF7 Q15005	Signal peptidase complex subunit 2 (SPCS2); *Microsomal signal peptidase 25 kDa subunit*	3 (5)	3.98	1.7361	± 1.4002	0.1184	2.1237	2 (5)	4.02	1.6131	± 0.3741	0.0148	1.3816
P14174	Macrophage migration inhibitory factor (MIF); *Glycosylation-inhibiting factor*	1 (8) *	7.83	1.6405	± 0.0927	4.162E-10	1.0403	1 (16) *	7.83	1.4427	± 0.1522	1.850E-11	1.0483
LEVEL 2													
P16949 A2A2D2	Stathmin 1/oncoprotein 18; *Leukemia-associated phosphoprotein p18*	1 (3) *	6.90	2.5295	± 0.3662	0.0078	1.4258	6 (18)	34.23	1.0283	± 0.2202	0.4639	1.0804
Q15738	NAD(P) dependent steroid dehydrogenase-like (NSDHL); *Sterol-4-alpha-carboxylate 3-dehydrogenase, decarboxylating*	1 (1) *	2.39	1.9351	N.A.	0.302209	7.862	4 (6)	16.09	1.0944	± 0.5346	0.5894	1.4731
P63000 A4D2P0	Ras-related C3 botulinum toxin substrate 1	2 (7)	9.95	1.6060	± 0.1425	8.814E-08	1.0719	3 (7)	17.18	1.1230	± 0.1668	0.0004	1.0782
UPI0000EFE353 P60953	Cell Division Cycle 42 (CDC42); *G25K GTP-binding protein*	5 (10)	27.75	1.5720	± 0.3572	6.150E-05	1.1653	5 (34)	31.41	1.0060	± 0.1871	0.8993	1.1154
Q06830	Peroxiredoxin-1 (PRDX1)	4 (14)	21.11	1.4477	± 0.2136	1.127E-06	1.0985	5 (11)	25.13	1.1125	± 0.0710	0.0075	1.0728
P30040	Endoplasmic reticulum protein ERp29 precursor	3 (10)	12.26	1.0516	± 0.3415	0.6662	1.2816	2 (5)	8.43	1.9656	± 0.5804	0.0076	1.4580
O95881	Thioredoxin domain-containing protein 12 precursor (TXD12); *Thioredoxin protein p19, ERP19*	1 (1) *	5.23	1.1338	N.A.	N.A.	N.A.	2 (4)	13.37	1.6015	± 0.2738	0.0170	1.3650
P07237	Protein disulfide-isomerase precursor (PDIA1); *procollagen-proline, 2-oxoglutarate 4-dioxygenase, beta polypeptide*	8 (23)	13.39	1.1377	± 0.1660	6.834E-05	1.0580	28 (230)	50.00	1.4980	± 0.3184	0.0000	1.0325
P13667	Protein disulfide-isomerase A4 precursor (PDIA4)	10 (30)	13.80	1.1750	± 0.3721	0.0019	1.1028	7 (18)	9.61	1.4855	± 0.3662	1.180E-06	1.1288
P30101	Protein disulfide-isomerase A3 precursor (PDIA3)	14 (38)	18.61	1.0449	± 0.2759	0.2092	1.0719	11 (61)	22.18	1.5080	± 0.2409	1.031E-24	1.0530
LEVEL 3													
Q5QNW6	Histone H2B type 2-F	8 (42)	34.92	2.8113	± 0.5410	1.285E-04	1.1363	N.D.					
Q5JQ37	Prosaposin (variant Gaucher disease and variant metachromatic leukodystrophy)	N.D.						4 (17)	4.29	1.6085	± 0.1582	4.105E-09	1.0960
UPI000054B38F A8K3K6	Carboxylesterase 1 isoform c precursor	N.D.						6 (15)	12.01	1.5551	± 0.1927	1.228E-09	1.0742
UPI000013D53C P20933	N(4)-(beta-N-acetylglucosaminyl)-L-asparaginase precursor; *Glycosylasparaginase beta c, Aspartylglucosaminidase*	N.D.						2 (7)	3.76	1.4754	± 0.5509	0.0154	1.3397
UPI00002263A8 NM198901	Sorcin isoform b	N.D.						3 (6)	10.93	1.4086	± 0.2776	0.0079	1.2389
Q05655	Protein kinase C delta type	N.D.						3 (9)	5.77	1.2469	± 0.2035	0.0026	1.1340

B

Accession Number	Name *Synonyms*	Experiment 1						Experiment 2					
		unique peptide (*total* count)	% Cov	Ratio	± S.D. or (± range)	P-Value	EF	*unique* peptide (*total* count)	% Cov	Ratio	± S.D. or (± range)	P-Value	EF
LEVEL 1													
Q10471	UDP-N-acetyl-alpha-D-galactosamine:polypeptide N-acetylgalactosaminyltransferase 2 (GalNAc-T2)	2 (4)	4.90	0.6784	± 0.1195	0.0231	1.3320	2 (2)	3.33	0.6820	(± 0.1356)	0.0176	1.3136
Q92896	Golgi apparatus protein 1 precursor (GSLG1); *Cysteine-rich fibroblast growth factor receptor, E-selectin ligand 1*	6 (8)	3.31	0.5613	± 0.0910	1.129E-06	1.1504	1 (1)*	0.84	0.7235	N.A.	0.2851	2.6198
LEVEL 2													
Q92520	Protein FAM3C precursor	3 (5)	7.93	0.5597	± 0.0946	0.0014	1.2345	2 (2)	11.45	0.9794	(± 0.3107)	0.9585	56.6481
Q9UIQ6	Leucyl/cystinyl aminopeptidase (LNPEP)	2 (4)	2.73	0.6625	± 0.1899	0.0814	1.6598	1 (12) *	1.46	0.9762	± 0.2302	0.8547	1.3205
LEVEL 3													
Q13425	Beta-2-syntrophin; *Dystrophin-associated protein A1*	2 (3)	4.81	0.6275	± 0.0464	0.0086	1.2059	N.D.					
Q8TAF6	Acyl-CoA synthetase long-chain family member 4	2 (3)	2.69	0.6921	± 0.0473	0.0021	1.1232	N.D.					
Q14321	High-mobility group box 1 (HMG-1)	4 (9)	13.49	0.6975	± 0.0988	1.324E-05	1.1176	N.D.					
Q9BXA0	C-X-C chemokine receptor type 4 (CXCR4); *CD184 antigen*	2 (2)	5.68	0.7067	(± 0.0422)	0.0085	1.2545	N.D.					
Q9BVA1	Tubulin beta-2B chain	N.D.						9 (93)	31.46	0.6916	± 0.2504	0.022414	1.2733

A: Up-regulated; B: Down-regulated; N.D.: Not-detected; N.A.:Not-applicable.
LEVEL 1: Differentially expressed in 2 experiments
LEVEL 2: Differentially expressed in 1 experiment and detected in 2 experiments
LEVEL 3: Differentially expressed in 1 experiment and detected in 1 experiment only
iTRAQ protein ratios (mz 117/114) were calculated by ProteinPilot software (v.2.0) based on the weighted average *Log ratios* of peptides;
and *ratio values* were corrected for experimental bias using the median average protein *ratio* as the correction factor.
Standard deviation ± S.D. were calculated from ratio values at *n* count ≥ 3, and *range* (± range) at *n* count = 2 **by** MicrosoftExcel software (v 11.2.3)
Significance of iTRAQ *protein ratios* is expressed as *p-value* calculated by ProteinPilot software (v.2.0)
Accuracy of i*TRAQ protein ratios* was assessed by the *error factors values* (EF), calculated by ProteinPilot software (v.2.0).
All peptides for identification and quantification of candidate proteins are listed in supplemental Table 2
For protein identification with *unique-peptide**, the annotated spectra are provided in supplemental Table 3

SUPPLEMENTAL

Proteomic analysis of enriched lysosomes at early phase of camptothecin-induced apoptosis in human U-937 cells

Nicolas Parent, Eric Winstall, Myriam Beauchemin, Claudie Paquet, Guy G. Poirier and Richard Bertrand

SUPPLEMENTAL Figure 1

SUPPLEMENTAL Table 1

SUPPLEMENTAL Table 2

SUPPLEMENTAL Table 3

SUPPLEMENTAL Table 4

SUPPLEMENTAL FIGURE 1

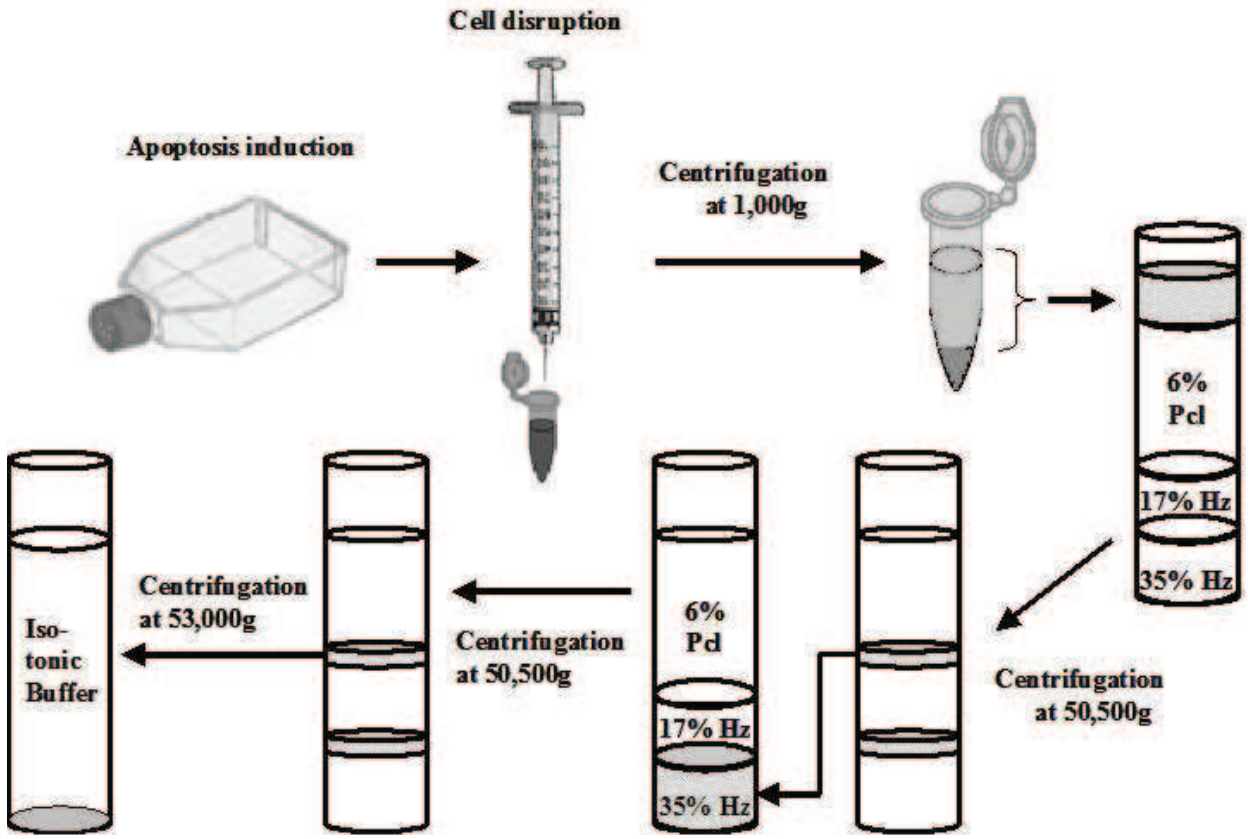

Schematic representation of the 2-step sequential density gradient procedure for preparation of enriched-lysosome fractions. Details are in *Experimental Procedures*.
Abbreviations are: Pcl, Percoll; Hz, histodenz.

SUPPLEMENTAL TABLE 1:
Listing of all proteins (313) indentified by more than 1 peptide in a reference experiment

GTP binding (7.9 %)

ACCESSION NUMBER	IDENTIFICATION	*unique* peptide	*total count*	% Cov	Ratio	± S.D.	P-Value	EF
P61204	ADP-ribosylation factor 3	2	3	11.60	1.0656	± 0.1206	0.286724865	1.154640317
UPI000006F0E6	ADP-ribosylation factor 6 interacting protein	2	5	4.14	1.3178	± 0.3187	0.44010219	18.21539879
Q9NVJ2	ADP-ribosylation factor-like protein 8B	5	36	31.18	0.7453	± 0.1574	5.15E-09	1.079476714
Q14344	Guanine nucleotide-binding protein, alpha-13 subunit	4	23	9.81	0.9514	± 0.1407	0.587433875	1.236842394
UPI0000F0A512	Guanine nucleotide-binding protein G(k) subunit	8	139	23.14	1.0159	± 0.2444	0.917421341	1.489065886
P04899	Guanine nucleotide-binding protein G(i), alpha-2 subunit	11	140	36.05	0.9466	± 0.2416	0.249151379	1.099268198
P62873	Guanine nucleotide-binding protein G(I)/G(S)/G(T) subunit beta 1	4	9	15.00	0.9654	± 0.1409	0.661128283	1.205447912
P62879	Guanine nucleotide-binding protein G(I)/G(S)/G(T) subunit beta 2	4	8	15.00	0.928	± 0.1078	0.083054177	1.091371775
P46940	Ras GTPase-activating-like protein IQGAP1	15	52	11.70	1.0943	± 0.3349	0.057226766	1.097498178
UPI000020CB2C	Ras GTPase-activating-like protein IQGAP2	4	11	3.80	0.9781	± 0.1270	0.772133946	1.248786926
UPI0000D611AF	Ras-related protein Rab-1A	4	20	30.71	0.8922	± 0.1946	0.000196659	1.048234105
Q9H0U4; Q6FIG4	Ras-related protein Rab-1B	4	26	21.39	1.1083	± 0.1691	N.D.	N.D.
UPI0000456691	Ras-related protein Rab-1C (Rab-35)	2	5	12.95	1.0439	± 0.0821	0.169161037	1.160516262
P51149	Ras-related protein Rab-7A	3	5	17.87	0.832	± 0.1042	0.042881776	1.190392137
P61006	Ras-related protein Rab-8A	2	8	12.07	1.0143	± 0.1276	0.54550612	1.055982709
P61026	Ras-related protein Rab-10	3	55	14.50	0.9635	± 0.2135	0.406632721	1.093530893
UPI0000132EC2	Ras-related protein Rab-11B	4	7	17.88	0.8408	± 0.0797	0.000592852	1.075786471
Q6IAS8	Ras-related protein Rab-27A	2	2	9.05	0.8218	(± 0.0506)	0.148011222	1.804259539
P11233	Ras-related protein Ral-A	4	15	19.90	1.0349	± 0.0578	0.204978645	1.060870647
Q5U0C3	Ras-related protein Rap-1A	5	56	20.10	0.9593	± 0.1933	0.206789806	1.067233562
P63000	Ras-related C3 Botulinum Toxin Substrate 1	3	7	17.18	1.1230	± 0.1668	0.000379681	1.078164816
Q53HM4	Ras homolog gene family, member A variant	5	9	18.13	1.2321	± 0.3169	0.000252395	1.102262616
UPI000049DEE3	Rho-associated protein kinase 2	2	2	1.29	0.9484	(± 0.0689)	0.88688755	4.119484901
P84095	Rho-related GTP-binding protein RhoG	3	4	25.13	0.8815	± 0.2105	0.307394534	1.386685729
UPI0000EFE353	Small GTP binding protein CDC42	5	34	31.41	1.006	± 0.1871	0.899345398	1.115411043

Vesicular and protein trafficking (8.9 %)

ACCESSION NUMBER	IDENTIFICATION	*unique* peptide	*total count*	% Cov	Ratio	± S.D.	P-Value	EF
UPI0000456CFE	Adapter-related protein complex 2 alpha 1 subunit	3	6	2.19	0.746	± 0.1758	0.262132317	2.259866953
UPI0000456A83	Adapter-related protein complex 2 beta 1 subunit	2	6	2.72	0.9854	± 0.2672	0.875606537	1.224721074
UPI00004571AB	Adapter-related protein complex 2 mu 1 subunit	2	4	6.89	0.8436	± 0.0360	0.000767679	1.052484274
P28838	Aminopeptidase	2	7	5.94	1.1643	± 0.1626	0.035799101	1.148130298
UPI000013D9C8	Armet protein precursor	2	7	13.67	1.2371	± 0.1862	0.002113307	1.122318149
UPI000013D798	Beta-hexosaminidase alpha chain precursor (EC 3.2.1.52)	3	4	5.67	1.0281	± 0.1019	0.710861087	1.323143005
P27824	Calnexin precursor	14	107	27.7	1.073	± 0.1942	0.000557733	1.039771914
P27797	Calreticulin precursor	9	38	20.83	1.3521	± 0.2573	1.38E-15	1.056571245
UPI00001FB052	Carboxypeptidase D precursor	2	2	0.51	0.9401	(± 0.1385)	1.59E-01	1.100624204
Q00610-2	Clathrin heavy chain 1 isoform 2	13	45	12.14	0.8778	± 0.2150	0.00787386	1.098753572
Q8IXZ9	Coatomer protein complex, alpha subunit	2	8	2.18	1.0824	± 0.2147	0.101524264	1.100403666
Q96A65	Exocyst complex component 4	2	8	2.87	0.8767	± 0.2388	0.155735776	1.211758494
O14745	Ezrin-radixin-moesin binding phosphoprotein 50 (EBP50)	9	39	25.97	1.1662	± 0.1501	7.26E-09	1.044194102
Q8NBJ4	Golgi membrane protein 1	3	3	9.98	0.8246	± 0.0614	0.21292755	1.475596547
P37235	Hippocalcin-like protein 1	3	8	16.06	1.0592	± 0.1527	0.113148913	1.108047009

A4D229	KIAA1228 protein (calcium binding)	5	9	5.37	1.0156	± 0.1840	0.80065161	1.147312641
P16150	Leukosialin precursor	4	25	13.75	1.0832	± 0.1108	0.06499505	1.059543848
UPI0000456FBC	Neuroendocrine secretory protein 55	2	2	4.18	0.9288	(± 0.2779)	0.510022521	1.327775598

Q10471	Polypeptide N-acetylgalactosaminyltransferase 2 (EC 2.4.1.41)	2	2	3.33	0.6820	(± 0.1356)	0.017632749	1.313616157
Q9HD89	Resistin precursor	2	16	17.59	1.0587	± 0.1374	0.134196445	1.078703523
Q7L7Q6	RTN4 protein	4	22	13.13	1.0048	± 0.1213	0.884903908	1.070528746
UPI00004DF217	Synapse-associated protein 97	2	3	2.35	0.9942	± 0.0632	0.892826974	1.176968455
Q12846	Syntaxin-4	2	7	8.41	0.9829	± 0.4440	0.883267641	1.299681067
Q9UNK0	Syntaxin-8	2	2	5.93	1.1542	(± 0.1466)	0.37852639	3.430858612
UPI0000161DE1	Syntaxin-7	2	7	9.19	1.0015	± 0.1321	0.98276329	1.180761933
Q12907	Vesicular integral-membrane protein VIP36 precursor	3	3	7.58	1.0695	± 0.1576	0.4330993	1.224867344
Q9BV40	Vesicle-associated membrane protein 8	5	36	41.00	1.11	± 0.2108	0.007313321	1.077425957
Q99536	Vesicle membrane protein VAT-1 homolog	2	4	5.34	0.9277	± 0.0911	0.155827835	1.126749039

Membrane / glucoside / lipid (12.3 %)

ACCESSION NUMBER	IDENTIFICATION	*unique* peptide	*total count*	% Cov	Ratio	± S.D.	P-Value	EF
P04083	Annexin A1	6	93	21.38	0.9566	± 0.3980	0.452989429	1.124497294
Q8TBV2	Annexin A2	18	164	51.91	0.8783	± 0.1464	7.54E-13	1.033630133
Q6P452	Annexin A4	3	117	12.37	0.8834	± 0.1854	0.151538342	1.199697375
P08758	Annexin A5	11	108	40.00	0.8269	± 0.2549	0.000216733	1.102268815
P08133	Annexin A6	30	491	53.34	0.8236	± 0.1633	6.11E-43	1.025136709
Q59EP1	Annexin A11	5	124	9.61	1.0187	± 0.1847	0.687671363	1.099552035
Q53HM8	Annexin VII isoform 1 variant	3	9	7.08	0.9406	± 0.1571	0.322606504	1.138025165
UPI0000190976	ASAH1 protein N-acylsphingosine amidohydrolase (acid ceramidase)	15	67	32.62	1.216	± 0.3966	0.000289124	1.107608438
P35613	Basigin precursor	6	30	15.32	0.9779	± 0.0821	0.261229247	1.040632963
UPI000003BC43	Beta-Glucuronidase	2	4	3.37	0.9815	± 0.1117	0.783967257	1.219124079
UPI000013D183	Beta-Hexosaminidase Beta Chain	7	12	10.61	0.9872	± 0.0687	0.545310318	1.046113849
Q99439	Calponin-2	2	3	8.73	1.3265	± 0.2302	0.028135832	1.271610618
Q99829	Copine I (phospholipid binding protein)	5	20	12.10	0.8295	± 0.2134	0.020934353	1.167599797
Q96FN4	Copine -2	2	23	4.38	1.1362	± 0.0975	0.039539531	1.126044869
O75131	Copine-3	4	23	8.00	0.982	± 0.0844	0.753427446	1.144200325
Q5VWA5	Dolichyl-diphosphooligosaccharide-protein glycosyltransferase	3	3	3.95	0.9608	± 0.0652	0.28704676	1.084081769
UPI0000D61084	Dolichyl-diphosphooligosaccharide--protein glycosyltransferase precursor	6	11	19.86	1.1872	± 0.2598	0.054096263	1.191600323
Q6IB58	Flotillin 1	3	5	5.62	0.8366	± 0.2239	0.433275819	2.200513601
UPI00001AE777	Flotillin-2	4	13	10.51	0.9158	± 0.1741	0.109986126	1.117038608
UPI00001AEC37	Ganglioside GM2 activator precursor (GM2-AP) (Sphingolipid acid)	4	7	9.32	1.2179	± 0.2210	0.019111447	1.168135047
UPI000049DDA7	Lysosomal-associated membrane glycoprotein-1	5	35	12.53	1.1659	± 0.1623	0.000150146	1.078181267
P13473-2	Lysosomal-associated membrane protein isoform 2	5	95	9.26	1.1518	± 0.1957	4.43E-10	1.041813135
Q16891-3	Mitofilin p87/p89 isoform 3	6	10	8.12	0.9145	± 0.1526	0.158382699	1.139526248
Q53HV6	Niemann-Pick disease, type C2 variant	4	14	30.46	1.304	± 0.1531	7.37E-06	1.080326796
Q92542	Nicastrin	3	4	4.37	0.9528	± 0.1020	0.458700538	1.198634505
UPI000013D53C	N(4)-(beta-N-acetylglucosaminyl)-L-asparaginase precursor	2	7	3.76	1.4754	± 0.5509	0.015410207	1.339689851
P30086	Phosphatidylethanolamine-binding protein (PEBP)	2	3	11.22	1.109	± 0.1057	0.23881191	1.307700396
Q9UMY2	3-Phosphoglycerate dehydrogenase	4	24	13.33	0.9545	± 0.3092	0.560873806	1.176116228
UPI00006C12C9	Phosphoglycerate mutase 1	2	3	12.28	1.0196	± 0.1523	0.882140994	1.468520045
Q5JQ37	Prosaposin (Variant Gaucher disease)	4	17	4.29	1.6085	± 0.1582	4.10E-09	1.096046567
Q8N5I0; Q14699	RFTN1 protein	3	3	3.19	0.9403	± 0.2085	0.565615237	1.31363225
P37268	Squalene synthetase	2	2	5.51	0.7196	(± 0.1861)	0.317859828	9.775856972
Q15738	Sterol-4-alpha-carboxylate 3-dehydrogenase, decarboxylating	4	6	16.08	1.0941	± 0.5346	0.58935374	1.473100066
P27105	Stomatin (7.2b)	10	93	20.13	1.1924	± 0.3772	0.013182091	1.147223234
P06703	S100-A6 protein	2	37	16.66	1.0152	± 0.1150	0.636699915	1.065685153

UPI00001D6EC0	Transmembrane emp24 domain containing protein 9 precursor	2	3	12.76	0.7999	± 0.0457	0.436343342	2.704771042
Q9BTV4	Transmembrane protein 43	3	6	7.75	0.7847	± 0.1449	0.021921966	1.20918262
UPI0000D61230	UDP-glucose ceramide glucosyltransferase-like 1	2	4	1.73	1.1412	± 0.1143	0.536215901	1.636914134

ACCESSION NUMBER	Channel/Transporter (6.4 %) IDENTIFICATION	*unique* peptide	*total count*	% Cov	Ratio	± S.D.	P-Value	EF
Q13884	Beta-1-syntrophin	3	3	5.76	0.7641	± 0.0794	0.055135615	1.32791841
P31949	Calgizzarin (Protein S100-A11)	4	81	34.28	1.1044	± 0.1822	2.43E-05	1.046087265
Q5T0B3	Cation-transporting ATPase	4	7	5.47	0.963	± 0.0825	0.360331863	1.100980759
Q59EV6	Carrier family 6 , member 8 variant	3	7	4.42	0.9784	± 0.1098	0.656707883	1.113237381
O00299	Chloride intracellular channel protein 1	7	49	51.03	1.2567	± 0.2283	2.15E-08	1.073123693
Q9Y696	Chloride intracellular channel protein 4	5	11	28.85	1.0932	± 0.5120	0.332645506	1.212293386
Q14974	Importin beta-1 subunit	3	13	5.02	0.9548	± 0.2384	0.536153674	1.171120644
UPI0000D61A8F	Importin beta-3	3	10	3.83	0.8869	± 0.3200	0.392638505	1.390682817
P53985	Monocarboxylate transporter 1	3	10	4.21	1.0264	± 0.1527	0.623299241	1.121728897
O15427	Monocarboxylate transporter 4	3	15	6.02	1.1995	± 0.2257	0.002991302	1.115041256
Q71UA6	Neutral amino acid transporter	4	35	10.53	0.8554	± 0.2239	0.003684097	1.107174277
Q6ZNE4	Potassium channel beta2 subunit (highly similar)	2	9	7.5	0.9659	± 0.2100	0.684381843	1.213202715
P05023	Sodium/potassium-transporting ATPase alpha-1 chain precursor	17	65	21.4	0.8754	± 0.1048	7.26E-10	1.038680434
P54709	Sodium/potassium-transporting ATPase beta-3 chain	9	40	24.73	0.9837	± 0.1971	0.554208338	1.056653261
Q53F03	Solute carrier family 1, member 4 variant	2	5	8.45	0.8347	± 0.1854	0.117377713	1.278584719
Q59GX2	Solute carrier family 2 (Facilitated glucose transporter)	2	10	3.48	1.0837	± 0.1738	0.223295689	1.150922537
Q8TDB8-2	Solute carrier family 2 (Facilitated glucose transporter) isoform 2	2	5	4.02	1.0839	± 0.0913	0.107758693	1.114374638
UPI00004EC299	solute carrier family 3 member 2 isoform e	13	51	25.52	0.9344	± 0.1961	0.067463763	1.075657129
Q6NVC0	Solute carrier family 25 (Adenine nucleotide translocator 2)	6	12	15.48	0.7166	± 0.1254	1.27E-06	1.098781943
Q9ULF5	Zinc transporter ZIP10 precursor	2	3	2.16	1.0678	± 0.0725	0.288309097	1.160557508

Structural / cytoskeleton / adhesion proteins (16.9 %)

ACCESSION NUMBER	IDENTIFICATION	*unique* peptide	*total count*	% Cov	Ratio	± S.D.	P-Value	EF
P68133	Actin alpha	11	437	27.85	1.0483	± 0.3932	0.338890076	1.121589065
P61158	Actin-like protein 3	3	11	6.69	0.9657	± 0.2037	0.698726296	1.222094297
UPI00006C0D04	Actin-related protein 2/3 complex subunit 1B	2	5	9.46	1.0493	± 0.0905	0.354574263	1.130828977
Q53G99	Actin beta variant	19	820	62.4	0.9934	± 0.3448	0.692229688	1.033056378
UPI00004EC29C	AHNAK nucleoprotein isoform 1	33	179	17.81	1.0858	± 0.0954	2.53E-30	1.01304388
Q1HE25	Alpha-actinin 1 isoform b	19	120	24.39	0.9432	± 0.1728	0.164130345	1.086812377
O43707	Alpha-actinin 4	31	148	39.95	1.0296	± 0.1609	0.131628692	1.038963914
P23528	Cofilin 1	9	30	54.20	1.082	± 0.2633	0.001486671	1.048451781
P31146	Coronin, actin binding protein, 1a variant	10	68	15.61	1.2514	± 0.1765	2.60E-20	1.036808848
Q59EA2	Coronin, actin binding protein, 1c variant	3	6	1.59	1.2986	± 0.2335	0.053825345	1.312521219
UPI0000D6223F	Cytoskeleton-associated protein 4	8	28	12.01	0.9908	± 0.1570	0.795187414	1.074196219
Q99497	Dj-1	2	4	22.22	1.0358	± 0.1532	0.837273002	5.543426514
Q0H395; O75923	Dysferlin	3	4	0.72	0.8598	± 0.1286	0.020911191	1.126263857
Q60FE6	Filamin A, alpha	49	202	25.27	1.2099	± 0.1949	2.14E-33	1.026326895
UPI0000457129	Filamin B, beta	9	28	3.76	1.0465	± 0.1540	0.472755671	1.145428181
O00291	Huntingtin-interacting protein 1	2	2	3.2	0.9593	(± 0.0337)	0.717142224	1.344538212
P08648	Integrin alpha-5 precursor	3	7	3.81	0.8322	± 0.1156	0.016779577	1.146729112
UPI000014ACA2	Integrin alpha-L precursor	2	4	1.96	0.7378	± 0.1053	0.025440345	1.262514949
Q6PJ75	Integrin beta	9	25	13.32	0.9379	± 0.2699	0.144066378	1.090899706
UPI0000160C2A	Integrin-beta 1 isoform c precursor	6	12	10.66	0.8804	± 0.1588	0.00246153	1.078623176
Q08722	integrin-associated protein (CD47 precursor)	2	17	5.88	0.8864	± 0.0736	5.38E-06	1.040569067
P05362	Intercellular adhesion molecule 1	5	6	11.46	1.0003	± 0.0918	0.995376825	1.16271162
Q6PD68	Intercellular adhesion molecule 3 precursor	2	5	3.11	1.0661	± 0.1082	0.213376448	1.127750635
Q5TBN4	L-plastin (Lymphocyte cytosolic protein 1)	19	71	35.09	1.0918	± 0.1606	0.000278379	1.047064066

UPI0000207FB5	LIM domains containing protein 1 (PINCH-1)	4	4	10.33	1.2447	± 0.4331	0.289047778	1.719777942
Q8WWI1	LIM domain only protein 7	2	3	1.66	1.0615	± 0.2183	0.685680926	1.731330276

P40121	Macrophage capping protein	6	28	22.41	1.1178	± 0.1658	2.68E-05	1.048765659
UPI000000DB01	Metadherin	2	15	3.95	0.7604	± 0.0980	4.93E-06	1.085598111
P26038	Moesin	33	359	43.67	1.1214	± 0.1439	1.30E-21	1.022394419
UPI00001D747C	Myosin IG	18	72	20.72	0.9122	± 0.1447	0.000336057	1.049814343
P35579	Myosin-9	21	86	12.55	1.0164	± 0.2303	0.556759775	1.056615233
Q96TA1	Niban-like protein	2	2	3.95	1.0603	(± 0.2599)	0.611758053	1.3446244
UPI0000457913	Plectin 1 (PLTN) (PCN) (Hemidesmosomal protein 1) (HD1)	6	6	1.65	1.0215	± 0.4511	0.797836244	1.189557076
P07737	Profilin 1	6	36	42.85	1.0208	± 0.1856	0.533237517	1.068657994
UPI00002263A8	Sorcin isoform b	3	6	10.93	1.4086	± 0.2776	0.0078554	1.238895297
Q13813-2	Spectrin alpha chain isoform 2	24	121	15.87	1.0786	± 0.2879	0.002880606	1.049997091
UPI0000D611A2	Spectrin beta chain, brain 1	18	38	8.70	1.0478	± 0.2787	0.272203714	1.088178515
P16949	Stathmin	6	18	34.23	1.0283	± 0.2202	0.463857919	1.080453992
UPI0000167B7F	Talin 1	11	70	6.7	0.816	± 0.1764	1.52E-06	1.078251481
UPI00001FE5FC	Talin 2 (TLN2)	7	27	4.64	0.8416	± 0.2758	0.184908137	1.304717541
UPI000020489E	Tropomyosin alpha 3 chain (Tropomyosin 3)	16	100	43.14	1.1939	± 0.1180	9.53E-15	1.035155892
P67936	Tropomyosin alpha 4 chain (Tropomyosin 4)	8	57	22.18	1.0297	± 0.1248	0.604928195	1.176033974
Q9BQE3; Q53GA7	Tubulin alpha-1C chain	10	104	24.72	0.9305	± 0.1913	N.D.	N.D.
P68363	Tubulin alpha-1 beta chain	11	98	28.38	0.8514	± 0.1681	0.004770451	1.108509541
P07437	Tubulin beta-2 chain	10	98	37.61	0.9326	± 0.2508	0.17868343	1.108967781
Q9BVA1	Tubulin beta-2b chain	9	93	31.46	0.6916	± 0.2504	0.022413997	1.273266315
Q8IWP6	Tubulin Class IVb beta	8	95	28.08	0.9926	± 0.2459	0.919574201	1.194827676
Q5SZ57	Utrophin	8	15	2.56	0.9724	± 0.1912	0.648127437	1.137969017
UPI0000D61508	Villin 2 (Erzin)	20	123	25.46	1.1794	± 0.3165	0.003169264	1.113456249
UPI00004A0D4A	Vimentin	9	34	20.88	1.1579	± 0.2896	8.55E-05	1.07134366
P18206-2	Vinculin Isoform 2	2	27	3.01	0.796	± 0.1216	0.010720001	1.165278077
UPI0000139021	XRP2 protein	2	4	4.86	0.9528	± 0.0696	0.31978029	1.137751102
Q15942	Zyxin	2	6	6.81	1.0912	± 0.0620	0.071036756	1.10657537

Hydrolase / peptidase / isomerase (6.1 %)

ACCESSION NUMBER	IDENTIFICATION	*unique* peptide	*total count*	% Cov	Ratio	± S.D.	P-Value	EF
Q1RMG2; P23526	Adenosylhomocysteinase	2	2	9.15	0.8673	(± 0.0256)	9.36E-02	1.306974649
Q59E93	Alanine aminopeptidase membrane variant	12	79	16.58	0.8196	± 0.2124	6.49E-07	1.075279593
UPI000054B38F	Carboxylesterase 1 isoform c precursor	6	15	12.01	1.5551	± 0.1927	1.23E-09	1.074197888
P07339	Cathepsin D precursor (EC 3.4.23.5)	11	128	30.34	0.9515	± 0.1845	0.007897845	1.036826134
P08311	Cathepsin G precursor	8	98	31.37	0.9394	± 0.1198	5.08E-05	1.029682279
UPI000013C5C2	Cystatin F	2	24	11.97	0.9326	± 0.1557	0.000906597	1.038604736
Q9UHL4	Dipeptidyl-peptidase 2 precursor	3	5	6.09	1.0749	± 0.1593	0.412850827	1.245677352
Q2Z2K8	Endothelin-converting enzyme 1c	3	6	6.89	0.8191	± 0.2729	0.284744591	1.566486001
P19440	Gamma-glutamyltranspeptidase 1 precursor (EC 2.3.2.2)	3	9	4.74	0.9297	± 0.1071	0.106785923	1.095553994
P08246	Leukocyte elastase precursor	2	10	3.74	1.0235	± 0.0702	0.281106055	1.045311928
UPI000013DB9E	Lysosomal alpha-glucosidase II	5	10	7.45	1.23	± 0.2208	0.002619215	1.125053167
P15586	N-acetylglucosamine-6-sulfatase precursor	4	10	6.88	1.1259	± 0.1315	0.059379306	1.132350087
P62937	Peptidyl-Prolyl Cis-Trans Isomerase A	6	47	35.75	1.0429	± 0.2090	0.04640862	1.042241096
Q6IBH5	Peptidyl-Prolyl cis-trans isomerase	7	42	31.48	1.2073	± 0.2179	3.76E-08	1.059878469
Q4VB08	Proteinase 3	4	58	20.70	0.7606	± 0.1527	2.64E-16	1.051420212
UPI0000456547	Signal peptidase complex subunit 2	2	5	4.02	1.6131	± 0.3741	0.01477547	1.381639838
P40939	Trifunctional enzyme alpha subunit	4	9	4.98	0.9809	± 0.1096	0.898776054	1.412520409
P60174-2	Triosephosphate isomerase isoform 2	2	3	18.88	1.2189	± 0.1009	0.06094547	1.246791482

UPI0000D625AE	Tripeptidyl-peptidase I precursor	3	15	8.64	1.0981	± 0.2098	0.235790983	1.175233603

ACCESSION NUMBER	IDENTIFICATION	*unique* peptide	*total count*	% Cov	Ratio	± S.D.	P-Value	EF
Receptor / Signal transduction (9.2 %)								
P30533	Alpha-2-macroglobulin receptor-associated protein precursor	5	5	25.56	1.3716	± 0.2304	0.007845682	1.230027914
Q9BUB1	cAMP-dependent protein kinase type II-alpha regulatory subunit	2	4	7.06	1.088	± 0.5794	0.736762524	2.071506977
Q9BRL5	Calmodulin3	4	97	11.56	1.1896	± 0.1482	4.02E-21	1.030591846
Q9UBC2; A2RRF3	Epidermal growth factor receptor substrate 15-like 1	2	3	0.92	1.0168	± 0.0903	0.617660224	1.362272024
Q4LE83	FASN variant protein	3	7	1.72	0.8987	± 0.2853	0.494402021	1.483668089
Q13418	Integrin-linked protein kinase 1	4	7	11.06	1.0173	± 0.2030	0.819246113	1.192229867
Q6NUK7	LYN protein	4	13	6.7	0.8841	± 0.1374	0.293248922	1.327100992
P14174	Macrophage migration inhibitory factor	1	16	7.83	1.4427	± 0.1522	1.85E-11	1.04828918
O00264	Membrane-associated progesterone receptor component 1	4	4	20.51	1.2066	± 0.1476	0.002146448	1.109373808
Q32Q12	Nucleoside diphosphate kinase	2	6	9.93	0.9354	± 0.1154	0.557998538	1.301000714
UPI0000130EB3	Osteoclast stimulating factor 1	3	14	13.08	1.0884	± 0.1669	0.097671606	1.107313514
Q9BTU6	Phosphatidylinositol 4-kinase type 2-alpha	2	4	4.59	0.8024	± 0.1955	0.177919179	1.454055786
UPI000006FDE7	Phosphatidylinositol glycan anchor biosynthesis, class G	2	4	3.18	1.0527	± 0.5497	0.900824785	4.800426483
Q8WUM4	Programmed cell death 6-interacting protein	2	7	2.99	1.0139	± 0.1053	0.85278523	1.214652419
P05771	Protein kinase C, beta type	3	7	5.05	0.9878	± 0.1562	0.830854356	1.133706927
Q05655	Protein kinase C, delta	3	9	5.77	1.2469	± 0.2035	0.002644603	1.134025693
Q6NSK0	Serine/threonine protein kinase 10	2	3	2.17	1.2641	± 0.2472	0.092338152	1.357172728
P30153	Serine/threonine protein phosphatase 2A (65 kDa subunit A alpha)	5	15	11.54	0.8682	± 0.2283	0.061765786	1.160838246
Q07161	Serine/threonine protein phosphatase type 1 catalytic subunit	2	8	6.45	0.9996	± 0.2742	0.997333944	1.275875926
P26447	S100 calcium-binding protein A4	4	58	35.64	1.2254	± 0.1454	1.21E-16	1.037096143
UPI0000073ADE	Signal regulatory protein alpha precursor	3	4	7.34	1.0411	± 0.0965	0.310318738	1.096284151
UPI000016789F	Signal sequence receptor, alpha	2	14	5.24	1.0801	± 0.2115	0.309557885	1.17588377
UPI000013D3E3	TAGLN2 protein	4	12	15.45	1.2736	± 0.1517	0.000134014	1.100362301
UPI0000136C97	Transferrin receptor	2	5	3.28	0.9646	± 0.4082	0.866854668	1.748900771
UPI00004709D1	Tyrosine protein kinase HCK	3	11	4.36	0.9031	± 0.4518	0.120792612	1.282476544
P31946-2	14-3-3 protein beta/alpha short isoform	4	71	18.44	1.0114	± 0.1237	0.863442302	1.214345098
P62258	14-3-3 protein epsilon	4	73	19.21	0.9303	± 0.1165	0.087127857	1.092887998
P61981	14-3-3 protein gamma	4	110	18.22	0.9595	± 0.1796	N.D.	N.D.
P63104	14-3-3 protein zeta/delta	4	75	18.36	0.8319	± 0.1299	0.127666578	1.283513665

Redox / Stress protein / Chaperone / Ubiquitin (10.0 %)

ACCESSION NUMBER	IDENTIFICATION	*unique* peptide	*total count*	% Cov	Ratio	± S.D.	P-Value	EF
Q9UNM1	Chaperonin 10-related protein	5	8	39.17	1.1734	± 0.1517	0.000539935	1.083340883
UPI00004CA9C4	Chaperonin containing TCP1, subunit 3 isoform	2	2	3.67	0.7971	(± 0.0309)	0.015160687	1.12918961
Q59ET3	Chaperonin containing TCP1, subunit 6A isoform	2	10	7.18	0.9831	± 0.2118	0.891955435	1.321945548
P61088	E2N Ubiquitin-conjugating enzyme	2	2	6.57	0.9963	(± 0.0506)	0.936191082	1.581386209
UPI0000D626C3	E3 ubiquitin-protein ligase HUWE1	2	3	0.62	0.9887	± 0.0745	0.904623806	1.278121829
P30040	ERp29 precursor	2	5	8.43	1.9656	± 0.5804	0.007619987	1.457954884
P78417	Glutathione transferase omega-1	2	3	3.19	1.0508	± 0.0957	0.330506116	1.146064281
Q2KHP4	Heat shock protein A5	19	139	32.67	1.322	± 0.2174	8.37E-37	1.032420516
P04792	Heat-shock protein Beta-1	3	4	14.14	0.9668	± 0.0621	0.409459174	1.118551016
UPI000013D97A	Heat shock protein 60 kDa	11	58	20.34	1.0138	± 0.3050	0.780431688	1.103503346
UPI000013CB7C	Heat shock protein 70kDa protein 1A	4	156	6.08	0.9664	± 0.1854	0.445044637	1.111575842
Q53H23	Heat shock protein 70kDa protein 9B variant	3	4	5.59	0.8836	± 0.0076	0.031869341	1.081920981
P11142	Heat shock protein 71 kDa protein	15	87	34.36	0.8888	± 0.1850	0.000186889	1.061069727
P07900-2	Heat shock protein 90 kDa isoform 1	11	28	12.19	0.8813	± 0.0979	0.006225117	1.083816648
UPI00001AE8D8	Heat shock protein 90 kDa beta	21	48	14.53	0.908	± 0.1564	0.015486835	1.079659581

Q04760	Lactoylglutathione lyase	6	59	27.71	1.089	± 0.1541	7.46E-05	1.04133594
Q9Y4L1	Oxygen/hypoxia-regulated protein precursor 150 kDa	2	2	2.21	1.299	(± 0.0628)	0.094761364	1.646378994

Q06830	Peroxiredoxin 1	5	11	25.13	1.1125	± 0.0710	0.007467468	1.07277894
P32119	Peroxiredoxin 2	3	6	18.68	0.8809	± 0.1832	0.615829468	10.34654903
P07237	Protein disulfide-isomerase precursor	28	230	50.00	1.4980	± 0.3184	0	1.032472253
P30101	Protein disulfide-isomerase A3 precursor	11	61	22.18	1.508	± 0.2409	1.03E-24	1.053023815
P13667	Protein disulfide-isomerase A4 precursor	7	18	9.61	1.4885	± 0.3662	1.18E-06	1.128838062
Q15084-2	Protein disulfide-isomerase A6 isoform 2	5	26	16.05	1.3934	± 0.3512	3.51E-06	1.125249386
Q6IBR0	RPN1 protein	12	85	22.24	0.9913	± 0.2336	0.770216763	1.060082316
P00441	Superoxide dismutase 1, (SOD1 protein).	5	28	44.80	1.2979	± 0.1782	2.94E-08	1.07986629
P10599	Thioredoxin-1	2	9	12.38	1.0433	± 0.0761	0.193051502	1.068310738
Q9H3N1	Thioredoxin domain-containing protein 1 precursor	3	6	7.14	1.1276	± 0.1715	0.206129342	1.247513652
O95881	Thioredoxin domain-containing protein 12 precursor (Erp19)	2	4	13.37	1.6015	± 0.2738	0.017047642	1.364967704
P78371	T-complex protein 1, beta subunit	2	19	5.61	0.9825	± 0.4766	0.82740587	1.18130815
P50991	T-complex protein 1, delta subunit	2	3	4.82	0.8317	± 0.2592	0.137318656	1.307233334
Q3MIH3	Ubiquitin A-52 residue ribosomal protein fusion product 1	4	39	25.56	1.0238	± 0.1715	0.342209309	1.050599337

Metabolism (7.0 %)

ACCESSION NUMBER	IDENTIFICATION	*unique* peptide	*total count*	% Cov	Ratio	± S.D.	P-Value	EF
Q5TIF8	Adenylate kinase 2, isoform b	3	9	23.27	1.3981	± 0.7322	0.045315851	1.386056781
UPI0000126EBE	Adenylyl cyclase-associated protein 1	5	15	14.31	0.9463	± 0.1286	0.192202285	1.089208007
P06576	ATP synthase subunit beta chain	6	28	16.06	0.9144	± 0.1465	0.04553286	1.091464877
Q6P666	Cytochrome c oxidase subunit VI isoform 1	2	4	10.66	0.9492	± 0.2139	0.642427742	1.379843712
Q53FT9	Enolase	15	133	43.77	0.9932	± 0.1841	0.745089889	1.041816235
P04075	Fructose-bisphosphate aldolase	7	20	20.87	0.9351	± 0.2660	0.064856529	1.074226737
UPI0000E9BBE7	Galactosidase, beta 1 isoform a	4	14	7.68	1.0919	± 0.1422	0.007199748	1.063044786
P09382	Galectin-1	5	14	31.85	1.1632	± 0.2306	0.011743126	1.117969751
P06744	Glucose-6-phosphate isomerase	7	50	14.15	1.0789		0.164045319	1.11476028
P04406	Glyceraldehyde-3-phosphate dehydrogenase	8	91	28.05	1.0251	± 0.1474	0.407416463	1.060962677
Q53GL5	Isocitrate dehydrogenase 2 (NADP+)	2	2	5.31	0.9335	(± 0.3887)	0.849749863	37.81287384
P00338-2	L-lactate dehydrogenase isoform 2	5	22	21.98	1.0126	± 0.3130	0.882367611	1.195253372
P07195	L-Lactate dehydrogenase B Chain	4	6	13.72	1.1061	± 0.1394	0.438738585	1.572227955
O60488	Long-chain-fatty-acid-CoA ligase 4	4	16	7.31	0.8578	± 0.2201	0.029499248	1.146251678
O00754	Lysosomal alpha-mannosidase precursor (alpha, 2B, member 1)	17	99	4.28	1.1912	± 0.3266	6.27E-06	1.074112773
Q13724	Mannosyl-oligosaccharide glucosidase	2	2	3.94	1.0011	(± 0.2172)	0.991800368	1.506832242
UPI0000161BEA	Methylenetetrahydrofolate dehydrogenase 1	5	8	7.7	0.8914	± 0.1605	0.654567301	1.789166093
Q5T0S6; P50897	Palmitoyl-protein thioesterase 1	2	2	4.31	0.9586	(± 0.1334)	0.741381526	3.484704733
P00558	Phosphoglycerate kinase 1	11	44	29.73	0.9545	± 0.2421	0.174354568	1.070074558
P14618	Pyruvate Kinase, M1/M2 Isozyme	12	34	25.98	0.9361	± 0.1027	0.005927233	1.047216773
UPI000013D771	Sorbitol dehydrogenase	2	2	6.72	1.0224	(± 0.2718)	0.860803902	1.615958929
UPI0000D6185A	TER ATPase (15S Mg(2+)- ATPase p97 subunit	4	14	3.72	0.7254	± 0.1630	0.002043229	1.189064264

DNA / RNA / translation (6.4 %)

ACCESSION NUMBER	IDENTIFICATION	*unique* peptide	*total count*	% Cov	Ratio	± S.D.	P-Value	EF
Q6IPT9	Elongation factor 1-alpha	8	26	23.8	1.084	± 0.2337	0.044904009	1.08191812
UPI000013EDA9	Elongation factor 1 gamma	2	5	4.57	1.0995	± 0.1333	0.151648685	1.171003222
P13639	Elongation factor 2	5	10	6.17	0.9471	± 0.2329	0.658623993	1.308337569
P63241-2	Eukaryotic translation initiation factor 5A variant	3	7	6.52	1.1296	± 0.3372	0.10911525	1.165890932

Q99879	Histone H2B TYPE1-M	3	22	7.08	0.8559	± 0.0798	2.02E-06	1.053041458
UPI00006C029D	Histone H3, family 2 isoform 2	3	15	12.77	0.8091	± 0.0496	4.95E-09	1.052234054
Q0VAS5	Histone H4	3	17	29.12	0.6211	± 0.1101	4.40E-10	1.092552662
UPI0000D61ADF	High-mobility group box 1	4	5	15.1	0.9784	± 0.2616	0.847518921	1.318649292
UPI00001AF3CE	Nucleo binding-2 precursor (DNA-binding protein NEFA)	5	7	9.76	1.2624	± 0.2739	0.003934251	1.149514318

Q9BYG9	Nucleophosmin/B23.2	4	10	14.67	1.2677	± 0.2786	0.01029263	1.180623412
UPI0000D6258B	Nucleosome assembly protein 1-like 4	2	7	6.89	1.06	± 0.2036	0.49684009	1.204914093
Q9H361	Poly(A) binding protein 3	2	6	4.59	1.2726	± 0.3551	0.114602067	1.383806109
P10153	Ribonuclease (Non-secretory)	3	3	19.87	1.1436	± 0.1183	0.439941794	4.098692894
O00584	Ribonuclease T2 precursor	4	8	15.23	1.1768	± 0.1214	0.000140317	1.069809794
Q59GY2	Ribosomal protein 60S L4	2	5	11.97	1.1229	± 0.1597	0.334794015	1.310795069
Q59GX9	Ribosomal protein 60S L5	4	6	14.52	1.0609	± 0.1418	0.356881797	1.156191587
Q9HBB3	Ribosomal protein 60S L6	3	5	8.31	1.1176	± 0.0433	0.067425638	1.129890919
UPI0000D6193A	Ribosomal protein 60S L7a	2	3	12.37	1.2167	± 0.2680	0.29223904	1.81443882
P05387	Ribosomal protein 60S P2	2	19	26.95	1.0334	± 0.1553	0.399815232	1.083583236
Q8N5K1	Zinc finger, CDGSH-type domain 2	3	17	43.7	0.9897	± 0.2384	0.952298045	1.653226733

Immunity (3.7 %)

ACCESSION NUMBER	IDENTIFICATION	*unique* peptide	*total count*	% Cov	Ratio	± S.D.	P-Value	EF
Q53G72	B-cell receptor-associated protein 31	11	60	32.11	1.064	± 0.1244	0.000916595	1.036385536
UPI0000126AFB	Bone marrow Stromal Cell Antigen 1	4	10	17.29	1.0904	± 0.1860	0.116938747	1.118123293
UPI000037848C	CD44 antigen isoform 2	8	27	11.02	1.1749	± 0.1213	2.56E-07	1.04871285
P08575	CD45 antigen	9	26	7.05	0.9966	± 0.1725	0.912026644	1.064027071
UPI0000D4D361	CD63 antigen isoform b	2	16	7.62	1.084	± 0.0636	4.07E-10	1.020315886
P48960-3	CD97 antigen isoform 3 precursor	4	13	18.13	0.9562	± 0.1870	0.482854784	1.140651584
P30498	MHC class I antigen HLA-B78	8	34	25.96	1.0628	± 0.7082	0.629662991	1.298284411
UPI000013F5FF	MHC class1 antigen HLA-G	7	24	22.91	1.2029	± 0.7615	0.219704792	1.359948874
A2RQE0	MHC class I antigen	5	9	26.73	1.1083	± 0.2662	N.D.	N.D.
UPI0000D61696	MHC class II antigen (HLA-DR invariant chain)	2	2	7.09	1.3757	(± 0.2832)	0.084307916	1.53102529
P16284-6	Splice isoform Delta15 of CD31	2	6	3.43	1.1751	± 0.3874	0.212538466	1.327235579
Q5CAQ5	Tumor rejection antigen (Gp96)	7	21	8.72	1.2679	± 0.5207	0.000249467	1.121475935

Miscellaneous / Hypothetical (5.1 %)

ACCESSION NUMBER	IDENTIFICATION	*unique* peptide	*total count*	% Cov	Ratio	± S.D.	P-Value	EF
P80723	Brain acid soluble protein 1	4	12	19.82	1.2007	± 0.1026	5.49E-06	1.058563948
Q6IAT8	B2M protein	4	40	49.57	1.1723	± 0.2895	3.75E-05	1.074123859
P21291	Cysteine and glycine-rich protein 1	4	8	18.13	1.1914	± 0.1357	0.005113306	1.111646771
Q9BSJ8	Family with sequence similarity 62 (C2 domain containing), member A	7	11	7.51	0.9686	± 0.2102	0.667384863	1.172287583
Q92520	FAM3C precursor	2	2	11.45	0.9794	(± 0.3107)	0.958453774	56.64810181
Q96AG4	Leucine-rich repeat-containing protein 59	5	40	19.86	1.3869	± 0.2385	1.72E-09	1.090105653
A4D1W8	Uncharacterized colorectal cancer gene 1	3	4	8.43	1.2426	± 0.1577	0.004716981	1.12231648
A6NGM3	Uncharacterized protein ENSP0000037405	2	4	5.07	0.9486	± 0.1969	0.585781813	1.262311935
A6NHK1	Uncharacterized protein MYL6	5	41	36.53	1.2517	± 0.2420	2.81E-09	1.064784884
A6NDZ0	Uncharacterized protein VAPA	3	11	4.87	1.0191	± 0.1258	0.625154555	1.086708784
Q53GF9	cDNA 5-PRIME end of clone CS0DF013YM24	2	9	11.11	0.9462	± 0.0983	0.326342106	1.12658155
Q86TY5	cDNA clone CS0DI041YE05	3	7	20.66	1.0391	± 0.1095	0.347887546	1.092955351
UPI00001B015C	cDNA FLJ40269 fis, clone TESTI2026597	4	7	5.11	0.7706	± 0.1015	0.005584539	1.14250052
Q8NCJ2	cDNA FLJ90221 fis, clone NT2RM1000462	3	10	12.96	1.007	± 0.4706	0.956046283	1.3341887
Q6ZS74	Hypothetical protein FLJ45773	4	19	17.62	1.1559	± 0.0929	0.007280972	1.093193054
Q9BVC6	Hypothetical protein Transmembrane109 precursor	2	3	8.64	0.8809	± 0.1086	0.071732	1.155658841

i) iTRAQ protein ratios (mz 117/114) were calculated by ProteinPilot software (v.2.0) based on the weighted average *Log ratios* of peptides, and values were corrected for experimental bias using the median average protein ratio as the correction factor.*ii) Standard variation* (S.D.) were calculated from ratio values at *n* count ≥ 3, and range (± range) at *n* count = 2, by MicrosoftExcel software (v 11.2.3)

iii) Significance of change in protein expression is expressed as *p-value* calculated by ProteinPilot software (v.2.0), reporting the probability that the observed ratio is different from 1 by chance.

iv) Accuracy of iTRAQ protein ratios was assessed by the *error factors values (EF)*, calculated by ProteinPilot software (v.2.0). N.D. , not-determined.

SUPPLEMENTAL TABLE 2

Peptide listing for identification and quantification of candidate proteins differentially expressed in enriched lysosome preparations from apoptotic U937 cell

UP10000456547 and UPI000047EFF7 and Q15005 / Signal peptidase complex subunit 2; Microsomal signal peptidase 25 kDa subunit

PEPTIDE SEQUENCE	CONF %	dMass	Prec MW	Prec m/z	Theor MW	Theor m/z	Theor z	Sc	Ratio	% Err
Experiment 1										
LHDSLAIER	99.00	-4.365988E-03	1.196659E+03	5.993369E+02	1.196664E+03	5.993390E+02	2	13	3.8561	7.7993
LHDSLAIER	99.00	-1.012769E-02	1.196653E+03	5.993340E+02	1.196664E+03	5.993390E+02	2	15	3.6720	5.2625
LHDSLAIER	99.00	-3.173271E-02	1.196632E+03	5.993232E+02	1.196664E+03	5.993390E+02	2	14	3.7188	3.9358
IDDKPVK	94.00	1.140282E-02	1.245777E+03	6.238959E+02	1.245766E+03	6.238902E+02	2	12	1.1375	4.1902
WDGSAVK	91.00	-3.106830E-02	1.049544E+03	5.257792E+02	1.049575E+03	5.257947E+02	2	12	1.0581	2.3159
Experiment 2										
LHDSLAIER	99.00	-1.497036E-02	1.196649E+03	5.993315E+02	1.196664E+03	5.993390E+02	2	14	2.0306	6.1889
LHDSLAIER	99.00	-7.768371E-03	1.196656E+03	5.993351E+02	1.196664E+03	5.993390E+02	2	15	1.9004	6.7218
LHDSLAIER	99.00	-1.396671E-02	1.196650E+03	5.993320E+02	1.196664E+03	5.993390E+02	2	15	1.8427	4.8245
LHDSLAIER	99.00	-1.274602E-02	1.196651E+03	5.993326E+02	1.196664E+03	5.993390E+02	2	14	1.7278	6.7976
WDGSAVK	94.00	-1.975770E-02	1.049555E+03	5.257849E+02	1.049575E+03	5.257947E+02	2	12	1.0750	4.0906

P14174 / Macrophage migration inhibitory factor (MIF); Glycosylation-inhibiting factor

PEPTIDE SEQUENCE	CONF %	dMass	Prec MW	Prec m/z	Theor MW	Theor m/z	Theor z	Sc	Ratio	% Err
Experiment 1										
LLCGLLAER	99.00	1.026870E-02	1.176658E+03	5.893364E+02	1.176648E+03	5.893313E+02	2	14	1.5394	5.9425
LLCGLLAER	99.00	5.852476E-02	1.176707E+03	5.893606E+02	1.176648E+03	5.893313E+02	2	13	1.5727	7.2086
LLCGLLAER	99.00	4.205719E-03	1.176652E+03	5.893334E+02	1.176648E+03	5.893313E+02	2	14	1.7098	7.2626
LLCGLLAER	99.00	-4.827110E-03	1.176643E+03	5.893289E+02	1.176648E+03	5.893313E+02	2	13	1.7748	7.3522
LLCGLLAER	99.00	2.141692E-02	1.176670E+03	5.893420E+02	1.176648E+03	5.893313E+02	2	15	1.7445	8.2847
LLCGLLAER	99.00	2.837464E-02	1.176677E+03	5.893455E+02	1.176648E+03	5.893313E+02	2	13	1.7291	10.2224
LLCGLLAER	98.00	-1.597423E-02	1.176632E+03	5.893233E+02	1.176648E+03	5.893313E+02	2	13	1.6904	5.6252
LLCGLLAER	93.00	4.693054E-02	1.176695E+03	5.893548E+02	1.176648E+03	5.893313E+02	2	12	1.5612	8.0512
Experiment 2										
LLCGLLAER	99.00	2.167794E-02	1.176670E+03	5.893422E+02	1.176648E+03	5.893313E+02	2	15	1.4487	10.3487
LLCGLLAER	99.00	-4.500257E-03	1.176644E+03	5.893290E+02	1.176648E+03	5.893313E+02	2	16	1.5158	3.0484
LLCGLLAER	99.00	-5.476779E-03	1.176643E+03	5.893286E+02	1.176648E+03	5.893313E+02	2	16	1.1890	3.6888
LLCGLLAER	99.00	-2.279710E-04	1.176648E+03	5.893312E+02	1.176648E+03	5.893313E+02	2	16	1.4826	4.5391
LLCGLLAER	99.00	7.618666E-03	1.176656E+03	5.893351E+02	1.176648E+03	5.893313E+02	2	16	1.5341	5.0715
LLCGLLAER	99.00	-1.862550E-02	1.176630E+03	5.893220E+02	1.176648E+03	5.893313E+02	2	16	1.4813	2.7945
LLCGLLAER	99.00	-1.801517E-02	1.176630E+03	5.893223E+02	1.176648E+03	5.893313E+02	2	16	1.5118	2.9339
LLCGLLAER	99.00	1.042618E-02	1.176659E+03	5.893365E+02	1.176648E+03	5.893313E+02	2	13	1.2577	13.6418
LLCGLLAER	99.00	7.781330E-03	1.176656E+03	5.893352E+02	1.176648E+03	5.893313E+02	2	14	1.3177	8.4118
LLCGLLAER	99.00	8.025460E-03	1.176656E+03	5.893353E+02	1.176648E+03	5.893313E+02	2	16	1.4157	6.7646
LLCGLLAER	99.00	7.781330E-03	1.176656E+03	5.893352E+02	1.176648E+03	5.893313E+02	2	15	1.4915	6.6438
LLCGLLAER	99.00	1.596852E-02	1.176664E+03	5.893393E+02	1.176648E+03	5.893313E+02	2	15	1.3539	8.6911
LLCGLLAER	99.00	1.145225E-02	1.176660E+03	5.893370E+02	1.176648E+03	5.893313E+02	2	15	1.4259	7.8228
LLCGLLAER	99.00	1.840975E-02	1.176667E+03	5.893405E+02	1.176648E+03	5.893313E+02	2	14	1.5397	9.2506
LLCGLLAER	99.00	1.424800E-02	1.176662E+03	5.893384E+02	1.176648E+03	5.893313E+02	2	15	1.4438	9.4612
LLCGLLAER	96.00	1.457642E-02	1.176663E+03	5.893386E+02	1.176648E+03	5.893313E+02	2	12	1.6234	14.7644

P16949 and A2A2D2 / Stathmin 1/oncoprotein 18; Leukemia-associated phosphoprotein p18

PEPTIDE SEQUENCE	CONF %	dMass	Prec MW	Prec m/z	Theor MW	Theor m/z	Theor z	Sc	Ratio	% Err
Experiment 1										
SHEAEVLK	99.00	-1.913221E-03	1.199673E+03	6.008440E+02	1.199675E+03	6.008450E+02	2	14	2.4734	6.9972
SHEAEVLK	98.00	-2.523532E-03	1.199673E+03	6.008437E+02	1.199675E+03	6.008450E+02	2	14	2.9334	7.2684
SHEAEVLK	97.00	4.356098E-02	1.199719E+03	6.008668E+02	1.199675E+03	6.008450E+02	2	11	2.2097	7.8765
Experiment 2										
ASGQAFELILSPR	99.00	-2.956520E-02	1.531818E+03	7.669165E+02	1.531848E+03	7.669313E+02	2	24	0.9171	3.2857
DLSLEEIQK	99.00	-7.943619E-03	1.361757E+03	6.818856E+02	1.361765E+03	6.818896E+02	2	16	0.9207	3.7055
ESVPEFPLSPPK	99.00	9.919097E-03	1.613901E+03	5.389742E+02	1.613891E+03	5.389709E+02	3	14	0.8613	7.0316
KLEAAEER	99.00	-2.231127E-02	1.232675E+03	6.173445E+02	1.232697E+03	6.173557E+02	2	14	1.0333	4.5457
KSHEAEVLK	99.00	-1.326605E-02	1.471859E+03	4.916270E+02	1.471872E+03	4.916314E+02	3	14	0.8516	9.2376
SHEAEVLK	99.00	-2.082695E-02	1.199655E+03	6.008345E+02	1.199675E+03	6.008450E+02	2	14	1.1564	7.0940
DLSLEEIQK	99.00	-1.120385E-02	1.361753E+03	6.818840E+02	1.361765E+03	6.818896E+02	2	15	0.8805	10.3334
ESVPEFPLSPPK	99.00	1.010219E-02	1.613901E+03	5.389742E+02	1.613891E+03	5.389709E+02	3	14	0.8272	5.8703
ESVPEFPLSPPK	99.00	1.907359E-02	1.613910E+03	5.389772E+02	1.613891E+03	5.389709E+02	3	14	1.0396	7.4993
SHEAEVLK	99.00	-4.142222E-03	1.199671E+03	6.008429E+02	1.199675E+03	6.008450E+02	2	14	1.4853	2.4621
SHEAEVLK	99.00	-3.050894E-02	1.199645E+03	6.008297E+02	1.199675E+03	6.008450E+02	2	14	1.3915	2.3252
SHEAEVLK	99.00	-1.685028E-02	1.199659E+03	6.008365E+02	1.199675E+03	6.008450E+02	2	14	1.4532	3.7717
SHEAEVLK	98.00	-1.072701E-02	1.055563E+03	5.287886E+02	1.055573E+03	5.287939E+02	2	13	0.9379	6.5352
SHEAEVLK	97.00	-9.377430E-03	1.055564E+03	5.287892E+02	1.055573E+03	5.287939E+02	2	13	0.8460	7.0856
KSHEAEVLK	89.00	-1.747716E-02	1.471855E+03	4.916256E+02	1.471872E+03	4.916314E+02	3	12	1.0184	7.3774
SHEAEVLK	88.00	-9.911290E-03	1.055563E+03	5.287890E+02	1.055573E+03	5.287939E+02	2	12	0.7456	12.8467
ESVPEFPLSPPK	83.00	1.522870E-02	1.613906E+03	5.389760E+02	1.613891E+03	5.389709E+02	3	12	0.9260	7.1622
ESVPEFPLSPPK	80.00	8.415494E-03	1.613899E+03	5.389737E+02	1.613891E+03	5.389709E+02	3	12	0.9069	4.9524

Q15738 / NAD(P) dependent steroid dehydrogenase-like (NSDHL); Sterol-4-alpha-carboxylate 3-dehydrogenase, decarboxylating

PEPTIDE SEQUENCE	CONF %	dMass	Prec MW	Prec m/z	Theor MW	Theor m/z	Theor z	Sc	Ratio	% Err
Experiment 1										
THLTEDTPK	99.00	-0.01761538	1328.700317	665.3574	1328.717964	665.3662585		13	4.5176	11.2508
Experiment 2										
AFHITNDEPIPFWTFLSR	99.00	2.06931E-02	2.33421E+03	7.79078E+02	2.33419E+03	7.79071E+02	3	14	0.9184	24.6509
FFLGDLCSR	99.00	6.39198E-03	1.24660E+03	6.24309E+02	1.24660E+03	6.24305E+02	2	15	0.9098	7.1690
NLVDFTFVENVVHGHILAAEQLSR	99.00	7.58876E-02	2.85159E+03	7.13904E+02	2.85151E+03	7.13885E+02	4	17	0.9801	17.6099
THLTEDTPK	99.00	-2.76633E-02	1.32869E+03	6.65352E+02	1.32872E+03	6.65366E+02	2	14	1.5444	15.1482
THLTEDTPK	99.00	-1.30357E-02	1.32870E+03	6.65360E+02	1.32872E+03	6.65366E+02	2	15	2.1696	6.6205
THLTEDTPK	97.00	3.08915E-02	1.18465E+03	5.93331E+02	1.18462E+03	5.93315E+02	2	13	0.7985	10.1057

P63000 and A4D2P0 / Ras-related C3 botulinum toxin substrate 1

PEPTIDE SEQUENCE	CONF %	dMass	Prec MW	Prec m/z	Theor MW	Theor m/z	Theor z	Sc	Ratio	% Err
Experiment 1										
YLECSALTQR	99.00	-4.946493E-03	1.372655E+03	6.873348E+02	1.372660E+03	6.873373E+02	2	16	1.5276	5.5237
CVVVGDGAVGK	99.00	2.443110E-02	1.336733E+03	6.693738E+02	1.336709E+03	6.693616E+02	2	19	1.2282	2.9714
CVVVGDGAVGK	99.00	-3.860337E-03	1.336705E+03	6.693597E+02	1.336709E+03	6.693616E+02	2	19	1.3108	3.7014
CVVVGDGAVGK	99.00	3.443985E-02	1.336743E+03	6.693788E+02	1.336709E+03	6.693616E+02	2	16	1.3071	7.1787
YLECSALTQR	99.00	1.291040E-02	1.372673E+03	6.873438E+02	1.372660E+03	6.873373E+02	2	15	1.5952	4.0542
YLECSALTQR	99.00	-7.717768E-03	1.372652E+03	6.873334E+02	1.372660E+03	6.873373E+02	2	14	1.5499	4.4749
YLECSALTQR	91.00	1.666392E-02	1.372677E+03	6.873456E+02	1.372660E+03	6.873373E+02	2	12	1.4577	6.3120
Experiment 2										

CVVVGDGAVGK	99.00	-2.755766E-02	1.336681E+03	6.693478E+02	1.336709E+03	6.693616E+02	2	20	1.2355	2.5963
TVFDEAIR	98.00	-1.975147E-02	1.093569E+03	5.477919E+02	1.093589E+03	5.478018E+02	2	13	0.7743	5.0377
TVFDEAIR	97.00	-1.433919E-02	1.093575E+03	5.477946E+02	1.093589E+03	5.478018E+02	2	13	0.9789	9.2786

TVFDEAIR	97.00	-5.777817E-03	1.093583E+03	5.477989E+02	1.093589E+03	5.478018E+02	2	13	1.0477	6.7866
LTPITYPQGLAMAK	96.00	3.076281E-02	1.791052E+03	5.980245E+02	1.791021E+03	5.980142E+02	3	13	1.3556	5.3704
LTPITYPQGLAMAK	96.00	3.390809E-02	1.791055E+03	5.980255E+02	1.791021E+03	5.980142E+02	3	13	1.3209	3.5379
TVFDEAIR	95.00	-8.853595E-03	1.093580E+03	5.477973E+02	1.093589E+03	5.478018E+02	2	13	0.8194	2.7794

UPI0000EFE353 and P60953 / Cell Division Cycle 42 (CDC42); G25K GTP-binding protein

PEPTIDE SEQUENCE	CONF %	dMass	Prec MW	Prec m/z	Theor MW	Theor m/z	Theor z	Sc	Ratio	% Err
Experiment 1										
CVVVGDGAVGK	99.00	2.44311E-02	1.33673E+03	6.69374E+02	1.33671E+03	6.69362E+02	2	19	1.2282	2.9714
DDPSTIEK	99.00	2.90973E-02	1.19165E+03	5.96833E+02	1.19162E+03	5.96819E+02	2	13	1.1273	9.8274
QKPITPETAEK	99.00	3.15841E-02	1.67300E+03	5.58675E+02	1.67297E+03	5.58665E+02	3	16	1.6772	3.4524
TPFLLVGTQIDLR	99.00	-8.97077E-02	1.61585E+03	8.08933E+02	1.61594E+03	8.08978E+02	2	13	2.3807	12.7663
YVECSALTQK	99.00	1.03249E-01	1.47484E+03	7.38429E+02	1.47474E+03	7.38377E+02	2	15	1.4675	3.0049
CVVVGDGAVGK	99.00	-3.86034E-03	1.33670E+03	6.69360E+02	1.33671E+03	6.69362E+02	2	19	1.3108	3.7014
CVVVGDGAVGK	99.00	3.44398E-02	1.33674E+03	6.69379E+02	1.33671E+03	6.69362E+02	2	16	1.3071	7.1787
TPFLLVGTQIDLR	99.00	-1.44625E-02	1.61691E+03	8.09463E+02	1.61693E+03	8.09470E+02	2	16	1.3574	10.4037
QKPITPETAEK	98.00	-1.78503E-02	1.67295E+03	5.58659E+02	1.67297E+03	5.58665E+02	3	13	1.6445	3.7424
DDPSTIEK	96.00	-3.07951E-02	1.19159E+03	5.96803E+02	1.19162E+03	5.96819E+02	2	12	1.6237	8.6193
Experiment 2										
CVVVGDGAVGK	99.00	-2.755766E-02	1.336681E+03	6.693478E+02	1.336709E+03	6.693616E+02	2	20	1.2355	2.5963
DDPSTIEK	99.00	-4.868878E-03	1.191618E+03	5.968162E+02	1.191623E+03	5.968186E+02	2	14	0.9984	6.9537
NVFDEAILAALEPPEPK	99.00	-2.685908E-03	2.140163E+03	7.143950E+02	2.140166E+03	7.143959E+02	3	16	0.8172	15.5832
QKPITPETAEK	99.00	-9.635041E-03	1.672963E+03	5.586616E+02	1.672973E+03	5.586648E+02	3	19	1.0313	3.3646
TPFLLVGTQIDLR	99.00	1.025086E-02	1.615952E+03	5.396580E+02	1.615942E+03	5.396546E+02	3	16	1.1782	8.5163
DDPSTIEK	99.00	-1.139645E-03	1.191622E+03	5.968181E+02	1.191623E+03	5.968186E+02	2	14	0.9948	4.8483
DDPSTIEK	99.00	9.278071E-03	1.191632E+03	5.968232E+02	1.191623E+03	5.968186E+02	2	14	1.0202	5.4880
NVFDEAILAALEPPEPK	99.00	-4.303141E-03	2.140162E+03	7.143945E+02	2.140166E+03	7.143959E+02	3	14	0.9326	29.9968
NVFDEAILAALEPPEPK	99.00	-1.444490E-02	2.140152E+03	7.143911E+02	2.140166E+03	7.143959E+02	3	16	1.2783	28.8865
NVFDEAILAALEPPEPK	99.00	-3.425733E-03	2.140163E+03	7.143948E+02	2.140166E+03	7.143959E+02	3	17	0.6509	28.6370
NVFDEAILAALEPPEPK	99.00	-1.411744E-03	2.140165E+03	7.143954E+02	2.140166E+03	7.143959E+02	3	14	0.8649	23.2764
NVFDEAILAALEPPEPK	99.00	-1.093242E-02	2.140155E+03	7.143923E+02	2.140166E+03	7.143959E+02	3	14	0.3630	31.7499
NVFDEAILAALEPPEPK	99.00	-3.235187E-03	2.140163E+03	7.143948E+02	2.140166E+03	7.143959E+02	3	14	0.7969	15.2642
NVFDEAILAALEPPEPK	99.00	6.097720E-04	2.140167E+03	7.143961E+02	2.140166E+03	7.143959E+02	3	15	0.8261	15.9071
NVFDEAILAALEPPEPK	99.00	-6.713960E-03	2.140159E+03	7.143937E+02	2.140166E+03	7.143959E+02	3	15	0.7316	21.3624
NVFDEAILAALEPPEPK	99.00	-9.277266E-03	2.140157E+03	7.143928E+02	2.140166E+03	7.143959E+02	3	15	0.9620	19.1651
QKPITPETAEK	99.00	-3.585840E-02	1.672937E+03	5.586528E+02	1.672973E+03	5.586648E+02	3	19	1.1201	3.1870
QKPITPETAEK	99.00	-2.888973E-02	1.672944E+03	5.586552E+02	1.672973E+03	5.586648E+02	3	18	1.0059	3.2136
QKPITPETAEK	99.00	-3.457671E-02	1.672938E+03	5.586533E+02	1.672973E+03	5.586648E+02	3	17	1.0387	3.0608
QKPITPETAEK	99.00	-6.632680E-04	1.672972E+03	5.586646E+02	1.672973E+03	5.586648E+02	3	17	0.9870	4.0395
QKPITPETAEK	99.00	-1.362679E-02	1.672959E+03	5.586602E+02	1.672973E+03	5.586648E+02	3	17	1.0624	4.1318
QKPITPETAEK	99.00	2.132787E-03	1.672975E+03	5.586655E+02	1.672973E+03	5.586648E+02	3	18	0.9979	4.3118
QKPITPETAEK	99.00	1.391976E-02	1.672986E+03	5.586694E+02	1.672973E+03	5.586648E+02	3	18	1.0318	5.2526
TPFLLVGTQIDLR	99.00	-2.932607E-03	1.615939E+03	5.396536E+02	1.615942E+03	5.396546E+02	3	16	1.2808	6.6468
QKPITPETAEK	98.00	3.106884E-02	1.673004E+03	5.586751E+02	1.672973E+03	5.586648E+02	3	13	1.0107	11.6761
NVFDEAILAALEPPEPK	97.00	2.257612E-03	2.140168E+03	7.143967E+02	2.140166E+03	7.143959E+02	3	13	0.9842	24.8852
TPFLLVGTQIDLR	97.00	2.443518E-02	1.615966E+03	5.396627E+02	1.615942E+03	5.396546E+02	3	13	1.2339	10.4090
NVFDEAILAALEPPEPK	96.00	-2.655342E-03	2.140163E+03	7.143950E+02	2.140166E+03	7.143959E+02	3	13	1.3764	26.4993
NVFDEAILAALEPPEPK	96.00	-4.707363E-03	2.140161E+03	7.143943E+02	2.140166E+03	7.143959E+02	3	13	0.5037	31.6953
NVFDEAILAALEPPEPK	95.00	-1.226010E-04	2.140166E+03	7.143959E+02	2.140166E+03	7.143959E+02	3	13	1.1498	22.1201

NVFDEAILAALEPPEPK	95.00	3.173078E-03	2.140169E+03	7.143970E+02	2.140166E+03	7.143959E+02	3	13	0.8579	21.6824
NVFDEAILAALEPPEPK	95.00	-2.869001E-03	2.140163E+03	7.143950E+02	2.140166E+03	7.143959E+02	3	13	0.8973	20.2889
NVFDEAILAALEPPEPK	94.00	2.140163E+03	7.143950E+02	2.140166E+03	7.143959E+02	7.143959E+02	3	12	0.9148	17.5219
NVFDEAILAALEPPEPK	84.00	2.140162E+03	7.143945E+02	2.140166E+03	7.143959E+02	7.143959E+02	3	12	1.1690	26.4404

Q06830 / Peroxiredoxin-1 (PRDX1)

PEPTIDE SEQUENCE	CONF %	dMass	Prec MW	Prec m/z	Theor MW	Theor m/z	Theor z	Sc	Ratio	% Err
Experiment 1										
ATAVMPDGQFK	99.00	9.734932E-03	1.451778E+03	7.268964E+02	1.451769E+03	7.268916E+02	2	15	1.3209	3.1198
LVQAFQFTDK	99.00	1.119718E-02	1.483839E+03	7.429268E+02	1.483828E+03	7.429212E+02	2	15	1.7746	5.0229
QITVNDLPVGR	99.00	7.418645E-02	1.354843E+03	6.784289E+02	1.354769E+03	6.783918E+02	2	18	1.5472	2.6465
TIAQDYGVLK	99.00	2.766854E-02	1.394829E+03	6.984218E+02	1.394801E+03	6.984079E+02	2	18	1.4359	1.9868
ATAVMPDGQFK	99.00	3.927293E-02	1.451808E+03	7.269112E+02	1.451769E+03	7.268916E+02	2	16	1.4842	2.9415
ATAVMPDGQFK	99.00	1.486136E-02	1.451783E+03	7.268990E+02	1.451769E+03	7.268916E+02	2	14	1.2010	5.7329
LVQAFQFTDK	99.00	-6.199519E-02	1.483766E+03	7.428902E+02	1.483828E+03	7.429212E+02	2	16	1.5689	2.0212
LVQAFQFTDK	99.00	-5.796759E-02	1.483770E+03	7.428922E+02	1.483828E+03	7.429212E+02	2	18	1.5020	1.8945
LVQAFQFTDK	99.00	-4.918008E-02	1.483779E+03	7.428966E+02	1.483828E+03	7.429212E+02	2	15	1.5748	3.5010
QITVNDLPVGR	99.00	2.876473E-02	1.354798E+03	6.784062E+02	1.354769E+03	6.783918E+02	2	14	0.9935	2.7742
TIAQDYGVLK	99.00	4.439047E-02	1.394846E+03	6.984301E+02	1.394801E+03	6.984079E+02	2	16	1.4823	3.6432
QITVNDLPVGR	98.00	4.025691E-02	1.354809E+03	6.784119E+02	1.354769E+03	6.783918E+02	2	13	1.4383	4.0980
LVQAFQFTDK	96.00	9.199948E-02	1.483920E+03	7.429672E+02	1.483828E+03	7.429212E+02	2	13	1.8315	6.6560
LVQAFQFTDK	96.00	3.778181E-02	1.484850E+03	7.434321E+02	1.484812E+03	7.434132E+02	2	13	1.4597	1.8359
Experiment 2										
ATAVMPDGQFK	99.00	-3.286617E-02	1.451736E+03	7.268752E+02	1.451769E+03	7.268916E+02	2	18	1.1628	3.2261
GLFIIDDK	99.00	1.692894E-02	1.207723E+03	6.048685E+02	1.207706E+03	6.048601E+02	2	14	0.9341	11.0009
LVQAFQFTDK	99.00	-1.751204E-02	1.483810E+03	7.429124E+02	1.483828E+03	7.429212E+02	2	18	1.1234	2.2968
QITVNDLPVGR	99.00	-3.668626E-02	1.354732E+03	6.783735E+02	1.354769E+03	6.783918E+02	2	17	1.1816	2.4212
TIAQDYGVLK	99.00	-3.529550E-03	1.394798E+03	6.984062E+02	1.394801E+03	6.984079E+02	2	17	1.0406	4.7388
GLFIIDDK	99.00	1.685047E-03	1.207707E+03	6.048609E+02	1.207706E+03	6.048601E+02	2	14	1.0925	5.4876
GLFIIDDK	99.00	2.051234E-03	1.207708E+03	6.048611E+02	1.207706E+03	6.048601E+02	2	14	1.1170	5.7211
GLFIIDDK	99.00	1.364714E-02	1.207719E+03	6.048669E+02	1.207706E+03	6.048601E+02	2	14	1.1148	6.7204
GLFIIDDK	99.00	-3.081646E-03	1.207703E+03	6.048585E+02	1.207706E+03	6.048601E+02	2	14	1.1668	8.7278
LVQAFQFTDK	99.00	-3.556886E-02	1.483792E+03	7.429034E+02	1.483828E+03	7.429212E+02	2	18	1.1637	2.1729
QITVNDLPVGR	99.00	-2.760528E-02	1.354741E+03	6.783780E+02	1.354769E+03	6.783918E+02	2	17	1.1190	5.1077

P30040 / Endoplasmic reticulum protein ERp29 precursor

PEPTIDE SEQUENCE	CONF %	dMass	Prec MW	Prec m/z	Theor MW	Theor m/z	Theor z	Sc	Ratio	% Err
Experiment 1										
ESYPVFYLFR	99.00	2.892410E-02	1.463786E+03	7.329003E+02	1.463757E+03	7.328858E+02	2	14	1.1235	10.3644
GALPLDTVTFYK	99.00	-9.719449E-02	1.611814E+03	8.069145E+02	1.611912E+03	8.069631E+02	2	21	1.1930	2.8461
QGQDNLSSVK	99.00	-2.723162E-03	1.362732E+03	6.823732E+02	1.362735E+03	6.823746E+02	2	16	0.5262	6.5033
GALPLDTVTFYK	99.00	-6.899913E-02	1.611843E+03	8.069286E+02	1.611912E+03	8.069631E+02	2	22	1.2533	2.8934
GALPLDTVTFYK	99.00	-9.585185E-02	1.611816E+03	8.069152E+02	1.611912E+03	8.069631E+02	2	20	1.1943	3.2143
GALPLDTVTFYK	99.00	-9.023719E-02	1.611821E+03	8.069180E+02	1.611912E+03	8.069631E+02	2	18	1.2414	4.2497
GALPLDTVTFYK	99.00	-5.162871E-03	1.611906E+03	8.069605E+02	1.611912E+03	8.069631E+02	2	15	1.2243	8.2484
QGQDNLSSVK	99.00	1.485170E-02	1.362750E+03	6.823820E+02	1.362735E+03	6.823746E+02	2	16	0.6021	4.9504
QGQDNLSSVK	99.00	4.971150E-02	1.362784E+03	6.823995E+02	1.362735E+03	6.823746E+02	2	16	0.6109	9.6605
ESYPVFYLFR	98.00	9.093065E-02	1.463848E+03	7.329313E+02	1.463757E+03	7.328858E+02	2	13	1.5266	8.8630
Experiment 2										
ESYPVFYLFR	99.00	2.338966E-02	1.463781E+03	7.328975E+02	1.463757E+03	7.328858E+02	2	17	2.8191	7.6254
GALPLDTVTFYK	99.00	3.163590E-02	1.611943E+03	5.383217E+02	1.611912E+03	5.383111E+02	3	14	1.9834	5.3473
ESYPVFYLFR	99.00	2.424413E-02	1.463781E+03	7.328979E+02	1.463757E+03	7.328858E+02	2	15	2.2346	10.0306
GALPLDTVTFYK	97.00	1.945923E-02	1.611931E+03	5.383176E+02	1.611912E+03	5.383111E+02	3	13	1.3567	8.8776
ESYPVFYLFR	93.00	5.000325E-02	1.463807E+03	7.329108E+02	1.463757E+03	7.328858E+02	2	12	1.5436	12.0909

O95881 / Thioredoxin domain-containing protein 12 precursor (TXD12); Thioredoxin-like protein p19, ERP19

PEPTIDE SEQUENCE	CONF %	dMass	Prec MW	Prec m/z	Theor MW	Theor m/z	Theor z	Sc	Ratio	% Err
Experiment 1										
ILFLDPSGK	97.00	1.652741E-02	1.276780E+03	6.393973E+02	1.276763E+03	6.393890E+02	2	13	1.1339	3.5865
Experiment 2										
ILFLDPSGK	99.00	1.177243E-02	1.276775E+03	6.393949E+02	1.276763E+03	6.393890E+02	2	13	1.8166	4.0373
YFYVSAEQVVQGMK	99.00	5.169906E-02	1.936052E+03	6.463581E+02	1.936001E+03	6.463409E+02	3	17	1.4128	6.3589
ILFLDPSGK	99.00	1.177243E-02	1.276775E+03	6.393949E+02	1.276763E+03	6.393890E+02	2	14	1.2584	11.4937
ILFLDPSGK	99.00	1.213885E-02	1.276776E+03	6.393951E+02	1.276763E+03	6.393890E+02	2	14	1.7761	10.9063

P07237 / Protein disulfide-isomerase precursor (PDIA1); procollagen-proline, 2-oxoglutarate 4-dioxygenase, beta polypeptide

PEPTIDE SEQUENCE	CONF %	dMass	Prec MW	Prec m/z	Theor MW	Theor m/z	Theor z	Sc	Ratio	% Err
Experiment 1										
ALAPEYAK	99.00	-4.512879E-02	1.149619E+03	5.758166E+02	1.149664E+03	5.758391E+02	2	14	1.1016	2.4310
DVESDSAK	99.00	5.061978E-02	1.137626E+03	5.698204E+02	1.137576E+03	5.697951E+02	2	13	0.9355	10.6074
HNQLPLVIEFTEQTAPK	99.00	-2.362321E-02	2.252217E+03	7.517463E+02	2.252241E+03	7.517542E+02	3	18	1.0328	6.9068
ILEFFGLK	99.00	-1.480706E-02	1.253748E+03	6.278812E+02	1.253763E+03	6.278886E+02	2	13	1.1865	3.5077
YQLDKDGVVLFK	99.00	5.477791E-02	1.856132E+03	6.197180E+02	1.856077E+03	6.196997E+02	3	18	1.2340	2.5075
DVESDSAK	99.00	2.359440E-02	1.137599E+03	5.698069E+02	1.137576E+03	5.697951E+02	2	14	1.1600	9.3409
HNQLPLVIEFTEQTAPK	99.00	-7.159378E-02	2.252169E+03	7.517303E+02	2.252241E+03	7.517542E+02	3	18	1.1181	6.5387
HNQLPLVIEFTEQTAPK	99.00	4.100891E-02	2.252282E+03	7.517679E+02	2.252241E+03	7.517542E+02	3	17	1.1784	11.1782
ILEFFGLK	99.00	6.099134E-02	1.253824E+03	6.279191E+02	1.253763E+03	6.278886E+02	2	13	1.4930	7.4881
ILEFFGLK	99.00	5.942904E-03	1.253769E+03	6.278916E+02	1.253763E+03	6.278886E+02	2	13	1.0999	4.2111
ILEFFGLK	99.00	-8.460013E-03	1.253754E+03	6.278844E+02	1.253763E+03	6.278886E+02	2	14	1.2103	3.2633
ILEFFGLK	99.00	-8.093838E-03	1.253755E+03	6.278846E+02	1.253763E+03	6.278886E+02	2	13	1.1932	3.4466
KEECPAVR	98.00	2.780726E-02	1.264679E+03	6.333467E+02	1.264651E+03	6.333328E+02	2	13	1.3085	6.8189
ALAPEYAK	97.00	-3.023763E-02	1.149634E+03	5.758240E+02	1.149664E+03	5.758391E+02	2	13	1.0207	1.9912
ILEFFGLK	97.00	4.658843E-02	1.253809E+03	6.279119E+02	1.253763E+03	6.278886E+02	2	13	0.9535	7.1009
TAAESFK	95.00	-2.634192E-02	1.040548E+03	5.212814E+02	1.040575E+03	5.212946E+02	2	12	1.0898	2.4117
KEECPAVR	95.00	4.442404E-03	1.264656E+03	6.333351E+02	1.264651E+03	6.333328E+02	2	12	1.2037	11.3233
TAAESFK	95.00	2.807171E-02	1.040603E+03	5.213086E+02	1.040575E+03	5.212946E+02	2	12	1.1545	3.9910
ILEFFGLK	94.00	5.354577E-02	1.253816E+03	6.279154E+02	1.253763E+03	6.278886E+02	2	12	0.9251	9.7800
KEECPAVR	94.00	4.063509E-02	1.264692E+03	6.333531E+02	1.264651E+03	6.333328E+02	2	12	1.5608	13.7679
TAAESFK	94.00	2.614329E-02	1.040601E+03	5.213076E+02	1.040575E+03	5.212946E+02	2	12	1.2508	3.4116
DHENIVIAK	87.00	-5.271332E-02	1.181600E+03	5.918073E+02	1.181653E+03	5.918336E+02	2	12	1.4675	19.7305
KEECPAVR	82.00	2.067708E-02	1.264672E+03	6.333432E+02	1.264651E+03	6.333328E+02	2	11	1.2562	10.7752
Experiment 2										
ALAPEYAK	99.00	-1.345107E-02	1.149650E+03	5.758324E+02	1.149664E+03	5.758391E+02	2	13	1.5426	4.2596
DHENIVIAK	99.00	-1.343455E-02	1.325741E+03	6.638779E+02	1.325755E+03	6.638846E+02	2	16	1.8182	4.1391
DVESDSAK	99.00	-1.889618E-02	1.137557E+03	5.697857E+02	1.137576E+03	5.697951E+02	2	14	1.4877	4.0326
ENLLDFIK	99.00	-7.149477E-03	1.278736E+03	6.403751E+02	1.278743E+03	6.403786E+02	2	14	1.5046	10.8123
FFPASADR	99.00	-8.469328E-03	1.053528E+03	5.277713E+02	1.053537E+03	5.277755E+02	2	14	1.7010	2.2893
FFRNGDTASPK	99.00	4.651565E-03	1.527797E+03	5.102730E+02	1.527793E+03	5.102715E+02	3	14	1.0813	5.1989
HNQLPLVIEFTEQTAPK	99.00	-3.567769E-02	2.252205E+03	7.517423E+02	2.252241E+03	7.517542E+02	3	21	1.7674	3.2752
ILEFFGLK	99.00	-1.917117E-02	1.253744E+03	6.278790E+02	1.253763E+03	6.278886E+02	2	14	1.8583	9.5764
ILFIFIDSDHTDNQR	99.00	2.665647E-02	1.977034E+03	6.600187E+02	1.977008E+03	6.600099E+02	3	20	1.5945	7.8047
KEECPAVR	99.00	-1.904077E-02	1.264632E+03	6.333233E+02	1.264651E+03	6.333328E+02	2	14	1.3047	3.8988
LGETYKDHENIVIAK	99.00	-2.356682E-02	2.017085E+03	6.733690E+02	2.017109E+03	6.733769E+02	3	20	1.6483	9.2616
MDSTANEVEAVK	99.00	6.180002E-03	1.596797E+03	5.332729E+02	1.596791E+03	5.332709E+02	3	14	1.3865	5.8032
NNFEGEVTK	99.00	-2.101507E-02	1.324666E+03	6.633401E+02	1.324687E+03	6.633506E+02	2	16	1.3486	3.5730

QFLQAAEAIDDIPFGITSNSDVFSK	99.00	7.400902E-03	3.000540E+03	1.001187E+03	3.000532E+03	1.001185E+03	3	25	1.5460	15.5883
QLAPIWDK	99.00	-3.101810E-02	1.257702E+03	6.298580E+02	1.257732E+03	6.298735E+02	2	14	1.6353	2.7302
SNFAEALAAHK	99.00	-3.846778E-02	1.445749E+03	4.829235E+02	1.445787E+03	4.829363E+02	3	14	1.2607	2.8294

THILLFLPK	99.00	-1.774897E-02	1.224754E+03	6.133842E+02	1.224772E+03	6.133931E+02	2	14	0.9197	8.6843
TVIDYNGER	99.00	-1.382336E-02	1.210581E+03	6.062980E+02	1.210595E+03	6.063049E+02	2	15	1.3692	5.1928
VDATEESDLAQQYGVR	99.00	1.418510E-02	1.923944E+03	6.423218E+02	1.923930E+03	6.423171E+02	3	21	1.1077	5.2083
YKPESEELTAER	99.00	-2.144130E-04	1.738898E+03	5.806399E+02	1.738898E+03	5.806400E+02	3	20	1.2695	3.3662
YQLDKDGVVLFK	99.00	-1.626153E-02	1.856061E+03	6.196943E+02	1.856077E+03	6.196997E+02	3	22	1.2453	3.5502
ALAPEYAK	99.00	-3.928500E-02	1.149625E+03	5.758195E+02	1.149664E+03	5.758391E+02	2	14	1.4790	1.4892
ALAPEYAK	99.00	-3.366993E-02	1.149630E+03	5.758223E+02	1.149664E+03	5.758391E+02	2	14	1.4339	2.2533
ALAPEYAK	99.00	-2.968657E-02	1.149634E+03	5.758243E+02	1.149664E+03	5.758391E+02	2	14	1.5865	2.7250
ALAPEYAK	99.00	-1.857863E-02	1.149645E+03	5.758298E+02	1.149664E+03	5.758391E+02	2	14	1.5049	4.2239
ALAPEYAK	99.00	-1.463649E-02	1.149649E+03	5.758318E+02	1.149664E+03	5.758391E+02	2	14	1.6181	3.6135
ALAPEYAK	99.00	-1.210839E-02	1.149652E+03	5.758331E+02	1.149664E+03	5.758391E+02	2	14	1.5646	4.8160
ALAPEYAK	99.00	-8.202435E-03	1.149656E+03	5.758350E+02	1.149664E+03	5.758391E+02	2	13	1.4660	7.4369
ALAPEYAK	99.00	-3.775981E-03	1.149660E+03	5.758373E+02	1.149664E+03	5.758391E+02	2	14	1.3382	5.9685
ALAPEYAK	99.00	-5.362804E-03	1.149658E+03	5.758365E+02	1.149664E+03	5.758391E+02	2	14	1.5212	5.4946
ALAPEYAK	99.00	-1.906757E-03	1.149662E+03	5.758382E+02	1.149664E+03	5.758391E+02	2	13	1.6041	7.4125
ALAPEYAK	99.00	-9.302550E-04	1.149663E+03	5.758387E+02	1.149664E+03	5.758391E+02	2	13	1.7522	9.6883
DHENIVIAK	99.00	-1.734247E-02	1.181635E+03	5.918249E+02	1.181653E+03	5.918336E+02	2	15	1.4983	5.5190
DHENIVIAK	99.00	-5.990238E-03	1.181647E+03	5.918306E+02	1.181653E+03	5.918336E+02	2	14	1.3925	7.9797
DHENIVIAK	99.00	-1.941586E-02	1.325735E+03	6.638749E+02	1.325755E+03	6.638846E+02	2	16	1.9797	3.9043
DHENIVIAK	99.00	-2.184566E-02	1.325733E+03	6.638737E+02	1.325755E+03	6.638846E+02	2	16	2.0127	3.7821
DHENIVIAK	99.00	-1.464364E-02	1.325740E+03	6.638773E+02	1.325755E+03	6.638846E+02	2	14	1.4425	9.0968
DVESDSAK	99.00	-1.563477E-02	1.137560E+03	5.697873E+02	1.137576E+03	5.697951E+02	2	13	1.6903	7.9673
DVESDSAK	99.00	-2.418280E-02	1.137552E+03	5.697830E+02	1.137576E+03	5.697951E+02	2	14	1.4303	3.2472
ENLLDFIK	99.00	1.446461E-02	1.278757E+03	6.403859E+02	1.278743E+03	6.403786E+02	2	13	1.4875	10.8690
ENLLDFIK	99.00	1.361019E-02	1.278756E+03	6.403854E+02	1.278743E+03	6.403786E+02	2	14	1.2126	10.6364
ENLLDFIK	99.00	7.060513E-03	1.278750E+03	6.403821E+02	1.278743E+03	6.403786E+02	2	14	1.7076	10.4364
ENLLDFIK	99.00	1.194288E-02	1.278755E+03	6.403846E+02	1.278743E+03	6.403786E+02	2	14	1.2219	7.7477
ENLLDFIK	99.00	1.841202E-02	1.278761E+03	6.403878E+02	1.278743E+03	6.403786E+02	2	13	1.0191	9.2662
ENLLDFIK	99.00	2.897866E-03	1.278746E+03	6.403801E+02	1.278743E+03	6.403786E+02	2	14	1.6016	12.3455
ENLLDFIK	99.00	1.339517E-02	1.278756E+03	6.403853E+02	1.278743E+03	6.403786E+02	2	14	1.4761	10.0866
ENLLDFIK	99.00	9.040000E-05	1.278743E+03	6.403787E+02	1.278743E+03	6.403786E+02	2	13	1.7173	9.6394
ENLLDFIK	99.00	1.068778E-02	1.278753E+03	6.403840E+02	1.278743E+03	6.403786E+02	2	13	1.4463	10.8207
ENLLDFIK	99.00	3.852425E-03	1.278747E+03	6.403806E+02	1.278743E+03	6.403786E+02	2	14	1.1588	9.8558
ENLLDFIK	99.00	-2.141398E-02	1.278721E+03	6.403679E+02	1.278743E+03	6.403786E+02	2	14	1.4610	21.1868
ENLLDFIK	99.00	4.044306E-03	1.278747E+03	6.403807E+02	1.278743E+03	6.403786E+02	2	14	1.6033	6.6939
ENLLDFIK	99.00	1.236876E-03	1.278744E+03	6.403793E+02	1.278743E+03	6.403786E+02	2	14	1.5009	4.9953
ENLLDFIK	99.00	-6.086857E-03	1.278737E+03	6.403756E+02	1.278743E+03	6.403786E+02	2	13	0.9634	17.6804
ENLLDFIK	99.00	-1.133553E-02	1.278731E+03	6.403730E+02	1.278743E+03	6.403786E+02	2	13	1.3755	17.1564
ENLLDFIK	99.00	-6.127532E-03	1.278737E+03	6.403755E+02	1.278743E+03	6.403786E+02	2	14	1.4797	5.1268
ENLLDFIK	99.00	1.108427E-02	1.278754E+03	6.403842E+02	1.278743E+03	6.403786E+02	2	14	1.0563	7.3798
ENLLDFIK	99.00	3.668001E-02	1.278779E+03	6.403970E+02	1.278743E+03	6.403786E+02	2	13	1.2723	9.9662
ENLLDFIK	99.00	-4.702410E-03	1.278738E+03	6.403763E+02	1.278743E+03	6.403786E+02	2	13	1.0435	23.0279
ENLLDFIK	99.00	-5.312746E-03	1.278737E+03	6.403760E+02	1.278743E+03	6.403786E+02	2	13	1.5380	16.2851
ENLLDFIK	99.00	-5.196444E-03	1.278738E+03	6.403760E+02	1.278743E+03	6.403786E+02	2	14	1.6509	6.9149
ENLLDFIK	99.00	7.374012E-03	1.278750E+03	6.403823E+02	1.278743E+03	6.403786E+02	2	14	1.3641	8.8160
ENLLDFIK	99.00	-1.227858E-02	1.278730E+03	6.403725E+02	1.278743E+03	6.403786E+02	2	14	1.4654	6.9138
ENLLDFIK	99.00	5.953563E-03	1.278749E+03	6.403816E+02	1.278743E+03	6.403786E+02	2	14	1.1600	11.1559
ENLLDFIK	99.00	3.512344E-03	1.278746E+03	6.403804E+02	1.278743E+03	6.403786E+02	2	14	0.9848	12.4438
FFPASADR	99.00	-1.821568E-03	1.053535E+03	5.277747E+02	1.053537E+03	5.277755E+02	2	13	1.5862	6.7178
FFRNGDTASPK	99.00	1.989670E-02	1.527812E+03	5.102781E+02	1.527793E+03	5.102715E+02	3	18	1.2037	4.9134

FFRNGDTASPK	99.00	-7.111459E-03	1.527785E+03	5.102691E+02	1.527793E+03	5.102715E+02	3	14	1.2640	4.0640
FFRNGDTASPK	99.00	6.757258E-03	1.527799E+03	5.102737E+02	1.527793E+03	5.102715E+02	3	15	1.0641	5.5786
HNQLPLVIEFTEQTAPK	99.00	1.247791E-02	2.252253E+03	7.517584E+02	2.252241E+03	7.517542E+02	3	22	1.8406	5.4365
HNQLPLVIEFTEQTAPK	99.00	-2.789964E-02	2.252213E+03	7.517449E+02	2.252241E+03	7.517542E+02	3	19	1.4169	12.6958
HNQLPLVIEFTEQTAPK	99.00	6.703667E-03	2.252248E+03	7.517565E+02	2.252241E+03	7.517542E+02	3	19	1.7622	10.9602

HNQLPLVIEFTEQTAPK	99.00	-1.068695E-02	2.108128E+03	7.037166E+02	2.108139E+03	7.037202E+02	3	17	1.4875	10.7080
ILEFFGLK	99.00	-2.557806E-03	1.253760E+03	6.278874E+02	1.253763E+03	6.278886E+02	2	13	2.2308	16.1511
ILEFFGLK	99.00	-6.283859E-03	1.253756E+03	6.278855E+02	1.253763E+03	6.278886E+02	2	13	1.1963	16.8676
ILEFFGLK	99.00	-2.570864E-02	1.253737E+03	6.278758E+02	1.253763E+03	6.278886E+02	2	14	1.9161	2.7499
ILEFFGLK	99.00	1.091154E-02	1.253774E+03	6.278941E+02	1.253763E+03	6.278886E+02	2	14	1.4865	11.4571
ILEFFGLK	99.00	-3.033967E-02	1.253732E+03	6.278735E+02	1.253763E+03	6.278886E+02	2	14	2.0107	2.4240
ILEFFGLK	99.00	-4.596423E-02	1.253717E+03	6.278657E+02	1.253763E+03	6.278886E+02	2	14	1.7510	1.8046
ILEFFGLK	99.00	-4.352289E-02	1.253719E+03	6.278669E+02	1.253763E+03	6.278886E+02	2	14	1.8368	2.0658
ILEFFGLK	99.00	7.256940E-03	1.253770E+03	6.278923E+02	1.253763E+03	6.278886E+02	2	14	1.3499	5.8957
ILEFFGLK	99.00	2.703178E-02	1.253790E+03	6.279022E+02	1.253763E+03	6.278886E+02	2	13	1.5421	10.1589
ILEFFGLK	99.00	-7.391088E-03	1.253755E+03	6.278849E+02	1.253763E+03	6.278886E+02	2	13	1.4544	12.3657
ILEFFGLK	99.00	4.815603E-03	1.253768E+03	6.278911E+02	1.253763E+03	6.278886E+02	2	13	1.4582	11.8622
ILEFFGLK	99.00	6.706775E-03	1.253769E+03	6.278920E+02	1.253763E+03	6.278886E+02	2	14	2.0271	4.8593
ILEFFGLK	99.00	2.339930E-03	1.253765E+03	6.278898E+02	1.253763E+03	6.278886E+02	2	13	1.9734	9.3150
ILEFFGLK	99.00	2.950259E-03	1.253766E+03	6.278901E+02	1.253763E+03	6.278886E+02	2	14	2.0348	7.2798
ILEFFGLK	99.00	4.142579E-03	1.253767E+03	6.278907E+02	1.253763E+03	6.278886E+02	2	13	1.7503	8.3111
ILEFFGLK	99.00	8.536793E-03	1.253771E+03	6.278929E+02	1.253763E+03	6.278886E+02	2	13	2.2400	9.3837
ILEFFGLK	99.00	-4.226695E-03	1.253759E+03	6.278865E+02	1.253763E+03	6.278886E+02	2	14	2.1672	9.8241
ILEFFGLK	99.00	1.021938E-03	1.253764E+03	6.278892E+02	1.253763E+03	6.278886E+02	2	14	2.2135	9.0430
ILFIFIDSDHTDNQR	99.00	4.210277E-02	1.977050E+03	6.600239E+02	1.977008E+03	6.600099E+02	3	14	2.1146	26.6568
ILFIFIDSDHTDNQR	99.00	3.800447E-02	1.977046E+03	6.600225E+02	1.977008E+03	6.600099E+02	3	16	1.0493	25.2530
ILFIFIDSDHTDNQR	99.00	1.878014E-02	1.977026E+03	6.600161E+02	1.977008E+03	6.600099E+02	3	15	0.9268	26.1837
ILFIFIDSDHTDNQR	99.00	2.830441E-02	1.977036E+03	6.600193E+02	1.977008E+03	6.600099E+02	3	17	1.4787	13.6577
KEECPAVR	99.00	-2.571043E-02	1.264625E+03	6.333200E+02	1.264651E+03	6.333328E+02	2	14	1.3467	5.2838
KEECPAVR	99.00	-1.684358E-02	1.264634E+03	6.333244E+02	1.264651E+03	6.333328E+02	2	13	1.1210	5.4920
LGETYKDHENIVIAK	99.00	-1.843999E-02	2.017090E+03	6.733707E+02	2.017109E+03	6.733769E+02	3	21	1.3621	11.0160
LGETYKDHENIVIAK	99.00	-2.075248E-02	2.017088E+03	6.733699E+02	2.017109E+03	6.733769E+02	3	21	1.3721	10.0199
MDSTANEVEAVK	99.00	1.987988E-03	1.596793E+03	5.332715E+02	1.596791E+03	5.332709E+02	3	14	1.5047	6.0383
NNFEGEVTK	99.00	-2.382245E-02	1.324663E+03	6.633387E+02	1.324687E+03	6.633506E+02	2	15	1.3214	4.8692
NNFEGEVTK	99.00	-3.860222E-03	1.324683E+03	6.633487E+02	1.324687E+03	6.633506E+02	2	16	1.2894	3.1771
NNFEGEVTK	99.00	-1.606644E-02	1.324671E+03	6.633426E+02	1.324687E+03	6.633506E+02	2	16	1.4046	3.6265
NNFEGEVTK	99.00	-8.846733E-03	1.324678E+03	6.633462E+02	1.324687E+03	6.633506E+02	2	15	1.0518	9.0374
QFLQAAEAIDDIPFGITSNSDVFSK	99.00	-3.452747E-02	3.000498E+03	1.001173E+03	3.000532E+03	1.001185E+03	3	22	2.0590	21.7413
QFLQAAEAIDDIPFGITSNSDVFSK	99.00	-2.738683E-02	3.000505E+03	1.001176E+03	3.000532E+03	1.001185E+03	3	21	1.0695	17.7987
QFLQAAEAIDDIPFGITSNSDVFSK	99.00	-4.428708E-02	3.000488E+03	1.001170E+03	3.000532E+03	1.001185E+03	3	17	1.5848	22.9029
QFLQAAEAIDDIPFGITSNSDVFSK	99.00	-1.786613E-02	3.000515E+03	7.511359E+02	3.000532E+03	7.511404E+02	4	17	2.5537	23.5761
QFLQAAEAIDDIPFGITSNSDVFSK	99.00	3.013688E-02	3.000563E+03	1.001195E+03	3.000532E+03	1.001185E+03	3	15	2.7552	25.5191
QFLQAAEAIDDIPFGITSNSDVFSK	99.00	1.835674E-02	3.000551E+03	7.511450E+02	3.000532E+03	7.511404E+02	4	18	1.7326	23.6867
QFLQAAEAIDDIPFGITSNSDVFSK	99.00	4.130432E-02	3.000574E+03	7.511507E+02	3.000532E+03	7.511404E+02	4	19	1.7245	24.6763
QFLQAAEAIDDIPFGITSNSDVFSK	99.00	4.452590E-03	3.000537E+03	1.001186E+03	3.000532E+03	1.001185E+03	3	15	1.9277	21.2370
QFLQAAEAIDDIPFGITSNSDVFSK	99.00	1.338466E-02	2.839417E+03	9.474797E+02	2.839404E+03	9.474752E+02	3	16	1.3077	24.7634
QFLQAAEAIDDIPFGITSNSDVFSK	99.00	-2.976704E-02	3.000503E+03	1.001175E+03	3.000532E+03	1.001185E+03	3	16	1.6671	21.2493
QFLQAAEAIDDIPFGITSNSDVFSK	99.00	7.087281E-02	3.000603E+03	7.511581E+02	3.000532E+03	7.511404E+02	4	15	1.5031	18.0284
QFLQAAEAIDDIPFGITSNSDVFSK	99.00	2.273842E-03	3.000535E+03	7.511409E+02	3.000532E+03	7.511404E+02	4	16	1.1755	14.6896
QFLQAAEAIDDIPFGITSNSDVFSK	99.00	-1.869349E-02	2.839385E+03	9.474690E+02	2.839404E+03	9.474752E+02	3	17	1.2175	27.8921
QLAPIWDK	99.00	-6.661833E-02	1.257666E+03	6.298402E+02	1.257732E+03	6.298735E+02	2	14	1.3749	1.1408
QLAPIWDK	99.00	-2.181977E-02	1.257711E+03	6.298626E+02	1.257732E+03	6.298735E+02	2	14	1.5250	2.3082
QLAPIWDK	99.00	-1.514966E-02	1.257717E+03	6.298660E+02	1.257732E+03	6.298735E+02	2	14	1.3090	7.6367
QLAPIWDK	99.00	-2.449814E-02	1.257708E+03	6.298613E+02	1.257732E+03	6.298735E+02	2	14	1.6500	3.0763
QLAPIWDK	99.00	-4.349312E-03	1.257728E+03	6.298713E+02	1.257732E+03	6.298735E+02	2	14	1.7616	5.7608

SNFAEALAAHK	99.00	-3.376683E-02	1.445753E+03	4.829250E+02	1.445787E+03	4.829363E+02	3	16	1.3951	2.2021
SNFAEALAAHK	99.00	-7.706638E-02	1.445710E+03	4.829106E+02	1.445787E+03	4.829363E+02	3	16	1.4849	1.4385
TVIDYNGER	99.00	-7.534907E-03	1.210588E+03	6.063011E+02	1.210595E+03	6.063049E+02	2	16	1.3923	5.2944
TVIDYNGER	99.00	-4.058568E-03	1.210591E+03	6.063029E+02	1.210595E+03	6.063049E+02	2	16	1.4199	5.3961
TVIDYNGER	99.00	-5.767407E-03	1.210589E+03	6.063020E+02	1.210595E+03	6.063049E+02	2	15	1.4502	5.2899

TVIDYNGER	99.00	2.316365E-03	1.210598E+03	6.063060E+02	1.210595E+03	6.063049E+02	2	15	1.4235	6.1922
VDATEESDLAQQYGVR	99.00	1.612882E-02	1.923946E+03	6.423225E+02	1.923930E+03	6.423171E+02	3	20	1.1415	5.1237
VDATEESDLAQQYGVR	99.00	2.153837E-02	1.923951E+03	6.423243E+02	1.923930E+03	6.423171E+02	3	20	0.9801	5.3815
YKPESEELTAER	99.00	-7.034354E-03	1.738891E+03	5.806376E+02	1.738898E+03	5.806400E+02	3	20	1.1133	4.7645
YKPESEELTAER	99.00	-2.676245E-02	1.738871E+03	5.806310E+02	1.738898E+03	5.806400E+02	3	20	1.2803	3.0009
YKPESEELTAER	99.00	5.541374E-03	1.738904E+03	5.806418E+02	1.738898E+03	5.806400E+02	3	20	1.3059	3.4176
YKPESEELTAER	99.00	-9.655371E-03	1.738889E+03	5.806368E+02	1.738898E+03	5.806400E+02	3	21	1.3414	2.9492
YKPESEELTAER	99.00	-1.175013E-02	1.738886E+03	5.806360E+02	1.738898E+03	5.806400E+02	3	18	1.1045	5.7575
YKPESEELTAER	99.00	-1.614370E-02	1.882984E+03	6.286686E+02	1.883000E+03	6.286740E+02	3	14	1.6241	6.8889
YKPESEELTAER	99.00	-1.566097E-02	1.738882E+03	5.806348E+02	1.738898E+03	5.806400E+02	3	18	1.2557	6.3977
VHSFPTLK	98.00	-3.218664E-02	1.215690E+03	6.088522E+02	1.215722E+03	6.088682E+02	2	13	1.9620	2.6799
ALAPEYAK	98.00	-1.118312E-02	1.149653E+03	5.758336E+02	1.149664E+03	5.758391E+02	2	13	1.5355	4.2309
ALAPEYAK	98.00	3.126164E-03	1.149667E+03	5.758407E+02	1.149664E+03	5.758391E+02	2	12	1.3836	21.1998
ENLLDFIK	98.00	-1.494481E-02	1.278728E+03	6.403712E+02	1.278743E+03	6.403786E+02	2	12	1.2176	24.7152
FFPASADR	98.00	-1.093507E-02	1.053526E+03	5.277701E+02	1.053537E+03	5.277755E+02	2	13	1.6817	3.7498
FFPASADR	98.00	-2.281073E-02	1.053514E+03	5.277642E+02	1.053537E+03	5.277755E+02	2	13	1.5641	2.5654
FFPASADR	98.00	-5.009587E-02	1.053486E+03	5.277505E+02	1.053537E+03	5.277755E+02	2	13	1.5582	1.2867
FFPASADR	98.00	-4.643385E-02	1.053490E+03	5.277523E+02	1.053537E+03	5.277755E+02	2	13	1.6366	1.8278
FFPASADR	98.00	-2.400908E-02	1.053513E+03	5.277635E+02	1.053537E+03	5.277755E+02	2	13	1.6798	2.1478
FFPASADR	98.00	-9.772343E-03	1.053527E+03	5.277706E+02	1.053537E+03	5.277755E+02	2	13	1.7650	2.5266
FFPASADR	98.00	-1.636385E-02	1.053520E+03	5.277673E+02	1.053537E+03	5.277755E+02	2	13	1.7260	3.1786
FFPASADR	98.00	-2.021812E-02	1.053516E+03	5.277654E+02	1.053537E+03	5.277755E+02	2	13	1.7221	2.2871
FFPASADR	98.00	-2.082842E-02	1.053516E+03	5.277651E+02	1.053537E+03	5.277755E+02	2	13	1.6090	2.8624
FFPASADR	98.00	-3.349188E-02	1.053503E+03	5.277588E+02	1.053537E+03	5.277755E+02	2	13	1.8070	2.4772
FFPASADR	98.00	-2.426650E-02	1.053512E+03	5.277634E+02	1.053537E+03	5.277755E+02	2	13	1.7512	2.5973
FFPASADR	98.00	-1.900668E-02	1.053518E+03	5.277661E+02	1.053537E+03	5.277755E+02	2	13	1.7651	3.1909
FFPASADR	98.00	-8.963604E-03	1.053528E+03	5.277711E+02	1.053537E+03	5.277755E+02	2	13	1.7731	5.2810
ILEFFGLK	98.00	1.469562E-02	1.253777E+03	6.278960E+02	1.253763E+03	6.278886E+02	2	14	2.6559	8.4452
ILEFFGLK	98.00	2.028264E-03	1.253765E+03	6.278896E+02	1.253763E+03	6.278886E+02	2	13	1.3338	13.2178
QFLQAAEAIDDIPFGITSNSDVFSK	98.00	1.181296E-03	3.000533E+03	1.001185E+03	3.000532E+03	1.001185E+03	3	14	0.6086	26.6727
QFLQAAEAIDDIPFGITSNSDVFSK	98.00	-2.424339E-02	3.001492E+03	1.001505E+03	3.001516E+03	1.001513E+03	3	14	1.5557	20.5904
QFLQAAEAIDDIPFGITSNSDVFSK	98.00	-7.944119E-03	2.840380E+03	9.478005E+02	2.840388E+03	9.478032E+02	3	14	1.5560	29.1219
QLAPIWDK	98.00	-1.681127E-02	1.257716E+03	6.298651E+02	1.257732E+03	6.298735E+02	2	13	1.3820	3.5205
QLAPIWDK	98.00	-1.936976E-02	1.257713E+03	6.298638E+02	1.257732E+03	6.298735E+02	2	14	1.6352	2.1613
QLAPIWDK	98.00	-1.883955E-02	1.257714E+03	6.298641E+02	1.257732E+03	6.298735E+02	2	14	1.4805	4.0158
QLAPIWDK	98.00	-1.888312E-02	1.257714E+03	6.298641E+02	1.257732E+03	6.298735E+02	2	14	1.5073	4.5091
THILLFLPK	98.00	-3.258400E-02	1.224739E+03	6.133768E+02	1.224772E+03	6.133931E+02	2	13	0.9394	10.3463
TVIDYNGER	98.00	-4.361304E-03	1.210591E+03	6.063027E+02	1.210595E+03	6.063049E+02	2	13	1.3683	5.1968
DHENIVIAK	97.00	-2.814973E-03	1.181650E+03	5.918322E+02	1.181653E+03	5.918336E+02	2	13	1.4781	6.5595
ENLLDFIK	97.00	-2.891249E-02	1.278714E+03	6.403642E+02	1.278743E+03	6.403786E+02	2	12	0.9355	20.4781
ILEFFGLK	97.00	6.646606E-03	1.253769E+03	6.278920E+02	1.253763E+03	6.278886E+02	2	13	1.4848	5.7461
ILEFFGLK	97.00	1.336029E-02	1.253776E+03	6.278953E+02	1.253763E+03	6.278886E+02	2	13	1.4589	6.8473
THILLFLPK	97.00	-1.891309E-02	1.224753E+03	6.133836E+02	1.224772E+03	6.133931E+02	2	13	1.2425	9.5778
TAAESFK	96.00	1.186375E-02	1.040586E+03	5.213005E+02	1.040575E+03	5.212946E+02	2	12	1.4944	6.8107
ALAPEYAK	96.00	-1.066701E-02	1.149653E+03	5.758338E+02	1.149664E+03	5.758391E+02	2	12	1.2458	14.1261
ENLLDFIK	96.00	-1.958309E-02	1.278723E+03	6.403688E+02	1.278743E+03	6.403786E+02	2	12	1.1819	22.5951
ENLLDFIK	96.00	-1.775219E-02	1.278725E+03	6.403698E+02	1.278743E+03	6.403786E+02	2	12	1.0283	21.9662
ILEFFGLK	96.00	8.843810E-03	1.253772E+03	6.278931E+02	1.253763E+03	6.278886E+02	2	12	1.3603	12.5072
ILEFFGLK	96.00	1.043068E-02	1.253773E+03	6.278939E+02	1.253763E+03	6.278886E+02	2	12	1.5133	17.6045
ILEFFGLK	96.00	1.043068E-02	1.253773E+03	6.278939E+02	1.253763E+03	6.278886E+02	2	12	1.6979	19.6645

ILEFFGLK	96.00	-1.945517E-02	1.253743E+03	6.278789E+02	1.253763E+03	6.278886E+02	2	12	1.6647	16.9076
ILFIFIDSDHTDNQR	96.00	-6.818503E-03	1.977001E+03	6.600076E+02	1.977008E+03	6.600099E+02	3	13	1.3389	28.5753
TAAESFK	96.00	1.519527E-03	1.040576E+03	5.212953E+02	1.040575E+03	5.212946E+02	2	12	1.3727	3.4380
TAAESFK	96.00	5.711519E-03	1.040580E+03	5.212974E+02	1.040575E+03	5.212946E+02	2	12	1.6430	4.6792
TAAESFK	96.00	4.154149E-03	1.040579E+03	5.212966E+02	1.040575E+03	5.212946E+02	2	12	1.4314	9.1227

THILLFLPK	96.00	-1.672023E-02	1.224755E+03	6.133847E+02	1.224772E+03	6.133931E+02	2	14	1.0513	8.9341
LITLEEEMTK	95.00	-3.719554E-03	1.509817E+03	5.042795E+02	1.509820E+03	5.042807E+02	3	13	1.4615	3.1268
ALAPEYAK	95.00	-1.463649E-02	1.149649E+03	5.758318E+02	1.149664E+03	5.758391E+02	2	12	1.4260	4.4323
ENLLDFIK	95.00	-1.311391E-02	1.278730E+03	6.403721E+02	1.278743E+03	6.403786E+02	2	12	0.9514	19.7588
ENLLDFIK	95.00	-1.609596E-02	1.278727E+03	6.403706E+02	1.278743E+03	6.403786E+02	2	12	0.6377	24.3226
ENLLDFIK	95.00	-3.635829E-02	1.278706E+03	6.403605E+02	1.278743E+03	6.403786E+02	2	12	1.4458	22.2003
ILEFFGLK	95.00	1.686956E-02	1.253780E+03	6.278971E+02	1.253763E+03	6.278886E+02	2	12	1.6358	13.1234
ILEFFGLK	95.00	2.947312E-02	1.253792E+03	6.279034E+02	1.253763E+03	6.278886E+02	2	12	1.5817	9.3235
ILEFFGLK	95.00	-2.020144E-03	1.253761E+03	6.278876E+02	1.253763E+03	6.278886E+02	2	12	1.9743	19.3487
TAAESFK	95.00	-1.626554E-02	1.040558E+03	5.212864E+02	1.040575E+03	5.212946E+02	2	12	1.4918	2.5873
TAAESFK	95.00	-5.157594E-03	1.040569E+03	5.212920E+02	1.040575E+03	5.212946E+02	2	12	1.4294	3.2609
TAAESFK	95.00	1.360194E-02	1.040588E+03	5.213014E+02	1.040575E+03	5.212946E+02	2	12	1.4375	7.3521
ILEFFGLK	94.00	-8.969163E-03	1.253754E+03	6.278842E+02	1.253763E+03	6.278886E+02	2	12	1.6750	14.9727
ILEFFGLK	94.00	2.367385E-02	1.253786E+03	6.279005E+02	1.253763E+03	6.278886E+02	2	12	1.8915	7.2007
ILEFFGLK	94.00	-4.563243E-03	1.253758E+03	6.278864E+02	1.253763E+03	6.278886E+02	2	12	1.7634	12.7076
MDSTANEVEAVK	94.00	3.810233E-03	1.596795E+03	5.332722E+02	1.596791E+03	5.332709E+02	3	13	1.6369	5.2092
MDSTANEVEAVK	94.00	7.838286E-03	1.596799E+03	5.332735E+02	1.596791E+03	5.332709E+02	3	13	1.3580	7.0148
TAAESFK	94.00	2.146354E-02	1.040596E+03	5.213053E+02	1.040575E+03	5.212946E+02	2	12	1.3448	6.0153
TAAESFK	94.00	1.839400E-02	1.040593E+03	5.213038E+02	1.040575E+03	5.212946E+02	2	12	1.0880	7.8870
ALAPEYAK	93.00	-4.020107E-03	1.149660E+03	5.758372E+02	1.149664E+03	5.758391E+02	2	12	1.3451	9.1148
ALAPEYAK	93.00	-2.111627E-02	1.149643E+03	5.758286E+02	1.149664E+03	5.758391E+02	2	12	1.3784	9.9403
ILEFFGLK	93.00	-8.040740E-04	1.253762E+03	6.278882E+02	1.253763E+03	6.278886E+02	2	12	1.9356	18.9767
ILEFFGLK	93.00	1.142726E-02	1.253774E+03	6.278943E+02	1.253763E+03	6.278886E+02	2	12	2.4038	10.5159
TAAESFK	93.00	-2.045251E-02	1.040554E+03	5.212844E+02	1.040575E+03	5.212946E+02	2	12	1.4973	1.8165
DGVVLFK	92.00	-1.252791E-02	1.064635E+03	5.333247E+02	1.064647E+03	5.333310E+02	2	12	1.1931	3.9475
DVESDSAK	92.00	-1.671985E-02	1.137559E+03	5.697868E+02	1.137576E+03	5.697951E+02	2	14	1.5918	2.9064
FFPASADR	92.00	-6.400270E-03	1.053530E+03	5.277723E+02	1.053537E+03	5.277755E+02	2	12	1.6918	6.9688
ILEFFGLK	92.00	-1.891425E-02	1.253744E+03	6.278792E+02	1.253763E+03	6.278886E+02	2	12	1.5220	19.6217
ILEFFGLK	92.00	7.211355E-03	1.253770E+03	6.278923E+02	1.253763E+03	6.278886E+02	2	12	1.1004	18.6229
ILEFFGLK	92.00	5.067650E-03	1.253768E+03	6.278912E+02	1.253763E+03	6.278886E+02	2	12	1.4531	22.5326
THILLFLPK	92.00	-6.344889E-03	1.224765E+03	6.133899E+02	1.224772E+03	6.133931E+02	2	13	0.9697	8.3976
NFEDVAFDEK	91.00	-1.359780E-03	1.356631E+03	6.793226E+02	1.356632E+03	6.793232E+02	2	13	1.3680	5.2799
FFPASADR	91.00	-8.812224E-03	1.053528E+03	5.277711E+02	1.053537E+03	5.277755E+02	2	12	1.3991	4.3714
ILEFFGLK	91.00	-7.802012E-03	1.253755E+03	6.278848E+02	1.253763E+03	6.278886E+02	2	12	1.3684	19.8791
FFPASADR	90.00	-2.158218E-02	1.053515E+03	5.277648E+02	1.053537E+03	5.277755E+02	2	12	1.4925	4.8212
QLAPIWDK	90.00	-1.546367E-02	1.257717E+03	6.298658E+02	1.257732E+03	6.298735E+02	2	12	1.3378	4.9190
IFGGEIK	89.00	-1.205698E-02	1.050620E+03	5.263171E+02	1.050632E+03	5.263231E+02	2	12	1.1720	4.4618
DHENIVIAK	89.00	-1.393100E-02	1.181639E+03	5.918266E+02	1.181653E+03	5.918336E+02	2	12	1.4019	10.1168
DVESDSAK	88.00	-1.917834E-02	1.137557E+03	5.697855E+02	1.137576E+03	5.697951E+02	2	12	0.9340	3.1760
EADDIVNWLK	87.00	9.307970E-03	1.489811E+03	4.976111E+02	1.489802E+03	4.976080E+02	3	12	1.0472	8.8816
ENLLDFIK	87.00	-1.255615E-02	1.278730E+03	6.403724E+02	1.278743E+03	6.403786E+02	2	11	1.6596	18.8336
ILFIFIDSDHTDNQR	87.00	2.485649E-02	1.977033E+03	6.600181E+02	1.977008E+03	6.600099E+02	3	12	1.3917	27.6448
ENLLDFIK	86.00	-1.658421E-02	1.278726E+03	6.403704E+02	1.278743E+03	6.403786E+02	2	11	1.4373	18.9585
ILEFFGLK	85.00	1.032868E-02	1.253773E+03	6.278938E+02	1.253763E+03	6.278886E+02	2	12	1.3753	12.6472
ILEFFGLK	84.00	2.263737E-02	1.253785E+03	6.279000E+02	1.253763E+03	6.278886E+02	2	11	1.7201	16.6468
ILFIFIDSDHTDNQR	81.00	3.132960E-02	1.977039E+03	6.600203E+02	1.977008E+03	6.600099E+02	3	12	1.4419	14.3534

P13667 / Protein disulfide-isomerase A4 precursor (PDIA4)

PEPTIDE SEQUENCE	CONF %	dMass	Prec MW	Prec m/z	Theor MW	Theor m/z	Theor z	Sc	Ratio	% Err

Experiment 1

DKDPPIPVAK	99.00	5.319559E-02	1.510962E+03	7.564881E+02	1.510908E+03	7.564615E+02	2	16	1.2180	5.7978
FDVSGYPTLK	99.00	2.084649E-02	1.413796E+03	7.079051E+02	1.413775E+03	7.078947E+02	2	16	1.2263	1.9825
FIEEHATK	99.00	-8.312699E-03	1.261683E+03	6.318486E+02	1.261691E+03	6.318528E+02	2	13	1.1620	6.8788
IDATSASVLASR	99.00	-2.843484E-02	1.333704E+03	6.678593E+02	1.333732E+03	6.678734E+02	2	14	1.0264	3.4885

MDATANDVPSDR	99.00	1.349413E-03	1.450649E+03	7.263320E+02	1.450648E+03	7.263313E+02	2	14	1.4685	14.5247
SHMMDVQGSTQDSAIK	99.00	-4.193257E-02	2.021933E+03	6.749851E+02	2.021975E+03	6.749991E+02	3	15	1.7708	7.1057
VDATAETDLAK	99.00	2.319837E-02	1.420789E+03	7.114016E+02	1.420765E+03	7.113899E+02	2	16	1.1482	7.3943
DKDPPIPVAK	99.00	3.061489E-02	1.510939E+03	7.564768E+02	1.510908E+03	7.564615E+02	2	13	1.1360	10.5979
FDVSGYPTIK	99.00	4.322842E-02	1.413818E+03	7.079163E+02	1.413775E+03	7.078947E+02	2	16	1.1139	6.0744
FDVSGYPTIK	99.00	2.084649E-02	1.413796E+03	7.079051E+02	1.413775E+03	7.078947E+02	2	16	1.2263	1.9825
FDVSGYPTIK	99.00	1.584254E-02	1.413791E+03	7.079026E+02	1.413775E+03	7.078947E+02	2	15	1.1594	2.3206
FDVSGYPTIK	99.00	4.452374E-02	1.413819E+03	7.079169E+02	1.413775E+03	7.078947E+02	2	16	1.3758	3.0391
FDVSGYPTIK	99.00	3.329536E-02	1.413808E+03	7.079113E+02	1.413775E+03	7.078947E+02	2	15	1.3709	6.4876
FDVSGYPTLK	99.00	4.322842E-02	1.413818E+03	7.079163E+02	1.413775E+03	7.078947E+02	2	16	1.1139	6.0744
FDVSGYPTLK	99.00	1.584254E-02	1.413791E+03	7.079026E+02	1.413775E+03	7.078947E+02	2	15	1.1594	2.3206
FDVSGYPTLK	99.00	4.452374E-02	1.413819E+03	7.079169E+02	1.413775E+03	7.078947E+02	2	16	1.3758	3.0391
FDVSGYPTLK	99.00	3.329536E-02	1.413808E+03	7.079113E+02	1.413775E+03	7.078947E+02	2	15	1.3709	6.4876
FIEEHATK	99.00	-1.186129E-02	1.261679E+03	6.318469E+02	1.261691E+03	6.318528E+02	2	13	1.2649	3.5439
FIEEHATK	99.00	-4.408444E-02	1.261647E+03	6.318307E+02	1.261691E+03	6.318528E+02	2	13	1.1580	3.2556
FIEEHATK	99.00	-3.089302E-02	1.261660E+03	6.318373E+02	1.261691E+03	6.318528E+02	2	14	1.2082	2.7936
IDATSASVLASR	99.00	4.183810E-02	1.333774E+03	6.678943E+02	1.333732E+03	6.678734E+02	2	17	1.1797	2.8831
IDATSASVLASR	99.00	-8.205622E-03	1.333724E+03	6.678693E+02	1.333732E+03	6.678734E+02	2	16	1.1928	2.7403
SHMMDVQGSTQDSAIK	99.00	6.410150E-03	2.021982E+03	6.750012E+02	2.021975E+03	6.749991E+02	3	19	2.1942	7.0962
SHMMDVQGSTQDSAIK	99.00	1.894571E-02	2.021994E+03	6.750054E+02	2.021975E+03	6.749991E+02	3	16	2.7312	11.6965
DLEHLSK	94.00	-6.217238E-02	1.128576E+03	5.652953E+02	1.128638E+03	5.653264E+02	2	12	1.0718	3.4321
EFVTAFK	94.00	-3.915879E-02	1.128603E+03	5.653088E+02	1.128642E+03	5.653284E+02	2	12	1.1292	1.7055
DLEHLSK	93.00	-6.023728E-03	1.128632E+03	5.653234E+02	1.128638E+03	5.653264E+02	2	12	0.7584	6.6749
EFVTAFK	93.00	-3.378865E-02	1.128609E+03	5.653115E+02	1.128642E+03	5.653284E+02	2	12	1.1066	1.7932
FIEEHATK	92.00	1.745401E-02	1.261708E+03	6.318615E+02	1.261691E+03	6.318528E+02	2	12	1.1582	7.2522
VDATAETDLAK	90.00	4.492531E-02	1.420810E+03	7.114124E+02	1.420765E+03	7.113899E+02	2	12	0.8528	11.5867
Experiment 2										
FDVSGYPTLK	99.00	-5.657232E-03	1.413769E+03	7.078918E+02	1.413775E+03	7.078947E+02	2	14	1.4448	6.0708
FIEEHATK	99.00	-1.674539E-02	1.261674E+03	6.318444E+02	1.261691E+03	6.318528E+02	2	14	1.9028	10.1368
IDATSASVLASR	99.00	-2.764041E-02	1.333705E+03	6.678596E+02	1.333732E+03	6.678734E+02	2	14	1.4255	5.9960
VEGFPTIYFAPSGDK	99.00	1.462843E-02	1.915012E+03	6.393445E+02	1.914997E+03	6.393396E+02	3	16	1.6355	14.6495
FDVSGYPTIK	99.00	-1.750011E-02	1.413757E+03	7.078859E+02	1.413775E+03	7.078947E+02	2	17	1.1767	6.8773
FDVSGYPTIK	99.00	-5.657232E-03	1.413769E+03	7.078918E+02	1.413775E+03	7.078947E+02	2	14	1.4448	6.0708
FDVSGYPTLK	99.00	-1.750011E-02	1.413757E+03	7.078859E+02	1.413775E+03	7.078947E+02	2	17	1.1767	6.8773
FIEEHATK	99.00	-1.326064E-02	1.261678E+03	6.318461E+02	1.261691E+03	6.318528E+02	2	14	1.7310	3.6763
FIEEHATK	99.00	-1.277236E-02	1.261678E+03	6.318464E+02	1.261691E+03	6.318528E+02	2	13	1.6712	4.3377
VEGFPTIYFAPSGDK	99.00	3.055725E-02	1.915028E+03	6.393499E+02	1.914997E+03	6.393396E+02	3	16	1.8184	12.9072
VEGFPTIYFAPSGDK	99.00	1.357701E-02	1.915011E+03	6.393442E+02	1.914997E+03	6.393396E+02	3	14	1.3702	10.2161
VEGFPTIYFAPSGDK	99.00	1.687269E-02	1.915014E+03	6.393453E+02	1.914997E+03	6.393396E+02	3	15	1.1124	11.8090
VEGFPTIYFAPSGDK	99.00	-9.349778E-03	1.914988E+03	6.393365E+02	1.914997E+03	6.393396E+02	3	15	2.1553	18.8145
DLEHLSK	96.00	-5.320731E-03	1.128633E+03	5.653237E+02	1.128638E+03	5.653264E+02	2	12	1.7981	4.8335
DLEHLSK	96.00	-1.154621E-02	1.128627E+03	5.653206E+02	1.128638E+03	5.653264E+02	2	12	1.7197	3.4134
EFVTAFK	94.00	-1.906131E-02	1.128623E+03	5.653189E+02	1.128642E+03	5.653284E+02	2	12	1.2106	2.4685
VEGFPTIYFAPSGDK	86.00	-1.206294E-02	1.914985E+03	6.393356E+02	1.914997E+03	6.393396E+02	3	12	2.4934	24.6496
VEGFPTIYFAPSGDK	80.00	6.579802E-03	1.915004E+03	6.393419E+02	1.914997E+03	6.393396E+02	3	12	1.3160	20.8366

P30101 / Protein disulfide-isomerase A3 precursor (PDIA3)

PEPTIDE SEQUENCE	CONF %	dMass	Prec MW	Prec m/z	Theor MW	Theor m/z	Theor z	Sc	Ratio	% Err
Experiment 1										

DASIVGFFDDSFSEAHSEFLK	99.00	-4.880789E-02	2.635220E+03	8.794139E+02	2.635269E+03	8.794301E+02	3	18	0.9556	12.1305
DPNIVIAK	99.00	-1.010168E-01	1.156605E+03	5.793098E+02	1.156706E+03	5.793602E+02	2	14	1.1274	1.8393
EATNPPVIQEEKPK	99.00	8.710539E-02	2.011219E+03	6.714135E+02	2.011132E+03	6.713845E+02	3	16	0.9328	9.4727
LAPEYEAAATR	99.00	2.073262E-02	1.334716E+03	6.683652E+02	1.334695E+03	6.683549E+02	2	16	1.0102	4.9359
TADGIVSHLK	99.00	1.587938E-02	1.327786E+03	6.649004E+02	1.327770E+03	6.648924E+02	2	14	1.3461	9.8831

TVAYTEQK	99.00	-2.465011E-02	1.226650E+03	6.143325E+02	1.226675E+03	6.143448E+02	2	13	0.9917	2.9879
VDCTANTNTCNK	99.00	-1.038372E-01	1.662604E+03	8.323092E+02	1.662708E+03	8.323612E+02	2	19	0.9158	3.8799
DASIVGFFDDSFSEAHSEFLK	99.00	-1.420227E-02	2.635254E+03	8.794254E+02	2.635269E+03	8.794301E+02	3	18	1.1201	13.2888
DPNIVIAK	99.00	-4.454628E-02	1.156661E+03	5.793380E+02	1.156706E+03	5.793602E+02	2	14	1.2394	3.1720
DPNIVIAK	99.00	-8.100066E-02	1.156625E+03	5.793198E+02	1.156706E+03	5.793602E+02	2	14	1.1752	1.8996
EATNPPVIQEEKPK	99.00	5.814133E-02	2.011190E+03	6.714038E+02	2.011132E+03	6.713845E+02	3	15	1.2027	5.2132
EATNPPVIQEEKPK	99.00	2.774206E-02	2.011159E+03	6.713937E+02	2.011132E+03	6.713845E+02	3	14	1.1030	12.7186
TADGIVSHLK	99.00	2.144482E-02	1.327792E+03	6.649031E+02	1.327770E+03	6.648924E+02	2	16	1.0872	10.4030
TADGIVSHLK	99.00	-9.568524E-02	1.183573E+03	5.927936E+02	1.183668E+03	5.928414E+02	2	15	2.6372	6.8831
TADGIVSHLK	99.00	5.563915E-03	1.327776E+03	6.648952E+02	1.327770E+03	6.648924E+02	2	17	1.2258	5.8112
TADGIVSHLK	99.00	-4.417147E-02	1.327726E+03	6.648704E+02	1.327770E+03	6.648924E+02	2	18	1.0834	2.1430
TADGIVSHLK	99.00	-4.514791E-02	1.327725E+03	6.648699E+02	1.327770E+03	6.648924E+02	2	18	0.9756	2.7274
TADGIVSHLK	99.00	-3.208807E-02	1.327738E+03	6.648764E+02	1.327770E+03	6.648924E+02	2	17	1.0559	4.3527
TADGIVSHLK	99.00	2.947825E-02	1.327800E+03	4.436072E+02	1.327770E+03	4.435974E+02	3	14	1.0905	4.0201
TVAYTEQK	99.00	4.189634E-03	1.226679E+03	6.143469E+02	1.226675E+03	6.143448E+02	2	14	1.0613	1.9230
TVAYTEQK	99.00	-1.131181E-02	1.226664E+03	6.143391E+02	1.226675E+03	6.143448E+02	2	13	1.0019	1.8622
TVAYTEQK	99.00	-9.602990E-03	1.226665E+03	6.143400E+02	1.226675E+03	6.143448E+02	2	14	0.8808	2.2180
QAGPASVPLR	98.00	-6.913961E-02	1.138589E+03	5.703017E+02	1.138658E+03	5.703363E+02	2	13	1.1919	3.2657
DPNIVIAK	98.00	-5.211373E-02	1.156654E+03	5.793342E+02	1.156706E+03	5.793602E+02	2	13	1.1748	3.9443
TVAYTEQK	97.00	8.492417E-03	1.226684E+03	6.143491E+02	1.226675E+03	6.143448E+02	2	12	0.7985	8.3117
TADGIVSHLK	96.00	4.894467E-03	1.327775E+03	6.648949E+02	1.327770E+03	6.648924E+02	2	12	1.1013	8.4834
TVAYTEQK	96.00	7.085525E-03	1.226682E+03	6.143483E+02	1.226675E+03	6.143448E+02	2	12	0.9003	3.1028
FLDAGHK	92.00	-7.914594E-03	1.074599E+03	5.383066E+02	1.074607E+03	5.383106E+02	2	12	1.0175	2.5183
EATNPPVIQEEKPK	90.00	4.757522E-02	2.011179E+03	6.714003E+02	2.011132E+03	6.713845E+02	3	12	0.7343	12.5097
QAGPASVPLR	90.00	7.490844E-03	1.138666E+03	5.703400E+02	1.138658E+03	5.703363E+02	2	12	1.1521	3.1347
FVMQEEFSR	89.00	1.439298E-02	1.315650E+03	6.588321E+02	1.315635E+03	6.588249E+02	2	12	1.0236	4.8849
SEPIPESNDGPVK	89.00	1.623699E-02	1.655877E+03	8.289459E+02	1.655861E+03	8.289378E+02	2	11	1.0265	8.5758
QAGPASVPLR	89.00	-2.009268E-02	1.138638E+03	5.703262E+02	1.138658E+03	5.703363E+02	2	12	1.1483	3.0337
SEPIPESNDGPVK	89.00	-6.131131E-02	1.655800E+03	8.289071E+02	1.655861E+03	8.289378E+02	2	12	0.9525	13.1505
YGVSGYPTLK	86.00	6.731486E-02	1.371832E+03	6.869230E+02	1.371764E+03	6.868894E+02	2	12	0.8115	4.3520
TADGIVSHLK	85.00	-1.805311E-02	1.183650E+03	5.928324E+02	1.183668E+03	5.928414E+02	2	13	2.1005	15.0159
TEEEFKK	83.00	-2.168384E-02	1.341729E+03	6.718717E+02	1.341751E+03	6.718826E+02	2	11	1.3418	8.6688
TVAYTEQK	81.00	2.734751E-02	1.226702E+03	6.143585E+02	1.226675E+03	6.143448E+02	2	11	0.7231	4.1136
Experiment 2										
DPNIVIAK	99.00	-3.335359E-02	1.156673E+03	5.793436E+02	1.156706E+03	5.793602E+02	2	13	1.2240	6.9513
EATNPPVIQEEKPK	99.00	-4.354776E-02	2.011088E+03	6.713699E+02	2.011132E+03	6.713845E+02	3	20	1.6064	3.1418
ELSDFISYLQR	99.00	-7.801795E-03	1.513782E+03	7.578983E+02	1.513790E+03	7.579022E+02	2	14	1.7063	19.9224
LAPEYEAAATR	99.00	-2.149697E-02	1.334674E+03	6.683441E+02	1.334695E+03	6.683549E+02	2	18	1.5378	3.0813
QAGPASVPLR	99.00	-8.456305E-03	9.775210E+02	4.897678E+02	9.775294E+02	4.897720E+02	2	14	1.2100	7.3812
SEPIPESNDGPVK	99.00	1.558167E-02	1.655877E+03	5.529661E+02	1.655861E+03	5.529609E+02	3	16	1.4351	8.8652
TADGIVSHLK	99.00	-3.065159E-02	1.327740E+03	4.435872E+02	1.327770E+03	4.435974E+02	3	15	1.4347	2.9477
VVVAENFDEIVNNENK	99.00	5.879533E-03	2.120105E+03	7.077090E+02	2.120099E+03	7.077071E+02	3	19	1.4876	8.5578
DPNIVIAK	99.00	-2.854089E-02	1.156677E+03	5.793459E+02	1.156706E+03	5.793602E+02	2	14	1.5855	3.0304
DPNIVIAK	99.00	-3.236136E-02	1.156674E+03	5.793441E+02	1.156706E+03	5.793602E+02	2	14	1.5774	2.5438
DPNIVIAK	99.00	-2.322660E-02	1.156683E+03	5.793486E+02	1.156706E+03	5.793602E+02	2	14	1.4574	8.0700
DPNIVIAK	99.00	-1.587262E-02	1.156690E+03	5.793523E+02	1.156706E+03	5.793602E+02	2	14	1.6346	3.7787
DPNIVIAK	99.00	-2.173186E-02	1.156684E+03	5.793494E+02	1.156706E+03	5.793602E+02	2	14	1.6064	3.3505
DPNIVIAK	99.00	-1.294300E-02	1.156693E+03	5.793538E+02	1.156706E+03	5.793602E+02	2	13	1.5142	6.5779
DPNIVIAK	99.00	-2.915665E-02	1.156677E+03	5.793456E+02	1.156706E+03	5.793602E+02	2	14	1.6830	2.8232
DPNIVIAK	99.00	-3.648071E-02	1.156669E+03	5.793420E+02	1.156706E+03	5.793602E+02	2	14	1.6363	2.3076

DPNIVIAK	99.00	-2.308825E-02	1.156683E+03	5.793487E+02	1.156706E+03	5.793602E+02	2	14	1.5686	2.8639
DPNIVIAK	99.00	-4.213088E-02	1.156664E+03	5.793392E+02	1.156706E+03	5.793602E+02	2	14	1.6350	2.0187
DPNIVIAK	99.00	-4.054399E-02	1.156665E+03	5.793400E+02	1.156706E+03	5.793602E+02	2	14	1.6732	2.0691
DPNIVIAK	99.00	-3.286244E-02	1.156673E+03	5.793438E+02	1.156706E+03	5.793602E+02	2	14	1.6331	2.9911
DPNIVIAK	99.00	-2.907835E-02	1.156677E+03	5.793457E+02	1.156706E+03	5.793602E+02	2	14	1.6701	3.5551

DPNIVIAK	99.00	-2.373784E-02	1.156682E+03	5.793484E+02	1.156706E+03	5.793602E+02	2	14	1.5683	3.4145
DPNIVIAK	99.00	-2.410405E-02	1.156682E+03	5.793482E+02	1.156706E+03	5.793602E+02	2	14	1.5443	4.5047
DPNIVIAK	99.00	-1.922122E-02	1.156687E+03	5.793506E+02	1.156706E+03	5.793602E+02	2	13	1.4472	6.0142
EATNPPVIQEEKPK	99.00	-4.903671E-02	2.011083E+03	6.713681E+02	2.011132E+03	6.713845E+02	3	23	1.5911	3.5406
EATNPPVIQEEKPK	99.00	-4.171311E-02	2.011090E+03	6.713705E+02	2.011132E+03	6.713845E+02	3	23	1.5204	4.1309
EATNPPVIQEEKPK	99.00	-2.285822E-02	2.011109E+03	6.713768E+02	2.011132E+03	6.713845E+02	3	23	1.7245	3.1224
EATNPPVIQEEKPK	99.00	-2.157516E-02	2.011110E+03	6.713773E+02	2.011132E+03	6.713845E+02	3	17	1.6206	8.7603
ELSDFISYLQR	99.00	2.890868E-02	1.657921E+03	5.536475E+02	1.657892E+03	5.536379E+02	3	18	1.9496	6.0003
LAPEYEAAATR	99.00	-2.095937E-02	1.334674E+03	6.683444E+02	1.334695E+03	6.683549E+02	2	18	1.5218	4.0391
LAPEYEAAATR	99.00	-2.345737E-02	1.334672E+03	6.683431E+02	1.334695E+03	6.683549E+02	2	18	1.5321	3.1897
LAPEYEAAATR	99.00	-9.041091E-03	1.334686E+03	6.683503E+02	1.334695E+03	6.683549E+02	2	18	1.5148	7.1450
QAGPASVPLR	99.00	-3.642150E-02	1.138622E+03	5.703181E+02	1.138658E+03	5.703363E+02	2	15	1.4909	2.5335
QAGPASVPLR	99.00	-4.130408E-02	1.138617E+03	5.703157E+02	1.138658E+03	5.703363E+02	2	14	1.4460	2.4572
QAGPASVPLR	99.00	-4.163391E-02	1.138616E+03	5.703155E+02	1.138658E+03	5.703363E+02	2	14	1.3108	2.6541
QAGPASVPLR	99.00	-2.600987E-02	1.138632E+03	5.703233E+02	1.138658E+03	5.703363E+02	2	15	1.2455	3.6342
SEPIPESNDGPVK	99.00	1.416945E-02	1.655875E+03	5.529656E+02	1.655861E+03	5.529609E+02	3	15	1.2365	7.0377
SEPIPESNDGPVK	99.00	1.746522E-02	1.655878E+03	5.529667E+02	1.655861E+03	5.529609E+02	3	14	1.6138	10.9226
TADGIVSHLK	99.00	-8.297915E-03	1.183660E+03	5.928373E+02	1.183668E+03	5.928414E+02	2	16	1.8247	6.7340
TADGIVSHLK	99.00	-2.804889E-03	1.183666E+03	5.928400E+02	1.183668E+03	5.928414E+02	2	16	1.4485	15.8704
TADGIVSHLK	99.00	-4.900599E-03	1.183663E+03	5.928390E+02	1.183668E+03	5.928414E+02	2	16	1.5786	3.8122
TADGIVSHLK	99.00	-2.093113E-03	1.183666E+03	5.928404E+02	1.183668E+03	5.928414E+02	2	15	1.2176	8.7347
TADGIVSHLK	99.00	-4.233755E-02	1.327728E+03	6.648713E+02	1.327770E+03	6.648924E+02	2	17	1.1330	3.7554
VVVAENFDEIVNNENK	99.00	1.741420E-02	2.120117E+03	7.077128E+02	2.120099E+03	7.077071E+02	3	19	1.4907	8.9679
VVVAENFDEIVNNENK	99.00	1.247077E-02	2.120112E+03	7.077112E+02	2.120099E+03	7.077071E+02	3	18	1.6098	8.7388
DPNIVIAK	98.00	-2.350026E-02	1.156682E+03	5.793485E+02	1.156706E+03	5.793602E+02	2	13	1.4850	3.9965
GFPTIYFSPANK	97.00	2.585292E-02	1.628906E+03	5.439761E+02	1.628881E+03	5.439675E+02	3	13	1.9415	4.0646
DPNIVIAK	96.00	-1.198891E-02	1.156694E+03	5.793542E+02	1.156706E+03	5.793602E+02	2	12	1.5294	6.8347
GFPTIYFSPANK	96.00	2.621910E-02	1.628907E+03	5.439762E+02	1.628881E+03	5.439675E+02	3	13	1.6774	4.4921
GFPTIYFSPANK	96.00	-4.349814E-03	1.628876E+03	5.439660E+02	1.628881E+03	5.439675E+02	3	13	1.8635	3.7770
TEEEFKK	95.00	-1.803677E-02	1.341733E+03	6.718735E+02	1.341751E+03	6.718826E+02	2	12	1.6110	5.6723
DPNIVIAK	92.00	-2.500116E-02	1.156681E+03	5.793477E+02	1.156706E+03	5.793602E+02	2	12	1.3707	5.5278
GFPTIYFSPANK	91.00	5.286870E-03	1.628886E+03	5.439692E+02	1.628881E+03	5.439675E+02	3	12	2.7388	22.7244
FLQDYFDGNLK	90.00	1.561979E-02	1.646870E+03	5.499641E+02	1.646855E+03	5.499589E+02	3	12	1.0970	12.8257
FLQDYFDGNLK	87.00	1.833272E-02	1.646873E+03	5.499650E+02	1.646855E+03	5.499589E+02	3	12	1.2992	10.6683
TADGIVSHLK	87.00	5.891983E-03	1.183674E+03	5.928444E+02	1.183668E+03	5.928414E+02	2	12	1.2814	14.4789
FLQDYFDGNLK	86.00	5.549463E-03	1.646860E+03	5.499607E+02	1.646855E+03	5.499589E+02	3	12	1.4958	13.9402
GFPTIYFSPANK	84.00	6.751622E-03	1.628887E+03	5.439697E+02	1.628881E+03	5.439675E+02	3	12	1.3914	19.5507
GFPTIYFSPANK	82.00	4.099659E-02	1.628922E+03	5.439811E+02	1.628881E+03	5.439675E+02	3	12	1.6639	5.7880
GFPTIYFSPANK	82.00	3.257414E-02	1.628913E+03	5.439783E+02	1.628881E+03	5.439675E+02	3	12	1.5413	5.5096
GFPTIYFSPANK	80.00	1.597364E-02	1.628896E+03	5.439728E+02	1.628881E+03	5.439675E+02	3	12	1.9416	4.2981

Q5QNW6 / Histone H2B type 2-F

PEPTIDE SEQUENCE	CONF %	dMass	Prec MW	Prec m/z	Theor MW	Theor m/z	Theor z	Sc	Ratio	% Err
Experiment 1										
ESYSVYVYK	99.00	2.914932E-02	1.424772E+03	7.133934E+02	1.424743E+03	7.133788E+02	2	15	2.8476	2.2135
HAVSEGTK	99.00	-1.105178E-01	1.115507E+03	5.587609E+02	1.115618E+03	5.588162E+02	2	14	1.9504	1.5783
KESYSVYVYK	99.00	3.165387E-02	1.696972E+03	8.494932E+02	1.696940E+03	8.494773E+02	2	14	2.5705	6.7070
LLLPGELAK	99.00	-6.910653E-02	1.240731E+03	6.213726E+02	1.240800E+03	6.214072E+02	2	16	1.3514	1.2356
QVHPDTGISSK	99.00	-5.070264E-02	1.455742E+03	7.288782E+02	1.455793E+03	7.289035E+02	2	19	3.0755	2.5012

ESYSVYVYK	99.00	2.072796E-02	1.424764E+03	7.133892E+02	1.424743E+03	7.133788E+02	2	15	3.0646	3.4977
ESYSVYVYK	99.00	-2.626080E-02	1.424717E+03	7.133657E+02	1.424743E+03	7.133788E+02	2	15	2.6987	2.3955
HAVSEGTK	99.00	-7.353577E-02	1.115544E+03	5.587794E+02	1.115618E+03	5.588162E+02	2	13	2.1987	1.7497
LLLPGELAK	99.00	-6.971682E-02	1.240730E+03	6.213723E+02	1.240800E+03	6.214072E+02	2	16	1.6908	1.4188
LLLPGELAK	99.00	-6.031831E-02	1.240740E+03	6.213770E+02	1.240800E+03	6.214072E+02	2	16	1.2619	1.2078

LLLPGELAK	99.00	-5.433743E-02	1.240745E+03	6.213800E+02	1.240800E+03	6.214072E+02	2	15	1.7223	1.4757
LLLPGELAK	99.00	-4.284477E-02	1.240757E+03	6.213858E+02	1.240800E+03	6.214072E+02	2	15	2.5216	2.6073
LLLPGELAK	99.00	-1.033866E-01	1.240697E+03	6.213555E+02	1.240800E+03	6.214072E+02	2	14	2.1610	1.7874
LLLPGELAK	99.00	-1.174235E-01	1.240682E+03	6.213485E+02	1.240800E+03	6.214072E+02	2	14	2.0988	1.7739
LLLPGELAK	99.00	-1.180338E-01	1.240682E+03	6.213482E+02	1.240800E+03	6.214072E+02	2	15	2.2914	1.9229
QVHPDTGISSK	99.00	1.770155E-03	1.294666E+03	6.483401E+02	1.294664E+03	6.483392E+02	2	13	0.9670	13.0666
QVHPDTGISSK	99.00	1.751623E-02	1.294681E+03	6.483480E+02	1.294664E+03	6.483392E+02	2	14	1.6198	13.2848
QVHPDTGISSK	99.00	-2.107648E-02	1.294643E+03	6.483287E+02	1.294664E+03	6.483392E+02	2	16	2.3755	8.6318
QVHPDTGISSK	99.00	-5.818389E-02	1.294606E+03	6.483101E+02	1.294664E+03	6.483392E+02	2	17	2.8389	6.7176
QVHPDTGISSK	99.00	-4.927323E-02	1.294615E+03	6.483146E+02	1.294664E+03	6.483392E+02	2	18	2.5410	6.1849
QVHPDTGISSK	99.00	-6.599598E-02	1.294598E+03	6.483062E+02	1.294664E+03	6.483392E+02	2	16	2.5341	6.1840
QVHPDTGISSK	99.00	-2.717967E-02	1.294637E+03	6.483256E+02	1.294664E+03	6.483392E+02	2	13	1.4138	10.5607
QVHPDTGISSK	99.00	-1.064223E-02	1.294653E+03	6.483339E+02	1.294664E+03	6.483392E+02	2	14	2.5963	15.4290
QVHPDTGISSK	99.00	2.881010E-03	1.455795E+03	7.289050E+02	1.455793E+03	7.289035E+02	2	16	3.7587	5.4622
QVHPDTGISSK	99.00	-5.253352E-02	1.455740E+03	7.288773E+02	1.455793E+03	7.289035E+02	2	18	2.9257	2.8124
HAVSEGTK	98.00	-1.100295E-01	1.115508E+03	5.587612E+02	1.115618E+03	5.588162E+02	2	13	2.3239	1.7981
HAVSEGTK	98.00	-7.548862E-02	1.115542E+03	5.587784E+02	1.115618E+03	5.588162E+02	2	13	2.6502	3.1929
HAVSEGTK	98.00	-8.329999E-02	1.115535E+03	5.587745E+02	1.115618E+03	5.588162E+02	2	13	2.9128	3.2472
LLLPGELAK	98.00	-4.872274E-02	1.240751E+03	6.213828E+02	1.240800E+03	6.214072E+02	2	13	2.4515	2.4855
QVHPDTGISSK	98.00	-2.346037E-02	1.294641E+03	6.483275E+02	1.294664E+03	6.483392E+02	2	13	2.6045	17.5047
LAHYNK	97.00	-2.292699E-02	1.032573E+03	1.033580E+03	1.032596E+03	1.033603E+03	1	10	2.7933	10.8458
AMGIMNSFVNDIFER	94.00	-6.090954E-02	1.902848E+03	9.524313E+02	1.902909E+03	9.524618E+02	2	13	2.8675	16.0685
LLLPGELAK	92.00	-1.191782E-02	1.240788E+03	6.214012E+02	1.240800E+03	6.214072E+02	2	12	2.3120	4.4360
HAVSEGTK	90.00	-3.041180E-04	1.115618E+03	5.588160E+02	1.115618E+03	5.588162E+02	2	12	2.3178	7.0457
LLLPGELAK	90.00	-2.946917E-02	1.240770E+03	6.213925E+02	1.240800E+03	6.214072E+02	2	12	2.6412	3.5982
LLLPGELAK	89.00	-3.839255E-03	1.240796E+03	6.214053E+02	1.240800E+03	6.214072E+02	2	12	2.7054	4.8569
IAGEASR	86.00	-3.977320E-02	8.464283E+02	4.242214E+02	8.464681E+02	4.242413E+02	2	12	2.5075	2.7444
IAGEASR	84.00	-1.017238E-02	8.464579E+02	4.242362E+02	8.464681E+02	4.242413E+02	2	12	2.3293	3.2976
IAGEASR	84.00	6.803285E-02	8.465362E+02	4.242754E+02	8.464681E+02	4.242413E+02	2	12	2.6649	5.7319
IAGEASR	83.00	-2.003766E-02	8.464481E+02	4.242313E+02	8.464681E+02	4.242413E+02	2	12	2.1172	1.8740
IAGEASR	82.00	-6.141604E-02	8.464067E+02	4.242106E+02	8.464681E+02	4.242413E+02	2	12	1.8222	1.5838
IAGEASR	81.00	-1.082212E-02	8.464573E+02	4.242359E+02	8.464681E+02	4.242413E+02	2	12	2.1408	2.2574

Q5JQ37 / Prosaposin (variant Gaucher disease and variant metachromatic leukodystrophy)

PEPTIDE SEQUENCE	CONF %	dMass	Prec MW	Prec m/z	Theor MW	Theor m/z	Theor z	Sc	Ratio	% Err
Experiment 2										
EIVDSYLPVILDIIK	99.00	-2.100276E-02	2.017174E+03	6.733987E+02	2.017195E+03	6.734058E+02	3	14	N.D.	N.D.
QEILAALEK	99.00	-1.824803E-02	1.301762E+03	6.518881E+02	1.301780E+03	6.518972E+02	2	15	1.8199	5.4128
QEILAALEK	99.00	-5.431730E-03	1.301774E+03	6.518945E+02	1.301780E+03	6.518972E+02	2	16	1.8623	5.7096
QEILAALEK	99.00	-2.982270E-03	1.301777E+03	6.518957E+02	1.301780E+03	6.518972E+02	2	15	1.6053	3.0510
EIVDSYLPVILDIIK	96.00	-4.160648E-02	2.017154E+03	6.733919E+02	2.017195E+03	6.734058E+02	3	13	N.D.	N.D.
LVGYLDR	93.00	-2.18604E-02	9.78540E+02	4.90277E+02	9.78562E+02	4.90288E+02	2	12	1.6380	2.8511
LVGYLDR	93.00	-7.37349E-03	9.78555E+02	4.90285E+02	9.78562E+02	4.90288E+02	2	12	1.5692	6.5833
LVGYLDR	92.00	-5.03792E-02	9.78512E+02	4.90263E+02	9.78562E+02	4.90288E+02	2	12	1.6700	1.9730
LVGYLDR	92.00	-1.36708E-02	9.78548E+02	4.90282E+02	9.78562E+02	4.90288E+02	2	12	1.7099	3.0606
LVGYLDR	92.00	-1.54407E-02	9.78547E+02	4.90281E+02	9.78562E+02	4.90288E+02	2	12	1.5284	4.1991
LVGYLDR	91.00	-7.02990E-03	9.78555E+02	4.90285E+02	9.78562E+02	4.90288E+02	2	12	1.4628	4.3343
LVGYLDR	88.00	-1.18792E-02	9.78550E+02	4.90282E+02	9.78562E+02	4.90288E+02	2	12	1.4021	6.4830
LVGYLDR	87.00	-1.39715E-02	9.78548E+02	4.90281E+02	9.78562E+02	4.90288E+02	2	12	1.6359	4.1798

LVGYLDR	85.00	-2.75749E-02	9.78534E+02	4.90275E+02	9.78562E+02	4.90288E+02	2	12	1.5142	2.7842
LVGYLDR	84.00	-2.70098E-02	9.78535E+02	4.90275E+02	9.78562E+02	4.90288E+02	2	12	1.5489	3.3828
LVGYLDR	84.00	2.62136E-03	9.78565E+02	4.90290E+02	9.78562E+02	4.90288E+02	2	11	1.2580	10.0149
GCSFLPDPYQK	83.00	3.99846E-02	1.58781E+03	5.30276E+02	1.58777E+03	5.30263E+02	3	12	2.5329	6.6178

UPI000054B38F and A8K3K8 / Carboxylesterase 1 isoform c precursor

PEPTIDE SEQUENCE	CONF %	dMass	Prec MW	Prec m/z	Theor MW	Theor m/z	Theor z	Sc	Ratio	% Err
Experiment 2										
AVEKPPQTEHIEL	99.00	-1.263666E-03	1.777980E+03	5.936674E+02	1.777982E+03	5.936679E+02	3	14	1.6014	9.7535
DKEVAFWTNLFAK	99.00	3.876157E-02	2.000149E+03	6.677234E+02	2.000110E+03	6.677105E+02	3	18	1.6473	6.8122
EVAFWTNLFAK	99.00	1.707094E-02	1.612903E+03	5.386415E+02	1.612886E+03	5.386358E+02	3	14	1.7961	4.5614
FTPPQPAEPWSFVK	99.00	6.320823E-03	1.918030E+03	6.403505E+02	1.918023E+03	6.403484E+02	3	16	1.3225	6.3197
TAMSLLWK	99.00	1.875358E-02	1.236733E+03	6.193738E+02	1.236714E+03	6.193645E+02	2	14	1.4635	8.4537
DKEVAFWTNLFAK	99.00	2.177205E-02	2.000131E+03	6.677178E+02	2.000110E+03	6.677105E+02	3	17	1.8056	5.7173
EVAFWTNLFAK	99.00	1.189362E-02	1.612898E+03	5.386398E+02	1.612886E+03	5.386358E+02	3	14	1.7462	6.1795
EVAFWTNLFAK	99.00	7.499203E-03	1.612893E+03	5.386384E+02	1.612886E+03	5.386358E+02	3	15	1.5626	5.3342
FTPPQPAEPWSFVK	99.00	3.381797E-02	1.918057E+03	6.403596E+02	1.918023E+03	6.403484E+02	3	17	1.1790	10.0507
TAMSLLWK	99.00	-6.972889E-03	1.236707E+03	6.193610E+02	1.236714E+03	6.193645E+02	2	14	1.4291	8.4860
TAMSLLWK	99.00	6.309933E-03	1.236721E+03	6.193676E+02	1.236714E+03	6.193645E+02	2	14	1.4709	7.7380
TAMSLLWK	99.00	6.309933E-03	1.236721E+03	6.193676E+02	1.236714E+03	6.193645E+02	2	14	1.2557	8.4400
DKEVAFWTNLFAK	97.00	2.850792E-02	2.000138E+03	6.677200E+02	2.000110E+03	6.677105E+02	3	13	1.6465	11.9313
EVAFWTNLFAK	97.00	1.432439E-02	1.612900E+03	5.386406E+02	1.612886E+03	5.386358E+02	3	13	1.7008	4.1862
EVAFWTNLFAK	86.00	2.909764E-02	1.612915E+03	5.386456E+02	1.612886E+03	5.386358E+02	3	12	1.6355	17.1426

UPI000013D53C and P20933 / N(4)-(beta-N-acetylglucosaminyl)-L-asparaginase precursor; Glycosylasparaginase beta c, Aspartylglucosaminidase

PEPTIDE SEQUENCE	CONF %	dMass	Prec MW	Prec m/z	Theor MW	Theor m/z	Theor z	Sc	Ratio	% Err
Experiment 2										
SPLPLVVNTWPFK	99.00	5.486240E-03	1.785049E+03	5.960235E+02	1.785043E+03	5.960217E+02	3	13	2.7009	19.4498
SPLPLVVNTWPFK	98.00	1.764489E-02	1.785061E+03	5.960276E+02	1.785043E+03	5.960217E+02	3	13	1.8467	16.2550
SPLPLVVNTWPFK	97.00	-4.875697E-03	1.785038E+03	5.960201E+02	1.785043E+03	5.960217E+02	3	13	1.2766	14.2209
SPLPLVVNTWPFK	97.00	4.108094E-02	1.785084E+03	5.960354E+02	1.785043E+03	5.960217E+02	3	13	1.7817	17.0089
NVIPDPSK	90.00	-1.845423E-02	1.156651E+03	5.793328E+02	1.156670E+03	5.793421E+02	2	12	1.3594	3.8289
NVIPDPSK	87.00	-1.735559E-02	1.156652E+03	5.793334E+02	1.156670E+03	5.793421E+02	2	12	1.3094	3.8461
SPLPLVVNTWPFK	84.00	4.064081E-02	1.785084E+03	5.960352E+02	1.785043E+03	5.960217E+02	3	12	2.3416	22.8310

UPI00002263A8 and NM198901 / Sorcin isoform b

PEPTIDE SEQUENCE	CONF %	dMass	Prec MW	Prec m/z	Theor MW	Theor m/z	Theor z	Sc	Ratio	% Err
Experiment 2										
QHFISFDTDR	99.00	-1.820910E-02	1.408667E+03	7.053410E+02	1.408686E+03	7.053501E+02	2	16	1.5595	3.9850
ELWAVLNGWR	99.00	8.017416E-03	1.386761E+03	6.943878E+02	1.386753E+03	6.943838E+02	2	16	1.6386	10.9324
ELWAVLNGWR	99.00	1.985791E-02	1.386773E+03	6.943937E+02	1.386753E+03	6.943838E+02	2	15	1.4618	9.0995
ELWAVLNGWR	98.00	1.729766E-02	1.386770E+03	6.943925E+02	1.386753E+03	6.943838E+02	2	13	1.8281	14.1195
ELWAVLNGWR	94.00	5.492302E-02	1.386808E+03	6.944113E+02	1.386753E+03	6.943838E+02	2	12	1.6042	14.6774
LMVSMLDR	88.00	-1.752483E-03	1.107589E+03	5.548015E+02	1.107590E+03	5.548024E+02	2	12	1.1575	4.1975

Q05655 / Protein kinase C delta type

PEPTIDE SEQUENCE	CONF %	dMass	Prec MW	Prec m/z	Theor MW	Theor m/z	Theor z	Sc	Ratio	% Err
Experiment 2										
CEDCGMNVHHK	99.00	-3.139432E-03	1.651661E+03	5.515609E+02	1.651664E+03	5.515620E+02	3	20	1.5533	4.5998
NHEFIATFFGQPTFCSVCK	99.00	1.540347E-02	2.555187E+03	6.398040E+02	2.555171E+03	6.398001E+02	4	17	N.D.	N.D.
TINWTLLEK	99.00	-9.598296E-03	1.404813E+03	7.034135E+02	1.404822E+03	7.034183E+02	2	15	0.9491	8.0491

CEDCGMNVHHK	99.00	7.718077E-03	1.667667E+03	5.568962E+02	1.667659E+03	5.568936E+02	3	15	1.4083	7.5512
CEDCGMNVHHK	99.00	1.126688E-03	1.667660E+03	5.568940E+02	1.667659E+03	5.568936E+02	3	15	1.5088	8.7234
CEDCGMNVHHK	99.00	-1.279396E-02	1.651651E+03	5.515577E+02	1.651664E+03	5.515620E+02	3	18	1.4095	3.6592
CEDCGMNVHHK	99.00	4.473578E-03	1.667663E+03	5.568951E+02	1.667659E+03	5.568936E+02	3	16	1.4925	11.0401
NHEFIATFFGQPTFCSVCK	99.00	2.370362E-02	2.555195E+03	6.398060E+02	2.555171E+03	6.398001E+02	4	15	N.D.	N.D.

Q10471 / UDP-N-acetyl-alpha-D-galactosamine:polypeptide N-acetylgalactosaminyltransferase 2 (GalNAc-T2)

PEPTIDE SEQUENCE	CONF %	dMass	Prec MW	Prec m/z	Theor MW	Theor m/z	Theor z	Sc	Ratio	% Err
Experiment 1										
HVGSNLCLDSR	99.00	4.725831E-02	1.389709E+03	6.958616E+02	1.389661E+03	6.958380E+02	2	16	0.6609	5.5582
VDLPATSVVITFHNEAR	99.00	5.586467E-02	2.012137E+03	6.717197E+02	2.012081E+03	6.717010E+02	3	15	0.8673	17.5863
HVGSNLCLDSR	99.00	5.104194E-02	1.389713E+03	6.958635E+02	1.389661E+03	6.958380E+02	2	14	0.6925	9.2757
VDLPATSVVITFHNEAR	99.00	5.256904E-02	2.012134E+03	6.717186E+02	2.012081E+03	6.717010E+02	3	16	0.5847	12.9809
Experiment 2										
FNQVESDK	99.00	-9.637223E-03	1.253640E+03	6.278272E+02	1.253650E+03	6.278321E+02	2	13	0.7273	6.0654
KDLHHSNGEEK	99.00	1.641851E-02	1.725917E+03	5.763131E+02	1.725901E+03	5.763077E+02	3	16	0.5355	8.7524

Q92896/ Golgi apparatus protein 1 precursor (GSLG1); Cysteine-rich fibroblast growth factor receptor, E-selectin ligand 1

PEPTIDE SEQUENCE	CONF %	dMass	Prec MW	Prec m/z	Theor MW	Theor m/z	Theor z	Sc	Ratio	% Err
Experiment 1										
GEIEHHCSGLHR	99.00	1.320187E-01	1.563848E+03	5.222899E+02	1.563716E+03	5.222458E+02	3	14	0.3941	13.5265
LLELQYFISR	99.00	-2.102026E-02	1.424794E+03	7.134042E+02	1.424815E+03	7.134147E+02	2	14	0.5487	9.6199
QITQNTDYR	99.00	2.687976E-02	1.281670E+03	6.418425E+02	1.281644E+03	6.418290E+02	2	14	0.6396	4.3809
QITQNTDYR	99.00	4.652960E-02	1.281690E+03	6.418523E+02	1.281644E+03	6.418290E+02	2	14	0.6567	4.1582
IQVSELCK	98.00	1.532809E-02	1.252692E+03	6.273531E+02	1.252676E+03	6.273454E+02	2	13	0.4821	2.7320
GEIEHHCSGLHR	97.00	8.899271E-02	1.563805E+03	5.222755E+02	1.563716E+03	5.222458E+02	3	13	0.4863	12.1301
CLIDLGK	93.00	-3.696290E-02	1.094570E+03	5.482924E+02	1.094607E+03	5.483109E+02	2	12	0.4909	2.2522
STITEIK	91.00	-2.165214E-02	1.078626E+03	5.403203E+02	1.078648E+03	5.403312E+02	2	12	0.6065	3.3850
Experiment 2										
LLELQYFISR	99.00	-7.613843E-03	1.424807E+03	7.134109E+02	1.424815E+03	7.134147E+02	2	16	0.5622	6.3183

Q92520 / Protein FAM3C precursor

PEPTIDE SEQUENCE	CONF %	dMass	Prec MW	Prec m/z	Theor MW	Theor m/z	Theor z	Sc	Ratio	% Err
Experiment 1										
GINVALANGK	99.00	-3.655792E-02	1.244697E+03	6.233556E+02	1.244733E+03	6.233739E+02	2	17	0.5545	4.5528
SALDTAAR	99.00	9.134338E-02	9.476072E+02	4.748109E+02	9.475158E+02	4.747652E+02	2	14	0.5120	4.2650
GINVALANGK	99.00	-2.994280E-03	1.244730E+03	6.233724E+02	1.244733E+03	6.233739E+02	2	15	0.7053	9.3868
SALDTAAR	95.00	1.011683E-01	9.476170E+02	4.748158E+02	9.475158E+02	4.747652E+02	2	13	0.4742	5.4421
DNWVFCGGK	92.00	1.2481149E-01	1.3587604E+03	6.8038750E+02	1.3586355E+03	6.8032502E+02	2	12	0.6406	8.8234
Experiment 2										
GINVALANGK	99.00	-3.956307E-03	1.244729E+03	6.233719E+02	1.244733E+03	6.233739E+02	2	15	1.322919	12.68258
LIADLGSTSITNLGFR	99.00	2.113148E-02	1.821033E+03	6.080182E+02	1.821012E+03	6.080112E+02	3	16	0.701377	14.08924

Q9UIQ6 / Leucyl/cystinyl aminopeptidase (LNPEP)

PEPTIDE SEQUENCE	CONF %	dMass	Prec MW	Prec m/z	Theor MW	Theor m/z	Theor z	Sc	Ratio	% Err
Experiment 1										
ANLINNIFELAGLGK	99.00	5.603376E-02	1.874143E+03	6.257216E+02	1.874087E+03	6.257029E+02	3	16	0.8785	7.9577
IGQVHYALETTVK	99.00	-3.848095E-02	1.745953E+03	5.829918E+02	1.745992E+03	5.830046E+02	3	14	0.4566	4.9012
ANLINNIFELAGLGK	99.00	1.616755E-01	1.874249E+03	6.257568E+02	1.874087E+03	6.257029E+02	3	17	0.8258	7.7051
ANLINNIFELAGLGK	98.00	9.027877E-02	1.874177E+03	6.257330E+02	1.874087E+03	6.257029E+02	3	13	0.7784	13.5261
Experiment 2										

ANLINNIFELAGLGK	99.00	-1.424943E-03	1.874086E+03	6.257025E+02	1.874087E+03	6.257029E+02	3	16	0.9834	23.1077
ANLINNIFELAGLGK	99.00	1.358933E-02	1.874101E+03	6.257075E+02	1.874087E+03	6.257029E+02	3	17	1.3231	26.7455
ANLINNIFELAGLGK	99.00	-8.719217E-03	1.874078E+03	6.257000E+02	1.874087E+03	6.257029E+02	3	17	0.7579	17.3583
ANLINNIFELAGLGK	99.00	-1.109952E-02	1.874076E+03	6.256992E+02	1.874087E+03	6.257029E+02	3	17	1.0590	10.9960

ANLINNIFELAGLGK	99.00	-4.874110E-03	1.874082E+03	6.257013E+02	1.874087E+03	6.257029E+02	3	15	0.5499	29.7483
ANLINNIFELAGLGK	99.00	2.625878E-03	1.874090E+03	6.257038E+02	1.874087E+03	6.257029E+02	3	16	1.3274	26.7805
ANLINNIFELAGLGK	99.00	1.049909E-02	1.874097E+03	6.257064E+02	1.874087E+03	6.257029E+02	3	16	1.0129	18.8726
ANLINNIFELAGLGK	99.00	1.853612E-03	1.874089E+03	6.257036E+02	1.874087E+03	6.257029E+02	3	17	1.0230	27.3687
ANLINNIFELAGLGK	99.00	1.686760E-02	1.874104E+03	6.257086E+02	1.874087E+03	6.257029E+02	3	17	0.8829	28.0408
ANLINNIFELAGLGK	99.00	8.871232E-03	1.874096E+03	6.257059E+02	1.874087E+03	6.257029E+02	3	14	1.3339	27.9288
ANLINNIFELAGLGK	99.00	1.637802E-02	1.874103E+03	6.257084E+02	1.874087E+03	6.257029E+02	3	15	0.8765	28.5791
ANLINNIFELAGLGK	99.00	1.683887E-02	1.874104E+03	6.257086E+02	1.874087E+03	6.257029E+02	3	16	1.1565	29.6279

Q13425 / Beta-2-syntrophin; Dystrophin-associated protein A1

PEPTIDE SEQUENCE	CONF %	dMass	Prec MW	Prec m/z	Theor MW	Theor m/z	Theor z	Sc	Ratio	% Err
Experiment 1										
ILVQGCHAAAELIK	99.00	4.660123E-02	1.799051E+03	6.006909E+02	1.799004E+03	6.006753E+02	3	14	0.6631	11.0173
QATHDQAVQALK	99.00	2.916539E-02	1.596912E+03	5.333112E+02	1.596883E+03	5.333015E+02	3	15	0.6493	11.6200
ILVQGCHAAAELIK	99.00	-2.875045E-02	1.799959E+03	6.009937E+02	1.799988E+03	6.010033E+02	3	15	0.5766	10.6647

Q8TAF6 / Acyl-CoA synthetase long-chain family member 4

PEPTIDE SEQUENCE	CONF %	dMass	Prec MW	Prec m/z	Theor MW	Theor m/z	Theor z	Sc	Ratio	% Err
Experiment 1										
TALLDISCVK	99.00	4.243724E-02	1.395813E+03	6.989139E+02	1.395771E+03	6.988927E+02	2	15	0.6557	5.6344
HIIYVDNK	98.00	-1.350016E-02	1.288725E+03	6.453697E+02	1.288738E+03	6.453764E+02	2	12	0.7410	7.1974
TALLDISCVK	98.00	-3.334450E-03	1.395768E+03	6.988911E+02	1.395771E+03	6.988927E+02	2	15	0.6627	5.5965

Q14321 / High-mobility group box 1 (HMG-1)

PEPTIDE SEQUENCE	CONF %	dMass	Prec MW	Prec m/z	Theor MW	Theor m/z	Theor z	Sc	Ratio	% Err
Experiment 1										
GEHPGLSIGDVAK	99.00	-2.025062E-02	1.566841E+03	7.844276E+02	1.566861E+03	7.844377E+02	2	19	0.5828	8.4637
IKGEHPGLSIGDVAK	99.00	4.242451E-02	1.952184E+03	6.517354E+02	1.952142E+03	6.517213E+02	3	23	0.5607	2.8890
KHPDASVNFSEFSK	99.00	4.835460E-04	2.024070E+03	6.756972E+02	2.024069E+03	6.756970E+02	3	20	0.7874	2.3964
GEHPGLSIGDVAK	99.00	-5.224909E-02	1.566809E+03	7.844116E+02	1.566861E+03	7.844377E+02	2	15	0.7021	11.9551
IKGEHPGLSIGDVAK	99.00	5.273747E-02	1.952195E+03	6.517389E+02	1.952142E+03	6.517213E+02	3	17	0.6832	6.4686
IKGEHPGLSIGDVAK	99.00	3.839677E-02	1.952180E+03	6.517341E+02	1.952142E+03	6.517213E+02	3	19	0.5397	3.0216
KHPDASVNFSEFSK	99.00	3.362270E-02	2.024103E+03	6.757083E+02	2.024069E+03	6.756970E+02	3	22	0.8119	3.1740
GEHPGLSIGDVAK	97.00	4.559240E-04	1.566861E+03	5.232944E+02	1.566861E+03	5.232943E+02	3	13	0.7349	9.0666
GEHPGLSIGDVAK	97.00	4.797740E-02	1.566909E+03	5.233102E+02	1.566861E+03	5.232943E+02	3	13	0.7295	8.4535

Q9BXA0 / C-X-C chemokine receptor type 4 (CXCR4); CD184 antigen

PEPTIDE SEQUENCE	CONF %	dMass	Prec MW	Prec m/z	Theor MW	Theor m/z	Theor z	Sc	Ratio	% Err
Experiment 1										
TSAQHALTSVSR	99.00	1.111270E-01	1.400860E+03	7.014375E+02	1.400749E+03	7.013820E+02	2	17	0.7089	6.7754
EENANFNK	97.00	3.468814E-03	1.252633E+03	6.273236E+02	1.252629E+03	6.273219E+02	2	12	0.7933	8.6030

Q9BVA1 / Tubulin beta-2B chain

PEPTIDE SEQUENCE	CONF %	dMass	Prec MW	Prec m/z	Theor MW	Theor m/z	Theor z	Sc	Ratio	% Err
Experiment 2										

MSATFIGNSTAIQELFK	99.00	3.320852E-02	2.145172E+03	7.160645E+02	2.145138E+03	7.160534E+02	3	22	0.6386	7.7651
EIVHIQAGQCGNQIGAK	99.00	-4.203430E-03	2.100066E+03	7.010292E+02	2.100070E+03	7.010306E+02	3	25	0.7218	6.3351
EIVHIQAGQCGNQIGAK	99.00	6.775599E-03	2.099093E+03	7.007048E+02	2.099086E+03	7.007026E+02	3	25	0.9979	6.9692
EIVHIQAGQCGNQIGAK	99.00	1.294432E-02	2.101067E+03	7.013629E+02	2.101054E+03	7.013586E+02	3	15	0.9713	10.3016
EIVHIQAGQCGNQIGAK	99.00	1.074706E-02	2.101065E+03	7.013622E+02	2.101054E+03	7.013586E+02	3	16	0.8696	12.5796

EIVHIQAGQCGNQIGAK	99.00	1.443904E-02	2.101068E+03	7.013634E+02	2.101054E+03	7.013586E+02	3	15	0.6600	15.0971
EIVHIQAGQCGNQIGAK	99.00	-1.078121E-02	1.954973E+03	6.526650E+02	1.954984E+03	6.526686E+02	3	18	0.9401	7.0219
FPGQLNADLR	99.00	-4.432557E-02	1.273646E+03	6.378301E+02	1.273690E+03	6.378523E+02	2	15	0.8742	2.1416
FPGQLNADLR	99.00	-4.627868E-02	1.273644E+03	6.378292E+02	1.273690E+03	6.378523E+02	2	16	0.9690	2.2107
GHYTEGAELVDSVLDVVR	99.00	2.090504E-02	2.102097E+03	7.017064E+02	2.102077E+03	7.016995E+02	3	19	N.D.	N.D.
GHYTEGAELVDSVLDVVR	99.00	2.341780E-02	2.102100E+03	7.017073E+02	2.102077E+03	7.016995E+02	3	21	1.6523	23.0387
GHYTEGAELVDSVLDVVR	99.00	5.287572E-02	2.102129E+03	7.017171E+02	2.102077E+03	7.016995E+02	3	20	0.5765	26.4286
GHYTEGAELVDSVLDVVR	99.00	3.591840E-02	2.102113E+03	7.017114E+02	2.102077E+03	7.016995E+02	3	17	N.D.	N.D.
GHYTEGAELVDSVLDVVR	99.00	1.779251E-02	2.102094E+03	7.017054E+02	2.102077E+03	7.016995E+02	3	19	N.D.	N.D.
GHYTEGAELVDSVLDVVR	99.00	2.730505E-02	2.102104E+03	7.017086E+02	2.102077E+03	7.016995E+02	3	19	0.7749	31.5957
GHYTEGAELVDSVLDVVR	99.00	2.400945E-02	2.102101E+03	7.017075E+02	2.102077E+03	7.016995E+02	3	19	0.8501	21.1204
GHYTEGAELVDSVLDVVR	99.00	8.546196E-03	2.102085E+03	7.017023E+02	2.102077E+03	7.016995E+02	3	18	0.6879	32.1146
GHYTEGAELVDSVLDVVR	99.00	8.729288E-03	2.102085E+03	7.017024E+02	2.102077E+03	7.016995E+02	3	19	0.9159	21.0951
GHYTEGAELVDSVLDVVR	99.00	-1.196016E-02	2.102065E+03	7.016955E+02	2.102077E+03	7.016995E+02	3	19	1.0058	20.2620
GHYTEGAELVDSVLDVVR	99.00	-1.665979E-03	2.102075E+03	7.016989E+02	2.102077E+03	7.016995E+02	3	18	1.1774	17.8351
GHYTEGAELVDSVLDVVR	99.00	1.755882E-02	2.102094E+03	7.017053E+02	2.102077E+03	7.016995E+02	3	18	1.1175	16.5007
GHYTEGAELVDSVLDVVR	99.00	2.598111E-02	2.102103E+03	7.017081E+02	2.102077E+03	7.016995E+02	3	18	0.8523	24.8160
GHYTEGAELVDSVLDVVR	99.00	1.774191E-02	2.102094E+03	7.017054E+02	2.102077E+03	7.016995E+02	3	16	0.4996	27.4216
GHYTEGAELVDSVLDVVR	99.00	4.559193E-03	2.102081E+03	7.017010E+02	2.102077E+03	7.016995E+02	3	18	0.8640	25.7806
GHYTEGAELVDSVLDVVR	99.00	-8.989712E-03	2.102068E+03	7.016965E+02	2.102077E+03	7.016995E+02	3	18	1.1811	21.7590
GHYTEGAELVDSVLDVVR	99.00	2.086439E-02	2.246199E+03	7.497404E+02	2.246179E+03	7.497335E+02	3	16	0.9565	18.0420
GHYTEGAELVDSVLDVVR	99.00	1.200881E-02	2.102089E+03	7.017035E+02	2.102077E+03	7.016995E+02	3	19	0.7136	18.8785
GHYTEGAELVDSVLDVVR	99.00	2.852384E-02	2.102105E+03	7.017090E+02	2.102077E+03	7.016995E+02	3	18	N.D.	N.D.
GHYTEGAELVDSVLDVVR	99.00	6.799801E-02	2.102145E+03	7.017221E+02	2.102077E+03	7.016995E+02	3	19	0.9056	20.7283
GHYTEGAELVDSVLDVVR	99.00	6.909660E-02	2.102146E+03	7.017225E+02	2.102077E+03	7.016995E+02	3	18	0.8245	21.9787
ISEQFTAMFR	99.00	-2.812615E-02	1.372665E+03	6.873398E+02	1.372693E+03	6.873538E+02	2	16	0.8428	1.7030
ISEQFTAMFR	99.00	-1.347812E-02	1.372680E+03	6.873471E+02	1.372693E+03	6.873538E+02	2	18	0.7684	2.5121
ISEQFTAMFR	99.00	-1.155281E-02	1.372682E+03	6.873481E+02	1.372693E+03	6.873538E+02	2	18	0.9242	1.6283
ISEQFTAMFR	99.00	-3.352457E-02	1.372660E+03	6.873371E+02	1.372693E+03	6.873538E+02	2	18	0.8699	1.7828
ISEQFTAMFR	99.00	7.245246E-03	1.372700E+03	6.873574E+02	1.372693E+03	6.873538E+02	2	17	0.7142	5.0360
ISEQFTAMFR	99.00	2.650294E-02	1.372720E+03	6.873671E+02	1.372693E+03	6.873538E+02	2	17	0.8931	5.2918
ISEQFTAMFR	99.00	1.538397E-02	1.372708E+03	6.873615E+02	1.372693E+03	6.873538E+02	2	17	0.7547	5.1211
ISEQFTAMFR	99.00	-2.932872E-03	1.372690E+03	6.873524E+02	1.372693E+03	6.873538E+02	2	18	0.7745	4.5332
ISEQFTAMFR	99.00	-1.389818E-02	1.372679E+03	6.873469E+02	1.372693E+03	6.873538E+02	2	18	0.8925	4.8298
ISEQFTAMFR	99.00	4.533069E-03	1.372698E+03	6.873561E+02	1.372693E+03	6.873538E+02	2	18	0.7955	5.6177
ISEQFTAMFR	99.00	1.116300E-03	1.372694E+03	6.873544E+02	1.372693E+03	6.873538E+02	2	17	0.8569	7.6147
ISEQFTAMFR	99.00	9.117627E-03	1.372702E+03	6.873584E+02	1.372693E+03	6.873538E+02	2	17	0.8180	7.5513
ISEQFTAMFR	99.00	-9.069724E-03	1.372684E+03	6.873493E+02	1.372693E+03	6.873538E+02	2	17	0.6769	8.6029
ISEQFTAMFR	99.00	3.713362E-03	1.372697E+03	6.873557E+02	1.372693E+03	6.873538E+02	2	14	0.6953	14.9852
ISEQFTAMFR	99.00	4.857368E-03	1.372698E+03	6.873563E+02	1.372693E+03	6.873538E+02	2	13	0.7771	16.5663
LHFFMPGFAPLTSR	99.00	9.742874E-03	1.619838E+03	5.409532E+02	1.619828E+03	5.409500E+02	3	14	N.D.	N.D.
LHFFMPGFAPLTSR	99.00	2.164416E-02	1.619850E+03	5.409572E+02	1.619828E+03	5.409500E+02	3	15	N.D.	N.D.
LHFFMPGFAPLTSR	99.00	3.165794E-03	1.763933E+03	5.889851E+02	1.763930E+03	5.889840E+02	3	17	1.2607	10.8248
LHFFMPGFAPLTSR	99.00	4.081277E-03	1.763934E+03	5.889854E+02	1.763930E+03	5.889840E+02	3	17	1.4279	8.6848
LHFFMPGFAPLTSR	99.00	3.008102E-02	1.763960E+03	5.889941E+02	1.763930E+03	5.889840E+02	3	16	1.3974	9.2947
LHFFMPGFAPLTSR	99.00	5.132313E-02	1.763982E+03	5.890012E+02	1.763930E+03	5.889840E+02	3	16	1.1763	10.8982
LHFFMPGFAPLTSR	99.00	2.129569E-02	1.763952E+03	5.889911E+02	1.763930E+03	5.889840E+02	3	16	1.8217	8.0024
LHFFMPGFAPLTSR	99.00	3.319681E-02	1.763964E+03	5.889951E+02	1.763930E+03	5.889840E+02	3	15	1.1515	7.8625
LTTPTYGDLNHLVSATMSGVTTCLR	99.00	5.205248E-02	2.840451E+03	9.478244E+02	2.840399E+03	9.478070E+02	3	27	0.8922	7.5170
LTTPTYGDLNHLVSATMSGVTTCLR	99.00	-1.122825E-02	2.840388E+03	7.111043E+02	2.840399E+03	7.111071E+02	4	23	1.0399	14.3860

LTTPTYGDLNHLVSATMSGVTTCLR	99.00	-3.660360E-03	2.840396E+03	7.111062E+02	2.840399E+03	7.111071E+02	4	26	0.9871	13.2895
LTTPTYGDLNHLVSATMSGVTTCLR	99.00	1.195575E-02	2.840411E+03	7.111101E+02	2.840399E+03	7.111071E+02	4	18	N.D.	N.D.
LTTPTYGDLNHLVSATMSGVTTCLR	99.00	3.434996E-03	2.840403E+03	7.111080E+02	2.840399E+03	7.111071E+02	4	19	1.3913	24.4253
LTTPTYGDLNHLVSATMSGVTTCLR	99.00	5.055082E-02	2.840450E+03	7.111198E+02	2.840399E+03	7.111071E+02	4	19	1.5761	13.4012
LTTPTYGDLNHLVSATMSGVTTCLR	99.00	3.053270E-02	2.840430E+03	7.111147E+02	2.840399E+03	7.111071E+02	4	19	0.9693	15.6923

LTTPTYGDLNHLVSATMSGVTTCLR	99.00	3.370630E-02	2.840433E+03	7.111155E+02	2.840399E+03	7.111071E+02	4	15	1.1508	22.4691
LTTPTYGDLNHLVSATMSGVTTCLR	99.00	4.908203E-02	2.840448E+03	9.478234E+02	2.840399E+03	9.478070E+02	3	17	0.9527	14.6620
LTTPTYGDLNHLVSATMSGVTTCLR	99.00	4.809426E-02	2.840448E+03	7.111191E+02	2.840399E+03	7.111071E+02	4	17	1.3289	19.6343
LTTPTYGDLNHLVSATMSGVTTCLR	99.00	4.638538E-02	2.840446E+03	7.111187E+02	2.840399E+03	7.111071E+02	4	15	1.0825	22.8585
MSATFIGNSTAIQELFK	99.00	1.764520E-02	2.145156E+03	7.160593E+02	2.145138E+03	7.160534E+02	3	21	0.7728	9.2567
MSATFIGNSTAIQELFK	99.00	1.624815E-02	2.145155E+03	7.160588E+02	2.145138E+03	7.160534E+02	3	19	0.6815	8.6368
NSSYFVEWIPNNVK	99.00	3.550207E-02	1.984065E+03	6.623624E+02	1.984030E+03	6.623505E+02	3	16	1.0006	6.2805
AILVDLEPGTMDSVR	98.00	-9.840870E-04	1.774925E+03	5.926489E+02	1.774926E+03	5.926492E+02	3	14	1.0227	7.0897
ISEQFTAMFR	98.00	-1.518724E-02	1.388673E+03	6.953437E+02	1.388688E+03	6.953513E+02	2	13	0.8293	5.1313
LTTPTYGDLNHLVSATMSGVTTCLR	98.00	-1.874075E-03	2.696295E+03	8.997724E+02	2.696297E+03	8.997730E+02	3	14	N.D.	N.D.
LHFFMPGFAPLTSR	96.00	7.089718E-02	1.619899E+03	5.409736E+02	1.619828E+03	5.409500E+02	3	13	N.D.	N.D.
LTTPTYGDLNHLVSATMSGVTTCLR	87.00	-2.423350E-03	2.696295E+03	8.997722E+02	2.696297E+03	8.997730E+02	3	13	N.D.	N.D.
LHFFMPGFAPLTSR	86.00	4.813664E-03	1.763935E+03	5.889857E+02	1.763930E+03	5.889840E+02	3	12	1.0331	23.7490

SUPPLEMENTAL TABLE 3:

ANNOTATED SPECTRA FOR EXPERIMENTS WITH UNIQUE-PEPTIDE-BASED PROTEIN IDENTIFICATION

A

P14174 (86%), 12,476.5 Da
MIF_HUMAN Macrophage migration inhibitory factor [Homo sapiens (Human)]
1 unique peptides, 1 unique spectra, 7 total spectra, 9/115 amino acids (8% coverage)

M P M F I V N T N V P R A S V P D G F L S E L T Q Q L A Q A T G K P P Q Y I A V H V V P D Q L M A F
G G S S E P C A L C S L H S I G K I G G A Q N R S Y S K **L L** **C G L L A E R** L R I S P D R V Y I N Y Y
D M N A A N V G W N N S T F A

B

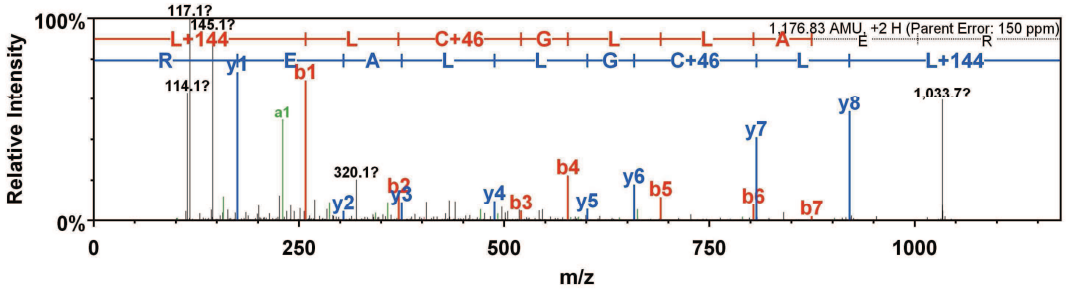

…	B Ions	B+2H	B-NH3	B-H2O	AA	Y Ions	Y+2H	Y-NH3	Y-H2O	…
1	258.2				L+144	1,177.7	589.3	1,160.6	1,159.6	9
2	371.3				L	920.5	460.7	903.4	902.5	8
3	520.3				C+46	807.4	404.2	790.4	789.4	7
4	577.3				G	658.4	329.7	641.4	640.4	6
5	690.4				L	601.4		584.3	583.4	5
6	803.5	402.2			L	488.3		471.3	470.3	4
7	874.5	437.8			A	375.2		358.2	357.2	3
8	1,003.5	502.3		985.5	E	304.2		287.1	286.2	2
9	1,177.7	589.3	1,160.6	1,159.6	R	175.1		158.1		1

C

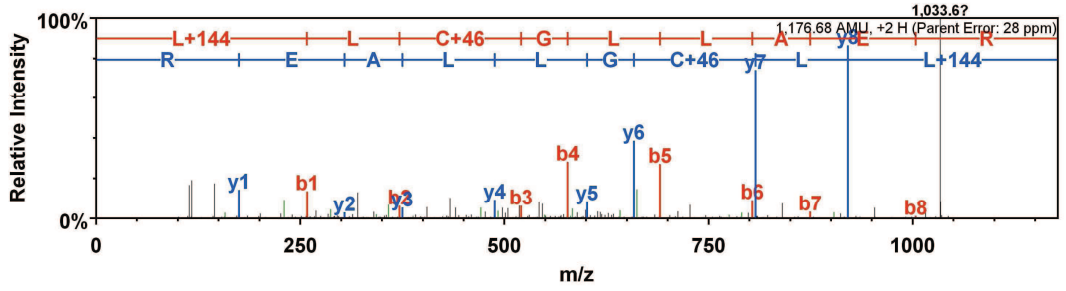

…	B Ions	B+2H	B-NH3	B-H2O	AA	Y Ions	Y+2H	Y-NH3	Y-H2O	…
1	258.2				L+144	1,177.7	589.3	1,160.6	1,159.6	9
2	371.3				L	920.5	460.7	903.4	902.5	8
3	520.3				C+46	807.4	404.2	790.4	789.4	7
4	577.3				G	658.4	329.7	641.4	640.4	6
5	690.4				L	601.4		584.3	583.4	5
6	803.5	402.2			L	488.3		471.3	470.3	4
7	874.5	437.8			A	375.2		358.2	357.2	3
8	1,003.5	502.3		985.5	E	304.2		287.1	286.2	2
9	1,177.7	589.3	1,160.6	1,159.6	R	175.1		158.1		1

A

Q15738 (86%), 41,900.8 Da
NSDHL_HUMAN Sterol-4-alpha-carboxylate 3-dehydrogenase, decarboxylating [Homo sapiens (Human)]
1 unique peptides, 1 unique spectra, 2 total spectra, 9/373 amino acids (2% coverage)

MEPAVSEPMR DQVARTHLTE DTPKVNADIE KVNQNQAKRC TVIGGSGFLG
QHMVEQLLAR GYAVNVFDIQ QGFDNPQVRF FLGDLCSRQD LYPALKGVNT
VFHCASPPPS SNNKELFYRV NYIGTKNVIE TCKEAGVQKL ILTSSASVIF
EGVDIKNGTE DLPYAMKPID YYTETKILQE RAVLGANDPE KNFLTTAIRP
HGIFGPRDPQ LVPILIEAAR NGKMKFVIGN GKNLVDFTFV ENVVHGHILA
AEQLSRDSTL GGKAFHITND EPIPFWTFLS RILTGLNYEA PKYHIPYWVA
YYLALLLSLL VMVISPVIQL QPTFTPMRVA LAGTFHYYSC ERAKKAMGYQ
PLVTMDDAME RTVQSFRHLR RVK

B

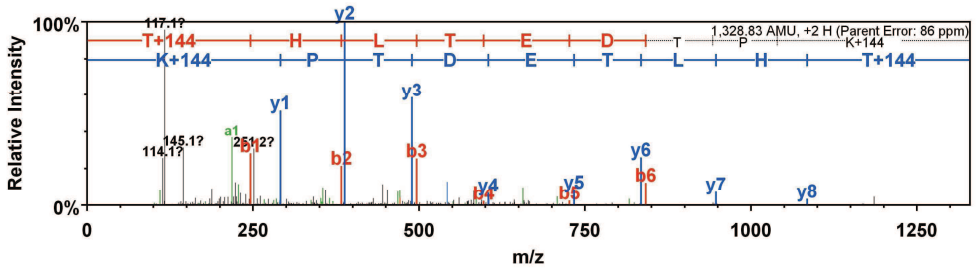

C

...	B Ions	B+2H	B-NH3	B-H2O	AA	Y Ions	Y+2H	Y-NH3	Y-H2O	...
1	246.2			228.1	T+144	1,329.7	665.4	1,312.7	1,311.7	9
2	383.2	192.1		365.2	H	1,084.6	542.8	1,067.5	1,066.6	8
3	496.3	248.7		478.3	L	947.5	474.3	930.5	929.5	7
4	597.3	299.2		579.3	T	834.4	417.7	817.4	816.4	6
5	726.4	363.7		708.4	E	733.4		716.4	715.4	5
6	841.4	421.2		823.4	D	604.3		587.3	586.3	4
7	942.5	471.7		924.5	T	489.3		472.3	471.3	3
8	1,039.5	520.3		1,021.5	P	388.3		371.2		2
9	1,329.7	665.4	1,312.7	1,311.7	K+144	291.2		274.2		1

A

P16949 (90%), 17,303.0 Da
STMN1_HUMAN Stathmin [Homo sapiens (Human)]
1 unique peptides, 1 unique spectra, 2 total spectra, 8/149 amino acids (5% coverage)

M A S S D I Q V K E L E K R A S G Q A F E L I L S P R S K E S V P E F P L S P P K K K D L S L E E I
Q K K L E A A E E R R K S H E A E V L K Q L A E K R E H E K E V L Q K A I E E N N N F S K M A E E K
L T H K M E A N K E N R E A Q M A A K L E R L R E K D K H I E E V R K N K E S K D P A D E T E A D

B

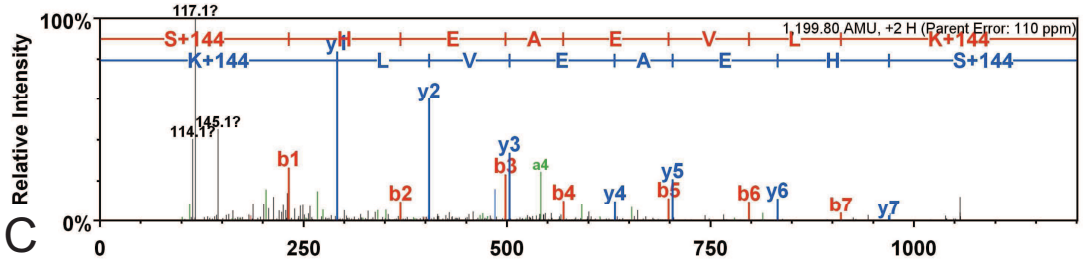

C

...	B Ions	B+2H	B-NH3	B-H2O	AA	Y Ions	Y+2H	Y-NH3	Y-H2O	...
1	232.1			214.1	S+144	1,200.7	600.8	1,183.7	1,182.7	8
2	369.2	185.1		351.2	H	969.5	485.3	952.5	951.5	7
3	498.2	249.6		480.2	E	832.5	416.7	815.5	814.5	6
4	569.3	285.1		551.3	A	703.4		686.4	685.4	5
5	698.3	349.7		680.3	E	632.4		615.4	614.4	4
6	797.4	399.2		779.4	V	503.4		486.3		3
7	910.5	455.7		892.5	L	404.3		387.3		2
8	1,200.7	600.8	1,183.7	1,182.7	K+144	291.2		274.2		1

A

O95881 (86%), 19,206.4 Da
TXD12_HUMAN Thioredoxin domain-containing protein 12 precursor [Homo sapiens (Human)]
1 unique peptides, 1 unique spectra, 1 total spectra, 9/172 amino acids (5% coverage)

```
METRPRLGAT  CLLGFSFLLL  VISSDGHNGL  GKGFGDHIHW  RTLEDGKKEA
AASGLPLMVI  IHKSWCGACK  ALKPKFAEST  EISELSHNFV  MVNLEDEEEP
KDEDFSPDGG  YIPRILFLDP  SGKVHPEIIN  ENGNPSYKYF  YVSAEQVVQG
MKEAQERLTG  DAFRKKHLED  EL
```

B

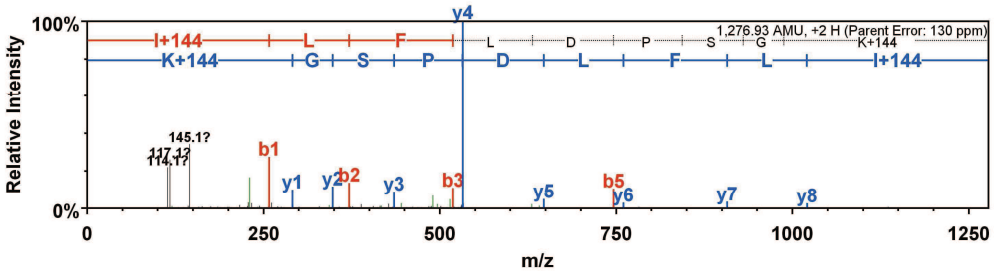

C

B	B Ions	B+2H	B-NH3	B-H2O	AA	Y Ions	Y+2H	Y-NH3	Y-H2O	Y
1	258.2				I+144	1,277.8	639.4	1,260.7	1,259.8	9
2	371.3				L	1,020.6	510.8	1,003.6	1,002.6	8
3	518.3				F	907.5	454.3	890.5	889.5	7
4	631.4				L	760.4	380.7	743.4	742.4	6
5	746.5			728.4	D	647.3		630.3	629.3	5
6	843.5	422.3		825.5	P	532.3		515.3	514.3	4
7	930.5	465.8		912.5	S	435.3		418.2	417.3	3
8	987.6	494.3		969.6	G	348.2		331.2		2
9	1,277.8	639.4	1,260.7	1,259.8	K+144	291.2		274.2		1

A

Q6P9D1 (86%), 137,223.9 Da
Q6P9D1_HUMAN Golgi apparatus protein 1 [Homo sapiens (Human)]
1 unique peptides, 1 unique spectra, 1 total spectra, 10/1203 amino acids (1% coverage)

M A A C G R V R R M F R L S A A L H L L L L F A A G A E K L P G Q G V H S Q G Q G G P G A N F V S F V
G Q A G G G G P A G Q Q L P Q L P Q S S Q L Q Q Q Q Q Q Q Q Q Q Q P Q P P Q P P F P A G G P P A R
R G G A G A G G G W K L A E E E S C R E D V T R V C P K H T W S N N L A V L E C L Q D V R E P E N E
I S S D C N H L L W N Y K L N L T T D P K F E S V A R E V C K S T I T E I K E C A D E P V G K G Y M
V S C L V D H R G N I T E Y Q C H Q Y I T K M T A I I F S D Y R L I C G F M D D C K N D I N I L K C
G S I R L G E K D A H S Q G E V V S C L E K G L V K E A E E R E P K I Q V S E L C K K A I L R V A E
L S S D D F H L D R H L Y F A C R D D R E R F C E N T Q A G E G R V Y K C L F N H K F E E S M S E K
C R E A L T T R Q K L I A Q D Y K V S Y S L A K S C K S D L K K Y R C N V E N L P R S R E A R L S Y
L L M C L E S A V H R G R Q V S S E C Q G E M L D Y R R M L M E D F S L S P E I I L S C R G E I E H
H C S G L H R K G R T L H C L M K V V R G E K G N L G M N C Q Q A L Q T L I Q E T D P G A D Y R I D
R A L N E A C E S V I Q T A C K H I R S G D P M I L S C L M E H L Y T E K M V E D C E H R **L L E L Q**
Y F I S R D W K L D P V L Y R K C Q G D A S R L C H T H G W N E T S E F M P Q G A V F S C L Y R H A
Y R T E E Q G R R L S R E C R A E V Q R I L H Q R A M D V K L D P A L Q D K C L I D L G K W C S E K
T E T G Q E L E C L Q D H L D D L V V E C R D I V G N L T E L E S E D I Q I E A L L M R A C E P I I
Q N F C H D V A D N Q I D S G D L M E C L I Q N K H Q K D M N E K C A I G V T H F Q L V Q M K D F R
F S Y K F K M A C K E D V L K L C P N I K K K V D V V I C L S T T V R N D T L Q E A K E H R V S L K

B

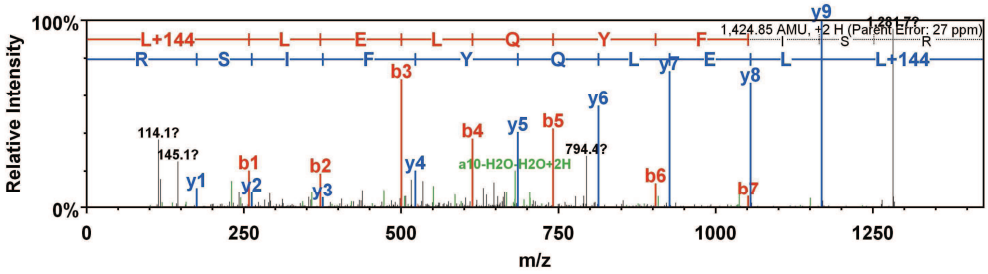

C

...	B Ions	B+2H	B-NH3	B-H2O	AA	Y Ions	Y+2H	Y-NH3	Y-H2O	...
1	258.2				L+144	1,425.8	713.4	1,408.8	1,407.8	10
2	371.3				L	1,168.6	584.8	1,151.6	1,150.6	9
3	500.3			482.3	E	1,055.6	528.3	1,038.5	1,037.5	8
4	613.4			595.4	L	926.5	463.8	909.5	908.5	7
5	741.5		724.4	723.5	Q	813.4	407.2	796.4	795.4	6
6	904.5	452.8	887.5	886.5	Y	685.4		668.3	667.4	5
7	1,051.6	526.3	1,034.6	1,033.6	F	522.3		505.3	504.3	4
8	1,164.7	582.8	1,147.7	1,146.7	I	375.2		358.2	357.2	3
9	1,251.7	626.4	1,234.7	1,233.7	S	262.2		245.1	244.1	2
10	1,425.8	713.4	1,408.8	1,407.8	R	175.1		158.1		1

A

Q9UIQ6 (86%), 117,353.2 Da
LCAP_HUMAN Leucyl-cystinyl aminopeptidase (EC 3.4.11.3) (Cystinyl aminopeptidase) (Oxytocinase) (OTase) (Insulin-regul
1 unique peptides, 1 unique spectra, 8 total spectra, 15/1025 amino acids (1% coverage)

```
MEPFTNDRLQ  LPRNMIENSM  FEEEPDVVDL  AKEPCLHPLE  PDEVEYEPRG
SRLLVRGLGE  HEMEEDEEDY  ESSAKLLGMS  FMNRSSGLRN  SATGYRQSPD
GACSVPSART  MVVCAFVIVV  AVSVIMVIYL  LPRCTFTKEG  CHKKNQSIGL
IQPFATNGKL  FPWAQIRLPT  AVVPLRYELS  LHPNLTSMTF  RGSVTISVQA
LQVTWNIILH  STGHNISRVT  FMSAVSSQEK  QAEILEYAYH  GQIAIVAPEA
LLAGHNYTLK  IEYSANISSS  YYGFYGFSYT  DESNEKKYFA  ATQFEPLAAR
SAFPCFDEPA  FKATFIIKII  RDEQYTALSN  MPKKSSVVLD  DGLVQDEFSE
SVKMSTYLVA  FIVGEMKNLS  QDVNGTLVSI  YAVPEKIGQV  HYALETTVKL
LEFFQNYFEI  QYPLKKLDLV  AIPDFEAGAM  ENWGLLTFRE  ETLLYDSNTS
SMADRKLVTK  IIAHELAHQW  FGNLVTMKWW  NDLWLNEGFA  TFMEYFSLEK
IFKELSSYED  FLDARFKTMK  KDSLNSSHPI  SSSVQSSEQI  EEMFDSLSYF
KGSSLLLMLK  TYLSEDVFQH  AVVLYLHNHS  YASIQSDDLW  DSFNEVTNQT
LDVKRMMKTW  TLQKGFPLVT  VQKKGKELFI  QQERFFLNMK  PEIQPSDTSY
LWHIPLSYVT  EGRNYSKYQS  VSLLDKKSGV  INLTEEVLWV  KVNINMNGYY
IVHYADDDWE  ALIHQLKINP  YVLSDKDRAN  LINNIFELAG  LGKVPLKRAF
DLINYLGNEN  HTAPITEALF  QTDLIYNLLE  KLGYMDLASR  LVTRVFKLLQ
NQIQQQTWTD  EGTPSMRELR  SALLEFACTH  NLGNCSTTAM  KLFDDWMASN
GTQSLPTDVM  TTVFKVGAKT  DKGWSFLLGK  YISIGSEAEK  NKILEALASS
EDVRKLYWLM  KSSLNGDNFR  TQKLSFIIRT  VGRHFPGHLL  AWDFVKENWN
KLVQKFPLGS  YTIQNIVAGS  TYLFSTKTHL  SEVQAFFENQ  SEATFRLRCV
QEALEVIQLN  IQWMEKNLKS  LTWWL
```

B

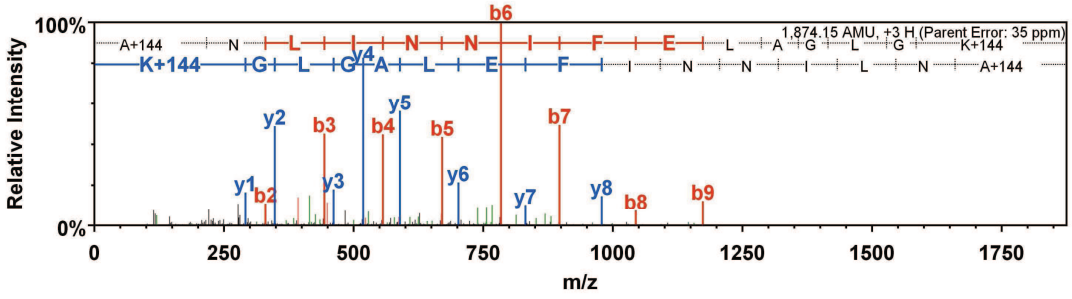

C

...	B Ions	B+2H	B-NH3	B-H2O	AA	Y Ions	Y+2H	Y-NH3	Y-H2O	...
1	216.1				A+144	1,875.1	938.1	1,858.1	1,857.1	15
2	330.2		313.2		N	1,660.0	830.5	1,642.9	1,641.9	14
3	443.3		426.2		L	1,545.9	773.5	1,528.9	1,527.9	13
4	556.4		539.3		I	1,432.8	716.9	1,415.8	1,414.8	12
5	670.4		653.4		N	1,319.7	660.4	1,302.7	1,301.7	11
6	784.4	392.7	767.4		N	1,205.7	603.4	1,188.7	1,187.7	10
7	897.5	449.3	880.5		I	1,091.7	546.3	1,074.6	1,073.6	9
8	1,044.6	522.8	1,027.6		F	978.6	489.8	961.5	960.6	8
9	1,173.6	587.3	1,156.6	1,155.6	E	831.5	416.3	814.5	813.5	7
10	1,286.7	643.9	1,269.7	1,268.7	L	702.5	351.7	685.4		6
11	1,357.8	679.4	1,340.7	1,339.7	A	589.4		572.4		5
12	1,414.8	707.9	1,397.8	1,396.8	G	518.3		501.3		4
13	1,527.9	764.4	1,510.8	1,509.9	L	461.3		444.3		3
14	1,584.9	792.9	1,567.9	1,566.9	G	348.2		331.2		2
15	1,875.1	938.1	1,858.1	1,857.1	K+144	291.2		274.2		1

SUPPLEMENTAL TABLE 4:

ANNOTATED SPECTRA FOR CANDIDATE PROTEINS VALIDATED IN FIGURE 4
NSDHL, PSAP, PKC delta

A

Q15738 (100%), 41,900.8 Da
NSDHL_HUMAN Sterol-4-alpha-carboxylate 3-dehydrogenase, decarboxylating [Homo sapiens (Human)]
3 unique peptides, 3 unique spectra, 4 total spectra, 34/373 amino acids (9% coverage)

```
MEPAVSEPMR DQVARTHLTE DTPKVNADIE KVNQNQAKRC TVIGGSGFLG
QHMVEQLLAR GYAVNVFDIQ QGFDNPQVRF FLGDLCSRQD LYPALKGVNT
VFHCASPPPS SNNKELFYRV NYIGTKNVIE TCKEAGVQKL ILTSSASVIF
EGVDIKNGTE DLPYAMKPID YYTETKILQE RAVLGANDPE KNFLTTAIRP
HGIFGPRDPQ LVPILIEAAR NGKMKFVIGN GKNLVDFTFV ENVVHGHILA
AEQLSRDSTL GGKAFHITND EPIPFWTFLS RILTGLNYEA PKYHIPYWVA
YYLALLLSLL VMVISPVIQL QPTFTPMRVA LAGTFHYYSC ERAKKAMGYQ
PLVTMDDAME RTVQSFRHLR RVK
```

B

...	B Ions	B+2H	B-NH3	B-H2O	AA	Y Ions	Y+2H	Y-NH3	Y-H2O	...
1	102.1			84.0	T+144	1,185.6	593.3	1,168.6	1,167.6	9
2	239.1	120.1		221.1	H	1,084.6	542.8	1,067.5	1,066.6	8
3	352.2	176.6		334.2	L	947.5	474.3	930.5	929.5	7
4	453.2	227.1		435.2	T	834.4	417.7	817.4	816.4	6
5	582.3	291.6		564.3	E	733.4		716.4	715.4	5
6	697.3	349.2		679.3	D	604.3		587.3	586.3	4
7	798.4	399.7		780.4	T	489.3		472.3	471.3	3
8	895.4	448.2		877.4	P	388.3		371.2		2
9	1,185.6	593.3	1,168.6	1,167.6	K+144	291.2		274.2		1

C

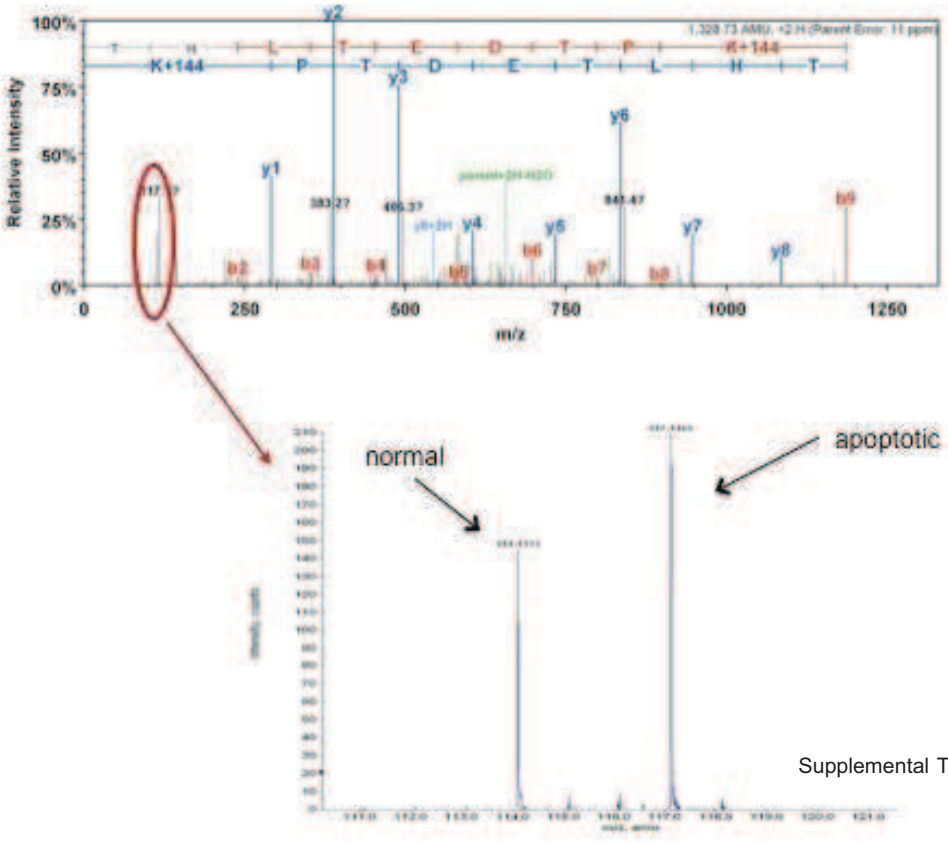

A

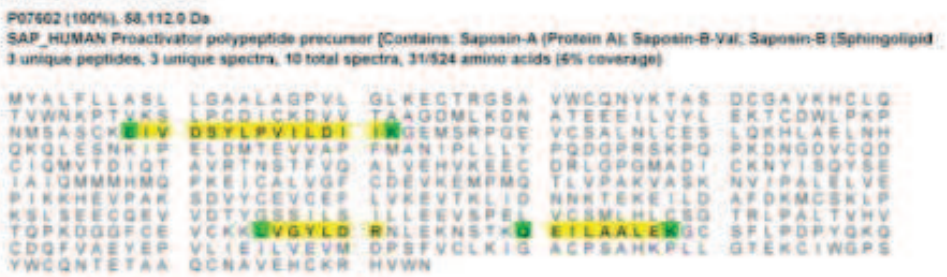

B

...	B Ions	B+2H	B-NH3	B-H2O	AA	Y Ions	Y+2H	Y-NH3	Y-H2O	...
1	129.1		112.0		Q+144	1,158.7	579.8	1,141.7	1,140.7	9
2	258.1		241.1	240.1	E	1,030.6	515.8	1,013.6	1,012.6	8
3	371.2		354.2	353.2	I	901.6	451.3	884.6	883.6	7
4	484.3		467.3	466.3	L	788.5	394.8	771.5	770.5	6
5	555.3		538.3	537.3	A	675.4		658.4	657.4	5
6	626.4	313.7	609.3	608.3	A	604.4		587.4	586.4	4
7	739.4	370.2	722.4	721.4	L	533.3		516.3	515.3	3
8	868.5	434.7	851.5	850.5	E	420.3		403.2	402.2	2
9	1,158.7	579.8	1,141.7	1,140.7	K+144	291.2		274.2		1

C

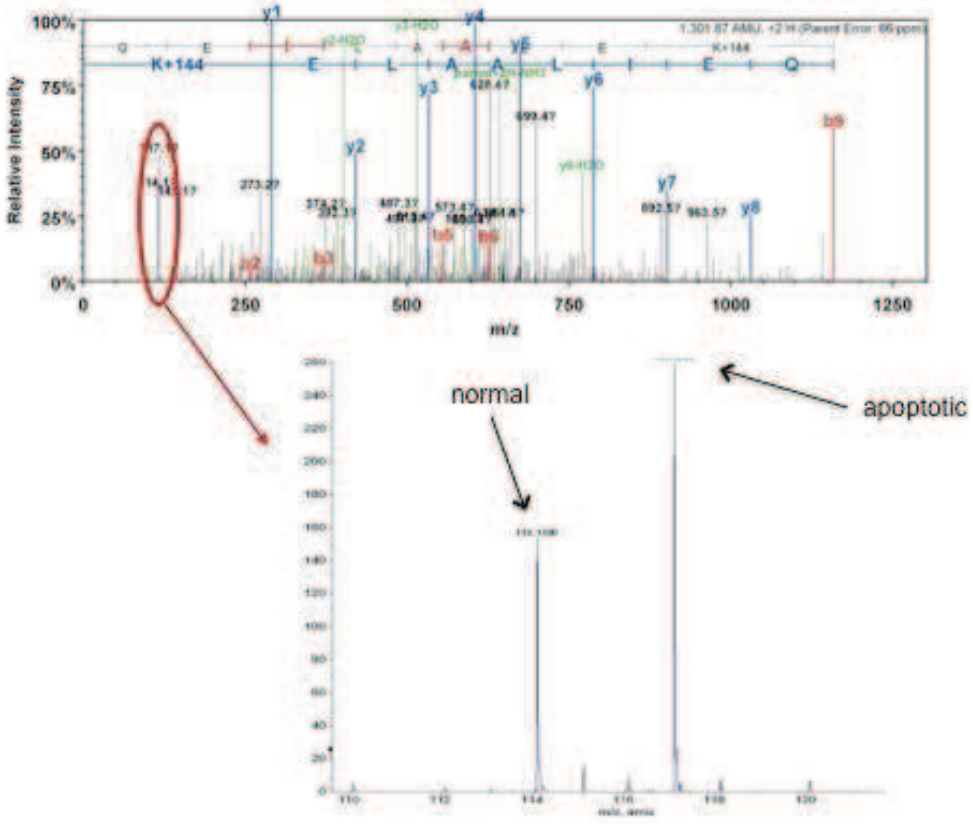

A

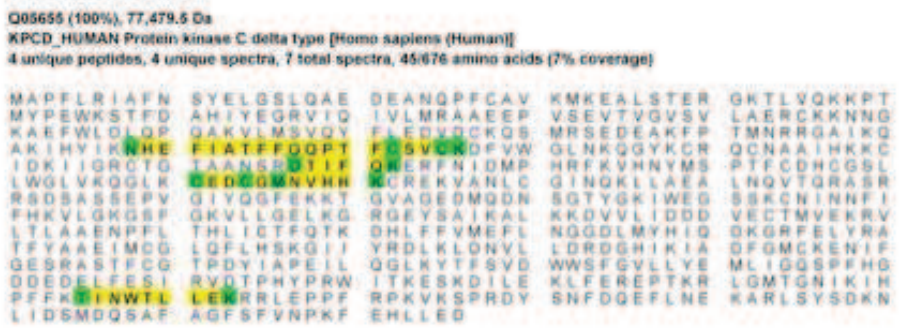

B

...	B Ions	B+2H	B-NH3	B-H2O	AA	Y Ions	Y+2H	Y-NH3	Y-H2O	...
1	104.0				C+190	1,462.6	731.8	1,445.6	1,444.6	11
2	233.1			215.0	E	1,359.6	680.3	1,342.5	1,341.6	10
3	348.1			330.1	D	1,230.5	615.8	1,213.5	1,212.5	9
4	497.1			479.1	C+46	1,115.5	558.3	1,098.5		8
5	554.1			536.1	G	966.5	483.8	949.5		7
6	685.1	343.1		667.1	M	909.5	455.2	892.5		6
7	799.2	400.1	782.2	781.2	N	778.4	389.7	761.4		5
8	898.3	449.6	881.2	880.2	V	664.4	332.7	647.4		4
9	1,035.3	518.2	1,018.3	1,017.3	H	565.3	283.2	548.3		3
10	1,172.4	586.7	1,155.3	1,154.4	H	428.3	214.6	411.2		2
11	1,462.6	731.8	1,445.6	1,444.6	K+144	291.2		274.2		1

C

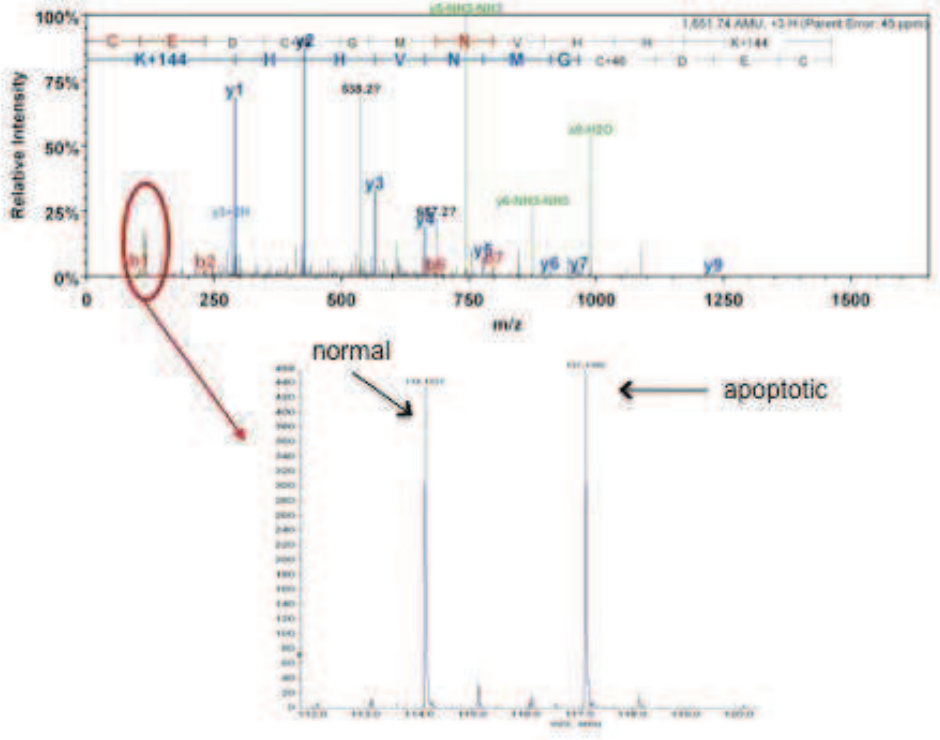

Protein kinase C delta isoform (PKC-δ) mediates lysosome labilization in DNA damage-induced apoptosis

Nicolas Parent[1], Max Scherer[2], Gerhard Liebisch[2], Gerd Schmitz[2], and Richard Bertrand[1, 3]

Affiliations des auteurs:

[1]Centre de recherche du Centre hospitalier de l'Université de Montréal (CHUM) - Hôpital Notre Dame et Institut du Cancer de Montréal, Montréal (Qc) H2L 4M1, Canada,

[2]Institute for Clinical Chemistry and Laboratory Medicine, University of Regensburg, D-93042 Regensburg, Germany et

[3]Département de Médecine, Université de Montréal, Montréal (Qc) H3C 3J7, Canada.

Manuscript en préparation

Contribution des co-auteurs :

Nicolas Parent : auteur principal : hypothèse et approches; article co-rédigé avec Richard Bertrand

Max Scherer et Gerhard Liebisch: mesures des lipides

Richard Bertrand : instigateur principal

PROTEIN KINASE C-DELTA ISOFORM (PKC-δ) MEDIATES LYSOSOME LABILIZATION IN DNA DAMAGE-INDUCED APOPTOSIS

Nicolas Parent[a], Max Scherer[b], Gerhard Liebisch[b], Gerd Schmitz[b], and Richard Bertrand[a, c, *]

[a] Centre de recherche du Centre hospitalier de l'Université of Montréal (CRCHUM), Hôpital Notre-Dame and Institut du cancer de Montréal, Montréal (QC) H2L 4M1, Canada,
[b] Institute for Clinical Chemistry and Laboratory Medicine, University of Regensburg, D-93042 Regensburg, Germany,
[c] Département de médecine, Université de Montréal, Montréal (QC) H3C 3J7, Canada

Running title: CPT-induced apoptosis

Corresponding author: Richard Bertrand, CRCHUM, Hôpital Notre-Dame and Institut du cancer de Montréal, 1560 Sherbrooke St. East (Room Y-5634), Montreal (Qc) H2L 4M1, Canada. Phone: (1-514) 890-8000 ext 26615; Fax: (1-514) 412-7591;

Abstract

A lysosomal pathway, characterized by partial rupture or labilization of lysosomal membranes (LLM) and cathepsin release into the cytosol, is evoked during the early events of 20-S-camptothecin lactone (CPT)-induced apoptosis in human cancer cells, including human histiocytic lymphoma U-937 cells. These lysosomal events begin rapidly and simultaneously with mitochondrial permeabilization and caspase activation within 3 h after drug treatment. Recently, in comparative proteomics analysis performed on highly-enriched lysosome extracts, we identified proteins whose translocation to lysosomes correlated with LLM induction after CPT treatment, including protein kinase C-delta (PKC-δ). Here, we show that PKC-δ translocation to lysosomes is required for LLM, as silencing its expression with RNA interference or suppressing its activity with the inhibitor rottlerin prevents CPT-induced LLM. PKC-δ translocation to lysosomes is associated with lysosomal acidic sphingomyelinase (ASM) phosphorylation and activation, which in turn leads to an increase of ceramide (CER) content at lysosomes. The accumulation of endogenous CER at lysosomes is a critical event for CPT-induced LLM as suppressing PKC-δ or ASM activity reduces both CPT-mediated CER generation at lysosomes and CPT-induced LLM. These findings reveal a novel mechanism by which PKC-δ mediates ASM phosphorylation/activation and CER accumulation at lysosomes in CPT-induced LLM, rapidly activating the lysosomal pathway of apoptosis after CPT treatment.

Keywords

Apoptosis, camptothecin, lysosome, PKC-δ, sphingolipids, ESI-MS/MS.

Abbreviations

The abbreviations used are: ↓ΔΨm: loss of mitochondrial inner membrane potential; AO, acridine orange; ASM, acidic sphingomyelinase; ATM, ataxia telangiectasia mutated kinase; cAbl, cytolosic Abelson oncogene homolog 1 kinase; CE, cholesterol ester; CER, ceramide; CNT, control; CPT, 20-S-camptothecin lactone; CRK-L, CT10 regulator of tyrosine kinase isoform L; CS, ceramide synthase; DESP, desipramine; dihSM, dihydro-sphingomyelin; DNA-PK, DNA-protein kinase; FB1, fumonisin B1; FC, free cholesterol; HexCER, hexosylceramide; IP, immunoprecipitation; JNK, Jun amino-terminal kinase; LacCER, lactosyl-ceramide; LAMP-1, lysosomal-associated membrane protein 1; ESI-MS/MS, electrospray ionization /tandem mass spectrometry; LLM, labilization of lysosomal membranes; LPC, lysophosphatidylcholine; p38MAPK, p38 mitogen-activated protein kinase, p73, tumor protein 73; PC, phosphatidylcholine; PCH, phosphorylcholine; PE, phosphatidylethanolamine; PG phosphatidyldiglycerol; PI, phosphatidylinositol; PKB/AKT, protein kinase B; PKC-□, protein kinase C-delta; PLA_2, phospholipase A_2; PLC, phospholipase C; PLASM, PE-based plasmalogen; PS, phosphatidylserine; ROTT, rottlerin; SEM, standard error of the mean; SPA, sphinganine; SPH, sphigosine; SM, sphingomyelin; TMRE, tetramethylrhodamine ethylester; TNF-α, tumor necrosis factor-alpha; UV, ultraviolet.

1. Introduction

Apoptosis is a controlled process involving many components of the cell, including organelles, such as the mitochondria, nucleus, endoplasmic reticulum and lysosome (for review see [1]). The lysosome compartment is associated with apoptosis signaling in a wide diversity of cells and with stimuli, such as oxidative stress [2-4], lysomotropic [5-8] and photo-sensitizer agents [9-11], photodamage [12], serum withdrawal [13], Fas and tumor necrosis factor-alpha (TNF-α) ligation [13-15], phospholipid and sphingolipid analogues [16-18], DNA-damaging [19, 20] and microtubule-stabilizing agents [21, 22], the quinolone class of antibiotics [23], artificial retinoics [24], zinc chloride [25] and silica [26]. Although participation of the lysosome compartment in apoptosis seems cell type and stimuli-specific, a shared feature among all models is the apparition of moderate lysosomal membrane ruptures, referred to here as labilization of lysosomal membranes (LLM), and subsequent release from the lysosomal lumen to the cytosol of lysosomal peptidases, the cathepsins, which contribute to cell death through various targets [27-30].

Several mechanisms underlying LLM have been proposed, including lipid alterations of lysosomal membrane composition. Indeed, oxidative stress, lysosome accumulation of redox-active iron and lipid peroxidation chain reaction can destabilize the lysosomal membrane (for review see [31]). Membrane accumulation of sphingosine (SPH) and lysophosphatidylcholine (LPC) has been reported to provoke LLM [16, 32, 33]. SPH is a sphingolipid with a long hydrophobic tail and a polar head that acts as a lysomotropic agent with detergent properties [16]. In addition, SPH accumulation can form channels in membranes [32]. In turn, LPC, a phospholipase A2 (PLA_2)-produced lipid metabolite, is

capable of eliciting relatively selective damage to lysosomal membranes by changing lysosomal osmotic sensitivity, provoking the entry of potassium ions and leading to losses of lysosomal membrane integrity [33].

A few proteins have been reported to induce or protect cells from LLM. It has been suggested that Bax, a proapoptotic member of the Bcl-2 family, can translocate to both the mitochondria and lysosome membranes in human fibroblasts exposed to the apoptosis-inducing drug staurosporine. Bax insertion into lysosomal membranes is believed to provoke LLM [34]. Some studies have suggested a role for PLA_2 [35], which could destabilize lysosomes, probably throughout the hydrolysis of phospholipids embedded within lysosome membranes [36] and LPC generation [33]. Others have proposed that PLA_2 and phospholipase C (PLC) could osmotically destabilize lysosome membranes via a K(+)/H(+) exchange process [37-40]. Another potential mechanism implicates the lysosome-associated apoptosis-inducing protein containing PH and FYVE domains (LAPF) that can mediate LLM through the phosphorylation and re-localization of p53 at lysosomes on TNF-α-treated murine fibrosarcoma cells [41]. Finally, heat shock protein 70 has been described as a stabilizing agent of lysosome membranes that effectively blocks LLM during diverse apoptotic treatments [42], Bcl-2 has been associated with the inhibition of PLA_2 activation and oxidative stress-induced LLM [43], while Bcl-xL overexpression prevents both 20-S-camptothecin lactone (CPT)-induced loss of mitochondrial membrane potential ($\downarrow\Delta\Psi m$) and LLM [19].

Human histiocytic lymphoma U-937 cells are highly sensitive to DNA damage and rapidly die by apoptosis after short treatment with the DNA-damaging drug CPT, a DNA topoisomerase I inhibitor, that traps transient intermediates of DNA topoisomerase I reactions where enzymes are linked to the 3' terminus of a DNA duplex [44, 45]. The

apoptotic death of these cells is associated with quick involvement of a mitochondrial and lysosomal pathway, within 2 to 3 h after drug treatment [19]. Recently, using comparative and quantitative proteomics approach on highly-enriched purified lysosomes obtained from control and CPT-treated human histiocytic lymphoma U-937 cells, we have reported that 27 proteins re-localize or de-localize at lysosomes in very early phases of CPT-induced LLM and apoptosis. Among the validated candidate proteins, protein kinase C-delta (PKC-δ) was identified as a protein that rapidly translocates to lysosomes after CPT treatment [46]. PKC-δ is an ubiquitously-expressed isoform of the multigenic family of PKC proteins related to serine/threonine kinase that acts in diverse cellular processes, including cell proliferation [47, 48] and apoptosis (reviewed in [49-51]) in a stimulus- and tissue-specific manner. So far, the apoptotic function of PKC-δ has been associated with its localization and activation of multiple signaling proteins, including Jun amino-terminal kinase (JNK), p38 mitogen-activated protein kinase (p38MAPK), ataxia telangiectasia mutated kinase (ATM), protein kinase B (PKB/AKT), cytolosic Abelson oncogene homolog 1 kinase (cAbl), tumor protein 73 (p73), DNA-protein kinase (DNA-PK), lamin, and scramblase [52, 53]. More recently, upon phorbol 12-myristate 13-acetate treatment, PKC-δ has been found to rapidly translocate to lysosomes where it phosphorylates and activates acidic sphingomyelinase (ASM), a key enzyme that catalyzes the degradation of membrane-bound sphingomyelin (SM) into phosphorylcholine (PCH) and ceramide (CER) [54]. More recently, PKC-δ has also been reported to mediate cytosolic CER accumulation through ASM activation in ultraviolet (UV)-treated cells [55].

In this study, we investigated the role of PKC-δ translocation at lysosomes for LLM in the early phase of CPT-induced apoptosis. We showed that PKC-δ is required for CPT-induced LLM, as silencing its expression by RNA interference (RNAi) or suppressing its

activity with the pharmacological inhibitor rottlerin (ROTT), prevents CPT-induced LLM in U-937 cells. PKC-δ translocation to lysosomes governs lysosomal ASM phosphorylation and activation, and depressing ASM activity with the pharmacological inhibitor desipramine (DESP) also prevents CPT-induced LLM. PKC-δ-mediated ASM activation leads to an increase of CER at lysosomes. This accumulation of endogenous CER at lysosomes is a critical event for LLM, given that suppression of PKC-δ or ASM activity reduces CPT-mediated CER generation at lysosome membranes and CPT-induced LLM. Theses results reveal a novel pathway where PKC-δ translocation to lysosomes mediates ASM phosphorylation/activation, CER generation and LLM during the early phase of CPT-induced apoptosis in U-937 cells.

2. Materials and methods

*2.1 Cell line, chemicals, drug treatments and RNAi transfection experiments***.** The human histiocytic lymphoma U-937 cell line from the American Type Culture Collection (Manassas, VA, USA) was grown in suspension at 37°C under 5% CO_2 in RPMI-1640 medium supplemented with 10% heat-inactivated fetal bovine serum, 100 U/ml penicillin and 100 μg/ml streptomycin (Gibco-BRL Life Technologies, Grand Island, NY, USA). CPT, ROTT, DESP, fumonisin B1 (FB1) and Histodenz™ were obtained from the Sigma-Aldrich Company (St. Louis, MO, USA). Percoll™ was purchased from GE Healthcare Bio-Sciences AB (Uppsala, Sweden). Acridine orange (AO) and tetramethylrhodamine ethylester (TMRE) were procured from Molecular Probes (Eugene, OR, USA). PKC-δ peptide substrate was from BioMol International (Plymouth Meeting, PA, USA). All other chemicals were of reagent grade and bought from either the Sigma-Aldrich Company, ICN

BioMedicals (Costa Mesa, CA, USA) or other local sources. For drug treatments, U-937 cells were exposed to CPT at a concentration of 1.0 μM for the indicated time. In the reported experiments, pre-incubation with DESP (10 μM), FB1 (10 μM) or ROTT (3.5 μM) was undertaken 1 h before CPT addition. Gene silencing of human PKC-δ was performed with the following duplex siRNA, sense, 5'-GGCUACAAAUGCAGGCAAUdTdT-3'; anti-sense, 5'-AUUGCCUGCAUUUGUAGCCdTdT-3' as reported previously [56]. siRNAs and negative control siRNAs were purchased from Thermo Scientific Dharmacon Products (Lafayette, CO, USA). For siRNA transfection, the cells were seeded without antibiotics, grown for 24 h, and transfected with Lipofectamine 2000 (Invitrogen Corporation, Carlsbad, CA, USA) according to the manufacturer's procedure. After 6 h of transfection, the medium was changed to complete growth medium containing serum and antibiotics, and the cells were grown for 48 h prior to CPT treatments.

2.2 Assessment of ↓ΔΨm and LLM. ↓ΔΨm was assessed by TMRE uptake [57]. At the indicated times (h) after CPT treatment, 1 x 10^6 cells were incubated with 100 nM TMRE in complete culture medium for 25 min at room temperature, washed 5-times and resuspended in 500 μL of ice-cold PBS and then, subjected to flow cytometry analysis. For LLM assessment, at various times after drug treatment, 1 x 10^6 cells were incubated with 1.5 μM AO in complete culture medium for 25 min at 37°C, washed 5 times and resuspended in 500 μL of ice-cold PBS before analysis by flow cytometry (uptake method) [2,19]. Loss of TMRE orange fluorescence was measured with the FL2 channel, loss of lysosomial AO red fluorescence with the FL3 channel and increase in cytosolic AO green fluorescence with the FL1 channel of a Coulter EPICS XL-MLC Flow Cytometer. At least

10,000 cells per sample were acquired in histograms, at least 3 independent experiments were conducted, and the results are expressed as the percentage of cells presenting $\downarrow\Delta\Psi m$ or LLM.

2.3 Immunofluorescence microscopy. Control and CPT-treated U-937 cells were allowed to adhere on glass slides previously treated with BD Cell-Tak^{TM} (BD Biosciences, Bedford, MA, USA) according to the manufacturer's specifications. Slides were then prepared as described elsewhere [46]. The first antibodies used were anti-cathepsin D of mouse origin (C47620, BD Biosciences; 10 □g/ml in 5% fetal bovine serum in PBS). The second antibodies used were Texas-red linked anti-mouse of goat origin (GE Healthcare Bio-Sciences AB; 1:25 v/v in 5% fetal bovine serum in PBS). Images were generated with a Nikon Optiphot-2 microscope equipped with a thermoelectrically-cooled CCD camera (Model DC330E, DageMTI Inc., Michigan City, IN, USA) and Clemex Vision software (Version 3.0.036, Clemex, Longueuil, QC, Canada).

2.4 Electron microscopy. Cells were processed as described earlier [44, 45]. Briefly, they were fixed in 0.1 M Millonig's phosphate buffer (pH 7.4; 292 mOsm containing 2.5% gluteraldehyde, stained with 2% uranyl acetate, and dehydrated with several ethanol treatments. Sections (500-700 Å) were mounted on copper grids and stained in lead citrate. Samples were examined (JFE Enterprises, Brookville, MD, USA) by transmission electron microscopy with a Ziess Em 10 CA microscope.

2.5 Analysis of DNA fragmentation. The kinetics of DNA fragmentation were monitored and quantified by DNA filter elution assays, and the results are expressed as percentages of DNA fragmentation [44, 45, 58].

*2.6 Subcellular fractionation***.** A 2-step sequential density gradient centrifugation protocol was modified from Storrie and Madden [59] and Paquet et al. [19] for lysosome isolation. Briefly, control and CPT-treated U-937 cells (5.0×10^8) were swelled in deionized water for 4 min on ice, and the samples adjusted to 220 mM mannitol, 70 mM sucrose, 10 mM Hepes-KOH (pH 7.4) and 1.0 mM EDTA (isotonic buffer). The cells were disrupted by passing the samples 30-fold through a 26G3/8 needle, and subsequently centrifuged at 1,000 x g for 15 min to pellet unbroken cells and nuclei. Supernatants containing mitochondria, lysosomes and other vesicles were adjusted to 8 mM calcium chloride and centrifuged at 5,000 g for 15 min to pellet the rough endoplasmic reticulum and mitochondria. Then, the supernatants were layered on top of the first gradient consisting, from bottom to top, of 2 ml of 35% (w/v) Histodenz™, 2 ml of 17% (w/v) Histodenz™, and 5 ml of 6% (v/v) Percoll™ in isotonic buffer. After centrifugation at 50,500 x g for 1 h at 4°C, a set of 2 discrete bands appeared at the interfaces of 17/35% Histodenz™ and 6% Percoll™/17% Histodenz™. The upper band, at the 6% Percoll™/17% Histodenz™ interface, contains small mitochondria and lysosomes that needed separation by the second gradient to obtain pure organelle fractions. This interface is collected and adjusted to 35% Histodenz™ by mixing with a 80% (w/v) Histodenz™ solution. The sample was then placed at the bottom of the second gradient and overlaid with 2 ml of 17% Histodenz™ and 5 ml of 5% Histodenz™. The tube was filled to the top with the isotonic buffer, and centrifuged at 50,500 x g for 1 h at 4°C. Two distinct bands appeared: the upper one at the

5/17% Histodenz™ interface contained lysosomes, while the lower one, at the 17/35% Histodenz™ interface, contained small mitochondria. To pellet the lysosomes, the interface was diluted with the largest possible volume of isotonic buffer and centrifuged at 53,000 x g for 1 h at 4°C, The purity of lysosome preparations are monitored by fluorescence microscopy following *in vitro* staining with the fluorescent biomarkers LysoTracker RED/DND-99 (lysosomes), MitoTracker Green/FM (mitochondria), ER-Tracker Red dye (endoplasmic reticulum, ER) and Hoechst 33342 (nucleus). In parallel, the purified preparations are also validated by fluorescence microscopy and Western blottings using specific antibodies directed against the protein biomarker LAMP-1 (lysosome), VDAC-1 (mitochondria), Calnexin (ER) and Nucleolin (nucleus). Purity of the lysosome extracts was documented in details recently [46].

2.7 Immunoprecipitation experiments and Western blotings. To prepare total protein extracts, cells were washed twice in PBS, homogenized and lysed in buffer containing 50 mM Tris (pH 7.4), 120 mM NaCl, 1% Triton X-100, 1 mM sodium orthovanadate, 2 mM phenylmethylsulfonyl fluoride, 5 mM sodium pyrophosphate and a cocktail of protease inhibitors (Complete™, Roche Molecular Biochemicals, Laval, QC, Canada) at 4°C for 30 min, centrifuged, and the supernatants collected. The same procedure was applied to prepare proteins from purified lysosome pellets. For co-immunoprecipitation experiments, 150 µg of purified lysosome proteins were used and 5% BSA (w/v) was added to lysis buffer. The supernatants were incubated overnight with primary antibodies (10 □g/ml) at 4°C. Immunocomplexes were captured with a protein A- and G-Sepharose mixture followed by several washes with lysis buffer prior to sodium dodecyl sulfate-polyacrylamide gel electrophoresis. The primary antibodies in Western blots and co-

immunoprecipitation experiments included anti-ASM rabbit polyclonal (sc-11352, Santa Cruz Biotechnology, Santa Cruz, CA, USA), anti-CT10 regulator of tyrosine kinase isoform L (CRK-L) rabbit polyclonal (sc-319, Santa Cruz Biotechnology), anti-caspase-3 rabbit polyclonal (556425, BD Biosciences), anti-lysosomal-associated membrane protein 1 (LAMP-1) mouse monoclonal (611042, BD Biosciences), anti-PKC-δ rabbit polyclonal (SA-148, Biomol International), anti-Phospho-(Ser) PKC substrate rabbit polyclonal (2261, Cell Signaling Technology, Danvers, MA, USA) and nonspecific normal rabbit and mouse IgG (Santa Cruz Biotechnology) as controls. The secondary antibodies were horseradish peroxidase-conjugated sheep anti-mouse Ig and donkey anti-rabbit Ig detected by enhanced chemiluminescence with reagents from GE Healthcare Bio-Sciences AB.

2.8 Enzymatic activity assays. PKC-δ activity was monitored according to a modified procedure described previously [60]. Briefly, the reaction mixture (100μl) consisted of 100 μM ATP with [γ-^{32}P]ATP (5 μCi), 1 mM DTT, 5 mM $MgCl_2$, 25 mM Tris-HCl (pH 7.5), 0.5 mM EGTA and 500 μM of the PKCδ-specific peptide substrate Ala-Arg-Arg-Lys-Arg-Lys-Gly-Ser-Phe-Phe-Gly-Gly. Reactions were initiated by the addition of lysosome-enriched extracts incubated at 30°C for 10 min and then stopped on ice. Reaction mixtures were spotted on PVDF membrane and washed 4-fold in 0.5 ml of 1% phosphoric acid. ^{32}P incorporation was measured by liquid scintillation counting. In each experimental assay, negative control reactions lacking the substrate peptide were included. The results are expressed as CPM min^{-1} mg^{-1}.

ASM activity was assayed according to the Hojjati and Jiang protocol, [61] with colorimetric-based kits purchased from the Cayman Chemical Company (Ann Arbor, MI, USA). Briefly, in this assay, SM is hydrolyzed by ASM to PCH and CER. Alkaline

phosphatase then generates choline from PCH and the newly-formed choline serves to generate hydrogen peroxide in a reaction catalyzed by choline oxidase. Finally, with peroxidase, hydrogen peroxide reacts with diamine oxidases and 4-aminoantipyrine to generate a blue color with an optimal absorption at 595 nm. ASM activity was evaluated from highly-enriched lysosome extracts in a reaction mixture containing excess SM (150 μM). Enzymatic reactions were carried out at room temperature under constant agitation, and enzyme activity measured at 10-min intervals for 60 min at the optimal absorption of 595 nm with a microplate reader (Model 3550**,** Bio-Rad Laboratories, Hercules, CA, USA). Control reactions consisted of lysosomal extracts incubated in the reaction buffer without SM or without protein extracts. The results are expressed as optical density (OD; 595nm) min^{-1} mg^{-1}.

2.9 Lipid species analysis by electrospray ionization tandem mass spectrometry (ESI-MS/MS). Lipid analysis was performed by the ESI-MS/MS as described previously [62, 63]. Briefly, samples were quantified by direct flow injection analysis using a precursor ion scan of *m/z* 184 specific for phosphocholine containing lipids including phosphatidylcholine (PC), sphingomyelin (SM) and lysophosphatidylcholine (LPC). Neutral loss scans of *m/z* 141 and *m/z* 185 were used for phosphatidylethanolamine (PE) and phosphatidylserine (PS), respectively. PE-based plasmalogens were analyzed by fragment ions of *m/z* 364, 380 and 382. Ammonium-adduct ions of phosphatidylglycerol (PG) and phoshatidylinositol (PI) were analysed by neutral loss scans of *m/z* 189 and 277, respectively [64]. Ceramide was analyzed similar to a previously described methodology [65] using N-heptadecanoyl-sphingosine as internal standard. Free cholesterol (FC) and cholesteryl ester (CE) were quantified using a fragment ion of *m/z* 369 after selective

derivatization of FC using acetyl chloride. Correction of isotopic overlap of lipid species as well as data analysis by self programmed Excel Macros was performed for all lipid classes. Sphingoid bases, hexosyl- and lactosylceramides were quantified by hydrophilic interaction chromatography (HILIC) coupled to ESI-MS/MS in a similar way as described by [66].

2.10 Statistical analysis. Mann-Whitney or Student's t tests were performed between data points as indicated in Figure legends with GraphPad InStat software (v3.0b). *P values* of 0.05 or less were considered as statistically significant.

3. Results

3.1 Lysosomal and mitochondrial pathways of apoptosis are quickly activated after CPT treatment in U-937 cells. Human histiocytic lymphoma U-937 cells are highly sensitive to DNA damage and rapidly die by apoptosis after treatment with the DNA topoisomerase I inhibitor CPT (1 μM) [19, 44-46]. Manifestations of apoptosis onset in these cells are illustrated by simultaneous activation of the mitochondrial and lysosomal pathways within 2 to 3 h after drug treatment, with $\downarrow\Delta\Psi m$, that reflects loss of mitochondrial inner membrane potential [67] (Fig. 1A), and LLM (Fig. 1B) accompanied by lysosomal cathepsin D release into the cytosol (Fig. 1C). Cleavage of the executioner procaspase-3 into catalytic fragments of the active caspase (Fig. 1D) also indicates that apoptosis has been initiated. These events correspond to the activation phase of apoptosis, followed by the execution phase where the morphological features of apoptotic cells become clearly apparent 4 h after CPT treatment (Fig. 1E).

3.2 PKC-δ is required for LLM in CPT-treated U-937 cells. Recently, taking a comparative proteomics approach on highly-enriched lysosome extracts, we identified PKC-δ as a protein that rapidly translocates at lysosomes after CPT treatment in U-937 cells [46]. PKC-δ translocation to lysosomes after CPT treatment (Fig 2A) correlated with increase PKC-δ activity in highly-enriched lysosome extracts (Fig 2B). Inhibition of PKC-δ activity with the pharmacological inhibitor ROTT [68] (Fig. 2B) or knocking down PKC-δ expression with siRNA [56] (Fig. 2C) had a significant effect on CPT-induced LLM (Fig. 2D), revealing that PKC-δ plays a key role in LLM induction by CPT. Inhibition of PKC-δ activity and subsequent reduction of LLM also had an effect on the kinetics of DNA fragmentation, a validated measure of apoptosis in CPT-treated U-937 cells (Fig. 2E). Purity of the lysosome extracts was documented in details recently [46].

3.3 PKC-δ mediates ASM phosphorylation and activation at lysosomes after CPT treatment. It has been reported that PKC-□at lysosomes phosphorylates and activates ASM, a key enzyme that catalyzes the degradation of membrane-bound SM into PCH and CER [54, 55]. To evaluate the effect of PKC-δ translocation and activity at lysosomes after CPT treatment, we first evaluated ASM expression in enriched lysosome extracts after CPT treatment. CPT treatment did not alter the lysosomal ASM expression level (Fig. 3A). However, reciprocal immunoprecipitation (IP) experiments performed on these highly-enriched lysosome extracts followed by Western blotting revealed that ASM phosphorylation increased significantly at lysosomes after CPT treatment (Fig. 3B). These experiments were conducted with specific antibodies recognizing specific PKC-δ Ser-phosphorylation consensus sequences and ASM (Fig. 3B). Co-treatment with ROTT

reduced ASM phosphorylation (Fig. 3B). The increment of ASM phosphorylation at lysosomes after CPT treatment also correlated with heightened ASM enzymatic activity (Fig. 3C). Inhibition of ASM activity by DESP [69] or suppression of PKC-δ by ROTT reduced ASM enzymatic activity in lysosomes during CPT treatment (Fig. 3C). Finally, inhibition of ASM activity by DESP also interfered with LLM (Fig. 3D). In contrast, inhibition of ceramide synthase (CS) by FB1 [70], a key enzyme involved in *de novo* CER generation had no effect on LLM after CPT treatment (Fig. 3D), confirming the importance of ASM activity for LLM.

3.4 PKC-δ-mediated activation of lysosomal ASM leads to CER generation and accumulation at lysosomes. ASM activation results in the hydrolysis of SM into CER. To investigate if the ASM activation mediated by PKC-δ after CPT treatment is associated with changes in lipid and sphingolipid distribution at lysosomes, highly-enriched lysosome extracts were analyzed for their lipid composition by ESI-MS/MS [62, 63]. Lipid profiling analysis revealed that CER and lactosyl-ceramide (LacCER) significantly increased in lysosomes after CPT treatment (Fig. 4A). Apparent LPC increment was also observed, although stastistically not significant due to variation among samples (Fig. 4A). All of the other lipid species analyzed including total SM, dihydro-sphingomyelin (dihSM), phosphatidylethanolamine (PE), phosphatidylcholine (PC), PE-based plasmalogen (PLASM), phosphatidylserine (PS), phosphatidyldiglycerol (PG), phosphatidylinositol (PI), hexosylceramide (HexCER), sphigosine (SPH), sphinganine (SPA), cholesterol ester (CE) and free cholesterol (FC) did not change (Fig. 4A). Inhibition of PKC-δ by ROTT during CPT treatment impeded CER and LacCER accumulation at lysosomes but had no effect on apparent LPC accumulation (Fig. 4B). Similarly, inhibition of ASM by DESP reduced

CER and LacCER accumulation induced by CPT treatment but had no effect on apparent LPC increment (Fig. 4C). Finally, inhibition of CS by FB1 did not alter CER accumulation at lysosomes after CPT treatment (Fig. 4D). Detailed quantitative distribution of CER (Fig. 5A) and SM (Fig. 5B) species generated at lysosomes after CPT treatment revealed a significant elevation in CER 16:0 (Fig. 5A). After an initial increment of SM 16:0 2h after CPT treatment (Fig. 5B), reduction of SM 16:0 paralleled the increase in CER 16:0.

Altogether, these results indicated that after CPT treatment, PKC-δ rapidly translocates to lysosomes, where it phosphorylates and activates ASM, which leads to CER accumulation and LLM.

4. Discussion

Many efforts have been invested in the past several years to understand the signaling pathways of caspase activation, a crucial step for apoptosis induction. The best-studied molecular mechanisms of caspase activation and apoptosis, the mitochondrial and cell death receptor pathways, are well characterized. However, alternative and amplification pathways of caspase activation are much less known, including the lysosomal pathway of apoptosis. The aim of this study was to investigate the role of PKC-δ in the induction of LLM during the early phase of CPT-induced apoptosis. Previously, we reported that PKC-δ rapidly translocates to lysosomes after CPT treatment in human histiocytic lymphoma U-937 cells [46]. Here, we show that PKC-δ regulates LLM via the phosphorylation and activation of lysosomal ASM, which leads to CER generation and accumulation at lysosomes after CPT.

PKC-δ is known to participate in the apoptotic process in diverse cell types with a plethora of stimuli (reviewed in [49-51]). The observations reported here correspond to the induction phase of apoptosis, in contrast to the execution phase where active caspases fire numerous substrates, including PKC-δ. PKC-δ activity and re-localization during apoptosis are regulated via threonine residue phosphorylation, or after cleavage of its regulatory domain mediated by caspase-3 [71]. The latter mode of activation is unlikely to play a role in our model as PKC-δ cleavage is not apparent in the early phase of CPT-induced apoptosis [46]. In agreement with our observations, others have reported that PKC-δ cleavage occurs only 24 h after NSC606985 treatment, a CPT analog, in U-937 cells [72].

PKC-δ pro-apoptotic functions are mediated through various targeted proteins. So far, the apoptotic functions of PKC-□have been associated with its cytosolic and nuclear localization and activation of multiple signaling proteins, including JNK, p38MAPK, ATM, PKB/AKT, cAbl, p73, DNA-PK, lamin, and scramblase [49-53]. More recently, upon phorbol 12-myristate 13-acetate treatment, PKC-□has been shown to rapidly translocate to lysosomes where it phosphorylates and activates ASM, a key enzyme that catalyzes the degradation of membrane-bound SM into PCH and CER [54]. After UV treatment, ASM has also been reported to be phosphorylated on Ser508 by PKC-δ in MCF-7 breast cancer cells, triggering cytosolic CER accumulation and provoking mitochondrial fragmentation and cytochrome c release [55].

CER generation has often been associated with apoptosis following a variety of insults in several studies [73]. CER accumulates in cells quickly but transiently [55], or progressively and continuously [74] after apoptosis-inducing treatment. While most attention is generally focused on total cellular CER content, and the mediated effects on

plasma membranes or mitochondria [55, 74], lipid and sphingolipid analyses in this study were performed on highly-enriched lysosome extracts after CPT treatment and the consequences of lysosomal CER accumulation were associated with LLM. Our experiments reveal that in addition to the PKC-□/ASM/CER pathway that regulates mitochondrial responses [55], a specific lysosomal PKC-□/ASM/CER pathway also regulates early lysosomal responses after CPT treament. It is unlikely that the increased lysosomal CER content observed in this study could also acts on the mitochondria, as it has been previously shown that lysosomal CER cannot exit into the cytosol unless it is deacylated to SPH [75].

In this study, we also observed an apparent increase of LPC content in lysosomes after CPT treatment, although this variation was statistically not significant. Lysosomal accumulation of LPC, a PLA_2-produced lipid metabolite, has been reported to provoke lysosomal rupture. It is believed that LPC, in concert with cytosolic PLA_2 and cytosolic PLC, osmotically destabilizes lysosome membranes via a K(+)/H(+) exchange process [33, 37-40]. Interestingly, our study suggests that the apparent LPC accumulation is independent of PKC-□ after CPT, and that CER accumulation is required for the destabilization of the lysosomal membranes, even in the presence of apparent high LPC levels. It is conceivable that CER and LPC cooperate for dynamic modifications of lysosomal membranes to activate the K(+)/H(+) exchange process associated with LLM, or to form novel channels inside lysosomal membranes. Indeed, it has been reported that CER can form channels inside lipid membranes, allowing the passage of molecules with size up to 60 kDa [76]. Considering that most lysosomal cathepsins are smaller than 60 kDa, such CER-formed channels could be implicated not only in LLM after CER accumulation at lysosome membranes but also in cathepsin release into the cytosol. Of interest, it has been reported

that CER could interact with cathepsin D leading to its auto-activation [17]. Finally, CER is generally generated in cells from SM hydrolysis mediated by ASM or from the *de novo* synthesis of CER mediated by CS [77]. Since both enzymes are found in lysosomes [78, 79], we also used in this study pharmacological inhibitors targeting both ASM and CS, to confirm that ASM was the major source of CER generation in lysosomes after CPT treatment. The detailed analysis of CER and SM species generated at lysosomes after CPT treatment indicating that SM 16:0 reduction paralleled CER 16:0 elevation, also confirmed the key role of ASM for CER generation after CPT treatment.

Cumulating evidence suggests that different intracellular organelles contribute together to amplify apoptosis initiation. After CPT treatment, both the mitochondrial and lysosomal pathways are engaged concomitantly, indicating cooperation between the 2 pathways to activate a variety of killer proteases, mainly caspases and cathepsins. Interestingly, PKC-δ inhibition reduced LLM (but also ↓ΔΨm; data not shown) and delayed apoptosis, suggesting that the lysosomal PKC-δ/ASM/CER pathway revealed in our study contributes, at least in part, to the activation of CPT-induced apoptosis. Because of all the pleotropic effects of PKC-δ in signaling apoptosis, it is however difficult to accurately quantitate or assess the importance of the lysosomal pathway. Indeed, we have reported previously that blocking caspase activity in these cells after CPT treatment will prevent typical manifestation of apoptosis, with cells dying by necrosis [80]. Blocking cathepsin B activity after CPT treatment will only slightly interfere with the kinetics and amplitude of apoptosis, while blocking the mitochondrial pathway of apoptosis either with either mitochondrial permeabilization inhibitors or Bcl-xL overexpression has a more pronounced effect on the kinetics of apoptosis [19]. Thus, it appears that the mitochondrial

pathway of apoptosis is predominant in these cells after CPT treatment, while the lysosomal pathway may act to amplify cell death signals.

A few compounds that induce significant cell death by triggering LLM and cathepsin-mediated killing of tumor cells have been identified. Boya et al. reported that widely-administered quinolone antibiotics, including ciprofloxacin and norfloxacin, could mediate LLM, cathepsin release and apoptosis, either alone or in combination with UV irradiation [23]. Similarly, cytotoxin 3-aminopropanal [81] and siramesine [82] specifically target the lysosomal compartment to induce LLM and apoptosis. More recently, screening of a small molecule library identified new compounds that induced significant LLM and cathepsin-mediated cell death in tumor cell lines [83]. Combination of DNA-damaging agents with the quinolone class of antibiotics enables lower doses of DNA-damaging agents to be used with the same apoptotic capacity when combined together [84]. Thus, the potential of activating the lysosomal death pathway is promising and under development for novel cancer therapeutic approaches [85].

References

[1] K.F. Ferri, G. Kroemer, Organelle-specific initiation of cell death pathways, Nat Cell Biol 3 (2001) E255-263.

[2] F. Antunes, E. Cadenas, U. T Brunk, Apoptosis induced by exposure to a low steady-state concentration of H2O2 is a consequence of lysosomal rupture, Biochem J 356 (2001) 459-555.

[3] K. Roberg, K. Ollinger, Oxidative stress causes relocation of the lysosomal enzyme cathepsin D with ensuing apoptosis in neonatal rat cardiomyocytes, Am J Pathol 152 (1998) 1151-1156.

[4] E. Dare, W. Li, B. Zhivotovsky, X. Yuan, S. Ceccatelli, Methylmercury and H_2O_2 provoke lysosomal damage in human astrocytoma D384 cells followed by apoptosis, Free Radic Biol Med 30 (2001) 1347-1356.

[5] U.T. Brunk, Lysosomotropic detergents induce time- and dose-dependent apoptosis/necrosis in cultured cells, Redox Rep 5 (2000) 87-88.

[6] T. Uchimoto, H. Nohara, R. Kamehara, M. Iwamura, N. Watanabe, Y. Kobayashi, Mechanism of apoptosis induced by a lysosomotropic agent, L-Leucyl-L-Leucine methyl ester, Apoptosis 4 (1999) 357-362.

[7] W. Li, X. Yuan, G. Nordgren, H. Dalen, G.M. Dubowchik, R.A. Firestone, U.T. Brunk, Induction of cell death by the lysosomotropic detergent MSDH, FEBS Lett 470 (2000) 35-39.

[8] K. van Nierop, F.J. Muller, J. Stap, C.J. van Noorden, M. van Eijk, C. de Groot, Lysosomal destabilization contributes to apoptosis of germinal center B-lymphocytes, J Histochem Cytochem 54 (2006) 1425-1435.

[9] U.T. Brunk, H. Dalen, K. Roberg, H.B. Hellquist, Photo-oxidative disruption of lysosomal membranes causes apoptosis of cultured human fibroblasts, Free Radic Biol Med 23 (1997) 616-626.

[10] D. Kessel, Y. Luo, P. Mathieu, J.J.J. Reiners, Determinants of the apoptotic response to lysosomal photodamage, Photochem Photobiol 71 (2000) 196-200.

[11] S. Nagata, A. Obana, Y. Gohto, S. Nakajima, Necrotic and apoptotic cell death of human malignant melanoma cells following photodynamic therapy using an amphiphilic photosensitizer, ATX-S10(Na), Lasers Surg Med 33 (2003) 64-70.

[12] S. Ichinose, J. Usuda, T. Hirata, T. Inoue, K. Ohtani, S. Maehara, M. Kubota, K. Imai, Y. Tsunoda, Y. Kuroiwa, K. Yamada, H. Tsutsui, K. Furukawa, T. Okunaka, N.L. Oleinick, H. Kato, Lysosomal cathepsin initiates apoptosis, which is regulated by photodamage to Bcl-2 at mitochondria in photodynamic therapy using a novel photosensitizer, ATX-s10 (Na), Int J Oncol 29 (2006) 349-355.

[13] U.T. Brunk, I. Svensson, Oxidative stress, growth factor starvation and Fas activation may all cause apoptosis through lysosomal leak, Redox Rep 4 (1999) 3-11.

[14] M.E. Guicciardi, J. Deussing, H. Miyoshi, S.F. Bronk, P.A. Svingen, C. Peters, S.H. Kaufmann, G.J. Gores, Cathepsin B contributes to TNF-alpha-mediated hepatocyte apoptosis by promoting mitochondrial release of cytochrome c, J Clin Invest 106 (2000) 1127-1137.

[15] M. Gyrd-Hansen, T. Farkas, N. Fehrenbacher, L. Bastholm, M. Hoyer-Hansen, F. Elling, D. Wallach, R. Flavell, G. Kroemer, J. Nylandsted, M. Jaattela, Apoptosome-independent activation of the lysosomal cell death pathway by caspase-9, Mol Cell Biol 26 (2006) 7880-7891.

[16] K. Kågedal, M. Zhao, I. Svensson, U.T. Brunk, Sphingosine-induced apoptosis is dependent on lysosomal proteases, Biochem J 359 (2001) 335-343.

[17] M. Heinrich, M. Wickel, W. Schneider-Brachert, C. Sandberg, J. Gahr, R. Schwandner, T. Weber, P. Saftig, C. Peters, J. Brunner, M. Krönke, S. Schütze,

Cathepsin D targeted by acid sphingomyelinase-derived ceramide, EMBO J 18 (1999) 5252-5263.

[18] C. Paris, J. Bertoglio, J. Bréard, Lysosomal and mitochondrial pathways in miltefosine-induced apoptosis in U937 cells, Apoptosis 12 (2007) 1257-1267.

[19] C. Paquet, A.T. Sané, M. Beauchemin, R. Bertrand, Caspase- and mitochondrial dysfunction-dependent mechanisms of lysosomal leakage and cathepsin B activation in DNA damage-induced apoptosis, Leukemia 19 (2005) 784-791.

[20] T. Hishita, T. Tada-Oikawa, K. Tohyama, Y. Miura, T. Nishihara, Y. Tohyama, Y. Yoshida, T. Uchiyama, S. Kawanishi, Caspase-3 activation by lysosomal enzymes in cytochrome c-independent apoptosis in myelodysplastic syndrome-derived cell line P39, Cancer Res 61 (2001) 2878-2884.

[21] L.E. Broker, C. Huisman, S.W. Span, J.A. Rodriguez, F.A. Kruyt, G. Giaccone, Cathepsin B mediates caspase-independent cell death induced by microtubule stabilizing agents in non-small cell lung cancer cells, Cancer Res 64 (2004) 27-30.

[22] L. Groth-Pedersen, M.S. Ostenfeld, M. Hoyer-Hansen, J. Nylandsted, M. Jaattela, Vincristine induces dramatic lysosomal changes and sensitizes cancer cells to lysosome-destabilizing siramesine, Cancer Res 67 (2007) 2217-2225.

[23] P. Boya, K. Andreau, D. Poncet, N. Zamzami, J.L. Perfettini, D. Metivier, D.M. Ojcius, M. Jaattela, G. Kroemer, Lysosomal membrane permeabilization induces cell death in a mitochondrion-dependent fashion, J Exp Med 197 (2003) 1323-1334.

[24] Y. Zang, R.L. Beard, R.A. Chandraratna, J.X. Kang, Evidence of a lysosomal pathway for apoptosis induced by the synthetic retinoid CD437 in human leukemia HL-60 cells, Cell Death Differ 8 (2001) 477-485.

[25] H. Yu, Y. Zhou, S.E. Lind, W.Q. Ding, Clioquinol targets zinc to lysosomes in human cancer cells, Biochem J 417 (2009) 133-139.

[26] M.S. Thibodeau, C. Giardina, D.A. Knecht, J. Helble, A.K. Hubbard, Silica-induced apoptosis in mouse alveolar macrophages is initiated by lysosomal enzyme activity, Toxicol Sci 80 (2004) 34-48.

[27] U.T. Brunk, J. Neuzil, J.W. Eaton, Lysosomal involvement in apoptosis, Redox Rep 6 (2001) 91-97.

[28] B. Turk, V. Stoka, J. Rozman-Pungercar, T. Cirman, G. Droga-Mazovec, K. Oreic, V. Turk, Apoptotic pathways: involvement of lysosomal proteases, Biol Chem 383 (2002) 1035-1044.

[29] M.E. Guicciardi, M. Leist, G.J. Gores, Lysosomes in cell death, Oncogene 23 (2004) 2881-2890.

[30] M. Leist, M. Jaattela, Triggering of apoptosis by cathepsins, Cell Death Differ 8 (2001) 324-326.

[31] A. Terman, T. Kurz, B. Gustafsson, U.T. Brunk, Lysosomal labilization, IUBMB Life 58 (2006) 531-539.

[32] L.J. Siskind, S. Fluss, M. Bui, M. Colombini, Sphingosine forms channels in membranes that differ greatly from those formed by ceramide, J Bioenerg Biomembr 37 (2005) 227-236.

[33] J.S. Hu, Y.B. Li, J.W. Wang, L. Sun, G.J. Zhang, Mechanism of lysophosphatidylcholine-induced lysosome destabilization, J Membr Biol 215 (2007) 27-35.

[34] K. Kågedal, A.C. Johansson, U. Johansson, G. Heimlich, K. Roberg, N.S. Wang, J.M. Jurgensmeier, K. Ollinger, Lysosomal membrane permeabilization during apoptosis--involvement of Bax?, Int J Exp Pathol 86 (2005) 309-321.

[35] M. Zhao, U.T. Brunk, J.W. Eaton, Delayed oxidant-induced cell death involves activation of phospholipase A2, FEBS Lett 509 (2001) 399-404.

[36] A.K. Mukherjee, S.K. Ghosal, C.R. Maity, Lysosomal membrane stabilization by a tocopherol against the damaging action of Vipera russelli venom phospholipase A_2, Cell Mol Life Sci 53 (1997) 152-155.

[37] M. Hiraoka, A. Abe, Y. Lu, K. Yang, X. Han, R.W. Gross, J.A. Shayman, Lysosomal phospholipase A2 and phospholipidosis, Mol Cell Biol 26 (2006) 6139-6148.

[38] J.W. Wang, L. Sun, J.S. Hu, Y.B. Li, G.J. Zhang, Effects of phospholipase A2 on the lysosomal ion permeability and osmotic sensitivity, Chem Phys Lipids 144 (2006) 117-126.

[39] X. Wang, L.L. Wang, G.J. Zhang, Guanosine 5'-[gamma-thio]triphosphate-mediated activation of cytosol phospholipase C caused lysosomal destabilization, J Membr Biol 211 (2006) 55-63.

[40] H.F. Zhao, X. Wang, G.J. Zhang, Lysosome destabilization by cytosolic extracts, putative involvement of Ca(2+)/phospholipase C, FEBS Lett 579 (2005) 1551-1556.

[41] N. Li, Y. Zheng, W. Chen, C. Wang, X. Liu, W. He, H. Xu, X. Cao, Adaptor protein LAPF recruits phosphorylated p53 to lysosomes and triggers lysosomal destabilization in apoptosis, Cancer Res 67 (2007) 11176-11185.

[42] J. Nylandsted, M. Gyrd-Hansen, A. Danielewicz, N. Fehrenbacher, U. Lademann, M. Hoyer-Hansen, E. Weber, G. Multhoff, M. Rohde, M. Jäättela, Heat shock

protein 70 promotes cell survival by inhibiting lysosomal membrane permeabilization, J Exp Med 200 (2004) 425-435.

[43] M. Zhao, J.W. Eaton, U.T. Brunk, Bcl-2 phosphorylation is required for inhibition of oxidative stress-induced lysosomal leak and ensuing apoptosis, FEBS Lett 509 (2001) 405-412.

[44] E. Schmitt, G. Cimoli, A. Steyaert, R. Bertrand, Bcl-xL modulates apoptosis induced by anticancer drugs and delays DEVDase and DNA fragmentation-promoting activities, Exp Cell Res 240 (1998) 107-121.

[45] A.T. Sané, R. Bertrand, Distinct steps in DNA fragmentation pathway during camptothecin-induced apoptosis involved caspase-, benzyloxycarbonyl- and N-tosyl-L-phenylalanylchloromethyl ketone-sensitive activities, Cancer Res 58 (1998) 3066-3072.

[46] N. Parent, E. Winstall, M. Beauchemin, C. Paquet, G.G. Poirier, R. Bertrand, Proteomic analysis of enriched lysosomes at early phase of camptothecin-induced apoptosis in human U-937 cells, J Proteomics 72 (2009) 960-973.

[47] S. Fukumoto, Y. Nishizawa, M. Hosoi, H. Koyama, K. Yamakawa, S. Ohno, H. Morii, Protein kinase Cδ inhibits the proliferation of vascular smooth muscle cells by suppressing G1 cyclin expression, J Biol Chem 272 (1997) 13816 -13822.

[48] O. You-Take, H.C. Kwang, I.O. Jeong, A.P. Jeong, U.K. Yong, K.L. Seung, PKC-δ modulates p21WAF1/CIP1 ability to bind to Cdk2 during TNF alpha -induced apoptosis., Biochem Biophys Res Com 339 (2006) 1138-1149.

[49] C. Brodie, P.M. Blumberg, Regulation of cell apoptosis by protein kinase c δ, Apoptosis 8 (2003) 19-27.

[50] M.E. Reyland, Protein kinase Cδ and apoptosis, Biochem Soc Trans 35 (2007) 1001-1004.

[51] M.E. Reyland, Protein kinase C isoforms: multi-functional regulators of cell life and death, Front Biosci 14 (2009) 2386-2399.

[52] K. Yoshida, PKC delta signaling: mechanisms of DNA damage response and apoptosis, Cell Signal 19 (2007) 892-901.

[53] R. Gomel, C. Xiang, S. Finniss, H.K. Lee, W. Lu, H. Okhrimenko, C. Brodie, The localization of protein kinase C-delta in different subcellular sites affects its proapoptotic and antiapoptotic functions and the activation of distinct downstream signaling pathways, Mol Cancer Res 5 (2007) 627-639.

[54] Y.H. Zeidan, Y.A. Hannun, Activation of acid sphingomyelinase by protein kinase C delta-mediated phosphorylation, J Biol Chem 282 (2007) 11549-11561.

[55] Y.H. Zeidan, B.X. Wu, R.W. Jenkins, L.M. Obeid, Y.A. Hannun, A novel role for protein kinase C delta-mediated phosphorylation of acid sphingomyelinase in UV light-induced mitochondrial injury, FASEB J 22 (2008) 183-193.

[56] M.L. Torgersen, S. Walchli, S. Grimmer, S.S. Skanland, K. Sandvig, Protein kinase C delta is activated by Shiga toxin and regulates its transport, J Biol Chem 282 (2007) 16317-16328.

[57] F.H. Labeed, H.M. Coley, M.P. Hughes, Differences in the biophysical properties of membrane and cytoplasm of apoptotic cells revealed using dielectrophoresis, Biochim Biophys Acta 1760 (2006) 922-929.

[58] R. Bertrand, M. Sarang, J. Jenkin, D. Kerrigan, Y. Pommier, Differential induction of secondary DNA fragmentation by topoisomerase II inhibitors in human tumor cell lines with amplified c-myc expression, Cancer Res 51 (1991) 6280-6285.

[59] B. Storrie, E.A. Madden, Isolation of subcellular organelles, Methods Enzymol 182 (1990) 203-225.

[60] K. Nishikawa, A. Toker, F.J. Johannes, Z. Songyang, L.C. Cantley, Determination of the specific substrate sequence motifs of protein kinase C isozymes, J Biol Chem 272 (1997) 952-960.

[61] M.R. Hojjati, X.C. Jiang, Rapid, specific, and sensitive measurements of plasma sphingomyelin and phosphatidylcholine, J Lipid Res 47 (2006) 673-676.

[62] M. Binder, G. Liebisch, T. Langmann, G. Schmitz, Metabolic profiling of glycerophospholipid synthesis in fibroblasts loaded with free cholesterol and modified low density lipoproteins, J Biol Chem 281 (2006) 21869-21877.

[63] P. Wiesner, K. Leidl, A. Boettcher, G. Schmitz, G. Liebisch, Lipid profiling of FPLC-separated lipoprotein fractions by electrospray ionization tandem mass spectrometry, J Lipid Res 50 (2009) 574-585.

[64] V. Matyash, G. Liebisch, T.V. Kurzchalia, A. Shevchenko, D. Schwudke, Lipid extraction by methyl-tert-butyl ether for high-throughput lipidomics, J Lipid Res 49 (2008) 1137-1146.

[65] G. Liebisch, W. Drobnik, M. Reil, B. Trumbach, R. Arnecke, B. Olgemoller, A. Roscher, G. Schmitz, Quantitative measurement of different ceramide species from crude cellular extracts by electrospray ionization tandem mass spectrometry (ESI-MS/MS), J Lipid Res 40 (1999) 1539-1546.

[66] M. Scherer, G. Schmitz, G. Liebisch, High-throughput analysis of sphingosine 1-phosphate, sphinganine 1-phosphate, and lysophosphatidic acid in plasma samples by liquid chromatography-tandem mass spectrometry, Clin Chem 55 (2009) 1218-1222.

[67] J.C. Goldstein, N.J. Waterhouse, P. Juin, G.I. Evan, D.R. Green, The coordinate release of cytochrome c during apoptosis is rapid, complete and kinetically invariant, Nat Cell Biol 2 (2000) 156-162.

[68] M. Gschwendt, H.-J. Müller, K. Kielbassa, R. Zang, W. Kittstein, G. Rincke, F. Marks, Rottlerin, a novel protein kinase inhibitor, Biochem Biophys Res Com 199 (1994) 93-98.

[69] S. Albouz, F. Le Saux, D. Wenger, J.J. Hauw, N. Baumann, Modifications of sphingomyelin and phosphatidylcholine metabolism by tricyclic antidepressants and phenothiazines, Life Science 38 (1986) 357-363.

[70] A.H. Merrill, G. van Echten, E. Wang, K. Sandhoff, Fumonisin B1 inhibits sphingosine (sphinganine) N-acyltransferase and de novo sphingolipid biosynthesis in cultured neurons in situ, J Biol Chem 268 (1993) 27299-27306.

[71] A. Khwaja, L. Tatton, Caspase-mediated proteolysis and activation of protein kinase C delta plays a central role in neutrophil apoptosis, Blood 94 (1999) 291-301.

[72] M.G. Song, S.M. Gao, K.M. Du, M. Xu, Y. Yu, Y.H. Zhou, Q. Wang, Z. Chen, Y.S. Zhu, G.Q. Chen, Nanomolar concentration of NSC606985, a camptothecin analog, induces leukemic-cell apoptosis through protein kinase C delta-dependent mechanisms, Blood 105 (2005) 3714-3721.

[73] B.J. Pettus, C.E. Chalfant, Y.A. Hannun, Ceramide in apoptosis: an overview and current perspectives, Biochim Biophys Acta 1585 (2002) 114 -125.

[74] H.E. Thomas, R. Darwiche, J.A. Corbett, T.W. Kay, Evidence that beta cell death in the nonobese diabetic mouse is Fas independent, J Immunol 163 (1999) 1562-1569.

[75] M. Chatelut, M. Leruth, K. Harzer, A. Daga, S. Marchesini, S. Gatt, R. Salvayre, P. Courtoy, T. Levade, Natural ceramide is unable to escape the lysosome, in contrast to a fuorescent analogue, FEBS Lett 426 (1998) 102-106.

[76] L.J. Siskind, R.N. Kolesnick, M. Colombini, Ceramide channels increase the permeability of the mitochondrial outer membrane to small proteins, J Biol Chem 277 (2002) 26796-26803.

[77] B. Ogretmen, Y.A. Hannun, Biologically active sphingolipids in cancer pathogenesis and treatment, Nat Rev Cancer 4 (2004) 604-616.

[78] W. Stoffel, Functional analysis of acid and neutral sphingomyelinases in vitro and in vivo, Chem Physic Lipids 102 (1999) 107-121.

[79] X. He, N. Okino, R. Dhami, A. Dagan, S. Gatt, H. Schulze, K. Sandhoff, E.H. Schuchman, Purification and characterization of recombinant human acid ceramidase, J Biol Chem 278 (2003) 32978-32986.

[80] A.T. Sané, R. Bertrand, Caspase inhibition in camptothecin-treated U-937 cells is coupled with a shift from apoptosis to transient G1 arrest followed by necrotic cell death, Cancer Res 59 (1999) 3565-3569.

[81] W. Li, X. Yuan, S. Ivanov, K.J. Tracey, J.W. Eaton, U.T. Brunk, 3-Aminopropanal, formed during cerebral ischaemia, is a potent lysosomotropic neurotoxin, Biochem J 371 (2003) 429-436.

[82] M.S. Ostenfeld, N. Fehrenbacher, M. Høyer-Hansen, C. Thomsen, T. Farkas, M. Jaattela, Effective tumor cell death by σ-2 receptor ligand siramesine involves lysosomal leakage and oxidative stress, Cancer Res 65 (2005) 8975-8983.

[83] H. Erdal, M. Berndtsson, J. Castro, U. Brunk, M.C. Shoshan, S. Linder, Induction of lysosomal membrane permeabilization by compounds that activate p53-independent apoptosis, Proc Natl Acad Sci USA 102 (2005) 192-197.

[84] B.F. El-Rayes, R. Grignon, N. Aslam, O. Aranha, F.H. Sarkar, Ciprofloxacin inhibits cell growth and synergises the effect of etoposide in hormone resistant prostate cancer cells, Int J Oncol 21 (2002) 207-211.

[85] N. Fehrenbacher, M. Jaattela, Lysosomes as targets for cancer therapy, Cancer Res 65 (2005) 2993-2995.

FIGURE LEGENDS

Fig. 1. CPT-induced apoptosis in U-937 cells. *A)* ↓ΔΨm and *B)* LLM were monitored in U-937 cells after CPT (1 μM) treatment. Bars are means of 4 independent determinations and error bars are SEM. *C)* Control and CPT-treated U-937 cells were stained with a specific antibody against cathepsin D to monitor the de-localization of lysosomal cathepsin D, 3 h after CPT treatment (1 μM). *D)* Western blotting of caspase-3. The active cleaved 17 and 12 kDa fragments of procaspase-3 (32 kDa) are clearly visible 4 h after CPT treatment (1 μM). *E)* Electron microscopy representative of control and CPT-treated U-937 cells (4 h).

Fig. 2. PKC-δ is required for LLM in CPT-treated U-937 cells. *A)* Expression of PKC-δ (80 kDa) in highly-enriched lysosome extracts from control and CPT-treated U-937 cells (1 μM; 3 h). Whole cell extract from control (CNT) cells is shown as PKC-δ antibody control. LAMP-1 expression is the loading control. *B)* PKC-δ activity monitored in highly-enriched lysosome extracts from CNT and CPT-treated U-937 cells (1 μM; 3 h) in the absence and presence of the PKC-δ inhibitor ROTT (3.5 μM). Bars are means of 4 independent determinations and error bars are SEM. *C)* Knock-down expression of PKC-δ by siRNA experiment. CRK-L expression is the loading control. The average of PKC-δ silencing efficiency in 3 independent experiments was 47±16%, based on densitometry analysis (not shown). *D)* LLM was monitored after CPT treatment (1 μM) in U-937 cells where PKC-δ was silenced by siRNA or PKC-δ activity inhibited by ROTT (3.5 μM). Bars are means of

3 independent determinations and error bars are SEM. *E)* The percentage of DNA fragmentation was monitored after CPT treatment (1 μM) in the absence or presence of the PKC-δ inhibitor ROTT (3.5 μM). Data points are the means of 3 duplicated independent determinations and error bars are SEM.

Fig. 3. PKC-δ mediates ASM phosphorylation and activation at lysosomes after CPT treatment. *A)* ASM expression in highly-enriched lysosome extracts from control and CPT-treated U-937 cells (1 μM; 3 h). Whole-cell control extract (CNT) is shown as ASM antibody control. LAMP-1 expression is the loading control. *B)* Western blottings reveal the ASM phosphorylation level after CPT-treatment (1 μM; 3 h). IP was performed from highly-enriched lysosome preparations. *Upper panel:* IP was undertaken with anti-ASM and Western blotting with anti-Phospho(Ser)PKC-substrate antibodies. The doublet may represent some protein degradation. *Lower panel*: Reciprocal experiment where IP was performed with anti-Phospho(Ser)PKC-substrate antibodies and Western blotting with anti-ASM. *C)* ASM activity monitored in highly-enriched lysosome extracts from CNT and CPT-treated U-937 cells (1 μM; 3 h) in the absence and presence of the PKC-δ inhibitor, ROTT (3.5 μM), and the ASM inhibitor, DESP (10 μM). Bars are means of 3 independent determinations and error bars are SEM. *D)* LLM was monitored after CPT treament in U-937 cells where ASM activity was inhibited by DESP (10 μM), and CS activity was inhibited by FB1 (10 μM). Bars are means of 3 independent determinations and error bars are SEM.

Fig. 4. PKC-δ-mediated activation of ASM leads to CER generation and accumulation at lysosomes. ESI-MS/MS lipid profiling of highly-enriched lysosome extracts obtained from

U-937 treated with *A)* CPT (1 μM), *B)* CPT (1 μM) in the presence of PKC-δ inhibitor ROTT (3.5 μM), *C)* CPT (1 μM) in the presence of ASM inhibitor DESP (10 μM), and *D)* CPT (1 μM) in the presence of CS inhibitor FB1 (10 μM). Bars are the means of 4 independent determinations and error bars are SEM. The data are presented as relative to untreated control cells. Abbreviations mean: *, significant differences between treated cells in comparision to control cells; SM, sphingomyelin; dihSM, dihydro-sphingomyelin; PE, phosphatidylethanolamine; PC, phosphatidylcholine; PLASM, PE-based plasmalogen; PS, phosphatidylserine; PG phosphatidyldiglycerol; PI, phosphatidylinositol; LPC, lysophosphatidylcholine; CER, ceramide; HexCER hexosylceramide; LacCER, lactosyl-ceramide SPH, sphingosine; SPA, sphinganine; CE, cholesterol ester; FC, free cholesterol.

Fig. 5. Quantitative distribution of CER and SM species generated at lysosomes after CPT treatment. *A)* CER and *B)* SM species were analyzed by ESI-MS/MS. Data points are the means of 4 independent determinations and error bars are SEM. Abbreviations mean: *, significant differences between treated cells versus control cells or between data points as indicated.

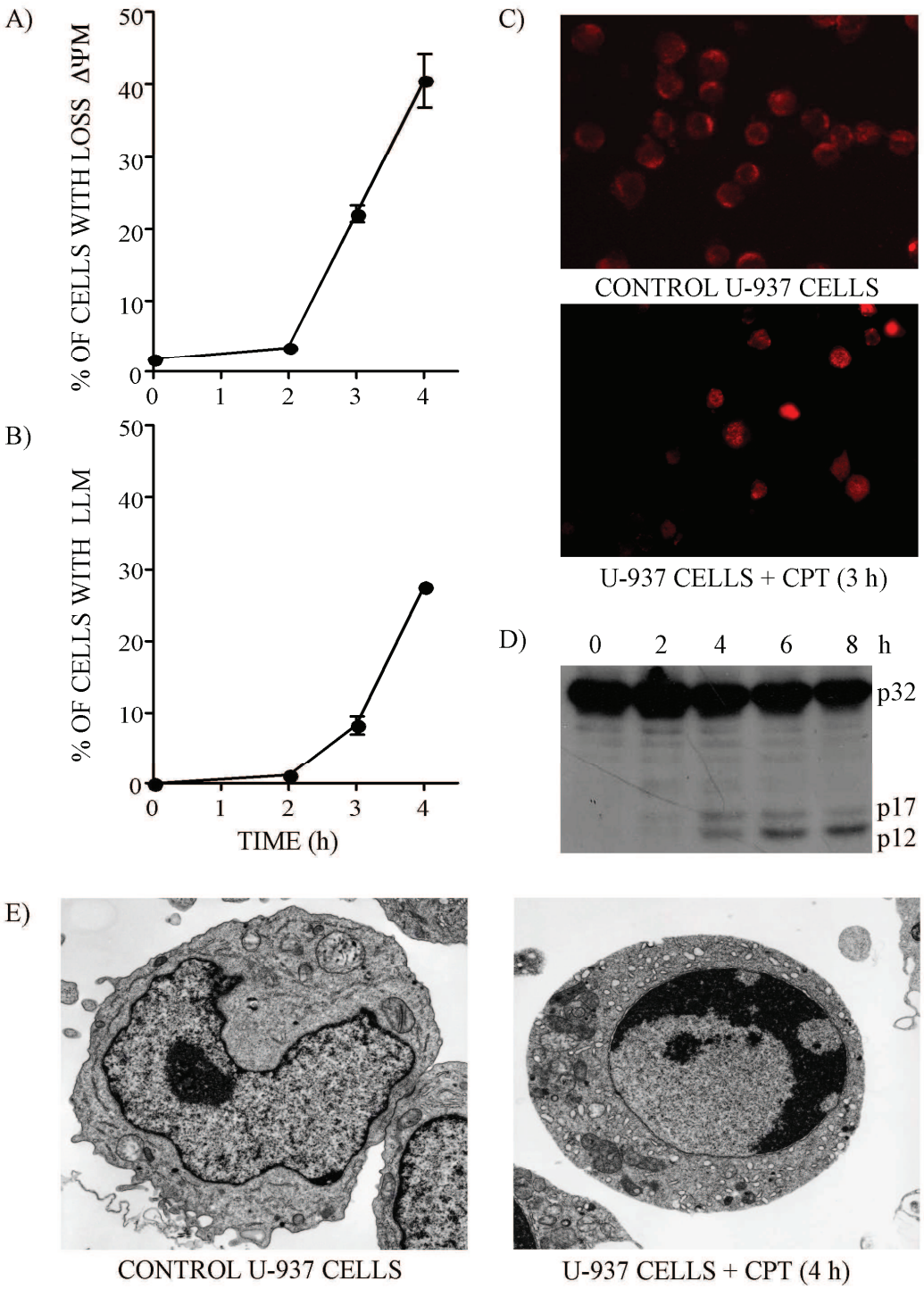
A)
% OF CELLS WITH LOSS ΔΨM
50
40
30
20
10
0
0 1 2 3 4
B)
% OF CELLS WITH LLM
50
40
30
20
10
0
0 1 2 3 4
TIME (h)
C)
CONTROL U-937 CELLS
U-937 CELLS + CPT (3 h)
D)
0 2 4 6 8 h
p32
p17
p12
E)
CONTROL U-937 CELLS
U-937 CELLS + CPT (4 h)

Figure 1

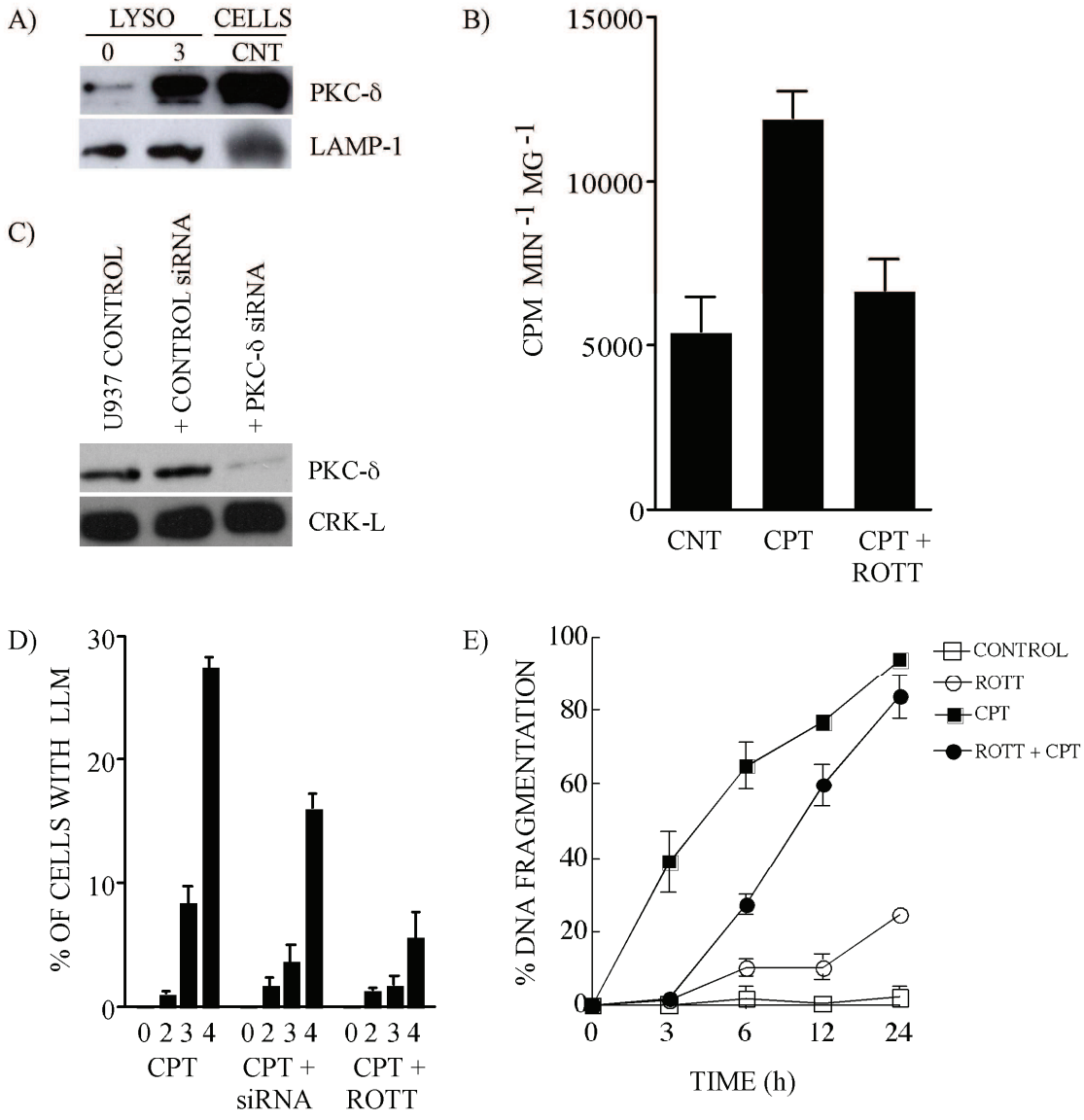
A)
LYSO
CELLS
0
3
CNT
PKC-δ
LAMP-1
B)
15000
10000
5000
0
CPM MIN -1 MG -1
CNT
CPT
CPT + ROTT
C)
U937 CONTROL
+ CONTROL siRNA
+ PKC-δ siRNA
PKC-δ
CRK-L
D)
30
20
10
0
% OF CELLS WITH LLM
0 2 3 4
CPT
CPT + siRNA
CPT + ROTT
E)
100
80
60
40
20
0
% DNA FRAGMENTATION
0
3
6
12
24
TIME (h)
CONTROL
ROTT
CPT
ROTT + CPT

Figure 2

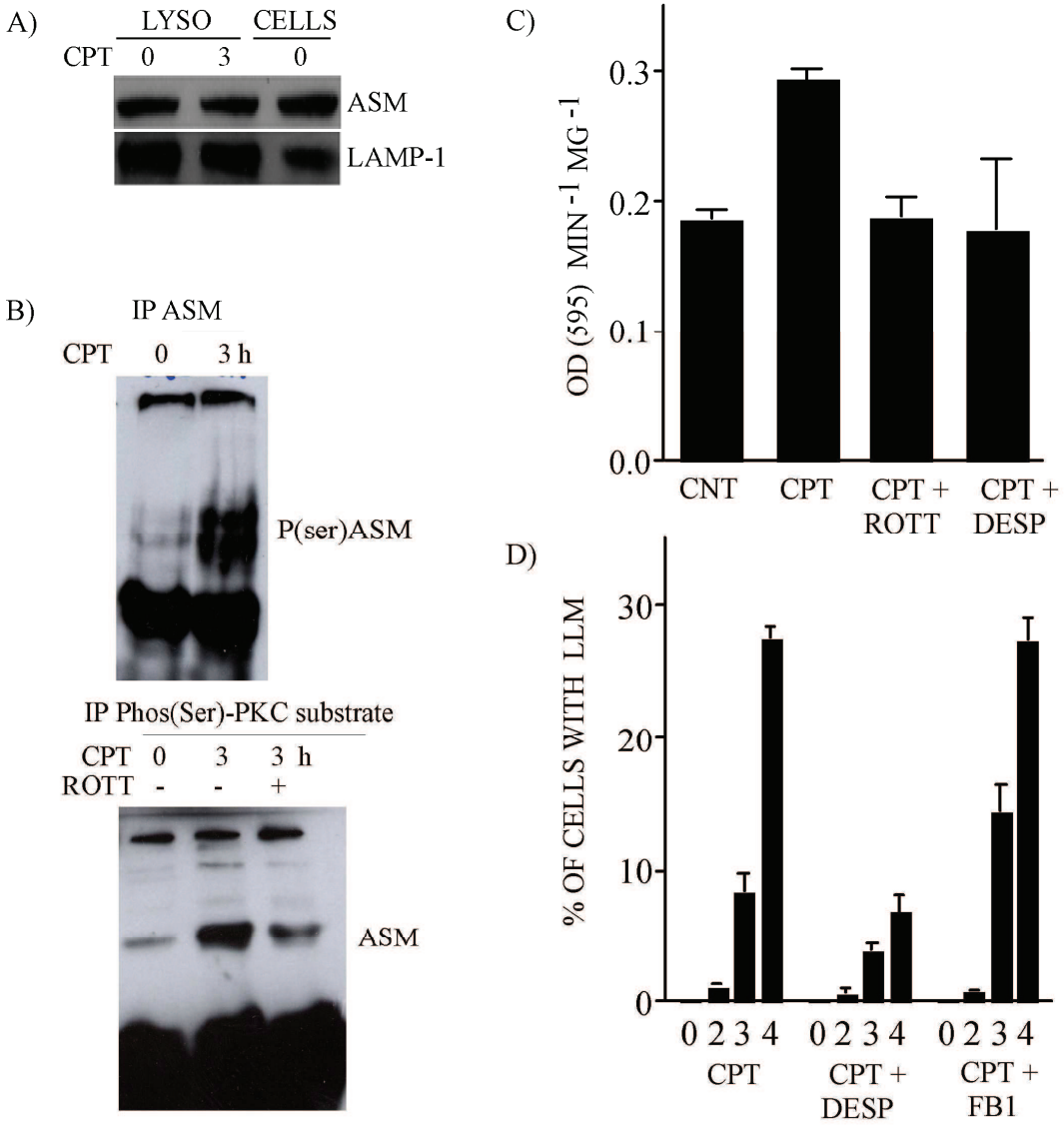
A)
LYSO
CELLS
CPT 0 3 0
ASM
LAMP-1
B)
IP ASM
CPT 0 3 h
P(ser)ASM
IP Phos(Ser)-PKC substrate
CPT 0 3 3 h
ROTT - - +
ASM
C)
OD (595) MIN -1 MG -1
0.3
0.2
0.1
0.0
CNT
CPT
CPT + ROTT
CPT + DESP
D)
% OF CELLS WITH LLM
30
20
10
0
0 2 3 4 0 2 3 4 0 2 3 4
CPT
CPT + DESP
CPT + FB1

Figure 3

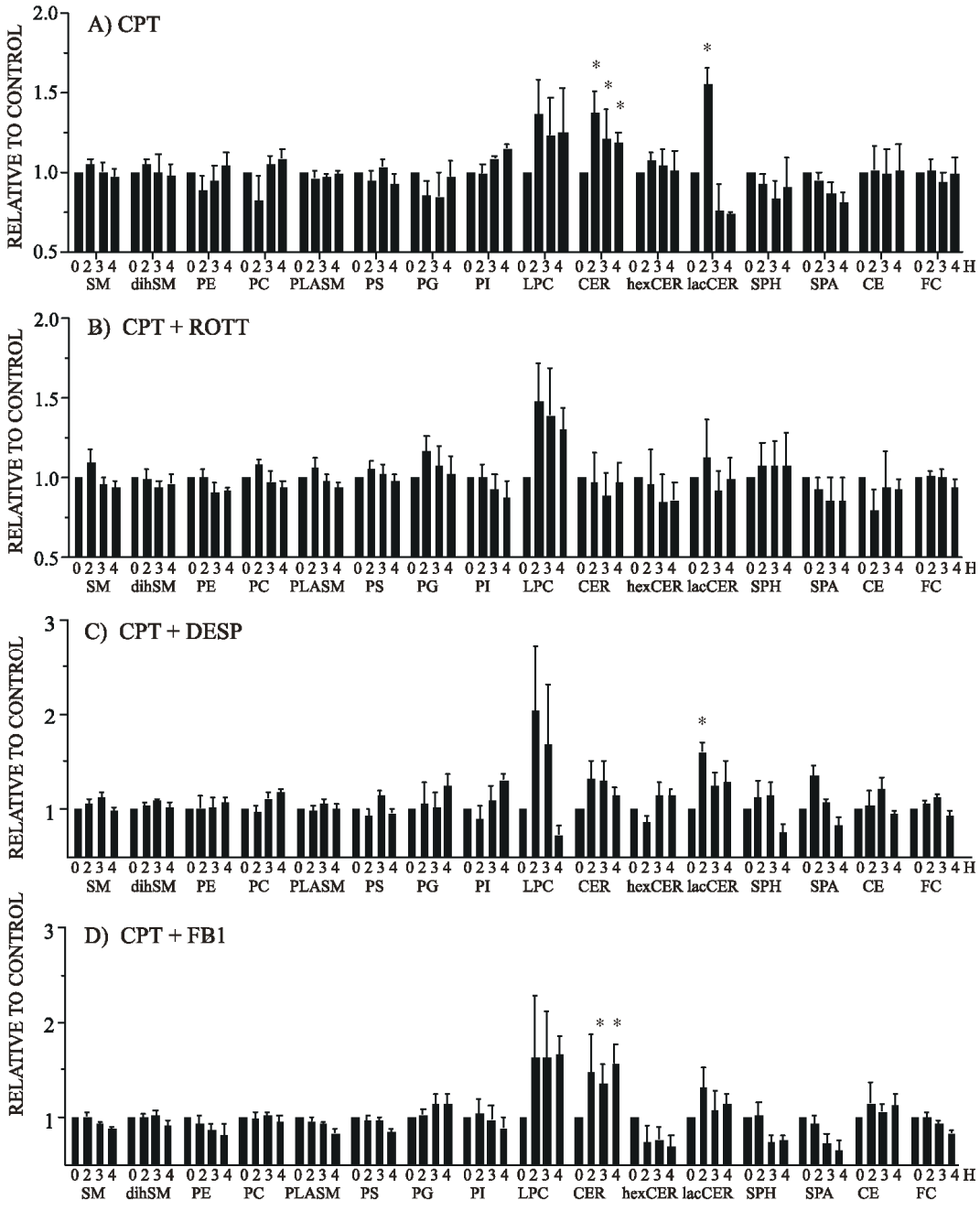
A) CPT
B) CPT + ROTT
C) CPT + DESP
D) CPT + FB1
RELATIVE TO CONTROL
2.0
1.5
1.0
0.5
3
2
1
0 2 3 4
SM
dihSM
PE
PC
PLASM
PS
PG
PI
LPC
CER
hexCER
lacCER
SPH
SPA
CE
FC
H

Figure 4

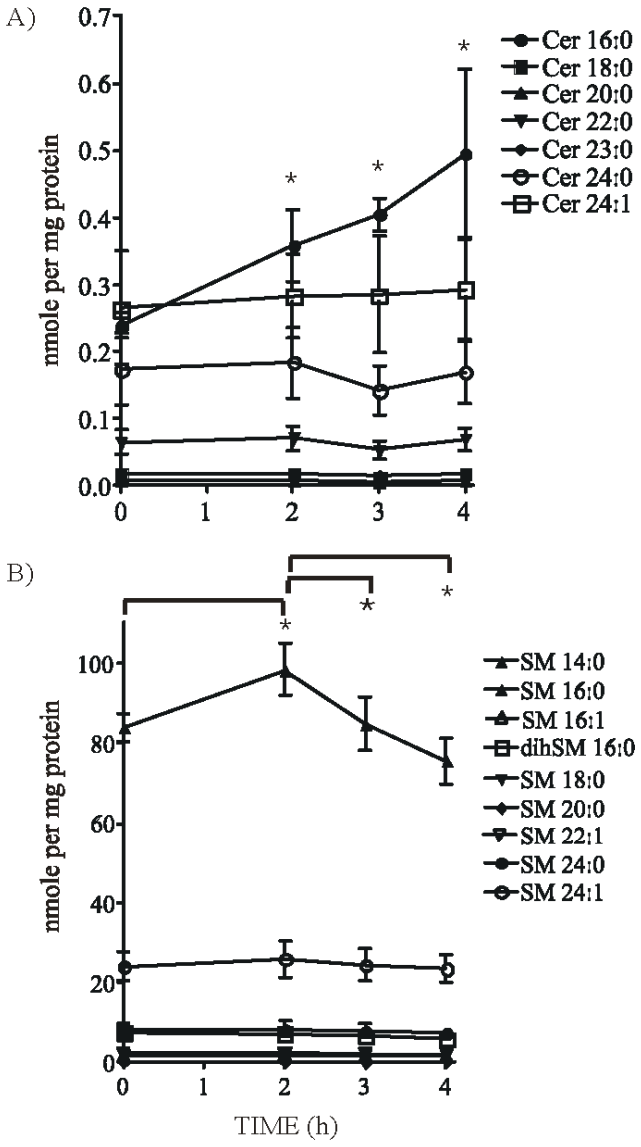
A)
nmole per mg protein
0.7
0.6
0.5
0.4
0.3
0.2
0.1
0.0
0
1
2
3
4
*
*
*
Cer 16:0
Cer 18:0
Cer 20:0
Cer 22:0
Cer 23:0
Cer 24:0
Cer 24:1
B)
nmole per mg protein
100
80
60
40
20
0
0
1
2
3
4
TIME (h)
*
*
*
SM 14:0
SM 16:0
SM 16:1
dihSM 16:0
SM 18:0
SM 20:0
SM 22:1
SM 24:0
SM 24:1

Figure 5

Synthèse des résultats de recherche

L'étude comparative des protéomes et des lipidomes de fractions enrichies en lysosomes démontre l'importance de la dynamique des lipides, en particulier des sphingolipides lors de la LML, un processus cellulaire participant à l'initiation de l'apoptose. Ainsi, trois protéines associées au métabolisme des lipides membranaires, la stérol-4-alpha-carboxylate 3-déhydrogénase (NSDHL), la prosaposin (PSAP) et la protéine kinase C delta (PKC-δ) sont quantitativement augmentées au niveau du compartiment lysosomale durant la phase précoce de l'induction de l'apoptose. Concomitamment, le contenu en lysophosphatidylcholines et en ceramides augmente à la membrane des lysosomes, suggérant un rôle direct des constituants de la membrane des lysosomes dans la LML. En effet, l'étude fonctionnelle de la PKC-δ dans le processus de la LML indique que l'accumulation du contenu en ceramides à la membrane lysosomale, gouvernée par l'activité combinée de la PKC-δ et de la sphingomyélinase acide, est indispensable pour l'induction de la LML durant l'apoptose suivant des dommages à l'ADN.

En somme, les travaux présentés dans cette thèse permettent de proposer un mécanisme, englobant la signalisation de protéines régulant le métabolisme des lipides et les modifications des sphingolipides à la membrane des lysosomes, responsable de la LML lors de l'initiation de l'apoptose induite par les dommages à l'ADN (Figure 6, page 145). Quoique plusieurs aspects de ce mécanisme restent à élucider, les résultats issus de ces travaux posent de nouvelles bases dans l'élaboration d'hypothèses quant à l'impact du métabolisme des sphingolipides lors de l'activation de la voie lysosomale dans l'apoptose induite par les dommages à l'ADN.

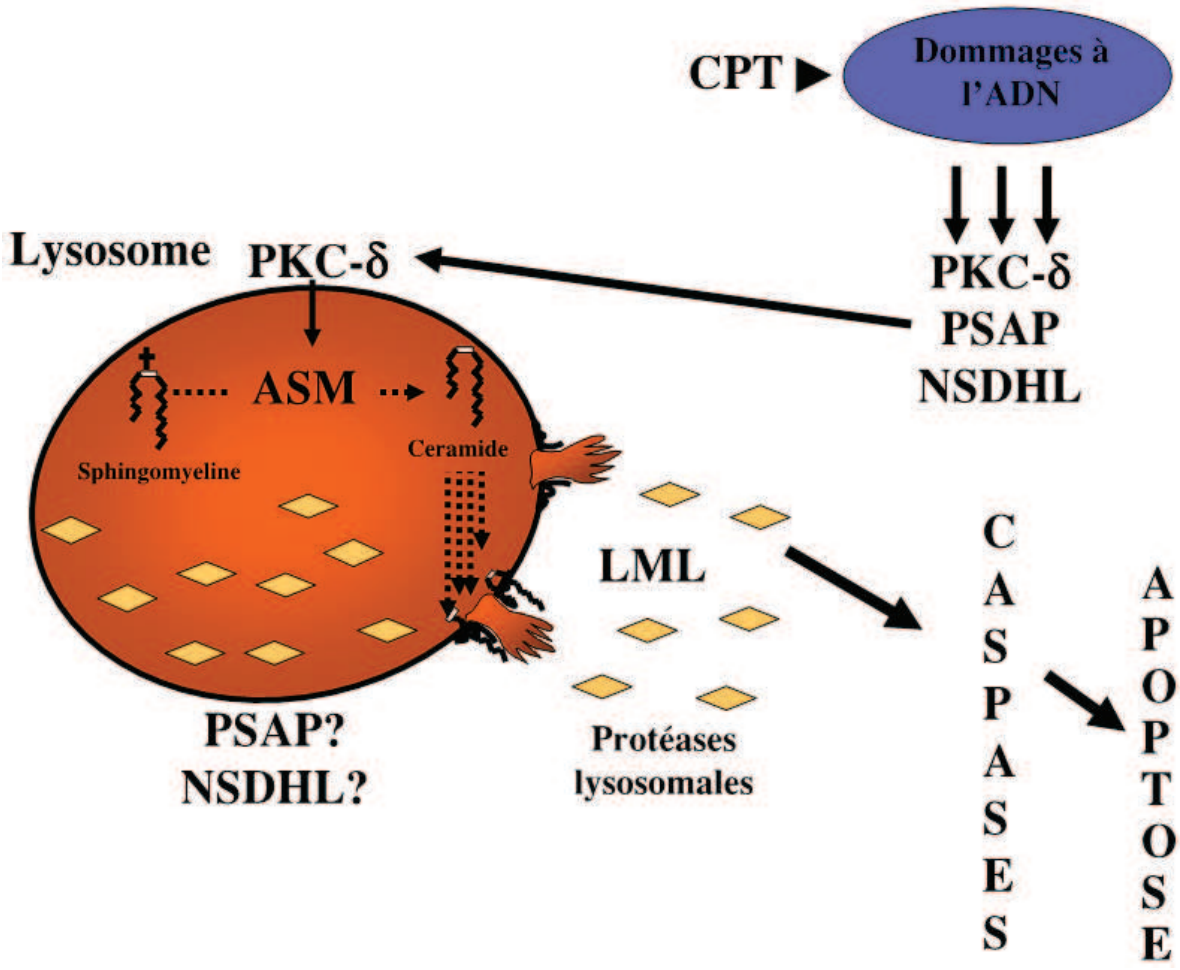

Figure 6 : Représentation schématisée des mécanismes responsables de l'activation de la voie lysosomale de l'apoptose dans les cellules U-937. Suivant les dommages à l'ADN induits par la camptothécine (CPT), les protéines stérol-4-alpha-carboxylate 3-déhydrogénase (NSDHL), la prosaposin (PSAP) et la protéine kinase C delta (PKC-δ) s'accumulent aux lysosomes. La PKC-δ phosphoryle et active directement la sphingomyélinase acide lysosomale (ASM) qui à son tour hydrolyse les sphingomyélines membranaires en céramide. L'augmentation du contenu membranaire en céramide est requise pour l'activation de la labilisation de la membrane lysosomale (LML) et l'activation de la voie lysosomale de l'apoptose.

Discussion

I- La spectrométrie de masse et les « omics »

L'avènement des techniques à haut débit alliées à des outils informatiques toujours plus puissants, a ouvert l'ère des « omics » : génome, transcriptome, interactome, protéome, lipidome, métabolome, dégradome, fluxome, etc. Que ce soit pour l'identification de substrats spécifiques, de médiateurs moléculaires précis ou pour dresser des réseaux de signalisation, les « omics » ont amené la production de données expérimentales à un niveau inégalé. Par exemple, le « phosphoprotéome » d'ATM et d'ATR, en réponse aux dommages à l'ADN, soit l'étude des substrats des protéines kinases ATM et ATR, a révélé la présence de plus de 900 sites de phosphorylation régulant plus de 700 protéines [242].

Dans un éditorial adressé aux lecteurs de la revue *Experimental Biology and Medicine*, Mark W. Ducan insistait sur l'importance d'un regard critique envers l'application des « omics » dans les domaines de la biologie et la médecine expérimentale. D'abord, bien qu'ils soient d'une puissance considérable, les « omics » ne sont et ne demeureront que de simples outils, et leur utilité ne reposera que sur les solutions qu'ils apportent à un problème. De plus, la quantité des données ne pourra jamais se substituer à la qualité de celles-ci. Enfin, la nécessité d'inclure les « omics » à des hypothèses falsifiables dans un contexte précis, puisque les « omics » à eux seuls ne constituent que des investigations observationnelles pouvant répondre à une multitude d'hypothèses parallèles mais distinctes [243]. Devant le potentiel incroyable promis par le développement de nouvelles, et toujours plus puissantes, techniques « omics », il est impératif de les utiliser en tenant compte de ces aspects.

Quantification en spectrométrie de masse

Le succès de l'étude comparative entre les protéomes d'échantillons différents repose sur la capacité à quantifier avec précision les milliers de peptides qui les composent. Traditionnellement, la quantification sur gels d'acrylamide, en une ou deux dimensions, s'effectue en mesurant le volume des points (bandes) où les protéines migrent. Toutefois, l'identification de chacun des points, pouvant contenir plusieurs protéines, et de l'ensemble des points représentant un protéome s'avère un travail considérable qui limite grandement le type d'analyse et la portée expérimentale de celle-ci. Des techniques de comparaison quantitative utilisant la spectrométrie de masse (MS) répondent à ces contraintes grâce à des procédures automatisées à haut débit d'analyse. Il existe différentes techniques reposant sur la MS qui permettent la quantification de protéines présentes dans un échantillon biologique et la comparaison entre plusieurs autres échantillons. Ces techniques requièrent un marquage préalable des échantillons avec une variété d'étiquettes de nature isotopiques, radioactives ou chimiques et présentent chacune leurs avantages et leurs inconvénients (revu dans [244]).

Le réactif iTRAQ a été développé récemment par Applied Biosystems. Il consiste en des étiquettes isobares non-radioactives qui forment des liens covalents spécifiquement avec les groupements ammonium des peptides issus de la digestion protéolytique des échantillons à investiguer [245]. Une étiquette est assignée à un échantillon puis une étiquette différente sera utilisée pour un autre échantillon à comparer (Figure 7, page 148). Le processus de quantification se déroule en deux étapes. En mode simple, soit le premier détecteur MS, les peptides à analyser sont sélectionnés selon leur masse sans discrimination quant à leur origine, les différentes versions de l'étiquette ayant une masse identique. En mode tandem, suivant la fragmentation, la masse des fragments peptidiques est mesurée afin d'identifier les peptides et chaque étiquette génèrera un groupement rapporteur distinctif. L'intensité relative de chacun des groupements rapporteurs dans le spectre MS/MS fournit une lecture directe de la contribution relative de chacun des échantillons dans le mélange analysé. Le principal avantage de l'utilisation des réactifs iTRAQ est la

possibilité d'analyser simultanément jusqu'à huit échantillons (pour un exemple, voir [246]).

La reproductibilité des analyses iTRAQ

Dans l'étude présentée dans cette thèse, les fractions enrichies de lysosomes de cellules U-937 normales et apoptotiques ont non seulement permit de relever plusieurs

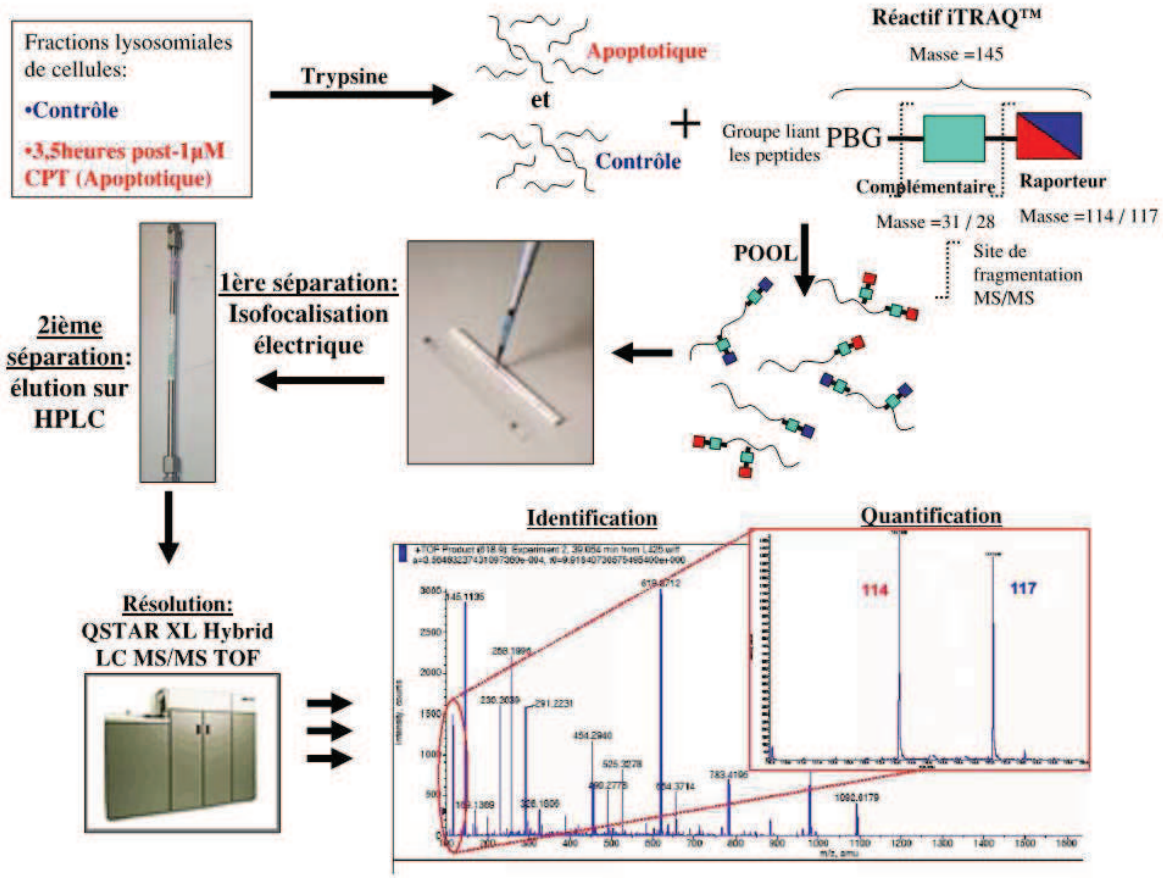

Figure 7 : Schématisation de l'approche en MS utilisant le réactif iTRAQ pour l'analyse protéomique quantitative.

différences dans la composition des protéomes respectifs, mais aussi dans l'efficacité de l'analyse iTRAQ. Dans la première expérience réalisée, les 1197 peptides analysés identifiaient 306 protéines différentes alors que la deuxième expérience, indépendamment

réalisée, a conduit à l'analyse de 5031 peptides identifiant 591 protéines différentes (résultats non-présentés). Bien que plusieurs des protéines identifiées dans l'une ou l'autre des expériences soient communes, la différence de reproductibilité entre les deux expériences est près de ±60%. Les causes de la variabilité observée pourraient découler de la nature hétérogène des échantillons, soit la variation biologique, de la reproductibilité des échantillons, soit la variation expérimentale, et des étapes de séparation des échantillons préalables à l'analyse, soit la variation technique. En effet, un des inconvénients principal de l'approche iTRAQ, comparativement aux autres approches quantitatives (ICAT, SILAC et marquage métabolique), est l'intervention de l'expérimentateur durant la préparation des échantillons en vue de l'analyse [247]. Une étude s'est attardée sur la responsabilité des trois types de variations sur les résultats lors de la répétition d'expériences avec l'approche iTRAQ et a permit d'établir que la variation technique comptait en moyenne pour ±11%, alors que la variation biologique et expérimentale pouvaient atteindre, en moyenne, près de ±25% et ±23% respectivement [248]. Considérant la complexité de la technique d'enrichissement des lysosomes, de même que la marginalisation du phénomène de la LML dans les cellules au moment de l'analyse, la variation biologique et la variation expérimentale sont sûrement les causes principales de la différence de reproductibilité observée dans l'analyse d'une expérience à l'autre. Il n'en demeure pas moins que la répétition de l'expérience a révélée la présence d'un grand nombre de protéines absentes dans l'une ou l'autre des expériences. Certaines d'entre-elles, dont la PKC-δ, étant d'ailleurs fonctionnellement pertinentes au processus de la LML. Ainsi, la répétition d'expériences indépendantes avec l'approche iTRAQ procure des avantages certains (pour un autre exemple, voir [249]).

Résolution des spectromètres de masse

Une limite inhérente des instruments de MS, des détecteurs TOF (*time-of-flight*) en particulier, est la résolution ions/temps lors de l'acquisition [247]. À chaque instant où les détecteurs enregistrent un signal, seul un certain nombre de peptides, généralement les plus abondants, sont sélectionnés pour les étapes ultérieures de fragmentation et de mesure de leur masse. C'est alors que la séparation préalable des peptides, habituellement effectuée en

appliquant différentes techniques de chromatographie, s'avère cruciale; une séparation plus étendue et une distribution plus étalée procurera une meilleure résolution de détection. Cette limite pourrait expliquer en partie la divergence entre les protéines identifiées dans l'une ou l'autre des expériences, mais aussi motiver l'absence de détection des protéines décrites comme des inducteurs de la voie lysosomale de l'apoptose dans la littérature. Ainsi, aucuns des peptides des protéines Bax, LAPF et des phospholipases C et A_2 n'ont été détectés dans le protéome des fractions enrichies en lysosomes. Cela dit, la présence de ces protéines n'a pas non plus été remarquée dans les autres études du protéome de la membrane des lysosomes [250, 251] ou du protéome des lysosomes sécrétoires [252]. La MS étant une technique extrêmement sensible, plus de mille fois supérieure aux techniques classiques (immuno-buvardage, ELISA, etc.), la résolution pourrait être mise en cause.

Une approche alternative en MS consiste à rechercher des profils d'ionisations moléculaires précis dans un mélange complexe. C'est d'ailleurs de cette manière que le lipidome des membranes lysosomales présenté dans cette thèse a pu être dressé. L'identification de protéines, ou de lipides, suivant la mesure expérimentale de leurs unités fragmentées s'appuie sur la recherche de profils de fragmentation spécifiques, aussi nommés empreintes de fragmentation, générés par des simulations théoriques de fragmentation *in silico* (revue dans [253]). À partir des masses théoriques des fragments de molécules d'intérêt, il est ainsi possible d'évaluer la présence ou non de cette molécule dans un échantillon complexe en commandant à l'appareil de ne détecter que les fragments des molécules recherchées. Une telle approche aurait pu être utilisée lors de l'étude comparative des protéomes de fractions enrichies en lysosomes afin de corroborer ou non, le rôle des protéines décrites dans d'autres modèles comme des inducteurs de la voie lysosomale de l'apoptose.

La fragmentation du réticulum endoplasmique durant l'apoptose chimio-induite.

La nature même des échantillons analysés est une source de confusion lors de l'analyse des résultats de l'étude protéomique. Le processus apoptotique va engendrer diverses modifications cellulaires qui vont éventuellement affecter le suivi d'organelles spécifiques tel qu'il est proposé dans l'étude présentée dans cette thèse. Ainsi, plusieurs protéines identifiées dans les fractions enrichies en lysosomes sont issues du réticulum endoplasmique (ER), suggérant que l'induction de l'apoptose à l'aide de la CPT s'accompagne aussi d'une perte de densité de cette organelle[1]. En effet, la déstabilisation du ER lors d'un stress tel que l'apoptose provoque la fragmentation du ER en structures de plus faible volume [255, 256]. En suivant la protéine Calnexin, une protéine résidente du ER, par immunofluorescence et microscopie confocale, une distribution diffuse de cette dernière apparaît 3 heures après le traitement des cellules U-937 à la CPT, indiquant que le ER subit des réarrangements morphologiques très tôt lors de la réponse apoptotique (Figure 8a, page 152). Parmi les protéines identifiées par l'analyse iTRAQ, on retrouve la protéines ERp19, une protéine décrite au ER [257]. La présence de ERp19 augmente dans les fractions enrichies en lysosomes suivant l'induction de l'apoptose par la CPT (Figure 8b, page 152). Cependant, les expériences de localisation démontrent que ERp19 co-localise avec la Calnexin suite à l'exposition des cellules à la CPT validant, tel qu'attendu, que ERp19 se retrouve au ER (Figure 8c, page 152). La présence de ERp19 aux lysosomes est minime puisqu'elle ne co-localise que très faiblement avec la protéine lysosomale LAMP-1 (Figure 8d, page 152). En somme, l'identification par l'approche iTRAQ et MS de protéines associées à d'autres compartiments que les lysosomes doit être considérée avec prudence. Dans le modèle expérimental utilisé dans cette étude, des protéines extra-lysosomales telles que ERp19 augmentent dans les fractions enrichies en lysosomes issues de cellules U-937 en cours d'apoptose. La présence de ces protéines, notamment des protéines associées au ER, dans les échantillons serait vraisemblablement due à une diminution de densité du ER, causée par des altérations morphologiques associées à

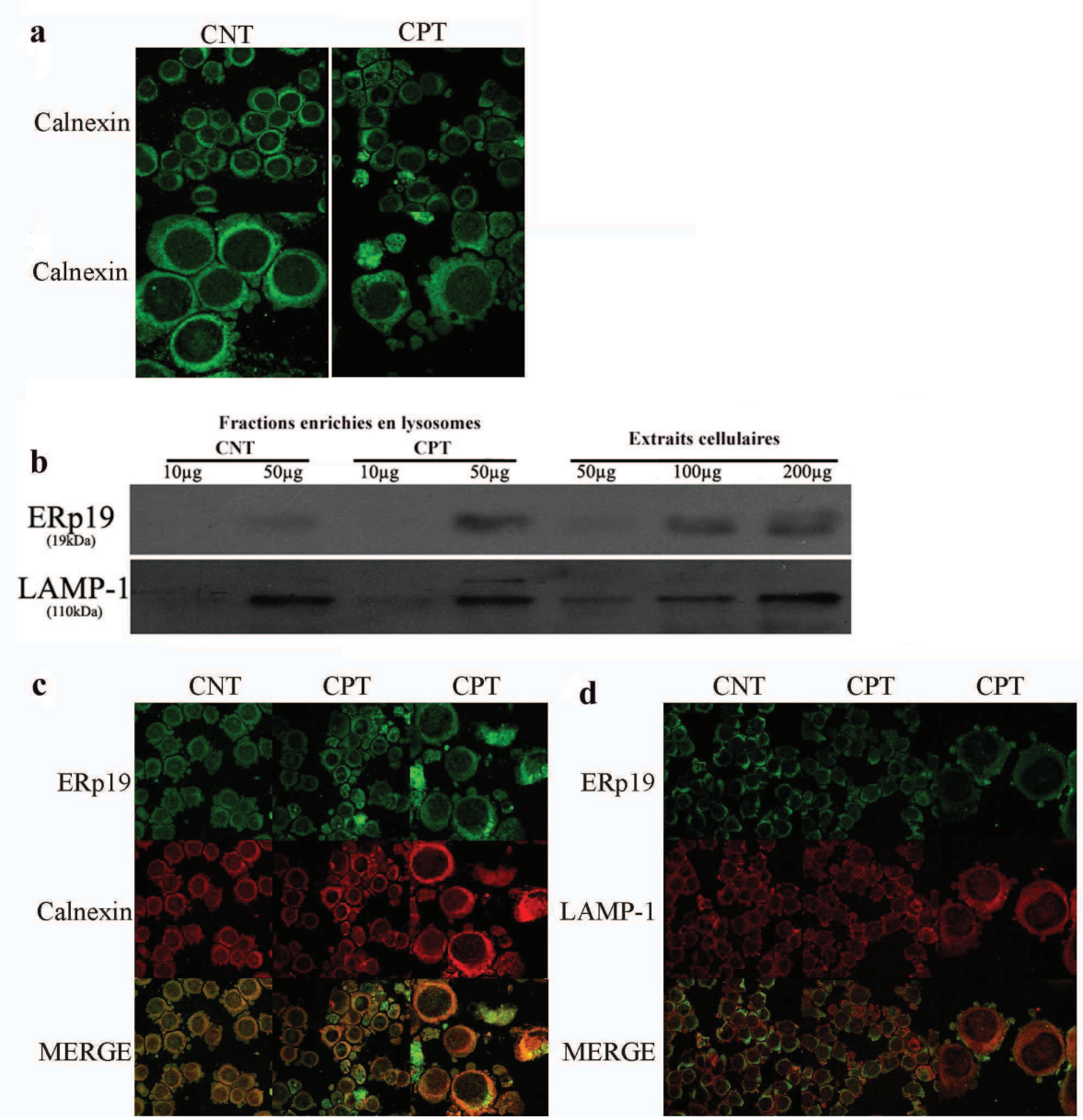

Figure 8: Localisation de la protéine ERp19 dans les cellules U-937[2]. La validation de localisation est effectuée à l'aide de biomarqueurs pour le lysosome, la protéine LAMP-1 et pour le ER, la protéine Calnexin. **a)** La morphologie du ER est modifiée après 3 heures suivant l'exposition à la CPT (CPT) comparativement à celle des cellules contrôles (CNT). **b)** La protéine ERp19 augmente dans les fractions enrichies en lysosomes issues de cellules U-937 traitées à la CPT (3 heures)[3]. **c)** Les protéines ERp19 et Calnexin co-localisent

---

[1] La densité du ER est normalement de 1,20 g/cm^3 alors que la densité du lysosome est de 1,12 g/cm^3) [254. Howell, K.E., E. Devaney, and J. Gruenberg, *Subcellular fractionation of tissue culture cells.* Trends Biochem Sci., 1989. **14**: p. 44-48.

[2] Images générées en microscopie confocale à fluorescence tel que décrit dans la section *Materials et Methods* de l'article *Proteomic analysis of enriched lysosomes at early phase of camptothecin-induced apoptosis in human U-937 cells* page 54.

[3] Idem, page 53.

fortement ensemble avec des valeurs de RCA[4] de 28,7 % ± 0,5 (n=3) et 33,0 % ± 1,4 (n=3) dans les contrôles et les cellules traitées à la CPT respectivement. **d)** Au contraire, la co-localisation des protéines ERp19 et LAMP-1 est plus faible avec des valeurs de RCA de 8,1 % ± 0,9 (n=3) et de 9,2 % ± 3,4 (n=3) dans les contrôles et les cellules traitées à la CPT respectivement. Les données présentées sont exprimées en valeur *Relative Colocalization Area* (*RCA*), et représente la moyenne de ± écart-type de (n) expériences indépendantes.

l'apoptose induite par la CPT. Ainsi, le ER, en situation de stress, se fragmente en vésicules plus petites [255, 256]. Ces vésicules de ER auraient pu être co-purifiées avec les lysosomes des cellules traitées à la CPT lors des préparations des échantillons. La validation des données obtenues par des analyses MS comparables est indispensable afin d'éviter toute confusion dans l'interprétation de ces résultats.

La mort cellulaire autophagique durant l'apoptose chimio-induite.

De par sa nature paradoxale, alliant la survie et la mort cellulaire, et combinée à sa capacité à éliminer des substrats aux potentiels letaux pour la cellule, on comprend bien l'importance de l'autophagie dans un contexte cellulaire toxique tel que celui créé par l'utilisation d'agents chimiothérapeutiques. Ainsi, l'autophagie contribue à la survie cellulaire dans les cellules humaines HeLa exposées à une diversité d'agents chimiothérapeutiques en éliminant les mitochondries endommagées au point d'induire la mort cellulaire [20]. Il semblerait qu'en plus d'éliminer un puissant inducteur de mort, en l'occurrence les mitochondries perméabilisées, l'autophagie pourrait contribuer à rétablir des niveaux d'énergie suffisants pour la mise en action des mécanismes de réparation nécessaires à la survie cellulaire [20]. Il est à noter toutefois que les mécanismes de protection contre la mort cellulaire conférés par l'autophagie nécessitent une période prolongée pour qu'ils opèrent, ce qui exclurait vraisemblablement une protection contre la réponse apoptotique rapide telle que celle induite par la CPT sur les cellules U-937.

---

[4] Images générées en microscopie confocale à fluorescence tel que décrit dans la section *Materials et Methods* de l'article *Proteomic analysis of enriched lysosomes at early phase of camptothecin-induced apoptosis in human U-937 cells* page 54

De plus, l'apoptose consituerait pour plusieurs auteurs la forme de mort cellulaire privilégiée par la cellule endommagée, et ce au détriment de la mort autophagique [63, 69-71]. La mort cellulaire autophagique est d'ailleurs rarement observée physiologiquement et les maladies associées à la dérégulation des mécanismes de l'autophagie sont presque exclusivement attribuables à un sous-fonctionnement plutôt qu'à un sur-fonctionnement de l'autophagie (revu dans [60]).

Enfin, le processus d'autophagie repose sur des bases moléculaires qui, à l'instar de l'apoptose, sont conservés au cours de l'évolution animale. Parmi elles, l'apparition de protéines spécifiques, telles que ULK1/2, Atg5, Beclin-1, LC3, Atg12, Atg13, Atg14, Atg16L1, FIP200 et Atg101 permet d'établir la présence d'autophagie active dans une population cellule (revu dans [258]). Or, aucune de ces protéines spécifiques à l'activation de l'autophagie n'ont été détectées dans l'analyse protéomique (résultats non-publiés). De même, la conjugaison de la protéine LC3-I en LC3-II, un essai classique de détermination de la progression de l'autophagie [259], ne montre pas d'activation de ce processus dans le modèle expérimental présenté dans cette thèse (résultats préliminaires non montrés).

Les protéines LAMP-1 et LAMP-2, des constituants majeurs de la membrane des lysosomes, partagent divers rôles notamment dans la maturation des autophagolysosomes [260]. Les protéines LAMP-1 et LAMP-2 aurait aussi la propriété de moduler la sensibilité de la membrane lysosomale lors d'insultes apoptotiques [261]. Bien qu'elles peuvent représenter jusqu'à près de 50 % de la quantité de protéines membranaires lysosomales dans certains types cellulaires [262], seule la protéine LAMP-1 a été identifiée lors des analyses protéomiques (résultats non-publiés). Il apparaît cependant que la présence de celle-ci n'est pas modulée par l'activation de l'apoptose par la CPT dans les cellules humaines U-937, du moins durant la période où les analyses ont été effectuées, justifiant du coup le choix de la protéine LAMP-1 comme protéine de référence pour les expériences subséquentes.

II- LE RÔLE DES SPHINGOLIPIDES DANS LA LML

Régulation du tropisme de la PKC-δ par les sphingolipides

L'étude comparative des protéomes des fractions enrichies en lysosomes de cellules U-937 en cours d'apoptose a permis d'identifier pour la première fois la PKC-δ comme un régulateur important dans le processus de la LML. La PKC-δ exerce ses fonctions à divers sites cellulaires incluant la membrane plasmique, l'appareil de Golgi, le réticulum endoplasmique, la mitochondrie, l'enveloppe nucléaire et les lysosomes [263-267]. La régulation de la translocation de la PKC-δ s'effectue suivant la phosphorylation des différents résidus sérine et thréonine retrouvés sur le domaine régulateur de la protéine. Les mécanismes exacts associés au tropisme de la PKC-δ suivant son activation demeurent toutefois inconnus.

Les modifications spécifiques des lipides membranaires, de même que la formation de micro-domaines riches en céramides pourraient être impliquées. Dans les cellules COS7 et CHOK1, il a été décrit que les PKC se liaient aux céramides, contrôlant ainsi leurs localisations intracellulaires [189]. Les céramides favoriseraient la translocation des PKC vers les organelles cytoplasmiques, alors que les esters de phorbol, utilisés pour stimuler l'activité des PKC, conduiraient à une redistribution à la membrane plasmique [268]. Enfin, des expériences de liaison entre le domaine C1B de la PKC-δ et les esters de phorbol indiquent que l'affinité entre eux est jusqu'à 80 fois plus forte lorsque l'ester de phorbol est inséré dans une phosphatidylsérine, comparativement à un ester de phorbol libre [269]. Ces observations démontrent la propension de la PKC-δ pour les membranes lipidiques.

Dans l'étude présentée dans cette thèse, l'accumulation des céramides à la membrane des lysosomes suivant l'apoptose induite par les dommages à l'ADN dans les cellules U-937 dépend de l'activité de la PKC-δ (Figure 4b du deuxième article, page 142). Dans ce cas, les céramides pourraient, tout au plus aider à soutenir la présence de la PKC-δ

aux lysosomes, mais cela n'expliquerait cependant pas la translocation initiale de celle-ci. Il devrait donc y avoir l'intervention d'une ou de plusieurs autres molécules, indépendantes de la régulation de la PKC-δ, qui permettrait le recrutement de la PKC-δ aux lysosomes suivant l'induction de l'apoptose.

Le lactosylcéramide

Le lipidome réalisé sur des fractions enrichies en lysosomes de cellules U-937 a permis de révéler que le comportement d'autres lipides que les céramides était aussi modifié durant l'induction de l'apoptose par la CPT, notamment le lactosylcéramide (LacCer). Le lactosylcéramide, aussi nommé cérébroside, est composé d'une base céramide à laquelle se lie le disaccharide lactose au niveau de la tête polaire. La synthèse du LacCer requiert l'action de la LacCer synthétase, qui permet le transfert d'une molécule de galactose sur un glucosylcéramide, lui-même issu de la glycosylation d'un céramide. Alternativement, le LacCer sera produite par l'action des sialidases, qui vont cataboliser le ganglioside G_{M3}.

Principalement situés sur le feuillet lipidique externe, les glycosphingolipides interagissent intimement avec le cholestérol pour former des micro-domaines lipidiques [270]. Le LacCer, en particulier, est décrit comme un constituant de micro-domaines lipidiques riche en céramides [271]. Jouant des fonctions cellulaires variées dont l'inflammation, la production d'espèces superoxides, la prolifération cellulaire, la migration et la phagocytose (revu dans [272] et [273]), le LacCer participe aussi au processus apoptotique *in vitro* [274, 275] et *in vivo* [276]. Dans des cellules d'ostéosarcomes humains traitées au TNF-α, il a été montré que l'induction de l'apoptose dépendait de l'accumulation de LacCer issus de l'hydrolyse des sphingomyélines et de l'action de la LacCer synthétase [274]. De même, l'apoptose induite par l'ajout de céramides dans ce modèle est bloquée par l'inhibition de la LacCer synthétase [274]. Il n'y a que très peu d'informations sur les cibles moléculaires des LacCer. La génération des LacCer est associée à la production de ROS lors de l'induction de l'apoptose [274]. Enfin, bien qu'il ait été observé dans des contextes physiologiques autres que l'apoptose, le LacCer

participe au recrutement et à l'activation de certaines isoformes de la PKC et de la phospholipase A_2 [277, 278].

L'augmentation des LacCer à la membrane des lysosomes est brève et se limite aux deux premières heures suivant l'induction de l'apoptose. Bien que l'accumulation soit, à l'instar des céramides, dépendante de l'activité de la PKC-δ, elle n'est au contraire que très faiblement influencée par l'inhibition de l'ASM (Figure 4b et 4c du deuxième article, page 142). L'utilisation de la fumonisine B_1, un inhibiteur de la céramide synthétase qui convertit les sphingosines en céramides, empêche l'accumulation de LacCer (Figure 4d du deuxième article, page 142). Ce résultat plutôt inattendu suggère que l'accumulation de LacCer observée dans les fractions enrichies en lysosomes dépendrait de la voie de synthèse *de novo* des céramides. Il est cependant utile de rappeler que la fumonisine B_1 n'a pas d'effet sur la LML (Figure 3d du deuxième article, page 142). La contribution des LacCer et de la voie de synthèse *de novo* des céramides, au processus de la LML durant l'apoptose chimio-induite, reste donc à élucider.

La lysophosphatidylcholine

Un autre sphingolipide mesuré dans les fractions enrichies en lysosomes de cellules U-937, la lysophosphatidylcholine (LPC) présente une accumulation relativement élevée, bien que statistiquement non significative, dès la première heure suivant l'induction de l'apoptose par des dommages à l'ADN. La LPC est formée de l'hydrolyse de la phosphatidylcholine par l'enzyme phospholipase A_2 et requiert la phosphocholine comme précurseur (revu dans [279]). La phosphocholine est un produit, avec les céramides, de l'hydrolyse de la sphingomyéline par la sphingomyélinase (Figure 1, page 26). Il est peu probable qu'il s'agisse de la source de phosphocholines responsable de l'accumulation observée à la membrane de fractions enrichies en lysosomes de cellules en cours d'apoptose puisque l'inhibition de l'hydrolyse des sphingomyélines, suivant l'inhibition de la PKC-δ ou de la ASM, n'affecte pas la génération de LPC (Figure 4b et 4c du deuxième article, page 142).

La LPC est surabondante dans plusieurs maladies associées à l'inflammation et le cancer (revu dans [280]). Au niveau moléculaire, il a été démontré que la LPC participait à différentes voies signalétiques par l'entremise de récepteurs couplés aux protéines G liant spécifiquement la LPC (revu dans [281]). Dans l'une de ces voies de signalisation, il est décrit que la LPC, ajoutée aux cellules, régulait l'activation des PKC : à faible dose la LPC active les PKC alors qu'à des doses 1,5 fois plus élevées, la LPC inhibe l'activité des PKC [282]. Il est difficile d'évaluer si la concentration de LPC mesurée dans les fractions enrichies en lysosomes correspond à l'une de ces valeurs de LPC ajoutée de façon exogène. Il est néanmoins invraisemblable que les LPC inhibent l'activité de la PKC-δ dans les fractions enrichies en lysosomes puisque l'accumulation de LPC corrèle avec l'augmentation de l'activité kinase de la PKC-δ dans un contexte apoptotique.

Ainsi, il a été montré que, dans les cellules U-937, l'ajout exogène de LPC avait pour conséquences, entre autres, de bloquer la synthèse de sphingomyéline à partir de céramides et de permettre l'accumulation soutenue de céramides [283], comme celle observée dans les fractions enrichies en lysosomes de cellules U-937 exposées à la CPT. De plus, les céramides, en particulier les C_{16}-céramides, conduisent à l'activation de la phospholipase A_2, possiblement en permettant à l'enzyme de s'insérer aux membranes rendues plus fluides [284].

Ces observations, si elles s'avéreraient intervenir également au niveau du compartiment lysosomal durant l'induction de l'apoptose, pourraient constituer une sorte de mécanisme en boucle permettant l'accumulation localisée de céramides à la membrane. En somme, contribuer à la formation des micro-domaines riches en céramides. D'ailleurs, des expériences réalisées sur des membranes artificielles indiquent que les C_{16}-céramides forment des micro-domaines à des concentrations plus faibles qu'il n'en est requis pour d'autres espèces de céramides [285]. Bien qu'il existe une variété importante de céramides, les C_{16}-céramides sont spécifiquement associés à l'apoptose. L'accumulation de l'espèce C_{16}-céramide est observée dans de nombreux modèles cellulaires apoptotiques différents [156, 157, 179, 286-290], incluant le nôtre.

Conclusion

En somme, les résultats présentés dans cette thèse mettent en évidence une régulation du métabolisme et du trafic des lipides très complexe durant le processus de la LML associée à l'induction de l'apoptose chimio-induite dans laquelle la PKC-δ participe de manière significative. D'une part, l'activité de la PKC-δ est indispensable aux modifications de la composition des fractions enrichies en lysosomes en céramides, en LacCer et en LPC suivant l'induction de l'apoptose par la CPT. D'une autre part, l'importance pour l'activation de la LML de l'accumulation de ces lipides n'est pas limpide. L'inhibition de l'hydrolyse des sphingomyélines, et conséquemment de la génération des céramides, supprime la LML, alors qu'elle n'affecte pas la génération des LacCer et des LPC. Ces dernières pourraient toutefois contribuer autrement, soit en favorisant la translocation et l'activation de la PKC-δ, soit en stabilisant les micro-domaines riches en céramide. Il est alors possible d'envisager le processus de la LML comme un ensemble de transformations de la composition lipidique et protéique de la membrane lysosomale, culminant avec la formation de micro-domaines riches en céramides.

Perspectives

Les études présentées dans cette thèse rendent possible l'élaboration de nouvelles hypothèses de travail qui pourront, à terme, approfondir la compréhension des mécanismes associés à l'induction de la LML durant la phase d'initiation de l'apoptose. De plus, il sera intéressant d'évaluer, sur la base de ces nouvelles connaissances, le potentiel thérapeutique que représente le processus de la LML dans le traitement du cancer. Voici quelques unes des stratégies envisagées afin de répondre à ces hypothèses.

Étude du rôle des changements lipidiques sur la labilisation de la membrane lysosomale

Des modifications de la composition de trois sphingolipides de la membrane des lysosomes ont été mises en évidence dans la description du lipidome présenté dans cette thèse : les céramides, les LPC et les LacCer. Il serait intéressant d'étudier avec plus de détails l'impact de ces modifications sur le processus de la LML.

1- Les C_{16}-céramides forment des micro-domaines enrichis en céramides et en PKC-δ à la membrane des lysosomes suivant l'induction de l'apoptose.

Les céramides, les C_{16}-céramides particulièrement, issus de l'hydrolyse des sphingomyélines sont indispensables à la LML lors de la phase de l'induction de l'apoptose des cellules U-937 induite par la CPT. L'accumulation locale de céramides à la membrane entraîne la formation de micro-domaines qui permettent le recrutement de protéines et leur assemblage en complexes impliqués dans la signalisation d'une diversité de processus cellulaires dont l'apoptose (revu dans [201]).

L'utilisation d'analogues de lipides marqués avec le fluorophore Bodipy et ses dérivés (*Invitrogen Corporation*) permet de suivre la formation des micro-domaines lipidiques aux membranes cellulaires. À des concentrations relativement faibles, le lipide-

Bodipy émet une couleur verte. Lorsque la concentration du lipide-Bodipy augmente, la lumière verte s'éteint partiellement et un second pic de fluorescence est observé dans la couleur rouge. La concentration du lipide marqué avec la Bodipy peut enfin être estimée en mesurant l'intensité des émissions vertes et rouges et en les comparant avec une courbe de calibration établie sur des liposomes artificiels (revu dans [291]). Ainsi, l'incubation préalable de sphingomyéline-Bodipy aux cellules U-937 permettrait de suivre la concentration membranaire en céramides issus de l'hydrolyse des sphingomyélines lors de l'induction de l'apoptose par la CPT. L'utilisation de biomarqueurs spécifiques pour les différents organelles de la cellule serait utile pour préciser le(s) lieu(x) où se forment d'éventuels micro-domaines enrichis en céramides.

Plusieurs techniques d'isolation de micro-domaines à partir de cellules en culture ont été publiées [292-295]. Ces techniques ont permis de mettre en évidence des protéines, des lipides et des sucres composants les micro-domaines dans une diversité de contextes cellulaires différents. Des micro-domaines pourront être isolés à partir de fractions enrichies en lysosomes issus de cellules apoptotiques et comparées à des fractions produites à partir de cellules non-traitées. Grâce à l'analyse de leur composition à l'aide d'approches en MS, immuno-buvardage et microscopie confocale, les présences de PKC-δ et des céramides seront évaluées.

2- L'accumulation des LPC et des LacCer à la membrane lysosomale contribue positivement au processus de la LML lors de l'induction de l'apoptose.

L'accumulation des LPC et des LacCer à la membrane des lysosomes accompagne le processus de la LML lors de l'induction de l'apoptose des cellules U-937. Il est décrit que ces deux sphingolipides participent à la signalisation d'une diversité de processus cellulaires (revu dans [272, 281]).

Les LacCer sont principalement issus de la glycosylation des céramides sous l'action de la LacCer synthétase. Alternativement, les LacCer peuvent provenir de la dégradation du ganglioside G_{M3}. Il existe des inhibiteurs pharmacologiques spécifiques à

ces enzymes : le D-Thréo-1-phényl-2-décanoylamino-3-morpholino-1-propanol-HCl (PDMP) inhibe la LacCer synthétase [296] alors que l'acide 2-déoxy-2,3-déhydro-N-acétylneuraminique (NeuAc2en) inhibe les sialidases [297] (Figure 9, page 161). L'utilisation seule ou combinée de ces inhibiteurs permettrait non seulement d'identifier la voie de synthèse responsable de

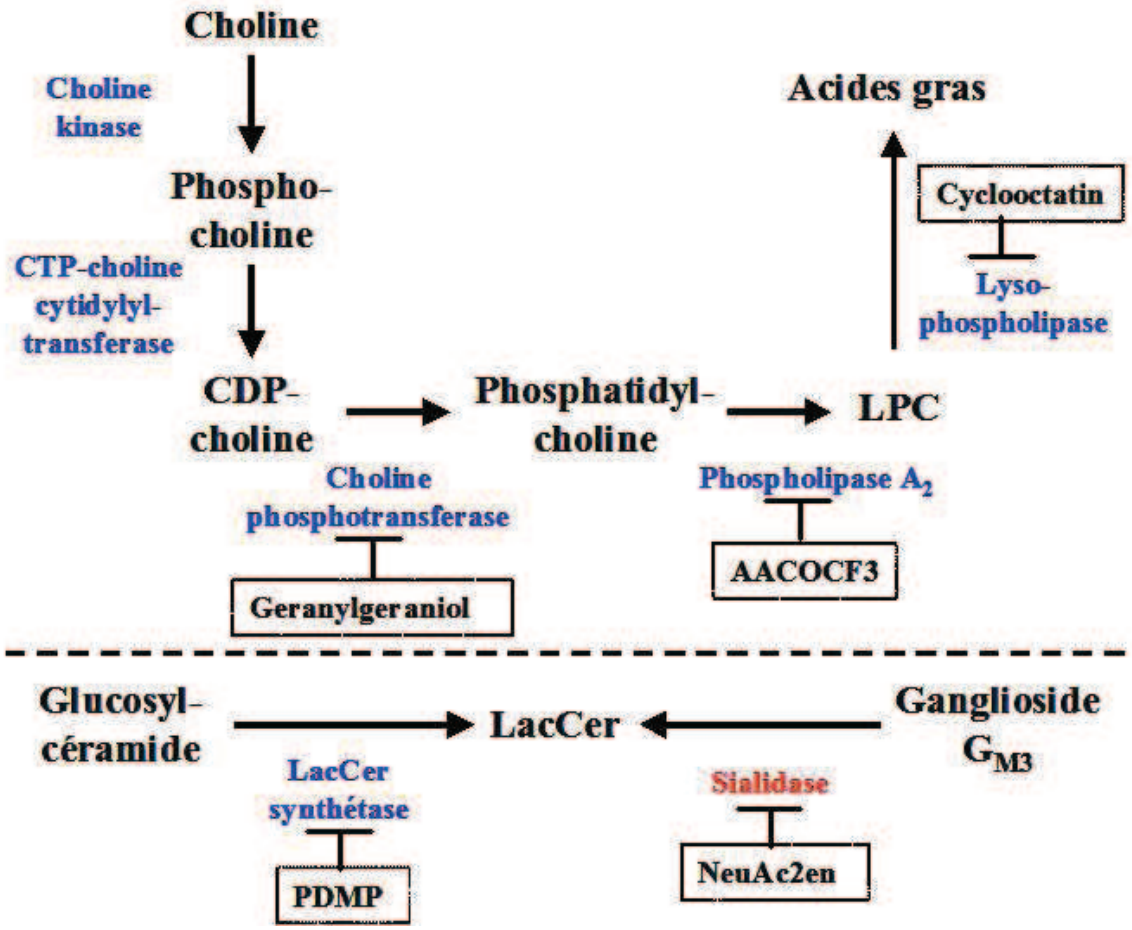

Figure 9 : Voies de biosynthèse de la LPC et du LacCer. Plusieurs inhibiteurs pharmacologiques spécifiques aux enzymes impliquées la génération des LPC (haut) et des LacCer (bas) sont indiqués.

l'accumulation de LacCer observée à la membrane lysosomale durant l'induction de l'apoptose, mais aussi d'apprécier l'importance de LacCer au processus de la LML.

Par ailleurs, il apparaît que l'accumulation de LacCer soit dépendante de l'action de la PKC-δ telle que montrée par l'utilisation du rottlerin. L'immunoprécipitation des

substrats phosphorylés spécifiquement par la PKC-δ a précédemment permit d'identifier l'ASM comme un substrat direct. Dans l'éventualité d'un effet sur la LML de l'utilisation des inhibiteurs des enzymes requises à la génération de LacCer, une telle approche permettrait d'évaluer le rôle joué par la PKC-δ sur la régulation de ces enzymes.

Quant à elles, les LPC sont issues exclusivement de la voie de biosynthèse des phosphatidylcholines (Figure 9, page 161). Cette voie peut être étudiée en détails du fait qu'il existe plusieurs inhibiteurs pharmacologiques spécifiques disponibles commercialement. Le geranylgeraniol permet d'inhiber la choline phosphotransferase [298] alors que l'arachidonyl trifluoromethyl ketone (AACOCF3) bloque l'action de la phospholipase A_2 [299]. L'utilisation de ces composés empêcherait la biosynthèse de LPC. À l'inverse, le cyclooctatin [300], un inhibiteur spécifique de la lysophospholipase, favoriserait l'accumulation de LPC.

Étude des autres candidats identifiés dans l'analyse quantitative du protéome des fractions enrichies en lysosomes de cellules en cours d'apoptose

Sur plus de 508 protéines identifiées dans le protéome des fractions enrichies en lysosomes, 27 d'entre-elles ont une expression altérée durant la phase précoce de l'induction de l'apoptose par la CPT. Seule la PKC-δ a fait l'objet d'une analyse fonctionnelle, qui s'est avérée fructueuse. Il serait intéressant d'étudier avec plus de détails le rôle des autres protéines et leurs impacts sur le processus de la LML.

1- Des protéines impliquées dans la régulation de la fluidité des membranes contribuent au processus de la LML lors de l'induction de l'apoptose.

Les deux autres protéines qui ont été validées, la PSAP et la NSDHL, quant à leur expression et leur localisation, participent toutes à la régulation de la composition lipidique des membranes cellulaires. D'une part, la PSAP est un précurseur qui donnera, suivant une dégradation protéolytique différentielle, les quatre isoformes de saposin (*sphingolipid-*

activator proteins). Les saposins (saposin A à D) sont des cofacteurs essentiels pour la dégradation de certains lipides, dont les sphingolipides, aux lysosomes (revu dans[301]). D'autre part, la NSDHL est une enzyme régulant la biosynthèse du cholestérol dans les membranes [302]. En modifiant la composition de la membrane, ces protéines peuvent contribuer à la régulation de la fluidité des membranes où elles sont présentes.

Bien qu'il n'existe pas d'inhibiteurs pharmacologiques spécifiques connus pour la PSAP et la NSDHL, il est possible d'interférer indirectement l'action de ces protéines. Le tricyclodecan-9-yl xanthate potassium (D609) empêche le transport de la PSAP aux lysosomes [303] alors que le 3-beta-(2-(diethylamino)ethoxy)androst-5-en-17-one (U18666A) bloque la sortie du cholestérol hors des lysosomes [304, 305]. Ces molécules seraient utilisées dans des expériences complémentaires à celles destinées à inhiber l'expression de la PSAP ou de la NSDHL à l'aide d'ARN interférents spécifiques.

2- Des protéines n'ayant pas de fonctions lysosomales connues contribuent au processus de la LML lors de l'induction de l'apoptose.

Afin d'exploiter pleinement les résultats de l'étude protéomique réalisée sur les fractions enrichies en lysosomes en cours d'apoptose, il serait judicieux d'évaluer la contribution au processus de la LML des autres protéines révélées dans cette étude (Table 1 du premier article, page 75). Plusieurs d'entre-elles sont associées à la régulation du stress oxydatif, telles que la Peroxiredoxin-1 [306]. Le stress oxydatif est un inducteur de la LML et est impliqué dans la peroxydation des lipides membranaires [131, 307-312]. D'autres protéines ont des propriétés oncogéniques et pro-apoptotiques décrites, soit la sthamine, la CDC42 (*cell division cycle protein 42*) et MIF (*macrophage migration inhibitory factor*) [313-319].

Des expériences de localisation par microscopie confocale et d'expression par immunobuvardage seraient effectuées afin de confirmer l'analyse iTRAQ en MS. Il est clair que certaines protéines retrouvées dans les fractions enrichies en lysosomes sont issues d'autres organelles, notamment du ER, altérées durant l'induction de l'apoptose. La

validation de la localisation est d'autant plus importante qu'il existe des protéines dont la localisation peut apparaître surprenante telle que l'histone H2B. Ainsi, il est décrit que certaines histones, incluant l'histone H1.2, migre rapidement à la mitochondrie suivant les dommages à l'ADN où elle contribue à l'activation de la voie mitochondriale de l'apoptose [320]. En somme, aucune des protéines identifiées par l'étude protéomique de fractions enrichies en lysosomes issues de cellules U-937 en apoptose induite par la CPT, un agent causant des dommages à l'ADN, ne peut être mises de côté sur la seule base de leurs fonctions et leurs origines. Enfin, des approches préconisant l'inhibition de l'expression des différentes protéines seraient utilisées pour valider fonctionnellement la contribution de celles-ci au processus de la LML.

Évaluation du potentiel thérapeutique du compartiment lysosomal

La découverte de nouveaux sites d'initiation et d'intégration du signal apoptotique a permis le développement de nouvelles stratégies pour lutter plus efficacement contre le cancer (revu dans [321, 322]) Plus spécifiquement, les lysosomes sont actuellement au centre de plusieurs approches expérimentales (revu dans [323]).

1- Des agents déstabilisants les lysosomes potentialisent les effets pro-apoptotiques des agents chimiothérapeutiques sur des cellules cancéreuses.

Plusieurs molécules sont reconnues pour induire la LML et l'activation de la voie lysosomale de l'apoptose (Tableau 2, page 22). Parmi celles-ci, les quinolones, telles que le ciprofloxacin, sont des antibiotiques aux propriétés lysosomotropes qui ont déjà prouvés leur efficacité à augmenter la sensibilité de certaines cellules cancéreuses aux effets des rayons ultra-violets [238] et à l'étoposide, un agent chimiothérapeutique causant des dommages à l'ADN [239]. La CPT et son analogue soluble à l'eau, le topotecan, induisent l'apoptose dans une variété de cellules cancéreuses humaines. Utilisée en combinaison avec des doses inoffensives de ciprofloxacin, la CPT augmente la mort cellulaire de cellules HeLa (Figure 10, page 165).

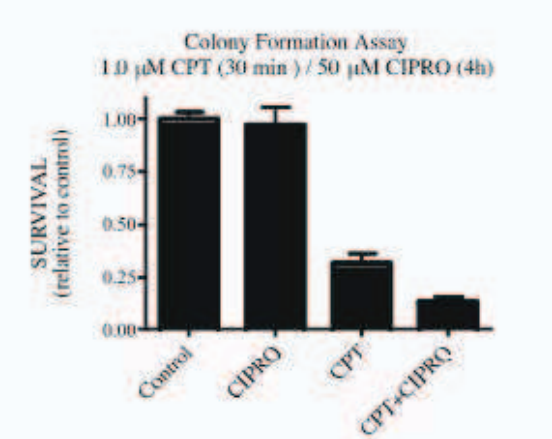

Figure 10 : Effet synergique d'un traitement combiné de ciprofloxacin et de CPT sur les cellules HeLa. Des cellules HeLa sont préalablement exposées à 50 µM de ciprofloxacin (CIPRO) pendant 4 heures directement dans le milieu de culture avant d'être traitées à la CPT pour 30 minutes. Les cellules sont ensuite diluées et cultivées dans un milieu complet pour une semaine avant d'être colorées au cristal violet (0,005% p/v), puis les colonies formées de cellules ayant proliférées ont été comptées. Résultats non-publiés de Jianfang Wang, Myriam Beauchemin et Richard Bertrand.

Il serait intéressant de poursuivre cette étude en élargissant l'éventail de cellules cancéreuses humaines traitées avec une combinaison de ciprofloxacin et de CPT/topotecan, incluant des cellules de cancer du sein (MCF-7 et MDA-MB-231), de l'ovaire (OVCAR-3 et A-2780), de la prostate (PC3 et LnCap), des poumons (A549 et Calu-1) et du côlon (HT-29 et Colo-320) déjà disponibles dans le laboratoire ou localement. Des essais de formation de colonies, ou essais clonogéniques, seraient réalisés en utilisant de faibles doses de ciprofloxacin et de CPT/topotecan seul ou en combinaison. Parallèlement, des paramètres apoptotiques tels que la LML, la perméablisation de la mitochondrie, la fragmentation de l'ADN, l'activation des caspase-3 et des cathepsine B seraient mesurés afin d'évaluer la contribution des lysosomes à l'apoptose, ou la mort cellulaire, observée. Enfin, cette étude permettrait d'identifier de nouveaux modèles cellulaires afin d'étendre l'application des connaissances sur les mécanismes de la LML. En somme, cette étude fournirait les informations nécessaires pour des expériences *in vivo* sur des modèles animaux sur le potentiel thérapeutique du compartiment lysosomal dans le traitement du cancer.

Bibliographie

1. Lockshin, R.A. and Z. Zakeri, *Apoptosis, autophagy, and more.* IJBCB, 2004. **36**: p. 2405-2419.
2. Joaquin, A.M. and S. Gollapudi, *Functional decline in aging and disease: a role for apoptosis.* J Am Geriatr Soc, 2001. **49**(9): p. 1234-1240.
3. Rudin, C.M. and C.B. Thompson, *Apoptosis and disease. Regulation and clinical relevance of programmed cell death.* Ann Rev Med, 1997. **48**: p. 267-281.
4. Thompson, C.B., *Apoptosis in the pathogenesis and treatment of disease.* Science, 1995. **267**(5203): p. 1456-1462.
5. Shen, Y. and T.E. Shenk, *Viruses and apoptosis.* Curr Op Genet Dev, 1995. **5**(1): p. 105-111.
6. Bedi, A., et al., *Inhibition of apoptosis during development of colorectal cancer.* Cancer Res, 1995. **55**(9): p. 1811-1816.
7. Kaufmann, S.H. and G.J. Gores, *Apoptosis in cancer: cause and cure.* Bioessays, 2000. **22**(11): p. 1007-1017.
8. Martin, S.J. and D.R. Green, *Apoptosis as a goal of cancer therapy.* Curr Op Oncology, 1994. **6**(6): p. 616-621.
9. Townson, J.L., G.N. Naumov, and A.F. Chambers, *The role of apoptosis in tumor progression and metastasis.* Curr Mol Med, 2003. **3**(7): p. 631-642.
10. Evan, G.I. and K.H. Vousden, *Proliferation, cell cycle and apoptosis in cancer.* Nature, 2001. **411**(6835): p. 342-348.
11. Johnstone, R.W., A.A. Ruefli, and S.W. Lowe, *Apoptosis. A link between cancer genetics and chemotherapy.* Cell, 2002. **108**(2): p. 153-164.
12. Kroemer, G., et al., *Classification of cell death: recommendations of the Nomenclature Committee on Cell Death 2009.* Cell Death Diff., 2008: p. 1-9.
13. Launay, S., et al., *Vital functions for lethal caspases.* Oncogene, 2005. **24**(5137-5148).
14. Lamkanfi, M., et al., *Alice in caspase land. A phylogenetic analysis of caspases from worm to man. .* Cell Death Differ., 2002. **9**: p. 358-361.
15. Boatright, K.M. and G.S. Salvesen, *Mechanisms of caspase activation.* Curr Opin Cell Biol, 2003. **15**: p. 725-731.
16. Nicholson, D.W., *Caspase structure, proteolytic substrates, and function during apoptotic cell death.* Cell Death Differ, 1999. **6**(11): p. 1028-1042.
17. Fischer, U., R.U. Janicke, and K. Schulze-Osthoff, *Many cuts to ruin: a comprehensive update of caspase substrates.* Cell Death Diff., 2003. **10**: p. 76-100.
18. Slee, E.A., C. Adrain, and S.J. Martin, *Serial killers: ordering caspase activation events in apoptosis.* Cell Death Differ, 1999. **6**(11): p. 1067-1074.
19. Khwaja, A. and L. Tatton, *Resistance to the cytotoxic effects of Tumor Necrosis Factor α can be overcome by inhibition of a FADD/Caspase-dependent signaling pathway.* J. Biol. Chem., 1999. **51**: p. 36817-36823.
20. Colell, A., et al., *GAPDH and autophagy preserve survival after apoptotic cytochrome c release in the absence of caspase activation.* Cell, 2007. **129**(983-997).

21. Tait, S.W.G. and D.R. Green, *Caspase-independent cell death: leaving the set without the final cut.* Oncogene, 2008. **27**: p. 6452-6461.
22. Lavrik, I., A. Golksand, and P.H. Krammer, *Death receptor signaling.* J Cell Sci, 2005. **118**: p. 265-267.
23. Scaffidi, C., et al., *Two Cd95 (Apo-1/Fas) signaling pathways.* EMBO J, 1998. **17**(6): p. 1675-1687.
24. Kroemer, G., L. Galluzzi, and C. Brenner, *Mitochondrial membrane permabilzation in cell death.* Physiol Rev, 2007. **87**: p. 99-163.
25. Cory, S. and J.M. Adams, *The bcl2 family: regulators of the cellular life-or-death switch.* Nat Rev Cancer, 2002. **2**(9): p. 647-656.
26. Paquet, C. and R. Bertrand, *Unique and multi-domain Bcl-2 family members: Post-translation modification and apoptosis regulation*, in *Recent Development in Biophysics and Biochemistry*. 2003, Research Signpost Publisher: Trivandrum. p. 291-325.
27. Kluck, R.M., et al., *Cytochrome C activation of Cpp32-like proteolysis plays a critical role in a Xenopus cell-free apoptosis system.* EMBO J, 1997. **16**(15): p. 4639-4649.
28. Yang, J., et al., *Prevention of apoptosis by Bcl-2: release of cytochrome C from mitochondria blocked.* Science, 1997. **275**(5303): p. 1129-1132.
29. Du, C., et al., *Smac, a mitochondrial protein that promotes cytochrome c-dependent caspase activation by eliminating IAP inhibition.* Cell, 2000. **102**(1): p. 33-42.
30. Verhagen, A.M., et al., *Identification of DIABLO, a mammalian protein that promotes apoptosis by binding to and antagonizing IAP proteins.* Cell, 2000. **102**(1): p. 43-53.
31. Suzuki, Y., et al., *A serine protease, Htra2, is released from the mitochondria and interacts with Xiap, inducing cell death.* Mol Cell, 2001. **8**(3): p. 613-621.
32. Hegde, R., et al., *Identification of Omi/HtrA2 as a mitochondrial apoptotic serine protease that disrupts inhibitor of apoptosis protein-caspase interaction.* J Biol Chem, 2002. **277**(1): p. 432-8.
33. Yang, Q.H., et al., *Omi/HtrA2 catalytic cleavage of inhibitor of apoptosis (IAP) irreversibly inactivates IAPs and facilitates caspase activity in apoptosis.* Genes Dev, 2003. **17**(12): p. 1487-1496.
34. Susin, S.A., et al., *Molecular characterization of mitochondrial apoptosis-inducing factor.* Nature, 1999. **397**(6718): p. 441-446.
35. Li, L.Y., X. Luo, and X. Wang, *Endonuclease G is an apoptotic DNase when released from mitochondria.* Nature, 2001. **412**(6842): p. 95-99.
36. Krajewski, S., et al., *Release of caspase-9 from mitochondria during neuronal apoptosis and cerebral ischemia.* Proc Natl Acad Sci (USA), 1999. **96**(10): p. 5752-5757.
37. Mancini, M., et al., *The caspase-3 precursor has a cytosolic and mitochondrial distribution: implications for apoptotic signaling.* J Cell Biol, 1998. **140**(6): p. 1485-1495.
38. Qin, Z.H., et al., *Pro-caspase-8 is predominantly localized in mitochondria and released into cytoplasm upon apoptotic stimulation.* J Biol Chem, 2001. **276**(11): p. 8079-8086.
39. Susin, S.A., et al., *Mitochondrial release of caspase-2 and -9 during the apoptotic process.* J Exp Med, 1999. **189**(2): p. 381-393.

40. Jiang, X. and X. Wang, *Cytochrome c-mediated apoptosis.* Annu Rev Biochem, 2004. **73**: p. 87-106.
41. Yin, Q., et al., *Caspase-9 holoenzyme is a specific and optimal procaspase-3 processing machine.* Mol Cell Biochem, 2006. **22**: p. 259-268.
42. McDonnell, M.A., et al., *Caspase-9 is activated in a cytochrome c-independent manner early during TNFalpha-induced apoptosis in murine cells.* Cell Death Differ, 2003. **10**(9): p. 1005-1015.
43. Forcet, C., et al., *The dependence receptor DCC (deleted in colorectal cancer) defines an alternative mechanism for caspase activation.* Proc Natl Acad Sci U S A, 2001. **98**(6): p. 3416-3421.
44. Gyrd-Hansen, M., et al., *Apoptosome-Independent Activation of the Lysosomal Cell Death Pathway by Caspase-9.* Mol Cell Biol, 2006. **26**(21): p. 7880-7891.
45. Nakagawa, T., et al., *Caspase-12 mediates endoplasmic-reticulum-specific apoptosis and cytotoxicity by amyloid-beta.* Nature, 2000. **403**(6765): p. 98-103.
46. Boya, P., et al., *Endoplasmic reticulum stress-induced cell death requires mitochondrialmembrane permeabilization.* Cell Death Differ, 2002. **9**: p. 465-467.
47. Morishima, N., et al., *An endoplasmic reticulum stress-specific caspase cascade in apoptosis. Cytochrome c-independent activation of caspase-9 by caspase-12.* J Biol Chem, 2002. **277**: p. 34287-34294.
48. Scorrano, L., et al., *Bax and Bak regulation of endoplasmic reticulum Ca^{2+}: a control point for apoptosis.* Science, 2003. **300**: p. 135-139.
49. Boyce, M., et al., *A selective inhibitor of eIF2alpha dephosphorylation protects cells from ER stress.* . Science, 2005. **307**: p. 935-939.
50. Boyce, M., et al., *A pharmacoproteomic approach implicates eukaryotic elongation factor 2 kinase in ER stress-induced cell death.* Cell Death Diff., 2008. **15**: p. 589-599.
51. de Duve, C., et al., *Tissue fractionation studies. 6. Intracellular distribution patterns of enzymes in ratliver tissue.* Biochem J, 1955. **60**: p. 604-617.
52. Kornfeld, S. and I. Mellman, *The biogenesis of lysosomes.* Annu Rev Cell Biol 1989. **5**: p. 483-525.
53. Ciechanover, A., *Intracellular protein degradation from a vague idea through the lysosome and the ubiquitin-proteasome system and on to human diseases and drug targeting. Nobel Lecture, December 8, 2004.* Ann N.Y. Acad Sci, 2007. **1116**: p. 1-28.
54. Rubinsztein, D.C., *The roles of intracellular protein-degradation pathways in neurodegeneration.* Nature, 2006. **443**: p. 780-186.
55. Terman, A., B. Gustafsson, and U.T. Brunk, *Autophagy, organelles and ageing.* J Pathol, 2007. **211**: p. 134-143.
56. Terman, A. and U.T. Brunk, *The aging myocardium: Role of mitochondrial damage and lysosomal degradation.* Heart Lung and Circulation, 2005. **14**: p. 107-114.
57. Anderson, N. and J. Borlak, *Drug-induced phospholipidosis.* FEBS Letters, 2006. **580**: p. 5533-5540.
58. Huizing, M., et al., *Disorders of lysosome-related organelle biogenesis: clinical and molecular genetics.* Annu Rev Genom Human Genet., 2008. **20**(2): p. 359-386.
59. Ono, K., S.O. Kim, and J. Han, *Susceptibility of lysosomes to rupture is a determinant for plasma membrane disruption in tumor necrosis factor alpha-induced cell death.* Mol Cell Biol, 2003. **23**(2): p. 665-676.

60. Mizushima, N., et al., *Autophagy fights disease through cellular self digestion.* Nature, 2008. **451**: p. 1069-1075.
61. Mizushima, N. and D.J. Klionsky, *Protein turnover via autophagy: implications for metabolism.* Annu. Rev. Nutrition & Cancer, 2007. **27**: p. 19-40.
62. Pattingre, S., et al., *Bcl-2 antiapoptotic proteins inhibit Beclin 1-dependent autophagy.* Cell, 2005. **122**: p. 927-939.
63. Levine, B. and J. Yuan, *Autophagy in cell death: an innocent convict?* J Clin Invest, 2005. **115**: p. 2679-2688.
64. Scott, R.C., G. Juhász, and T.P. Neufeld, *Direct induction of autophagy by Atg1 inhibits cell growth and induces apoptotic cell death.* Curr Biol, 2007. **17**: p. 1-11.
65. Yu, L., et al., *Regulation of an ATG7-beclin 1 program of autophagic cell death by caspase-8.* Science, 2004. **304**: p. 1500-1502.
66. Maiuri, M.C., et al., *Functional and physical interaction between Bcl-X(L) and a BH3-like domain in Beclin-1.* EMBO J, 2007. **26**: p. 2527-2539.
67. Wirawan, E., et al., *Caspase-mediated cleavage of Beclin-1 inactivates Beclin-1-induced autophagy and enhances apoptosis by promoting the release of proapoptotic factors from mitochondria.* Cell Death Dis., 2010. **1**: p. sous presses.
68. Sinha, S. and B. Levine, *The autophagy effector Beclin 1: a novel BH3-only protein.* Oncogene, 2009. **27**: p. S137-S148.
69. Shimizu, S., et al., *Role of Bcl-2 family proteins in a non-apoptotic programmed cell death dependent on autophagy genes.* Nat Cell Biol, 2004. **6**: p. 1221-1228.
70. Madden, D.T., L. Egger, and D.E. Bredesen, *A calpain-like protease inhibits autophagic cell death.* Autophagy, 2007. **3**: p. 519-522.
71. Boya, P., et al., *Inhibition of macroautophagy triggers apoptosis.* Mol Cell Biol, 2005. **25**: p. 1025-1040.
72. Gonzales-Polo, R.A., et al., *The apoptosis/autophagy paradox. Autophagic vacuolization before apoptotic death.* J Cell Sci 2005. **118**: p. 3091-3102.
73. Maiuri, C.M., et al., *Self-eating and self-killing: crosstalk between autophagy and apoptosis.* Nature Rev Mol Cell Biol, 2007. **8**: p. 741-743.
74. Liu, D., et al., *Caspase-8-mediated intracellular acidification precedes mitochondrial dysfunction in somatostatin-induced apoptosis.* J Biol Chem, 2000. **275**(13): p. 9244-50.
75. Matsuyama, S., et al., *Changes in intramitochondrial and cytosolic pH: early events that modulate caspase activation during apoptosis.* Nat Cell Biol, 2000. **2**(6): p. 318-325.
76. Nilsson, C., et al., *Analysis of cytosolic and lysosomal pH in apoptotic cells by fow cytometry.* Methods in Cell Sciences, 2003. **25**: p. 185-194.
77. Gottlieb, R.A., et al., *Apoptosis induced in Jurkat cells by several agents is preceded by intracellular acidification.* Proc Natl Acad Sci (USA), 1996. **93**(2): p. 654-658.
78. Li, J. and A. Eastman, *Apoptosis in an interleukin-2-dependent cytotoxic T lymphocyte cell line is associated with intracellular acidification. Role of the Na(+)/H(+)-antiport.* J Biol Chem., 1995. **270**(7): p. 3203-11.
79. Xie, Z.H., et al., *Acidic Ph Promotes Dimerization Of Bcl-2 Family Proteins.* Biochemistry, 1998. **37**(18): p. 6410-6418.
80. Turk, B., et al., *Kinetics of the pH-induced inactivation of human cathepsin L.* Biochemistry, 1993. **32**(1): p. 375-380.

81. Kirschke, H., et al., *Cathepsine S from bovine spleen.* Biochem J, 1989. **264**: p. 467-473.
82. Turk, B., D. Turk, and G.S. Salvesen, *Regulating cysteine protease activity: essential role of protease inhibitors as guardians and regulators.* Curr Pharm Des, 2002. **8**(18): p. 1623-1637.
83. Pennacchio, L.A., et al., *Progressive ataxia, myoclonic epilepsy and cerebellar apoptosis in cystatin B-deficient mice.* Nature Genet, 1998. **20**: p. 251-258.
84. Stoka, V., et al., *Lysosomal protease pathways to apoptosis. Cleavage of Bid, not pro-caspases, is the most likely route.* J Biol Chem, 2001. **276**(5): p. 3149-3157.
85. Schotte, P., et al., *Cathepsin B-mediated activation of the proinflammatory caspase-11.* Bichem Biophys Res Commun, 1998. **251**: p. 379-387.
86. Gorria, M., et al., *A new lactoferrin and iron-dependent lysosomal death pathway is inducedby benzo[a]pyrene in hepatic epithelial cells.* Toxicology and Applied Pharmacology 2008. **228**: p. 212-224.
87. Katunuma, N., et al., *New apoptosis cascade mediated by lysosomal enzyme and its protection by epigallo-catechin gallate.* Adv Enzyme Regul, 2004. **44**: p. 1-10.
88. Katunuma, N., et al., *A novel apoptosis cascade mediated by lysosomal lactoferrin and its participation in hepatocyte apoptosis induced by D-galactosamine.* FEBS Letters, 2006. **580**: p. 3699-3705.
89. Katunuma, N., et al., *Novel procaspase-3 activating cascade mediated by lysoapoptases and its biological significances in apoptosis.* Adv Enzyme Regul, 2001. **41**: p. 237-250.
90. Persson, H.L., et al., *Prevention of oxidant-induced cell death by lysosomotropic iron chelators.* Free Radic Biol Med, 2003. **34**: p. 1295-1305.
91. Castino, R., et al., *Cathepsin D –Bax death pathway in oxidative stressed neuroblastoma cells.* Free Radical Biology & Medicine, 2007. **42**: p. 1305-1316.
92. Petrat, F., H. de Groot, and U. Rauen, *Subcellular distribution of chelatable iron: a laser scanning microscopic study in isolated hepatocytes and liver endothelial cells.* Biochem J. , 2001. **356**: p. 61-69.
93. Hishita, T., et al., *Caspase-3 activation by lysosomal enzymes in cytochrome c-independent apoptosis in myelodysplastic syndrome-derived cell line P39.* Cancer Res, 2001. **61**: p. 2878-2884.
94. Paquet, C., et al., *Caspase- and mitochondrial dysfunction-dependent mechanisms of lysosomal leakage and cathepsin B activation in DNA damage-induced apoptosis.* Leukemia, 2005. **19**(5): p. 784-91.
95. Lamparska-Przybysz, M., B. Gajowska, and T. Motyl, *Cathepsines and Bid are involved in the molecular swithc beteen apoptosis and autophagy in breast cancer MCF-7 cells exposed to camptothecin.* J Physiol Pharmacol, 2005. **56**: p. 159-179.
96. Blomgran, R., L. Zheng, and O. Stendahl, *Cathepsin-cleaved Bid promotes apoptosis in human neutrophils via oxidative stress-induced lysosomal membrane permeabilization.* J Leukoc Biol, 2007. **81**: p. 1213-1223.
97. Roberg, K. and K. Ollinger, *Oxidative stress causes relocation of the lysosomal enzyme cathepsin D with ensuing apoptosis in neonatal rat cardiomyocytes.* Am J Pathol, 1998. **152**(5): p. 1151-1156.
98. Roberg, K., U. Johansson, and K. Ollinger, *Lysosomal release of cathepsin D precedes relocation of cytochrome c and loss of mitochondrial transmembrane*

potential during apoptosis induced by oxidative stress. Free Radic Biol Med, 1999. **27**(11-12): p. 1228-1237.

99. Antunes, F. and E. Cadenas, *Cellular titration of apoptosis with steady-state concentrations of H_2O_2. Sub-micromolar levels of H_2O_2 induce apoptosis through Fenton chemistry independent of cellular thiol state.* . Free Radical Biol. Med, 2001. **30**(9): p. 1008-1018.
100. Antunes, F., E. Cadenas, and U.T. Brunk, *Apoptosis induced by exposure to a low steady-state concentration of H_2O_2 is a consequence of lysosomal rupture.* Biochem J, 2001. **356**(Pt 2): p. 549-555.
101. Dare, E., et al., *Methylmercury and H_2O_2 provoke lysosomal damage in human astrocytoma D384 cells followed by apoptosis.* Free Radical Biology & Medicine, 2001. **30**: p. 1347-1356.
102. Yap, Y.W., et al., *Hypochlorous acid induces apoptosis of cultured cortical neurons through activation of calpains and rupture of lysosomes.* Journal of Neurochemistry, 2006. **98**: p. 1597-1609.
103. Guicciardi, M.E., et al., *Bid Is Upstream of Lysosome-Mediated Caspase 2 Activation in Tumor Necrosis Factor alpha–Induced Hepatocyte Apoptosis.* Gastroenterology 2005. **129**: p. 269–284.
104. Liu, N., et al., *NF-kappaB protects from the lysosomal pathway of cell death.* EMBO J, 2003. **22**(19): p. 5313-5322.
105. Werneburg, N., et al., *TNF-α-mediated lysosomal permeabilization is FAN and caspase 8/Bid dependent.* Am J Physiol Gastrointest Liver Physiol. , 2004. **287**: p. G436-G443.
106. Guicciardi, M.E., et al., *Cathepsin B knockout mice are resistant to tumor necrosis factor-alpha-mediated hepatocyte apoptosis and liver injury: implications for therapeutic applications.* Am J Pathol, 2001. **159**(6): p. 2045-2054.
107. Werneburg, N.W., et al., *Tumor necrosis factor--associated lysosomal permeabilization is cathepsin B dependent.* Am. J. Physiol. Gastrointest. Liver Physiol., 2002. **283**: p. G947-G956.
108. Deiss, L.P., et al., *Cathepsin D protease mediates programmed cell death induced by interferon-gamma, Fas/Apo-1 and TNF-alpha.* EMBO J, 1996. **15**(15): p. 3861-3870.
109. Van Eijk, M. and C. De Groot, *Germinal center B-cell apoptosis requires both caspase and cathepsin activity.* J Immunol, 1999. **163**: p. 2478-2482.
110. Akazawa, Y., et al., *Death Receptor 5 Internalization Is Required for Lysosomal Permeabilization by TRAIL in Malignant Liver Cell Lines.* Gastroenterology, 2009. **in press**.
111. Wilson, P.D., R.A. Firestone, and J. Lenard, *The role of lysosomal enzymes in killing of mammalian cells by the lysosomotropic detergent N-dodecylimidazole.* J Cell Biol., 1987. **104**: p. 1223-1229.
112. Van Nierop, K., et al., *Lysosomal Destabilization Contributes to Apoptosis of Germinal Center B-lymphocytes.* J Histochem Cytochem, 2006. **54**(12): p. 1425-1435.
113. Ditaranto-Desimone, K., et al., *Neuronal endosomal/lysosomal membrane destabilization activates caspases and induces abnormal accumulation of the lipid secondary messenger ceramide.* Brain Research Bulletin, 2003. **59**(6): p. 523-531.

114. Uchimoto, T., et al., *Mechanism of apoptosis induced by a lysosomotropic agent, L-Leucyl-L-Leucine methyl ester.* Apoptosis, 1999. **4**(5): p. 357-362.
115. Cirman, T., et al., *Selective disruption of lysosomes in HeLa cells triggers apoptosis mediated by cleavage of Bid by multiple papain like lysosomal cathepsins.* J Biol Chem, 2004. **279**: p. 3578-3587.
116. Boya, P., et al., *Lysosomal membrane permeabilization induces cell death in a mitochondrion-dependent fashion.* J Exp Med., 2003. **197**: p. 1323-1334.
117. Boya, P., et al., *Mitochondrial membrane permeabilization is a critical step of lysosome-initiated apoptosis induced by hydroxychloroquine.* Oncogene, 2003. **22**: p. 3927-3936.
118. Reiners, J.J.J., et al., *Release of cytochrome c and activation of pro-caspase-9 following lysosomal photodamage involves bid cleavage.* Cell Death Diff., 2002. **9**: p. 934-944.
119. Ichinose, S., et al., *Lysosomal cathepsin initiates apoptosis, which is regulated by photodamage to Bcl-2 at mitochondria in photodynamic therapy using a novel photosensitizer, ATX-s10 (Na).* Int J Oncol, 2006. **29**(2): p. 349-55.
120. Nagata, S., et al., *Necrotic and apoptotic cell death of human malignant melanoma cells following photodynamic therapy using an amphiphilic photosensitizer, ATX-S10(Na).* Lasers in Surgery and Medicine, 2003. **33**: p. 64-70.
121. Li, W., et al., *3-Aminopropanal, formed during cerebral ischaemia, is a potent lysosomotropic neurotoxin.* Biochem J., 2003. **371**: p. 429-436.
122. Kagedal, K., et al., *Sphingosine-induced apoptosis is dependent on lysosomal proteases.* Biochem J, 2001. **359**(Pt 2): p. 335-343.
123. Paris, C., J. Bertoglio, and J. Bréard, *Lysosomal and mitochondrial pathways in miltefosine-induced apoptosis in U937 cells.* Apoptosis, 2007. **12**(7): p. 1257-1267.
124. Holman, D.H., et al., *Lysosomotropic acid ceramidase inhibitor induces apoptosis in prostate cancer cells.* Cancer Chemother Pharmacol, 2008. **61**: p. 231-242.
125. Broker, L.E., et al., *Cathepsin B mediates caspase-independent cell death induced by microtubule stabilizing agents in non-small cell lung cancer cells.* Cancer Research, 2004. **64**(27-30).
126. Groth-Pedersen, L., et al., *Vincristine induces dramatic lysosomal changes and sensitizes cancer cells to lysosome-destabilizing siramesine.* Cancer Res., 2007. **67**: p. 2217-2225.
127. Nakashima, S., et al., *Vacuolar H+-ATPase Inhibitor Induces Apoptosis via Lysosomal Dysfunction in the Human Gastric Cancer Cell Line MKN-1.* J Biochem, 2003. **134**: p. 359-364.
128. Michallet, M.C., et al., *Cathepsin-B-dependent apoptosis triggered by antithymocyte globulins: a novel mechanism of T-cell deletion.* Blood, 2003. **102**: p. 3719-3726.
129. Laforge, M., et al., *Commitment to apoptosis in $CD4^+$ T lymphocytes productively infected with human immunodeficiency virus type 1 is initiated by lysosomal membrane permeabilization, itself induced by the isolated expression of the viral protein Nef.* J. Virol., 2007. **81**(20): p. 114026-11440.
130. Shibata, M., et al., *Participation of cathepsins B and D in apoptosis of PC12 cells following serum deprivation.* Biochem Biophys Res Com, 1998. **251**(1): p. 199-203.

131. Brunk, U.T. and I. Svensson, *Oxidative stress, growth factor starvation and Fas activation may all cause apoptosis through lysosomal leak.* Redox Rep, 1999. **4**(1-2): p. 3-11.
132. Nylandsted, J., et al., *Heat shock protein 70 promotes cell survival by inhibiting lysosomal membrane permeabilization.* J Exp Med, 2004. **200**: p. 425-435.
133. Yu, H., et al., *Clioquinol targets zinc to lysosomes in human cancer cells.* Biochem J., 2009. **417**: p. 133-139.
134. Thibodeau, M.S., et al., *Silica-Induced Apoptosis in Mouse Alveolar Macrophages Is Initiated by Lysosomal Enzyme Activity.* Toxicological Sciences, 2004. **80**(1): p. 34-48.
135. Zang, Y., et al., *Evidence of a lysosomal pathway for apoptosis induced by the synthetic retinoid CD437 in human leukemia HL-60 cells.* Cell Death Differ, 2001. **8**(5): p. 477-485.
136. Neuzil, J., et al., *Alpha-tocopheryl succinate-induced apoptosis in Jurkat T cells involves caspase-3 activation, and both lysosomal and mitochondrial destabilisation.* FEBS Lett, 1999. **445**(2-3): p. 295-300.
137. He, J., et al., *Lysosome is a primary organelle in B cell receptor-mediated apoptosis: an indispensable role of Syk in lysosomal function.* Genes to Cells, 2005. **10**: p. 23-35.
138. Yuan, X.M., et al., *Lysosomal destabilization in p53-induced apoptosis.* Proc Nat Acad Sci. (USA), 2002. **99**: p. 6286-6291.
139. Bidere, N., et al., *Cathepsin D triggers Bax activation, resulting in selective apoptosis-inducing factor (AIF) relocation in T lymphocytes entering the early commitment phase to apoptosis.* J Biol Chem, 2003. **278**(33): p. 31401-31411.
140. Johansson, A.C., et al., *Cathepsin D mediates cytochrome c release and caspase activation in human fibroblast apoptosis induced by staurosporine.* Cell Death Differ, 2003. **10**: p. 1253-1259.
141. Roberts, L.R., P.N. Adjei, and G.J. Gores, *Cathepsins as effector proteases in hepatocyte apoptosis.* Cell Biochem. Biophys, 1999. **30**: p. 71- 88.
142. Roberg, K., K. Kagedal, and K. Ollinger, *Microinjection of cathepsin D induces caspase-dependent apoptosis in fibroblasts.* Am J Pathol, 2002. **161**(1): p. 89-96.
143. Vancompernolle, K., et al., *Atractyloside-induced release of cathepsin B, a protease with caspase-processing activity.* FEBS Lett, 1998. **438**: p. 150-158.
144. López-Otin, C. and C.M. Overall, *Protease degradomics: a new challenge for proteomics.* Nat Mol Cell Reviews 2002. **3**: p. 509-519.
145. Zheng, W., et al., *Ceramides and other bioactive sphingolipid backbones in health and disease: Lipidomic analysis, metabolism and roles in membrane structure, dynamics, signaling and autophagy.* Biochimica et Biophysica Acta, 2006. **1758**: p. 1864 - 1884.
146. Hannun, Y.A., C. Luberto, and K.M. Argraves, *Enzymes of sphingolipid metabolism: From modular to integrative signaling.* Biochem, 2001. **40**(16): p. 4893-4904.
147. Mandon, E.C., et al., *Subcellular localization and membrane topology of serine palmitoyltransferase, 3-dehydrosphinganine reductase, and sphinganine N-acyltransferase in mouse liver.* J Biol Chem, 1992. **267**(16): p. 11144-11148.
148. Marchesini, N. and Y.A. Hannun, *Acid and neutral sphingomyelinases: roles and mechanisms of regulation.* Biochem. Cell Biol., 2004. **82**: p. 27-44.

149. Delamare, J., et al., *Dictionnaire des termes de médecine*, Maloine, Editor. 1999: Paris. p. 975.
150. Ogretmen, B. and Y.A. Hannun, *Biologically active sphingolipids in cancer pathogenesis and treatment.* Nat. Rev. Cancer, 2004. **4**: p. 604-616.
151. Riboni, L., G. Tettamanti, and P. Viani, *Ceramide levels are inversely associated with malignant progression of human glial tumors.* Glia, 2002. **39**: p. 105-113.
152. Okazaki, T., R.M. Bell, and Y.A. Hannun, *Sphingomyelin turnover induced by vitamin D3 in HL-60 cells. Role in cell differentiation.* J Biol Chem., 1989. **264**(32): p. 19076-19080.
153. Chalfant, C.E. and S. Spiegel, *Sphingosine 1-phosphate and ceramide 1-phosphate: expanding roles in cell signaling.* J Cell Sci., 2005. **118**(20): p. 4605-4612.
154. Hannun, Y.A. and L.M. Obeid, *Ceramide: an intracellular signal for apoptosis.* . Trends in Biochemical Sciences, 1995. **20**(2): p. 73-7.
155. Asakuma, J., et al., *Selective Akt inactivation and tumor necrosis actor-related apoptosis-inducing ligand sensitization of renal cancer cells by low concentrations of paclitaxel.* Cancer Res., 2003. **63**: p. 1365-1370.
156. Bose, R., et al., *Ceramide synthase mediates daunorubicin-induced apoptosis: an alternative mechanism for generating death signals.* Cell, 1995. **82**(3): p. 405-414.
157. Perry, D.K., et al., *Serine palmitoyltransferase regulates de novo ceramide generation during etoposide-induced apoptosis.* J Biol Chem, 2000. **275**(12): p. 9078-9084.
158. Hara, S., et al., *p53-independent ceramide formation in human glioma cells during γ-radiation-induced apoptosis.* Cell Death Diff., 2004. **11**: p. 853-861.
159. Galve-Roperh, I., et al., *Anti-tumoral action of cannabinoids: Involvement of sustained ceramide accumulation and extracellular signal-regulated kinase activation.* Nat Med, 2000. **6**(3): p. 313-319.
160. Cuvillier, O., L. Edsall, and S. Spiegel, *Involvement of sphingosine in mitochondria-dependent Fas-induced apoptosis of type II Jurkat T cells.* J Biol Chem, 2000. **275**(21): p. 15691-1700.
161. Cuvillier, O., et al., *Sphingosine generation, cytochrome c release, and activation of caspase-7 in doxorubicin-induced apoptosis of MCF7 breast adenocarcinoma cells.* Cell Death Differ, 2001. **8**(2): p. 162-171.
162. Lepine, S., et al., *Involvement of sphingosine in dexamethasone-induced thymocyte apoptosis.* Ann N Y Acad Sci, 2002. **973**: p. 190-193.
163. Isogai, C., et al., *Analysis of bax protein in sphingosine-induced apoptosis in the human leukemic cell line TF1 and its bcl-2 transfectants.* Exp Hematol, 1998. **26**(12): p. 1118-1125.
164. Nava, V.E., et al., *Sphingosine enhances apoptosis of radiation-resistant prostate cancer cells.* Cancer Res, 2000. **60**(16): p. 4468-4474.
165. Chang, H.C., et al., *Functional role of caspases in sphingosine-induced apoptosis in human hepatoma cells.* IUBMB Life, 2003. **55**(7): p. 403-407.
166. Obeid, L., et al., *Programmed cell death induced by ceramide.* Science, 1993. **259**: p. 1769-1771.
167. Hannun, Y.A., *Function of ceramide in coordinating cellular responses to stress.* Science, 1996. **274**(5294): p. 1855-1859.

168. Geley, S., B.L. Hartmann, and R. Kofler, *Ceramides induce a form of apoptosis in human acute lymphoblastic leukemia cells that is inhibited by Bcl-2, but not by Crma.* FEBS Letters, 1997. **400**(1): p. 15-18.
169. Zhang, P., et al., *Expression of neutral sphingomyelinase identifies a distinct pool of sphingomyelin involved in apoptosis.* J Biol Chem, 1997. **272**(15): p. 9609-9612.
170. Akao, Y., et al., *Ceramide accumulation is independent of camptothecin-induced apoptosis in prostate cancer LNCaP cells.* Biochem Biophys Res Commun, 2002. **294**(2): p. 363-370.
171. Higuchi, M., et al., *Acidic Sphingomyelinase-Generated Ceramide Is Needed But Not Sufficient For TNF-Induced Apoptosis and Nuclear Factor-Kappa-B Activation.* Journal of Immunology, 1996. **157**(1): p. 297-304.
172. Kreder, D., et al., *Impaired neutral sphingomyelinase activation and cutaneous barrier repair in FAN-deficient mice.* EMBO J., 1999. **18**(9): p. 2472-2479.
173. Lin, T., et al., *Role of acidic sphingomyelinase in Fas/CD95-mediated cell death.* J Biol Chem, 2000. **275**(12): p. 8657-63.
174. Pettus, B.J., C.E. Chalfant, and Y.A. Hannun, *Ceramide in apoptosis: an overview and current perspectives.* Biochimica et Biophysica Acta, 2002. **1585**: p. 114 - 125.
175. Lozano, J., et al., *Cell autonomous apoptosis defects in acid sphingomyelinase knockout fibroblasts.* J Biol Chem, 2001. **276**(1): p. 442-448.
176. Separovica, D., et al., *Suppression of sphingomyelin synthase 1 by small interference RNA is associated with enhanced ceramide production and apoptosis after photodamage.* Exp Cell Res, 2008. **314**(8): p. 1860-1868.
177. Ding, T., et al., *SMS overexpression and knockdown: impact on cellular sphingomyelin and diacylglycerol metabolism, and cell apoptosis.* J Lipid Res., 2008. **49**: p. 376-385.
178. Caruso, J.A., P.A. Mathieu, and J.J.J. Reiners, *Sphingomyelins suppress the targeted disruption of lysosomes/endosomes by the photosensitizer NPe6 during photodynamic therapy.* Biochem J., 2005. **392**: p. 325-334.
179. Seumois, G., et al., *De novo C_{16} and C_{24}-ceramide generation contributes to spontaneous neutrophil apoptosis.* J Leukoc Biol., 2007. **81**: p. 1477-1486.
180. Wells, G.B., R.C. Dickson, and R.L. Lester, *Heat-induced elevation of ceramide in Saccharomyces cerevisiae via de novo synthesis.* J Biol Chem., 1998. **273**(13): p. 7235-7243.
181. Zhang, Y., et al., *Kinase suppressor of Ras is ceramide-activated protein kinase.* Cell., 1997. **89**(1): p. 63-72.
182. Yan, F. and D.B. Polk, *Kinase suppressor of ras is necessary for tumor necrosis factor alpha activation of extracellular signal-regulated kinase/mitogen-activated protein kinase in intestinal epithelial cells.* Cancer Res., 2001. **61**(3): p. 963-969.
183. Chalfant, C.E., et al., *De novo ceramide regulates the alternative splicing of caspase 9 and Bcl-x in A549 lung adenocarcinoma cells. Dependence on protein phosphatase-1.* J Biol Chem., 2002. **277**(15): p. 12587-12595.
184. Huwiler, A., et al., *Ceramide-binding and activation defines protein kinase c-Raf as a ceramide-activated protein kinase.* Proc Natl Acad Sci USA 1996. **93**(14): p. 6959-6963.
185. Zhou, M., et al., *Solution structure and functional analysis of the cysteine-rich C1 domain of kinase suppressor of Ras (KSR).* J Mol Biol., 2002. **315**(3): p. 435-446.

186. Gulbins, E., et al., *Fas-Induced Apoptosis Is Mediated By Activation Of a Ras and Rac Protein-Regulated Signaling Pathway.* Journal of Biological Chemistry, 1996. **271**(42): p. 26389-26394.
187. Huwiler, A., et al., *Ceramide binds to the CaLB domain of cytosolic phospholipase A2 and facilitates its membrane docking and arachidonic acid release.* FASEB J., 2001. **15**(1): p. 7-9.
188. Heinrich, M., et al., *Cathepsin D targeted by acid sphingomyelinase-derived ceramide.* EMBO J., 1999. **18**: p. 5252 - 5263.
189. Kashiwagi, K., et al., *Importance of C1B domain for lipid messenger-induced targeting of protein kinase C.* J Biol Chem., 2002. **277**: p. 18037-18045.
190. Lepple-Wienhues, A., et al., *Stimulation of CD95 (Fas) blocks T lymphocyte calcium channels through sphingomyelinase and sphingolipids.* Proc Natl Acad Sci USA, 1999. **96**(24): p. 13795-13800.
191. Verheij, M., et al., *Requirement for ceramide-initiated Sapk/Jnk signalling In stress-induced apoptosis.* Nature, 1996. **380**(6569): p. 75-79.
192. Westwick, J.K., et al., *Ceramide activates the stress-activated protein kinases.* J Biol Chem., 1995. **270**(39): p. 22689-22692.
193. Basu, S., et al., *BAD enables ceramide to signal apoptosis via Ras and Raf-1.* J Biol Chem., 1998. **273**(46): p. 30419-30426.
194. Gudz, T.I., K.Y. Tserng, and C.L. Hoppel, *Direct Inhibition Of Mitochondrial Respiratory Chain Complex Iii By Cell-Permeable Ceramide.* Journal of Biological Chemistry, 1997. **272**(39): p. 24154-24158.
195. Garciaruiz, C., et al., *Direct Effect Of Ceramide On the Mitochondrial Electron Transport Chain Leads to Generation Of Reactive Oxygen Species - Role Of Mitochondrial Glutathione.* Journal of Biological Chemistry, 1997. **272**(17): p. 11369-11377.
196. Schissel, S.L., et al., *Zn^{2+}-stimulated sphingomyelinase is secreted by many cell types and is a product of the acid sphingomyelinase gene.* J Biol Chem., 1996. **271**(31): p. 18431-18436.
197. Cremesti, A., et al., *Ceramide enables Fas to cap and kill.* J Biol Chem, 2001. **276**(26): p. 23954-23961.
198. Grassme, H., et al., *Ceramide-rich membrane rafts mediate CD40 clustering.* J Immunol, 2002. **168**(1): p. 298-307.
199. Prinetti, A., et al., *Changes in the lipid turnover, composition, and organization, as sphingolipid-enriched membrane domains, in rat cerebellar granule cells developing in vitro.* J Biol Chem., 2001. **276**(24): p. 21136-21145.
200. Kolesnick, R.N., F.M. Goñi, and A. Alonso, *Compartmentalization of ceramide signaling: physical foundations and biological effects.* J Cell Physiol., 2000. **184**(3): p. 285-300.
201. Gulbins, E. and R. Kolesnick, *Raft ceramide in molecular medicine.* Oncogene, 2003. **22**: p. 7070-7077.
202. Zundel, W. and A. Giaccia, *Inhibition of the anti-apoptotic PI(3)K/Akt/Bad pathway by stress.* Genes & Development, 1998. **12**(13): p. 1941-1946.
203. Trajkovic, K., et al., *Ceramide triggers budding of exosome vesicles into multivesicular endosomes.* Science, 2008. **319**: p. 1244-1247.

204. Utermöhlen, O., et al., *Fusogenicity of membranes: The impact of acid sphingomyelinase on innate immune responses.* Immunobiology, 2008. **213**: p. 307-314.
205. Krönke, M., *Biophysics of ceramide signaling: interaction with proteins and phase transition of membranes.* Chem. Phys. Lipids, 1999. **101**: p. 109-121.
206. Kagedal, K., et al., *Lysosomal membrane permeabilization during apoptosis-involvement of Bax?* . Int J Exp Pathol, 2005. **86**: p. 309-321.
207. Ganesan, V., et al., *Ceramide and activated Bax act synergically to permeabilize the mitochondrial outer membrane.* Apoptosis, 2010. **sous presses**.
208. Chen, W., et al., *The lysosome-associated apoptosis-inducing protein containing the pleckstrin homology (PH) and FYVE domains (LAPF), representative of a novel family of PH and FYVE domain-containing proteins,induces caspase-independent apoptosis via the lysosomal-mitochondrial pathway.* J Biol Chem., 2005. **280**: p. 40985-40995.
209. Li, N., et al., *Adaptor Protein LAPF Recruits Phosphorylated p53 to Lysosomes and Triggers Lysosomal Destabilization in Apoptosis.* Cancer Res, 2007. **67**(23): p. 11176-11185.
210. Caelles, C., A. Helmberg, and M. Karin, *p53-dependent apotosis in the absence of transcriptional activation of p53-target genes.* Nature, 1994. **370**: p. 220-223.
211. Koumenis, C., et al., *Regulation of p53 by hypoxia: dissociation of transcriptional repression and apoptosis from p53-dependent transactivation.* . Mol Cell Biol, 2001. **21**: p. 1297-1310.
212. Ding, H.F., et al., *Essential role for caspase-8 in transcription-independent apoptosis triggered by p53.* J Biol Chem, 2000. **275**: p. 38905-38911.
213. Mihara, M., et al., *p53 has a direct apoptogenic role at the mitochondria.* Mol Cell, 2003. **11**(3): p. 577-590.
214. Zhao, H.F., X. Wang, and G.J. Zhang, *Lysosome destabilization by cytosolic extracts, putative involvement of Ca(2+)/phospholipase C.* FEBS Lett, 2005. **579**: p. 1551-1556.
215. Orrenius, S., B. Zhivotovsky, and P. Nicotera, *Regulation of cell death: the calcium-apoptosis link.* Nat Rev Mol Cell Biol, 2003. **4**(7): p. 552-565.
216. Zhao, M., U.T. Brunk, and J.W. Eaton, *Delayed oxidant-induced cell death involves activation of phospholipase A_2.* FEBS Lett., 2001. **509**: p. 399-404.
217. Wang, J.W., et al., *Effects of phospholipase A2 on the lysosomal ion permeability and osmotic sensitivity.* Chem Phys Lipids., 2006. **144**: p. 117-126.
218. Hu, J.S., et al., *Mechanism of lysophosphatidylcholine-induced lysosome destabilization.* J Membrane Biol., 2007. **215**: p. 27-35.
219. Siskind, L.J., et al., *Sphingosine forms channels in membranes that differ greatly from those formed by ceramide.* J Bioenerg. Biomembr. , 2005. **37**(4): p. 227-236.
220. Siskind, L.J. and M. Colombini, *The lipids C2- and C16-ceramide form large stable channels. Implications for apoptosis.* J Biol Chem. Dec 8;():, 2000. **275**(49): p. 38640-38644.
221. Stiban, J., D. Fistere, and M. Colombini, *Dihydroceramide hinders ceramide channel formation: Implications on apoptosis.* Apoptosis, 2006. **11**: p. 773-780.
222. Siskind, L.J., *Mitochondrial ceramide and the induction of apoptosis.* J Bioenerg Biomembr., 2005. **37**(3): p. 143-153.

223. Siskind, L.J., R.N. Kolesnick, and M. Colombini, *Ceramide channels increase the permeability of the mitochondrial outer membrane to small proteins.* J Biol Chem, 2002. **277**(30): p. 26796-26803.
224. Davies, K.J.A., *The broad spectrum of responses to oxidants in proliferating cells: a new paradigm for oxidative stress.* IUBMB Life 1999. **48**: p. 41-47.
225. Le Bras, M., et al., *Reactive oxygen species and the mitochondrial signaling pathway of cell death.* Histol. Histopathol., 2005. **20**: p. 205-220.
226. Catalá, A., *Lipid peroxidation of membrane phospholipids generates hydroxy-alkenals and oxidized phospholipids active in physiological and/or pathological conditions.* Chem Phys Lipids., 2009. **157**: p. 1-11.
227. Nigam, S. and T. Schewe, *Phospholipase A2s and lipid peroxidation.* Biochim. Biophys. Acta, 2000. **1488**: p. 167-181.
228. Nomura, K., et al., *Mitochondrial phospholipid hydroperoxide glutathione peroxidase suppresses apoptosis mediated by a mitochondrial death pathway.* J Biol Chem, 1999. **274**(41): p. 29294-29302.
229. OMS. *Le cancer*. 2009 [cited; Available from: http://www.who.int/mediacentre/factsheets/fs297/fr/index.html.
230. Lessene, G., P.E. Czabotar, and P.M. Colman, *BCL-2 family antagonists for cancer therapy.* Nat Rev Drug Discov., 2008. **7**: p. 989-1000.
231. Papenfuss, K., S.M. Cordier, and H. Walczak, *Death receptors as targets for anti-cancer therapy.* J Cell Mol Med., 2008. **12**: p. 2566-2285.
232. Glunde, K., et al., *Extracellular acidification alters lysosomal trafficking in human breast cancer cells.* Neoplasia, 2003. **5**: p. 533-545.
233. Rochefort, H., et al., *Cathepsin D in breast cancer: mechanisms and clinical applications, a 1999 overview.* Clin Chim Acta., 2000. **291**: p. 157-170.
234. Fehrenbacher, N., et al., *Sensitization to the lysosomal cell death pathway upon immortalization and transformation.* Cancer Res., 2004. **64**: p. 5301-5310.
235. Weylandt, K.H., et al., *ClC-3 expression enhances etoposide resistance by increasing acidification of the late endocytic compartment.* Mol Cancer Ther., 2007. **6**: p. 979-986.
236. Raghunand, N., et al., *pH and drug resistance. Turnover of acidic vesicles and resistance to weakly basic chemotherapeutic drugs.* Biochem Pharmacol., 1999. **57**: p. 1047-1058.
237. Gidding, C.E., et al., *Vincristine revisited.* Crit Rev Oncol Hematol., 1999. **29**: p. 267-287.
238. Herold, C., et al., *Ciprofloxacin induces apoptosis and inhibits proliferation of human colorectal carcinoma cells.* Br J Cancer., 2002. **86**: p. 443-448.
239. El-Rayes, B.F., et al., *Ciprofloxacin inhibits cell growth and synergises the effect of etoposide in hormone resistant prostate cancer cells.* Int J Oncol. , 2002. **21**: p. 207-211.
240. Ding, W.Q., et al., *Anticancer activity of the antibiotic clioquinol.* Cancer Res., 2005. **65**: p. 3389-3395.
241. Zhao, H., et al., *Chloroquine-mediated radiosensitization is due to the destabilization of the lysosomal membrane and subsequent inductionof cell death by necrosis.* Radiat Res., 2005. **164**: p. 250-257.
242. Matsuoka, S., et al., *ATM and ATR substrate analysis reveals extensive protein networks responsive to DNA damage.* Science, 2007. **316**: p. 1160-1165.

243. Ducan, M.W., *Omics and its 15 minutes.* Exp Biol Med. , 2007. **232**: p. 471-472.
244. Bantscheff, M., et al., *Quantitative mass spectrometry in proteomics: a critical review.* 2007. **389**: p. 1017-1031.
245. *Applied biosystems iTRAQ™ reagents. Chemistry reference guide.* 2004. p. 1-96.
246. Pierce, A., et al., *Eight-channel itraq enables comparison of the activity of 6 leukaemogenic tyrosine kinases.* Mol. Cell Proteomics, 2007. **7**: p. 853-863.
247. Wu, W.W., et al., *Comparative study of three proteomic quantitative methods, DIGE, cICAT, and iTRAQ, using 2D Gel- or LC-MALDI TOF/TOF.* J Proteome Res., 2006. **5**: p. 651-658.
248. Gan, C.S., et al., *Technical, experimental, and biological variations in isobaric tags for relative and absolute quantitation (iTRAQ).* J Proteome Res., 2007. **6**: p. 821-827.
249. Hsieh, H.C., et al., *Protein profilings in mouse liver regeneration after partial hepatectomy using iTRAQ technology.* J Proteome Res., 2009. **8**: p. 1004-1013.
250. Schroder, B., et al., *Integral and associated lysosomal membrane proteins.* Traffic, 2007. **8**: p. 1676-1686.
251. Bagshaw, R.D., D.J. Mahuran, and J.W. Callahan, *A proteomic analysis of lysosomal integral membrane proteins reveals the diverse composition of the organelle.* Mol Cell Proteomics, 2005. **4**: p. 133-143.
252. Casey, T.M., J.L. Meade, and E.W. Hewitt, *Organelle proteomics: identification of the exocytic machinery associated with the natural killer cell secretory lysosome. .* Mol Cell Proteomics, 2007. **6**: p. 767-780.
253. Canas, B., et al., *Mass spectrometry technologies for proteomics.* Briefings in functionnal genomics and proteomics, 2006. **4**: p. 295-320.
254. Howell, K.E., E. Devaney, and J. Gruenberg, *Subcellular fractionation of tissue culture cells.* Trends Biochem Sci., 1989. **14**: p. 44-48.
255. Terrinoni, A., et al., *p73-alpha is capable of inducing scotin and ER stress.* Oncogene, 2004. **23**(20): p. 3721-5.
256. Moenner, M., et al., *Integrated endoplasmic reticulum stress responses in cancer.* Cancer Res, 2007. **67**(22): p. 10631-4.
257. Knoblach, B., et al., *ERp19 and ERp46, new members of the thioredoxin family of endoplasmic reticulum proteins.* Mol Cell Proteomics, 2003. **2**: p. 1104-1119.
258. Mizushima, N., T. Yoshimori, and B. Levine, *Methods in mammalian autophagy research.* Cell, 2010. **140**: p. 313-326.
259. Klionsky, D.J., et al., *Guidelines for the use and interpretation of assays for monitoring autophagy in higher eukaryotes.* Autophagy, 2008. **4**: p. 151-175.
260. Jäger, S., et al., *Role for Rab7 in maturation of late autophagic vacuoles.* J Cell Sci, 2004. **117**: p. 4837-4848.
261. Fehrenbacher, N., et al., *Sensitization to the lysosomal cell death pathway by oncogene-induced down-regulation of lysosome-associated membrane proteins 1 and 2.* Cancer Res, 2008. **68**: p. 6623-6633.
262. Hunziker, W., T. Simmen, and S. Honing, *Trafficking of lysosomal membrane proteins in polarized kidney cells.* Nephrologie, 1996. **17**: p. 347-350.
263. Wang, Q.J., et al., *Differential localization of protein kinase C delta by phorbol esters and related compounds using a fusion protein with green fluorescent protein.* J Biol Chem. , 1999. **274**: p. 37233-37239.

264. Kazi, J.U. and J.-W. Soh, *Isoform-specific translocation of PKC isoforms in NIH3T3 cells by TPA.* Biochem Biophys Res Com. , 2007. **364**: p. 231-237.
265. Kajimoto, T., et al., *Ceramide-induced apoptosis by translocation, phosphorylation, and activation of protein kinase Cδ in the golgi complex.* J Biol Chem., 2004. **279**: p. 12668–12676.
266. Qi, X. and D. Mochly-Rosen, *The PKCδ-Abl complex communicates ER stress to the mitochondria – an essential step in subsequent apoptosis.* J Cell Sci. , 2008. **121**: p. 804-813.
267. Parent, N., et al., *Proteomic analysis of enriched lysosomes at early phase of camptothecin-induced apoptosis in human U-937 cells.* J Proteomics., 2009 **72**: p. 960-973.
268. Aschrafi, A., et al., *Ceramide induces translocation of protein kinase C-α to the Golgi compartment of human embryonic kidney cells by interacting with the C2 domain.* Biochimica et Biophysica Acta, 2003. **1634**: p. 30-39.
269. Kazanietz, M.G., et al., *Low affinity binding of phorbol esters to protein kinase C and its recombinant cystein-rich region in absence of phospholipids.* J Biol Chem., 1995. **270**: p. 14679-14684.
270. Simons, K. and D. Toomre, *Lipid rafts and signal transduction.* Nat Rev Mol Cell Biol., 2000. **1**: p. 31–39.
271. Grandl, M., et al., *E-LDL and Ox-LDL differentially regulate ceramide and cholesterol raft microdomains in human macrophages.* Cytometry, 2006. **69A**: p. 189-191.
272. Won, J.S., A.K. Singh, and I. Singh, *Lactosylceramide: a lipid second messenger in neuroinflammatory disease.* J Neurochem., 2007. **103**: p. 180-191.
273. Yoshizaki, F., et al., *Role of glycosphingolipid-enriched microdomains in innate immunity: Microdomain-dependent phagocytic cell functions.* Biochimica et Biophysica Acta, 2008. **1780**: p. 383-392.
274. Martin, S.F., N. Williams, and S. Chatterjee, *Lactosylceramide is required in apoptosis induced by N-Smase.* Glycoconj J., 2006. **23**: p. 147-157.
275. Garcia-Ruiz, C., et al., *Direct interaction of GD3 ganglioside with mitochondria generates reactive oxygen species followed by mitochondrial permeability transition, cytochrome c release, and caspase activation.* FASEB J., 2000. **14**: p. 847–858.
276. Kakugawa, Y., et al., *Up-regulation of plasma membrane-associated ganglioside sialidase [Neu3] in human colon cancer and its involvement in apoptosis suppression.* Proc Natl Acad Sci USA., 2002. **99**: p. 10718-10723.
277. Iwabuchi, K. and I. Nagaoka, *Lactosylceramide-enriched glycosphingolipid signaling domain mediates superoxide generation from human neutrophils.* Blood, 2002. **100**: p. 1454-1464.
278. Gong, N., et al., *Lactosylceramide recruits PKCα /epsilon and phospholipase A2 to stimulate PECAM-1 expression in human monocytes and adhesion to endothelial cells.* Proc Natl Acad Sci USA., 2004. **101**: p. 6490-6495.
279. Christie, W.W. *Lipid library*. [Web page] 2009 [cited; Available from: http://www.lipidlibrary.co.uk/.
280. Meyer zu Heringdorf, D. and K.H. Jakobs, *Lysophospholipid receptors: signalling, pharmacology and regulation by lysophospholipid metabolism.* Biochim Biophys Acta., 2007. **1768**: p. 923-940.

281. Xu, Y., *Sphingosylphosphorylcholine and lysophosphatidylcholine: G protein-coupled receptors and receptor-mediated signal transduction.* Biochim Biophys Acta, 2002. **1582**: p. 81 –88.
282. Prokazova, N.V., N.D. Zvezdina, and A.A. Korotaeva, *Effect of lysophosphatidylcholine on transmembrane signal transduction.* Biochemistry (Mosc), 1998. **63**: p. 31-37.
283. Muller, G., et al., *PKC ζ is a molecular switch in signal transduction of TNF-α, bifunctionally regulated by ceramide and arachidonic acid.* EMBO J., 1995. **14**(9): p. 1961-1969.
284. Huang, H.W., E.M. Goldberg, and R. Zidovetski, *Ceramides perturb the structure of phosphatidylcholine bilayers and modulate the activity of phospholipase A_2.* Eur Biophys J., 1998. **27**: p. 361-366.
285. Holopainen, J.M., M. Subramanian, and P.K.J. Kinnunen, *Sphingomyelinase induces lipid microdomain formation in a fluid phosphatidylcholine/sphingomyelin membrane.* Biochemistry, 1998. **37**: p. 17562-17570.
286. Osawa, Y., et al., *Roles for C_{16}-ceramide and sphingosine 1-phosphate in regulating hepatocyte apoptosis in response to tumor necrosis factor-α.* J Biol Chem., 2005. **280**: p. 27879-27887.
287. Panjarian, S., et al., *De novo N -palmitoylsphingosine synthesis is the major biochemical mechanism of ceramide accumulation following p53 up-regulation.* Prostaglandins & other Lipid Mediators, 2008. **86**: p. 41-48.
288. Kroesen, B.J., et al., *Induction of apoptosis through B-cell receptor cross-linking occurs via de novo generated C16-ceramide and involves mitochondria.* J Biol Chem., 2001. **276**: p. 13606-13614.
289. Eto, M., et al., *C_{16} ceramide accumulates following androgen ablation in LNCaP prostate cancer cells.* Prostate, 2003. **57**: p. 66-79.
290. Wieder, T., C.E. Orfanos, and C.C. Geilen, *Induction of ceramide-mediated apoptosis by the anticancer phospholipid analog, hexadecylphosphocholine.* J Biol Chem, 1998. **273**: p. 11025-11031.
291. Marks, D.L., R. Bittman, and R.E. Pagano, *Use of Bodipy-labeled sphingolipid and cholesterol analogs to examine membrane microdomains in cells.* Histochem Cell Biol., 2008. **130**: p. 819-832.
292. Smart, E.J., et al., *A detergent-free method for purifying caveolae membrane from tissue culture cells.* Proc Natl Acad Sci USA, 1995. **92**: p. 10104–10108.
293. Prinetti, A., K. Iwabuchi, and S. Hakomori, *Glycosphingolipid-enriched signaling domain in mouse neuroblastoma Neuro2a cells - Mechanism of ganglioside-dependent neuritogenesis.* J Biol Chem., 1999. **274**: p. 20916-20924.
294. Macdonald, J.L. and L.J. Pike, *A simplified method for the preparation of detergent-free lipid rafts.* J Lipid Res., 2005. **46**: p. 1061-1067.
295. Brown, D.A. and J.K. Rose, *Sorting of GPI-anchored proteins to glycolipid-enriched membrane subdomains during transport to the apical cell surface.* Cell, 1992. **68**: p. 533-544.
296. Pannu, R., A.K. Singh, and S. I., *A novel role of lactosylceramide in the regulation of tumor necrosis factor alpha-mediated proliferation of rat primary astrocytes. Implications for astrogliosis following neurotrauma.* J Biol Chem., 2005. **280**: p. 13742-13751.

297. Kopitz, J., et al., *Effects of cell surface ganglioside sialidase inhibition on growth control and differentiation of human neuroblastoma cells.* Eur J Cell Biol., 1997. **73**: p. 1-9.
298. Miquel, K., et al., *Competitive inhibition of choline phosphotransferase by geranylgeraniol and farnesol inhibits phosphatidylcholine synthesis and induces apoptosis in human lung adenocarcinoma A549 cells.* J Biol Chem., 1998. **273**: p. 26179-26186.
299. Vanags, D.M., et al., *Inhibitors of arachidonic acid metabolism reduce DNA and nuclear fragmentation induced by TNF plus cycloheximide in U937 cells.* Cell Death Differ., 1997. **4**: p. 479-486.
300. Aoyama, T., et al., *The structure of cyclooctatin, a new inhibitor of lysophospholipase.* J Antibiot (Tokyo). 1992. **45**: p. 1703-1704.
301. Schuette, C.G., et al., *Sphingolipid activator proteins: proteins with complex functions in lipid degradation and skin biogenesis.* Glycobiology, 2001. **11**(6): p. 81-90.
302. Caldas, H. and G.E. Herman, *NSDHL, an enzyme involved in cholesterol biosynthesis, traffics through the Golgi and accumulates on ER membranes and on the surface of lipid droplets.* Hum Mol Genet., 2003. **12**: p. 2981-2991.
303. Lefrancois, S., et al., *The lysosomal transport of prosaposin requires the conditional interaction of its highly conserved d domain with sphingomyelin.* J Biol Chem, 2002. **277**(19): p. 17188-99.
304. Koh, C.H., et al., *U18666A-mediated apoptosis in cultured murine cortical neurons: role of caspases, calpains and kinases.* Cell Signal, 2006. **18**(10): p. 1572-83.
305. Koh, C.H. and N.S. Cheung, *Cellular mechanism of U18666A-mediated apoptosis in cultured murine cortical neurons: bridging Niemann-Pick disease type C and Alzheimer's disease.* Cell Signal, 2006. **18**(11): p. 1844-53.
306. Kim, S.Y., T.J. Kim, and K.Y. Lee, *A novel function of peroxiredoxin 1 (Prx-1) in apoptosis signal-regulating kinase 1 (ASK1)-mediated signaling pathway.* FEBS Lett, 2008. **582**(13): p. 1913-8.
307. Brunk, U.T., et al., *Lethal hydrogen peroxide toxicity involves lysosomal iron-catalyzed reactions with membrane damage.* Redox Rep, 1995. **1**: p. 267-277.
308. Brunk, U.T., et al., *Photo-oxidative disruption of lysosomal membranes causes apoptosis of cultured human fibroblasts.* Free Radic Biol Med, 1997. **23**(4): p. 616-626.
309. Ouedraogo, G., et al., *Lysosomes are sites of fluoroquinolone photosensitization in human skin fibroblasts: a microspectrofluorometric approach.* Photochem Photobiol, 1999. **70**(2): p. 123-129.
310. Kagedal, K., U. Johansson, and K. Ollinger, *The lysosomal protease cathepsin D mediates apoptosis induced by oxidative stress.* FASEB J, 2001. **15**(9): p. 1592-1594.
311. Antunes, F., E. Cadenas, and U.T. Brunk, *Apoptosis induced by exposure to a low steady-state concentration of H2O2 is a consequence of lysosomal rupture.* Biochem J, 2001. **356**(Pt 2): p. 549-555.
312. Boya, P., et al., *Lysosomal membrane permeabilization induces cell death in a mitochondrion-dependent fashion.* J Exp Med, 2003. **197**(10): p. 1323-1334.

313. Mizumura, K., et al., *Identification of Op18/stathmin as a potential target of ASK1-p38 MAP kinase cascade.* J Cell Physiol, 2006. **206**(2): p. 363-70.
314. Cheng, T.L., M. Symons, and T.S. Jou, *Regulation of anoikis by Cdc42 and Rac1.* Exp Cell Res, 2004. **295**(2): p. 497-511.
315. Chuang, T.H., et al., *The small GTPase Cdc42 initiates an apoptotic signaling pathway in Jurkat T lymphocytes.* Mol Biol Cell, 1997. **8**(9): p. 1687-98.
316. Qin, W., et al., *BNIPL-2, a novel homologue of BNIP-2, interacts with Bcl-2 and Cdc42GAP in apoptosis.* Biochem Biophys Res Commun, 2003. **308**(2): p. 379-85.
317. Subauste, M.C., et al., *Rho family proteins modulate rapid apoptosis induced by cytotoxic T lymphocytes and Fas.* J Biol Chem, 2000. **275**(13): p. 9725-33.
318. Zhou, Y.T., G.R. Guy, and B.C. Low, *BNIP-Salpha induces cell rounding and apoptosis by displacing p50RhoGAP and facilitating RhoA activation via its unique motifs in the BNIP-2 and Cdc42GAP homology domain.* Oncogene, 2006. **25**(16): p. 2393-408.
319. Baumann, R., et al., *Macrophage migration inhibitory factor delays apoptosis in neutrophils by inhibiting the mitochondria-dependent death pathway.* Faseb J, 2003. **17**(15): p. 2221-30.
320. Konishi, A., et al., *Involvement of histone H1.2 in apoptosis induced by DNA double-strand breaks.* Cell, 2003. **114**: p. 673-688.
321. Kim, R., *Recent advances in understanding the cell death pathways activated by anticancer therapy.* Cancer, 2005. **103**: p. 1551-1561.
322. Reed, J.C., *Apoptosis-targeted therapies for cancer.* Cancer Cell, 2003. **3**(1): p. 17-22.
323. Fehrenbacher, N. and M. Jäättelä, *Lysosomes as targets for cancer therapy.* Cancer Res., 2005. **65**: p. 2993-2995.